GEOLOGICAL SURVEY CIRCULAR 98

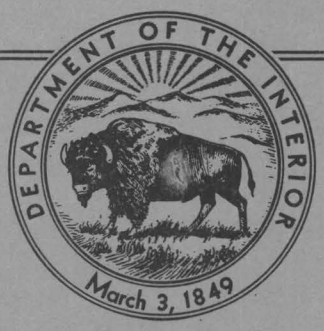

April 1951

TRENDS IN CLIMATE AND IN PRECIPITATION-RUNOFF RELATION IN MISSOURI RIVER BASIN

By

Roy E. Oltman and Hubert J. Tracy

Compiled as Part of Interior Department Program
for Development of Missouri River Basin

UNITED STATES DEPARTMENT OF THE INTERIOR
Oscar L. Chapman, Secretary
GEOLOGICAL SURVEY
W. E. Wrather, Director

Washington, D. C., 1952

Free on application to the Geological Survey, Washington 25, D. C.

TRENDS IN CLIMATE AND IN PRECIPITATION-RUNOFF RELATION IN MISSOURI RIVER BASIN

By Roy E. Oltman and Hubert J. Tracy

CONTENTS

	Page
Abstract	4
Introduction	4
Precipitation	4
Variation of precipitation distribution within the year	5
Areal variation of precipitation	5
Temperature trends	17
Trends in the precipitation-runoff relationship.	17
Possible explanation of trends	20
Map of limiting water loss	108
Conclusions	111
References Cited	113

ILLUSTRATIONS

		Page
Figure 1.	Plots of 10-year centered moving average annual precipitation with computed trend lines for selected weather stations in Missouri	6
2.	Plots of 10-year centered moving average annual precipitation with computed trend lines for selected weather stations in Kansas	7
3.	Plots of 10-year centered moving average annual precipitation with computed trend lines for selected weather stations in Nebraska	8
4.	Plots of 10-year centered moving average annual precipitation with computed trend lines for selected weather stations in Nebraska	9
5.	Plots of 10-year centered moving average annual precipitation with computed trend lines for selected weather stations in South Dakota	10
6.	Plots of 10-year centered moving average annual precipitation with computed trend lines for selected weather stations in Montana and North Dakota	11
7.	Plots of 10-year centered moving average annual precipitation with computed trend lines for selected weather stations in Colorado and Wyoming	12
8.	Long-term trends in annual precipitation in the Missouri River Basin	13
9.	Plot of 10-year centered moving average annual precipitation with computed trend lines for two periods at Milan, Italy	14
10.	Average monthly distribution of annual precipitation by decades for selected weather stations	15
11.	Roses showing correlation of annual precipitation at selected weather stations and surrounding stations	16
12.	Plots of 10-year centered moving average annual mean temperature with computed trend lines for selected weather stations	18
13.	Relationship of annual precipitation to mean annual temperature at selected weather stations	19
14.	Relationship of effective annual precipitation to annual runoff of Osage River near Bagnell, Mo.	21
15.	Double mass curve of measured runoff plotted against computed runoff for Osage River near Bagnell, Mo.	22
16.	Relationship of effective annual precipitation to annual runoff of Beaverhead River at Barratts, Mont.	23
17.	Double mass curve of measured runoff plotted against computed runoff for Beaverhead River at Barratts, Mont.	24
18.	Relationship of effective annual precipitation to annual runoff of Missouri River at Fort Benton, Mont.	25
19.	Double mass curve of measured runoff plotted against computed runoff for Missouri River at Fort Benton, Mont.	26
20.	Relationship of effective annual precipitation to annual runoff of Madison River near West Yellowstone, Mont.	27
21.	Double mass curve of measured runoff plotted against computed runoff for Madison River near West Yellowstone, Mont.	28
22.	Relationship of effective annual precipitation to annual runoff of Tenmile Creek near Rimini, Mont.	29
23.	Double mass curve of measured runoff plotted against computed runoff for Tenmile Creek near Rimini, Mont.	30
24.	Relationship of effective annual precipitation to annual runoff of North Fork Sun River near Augusta, Mont.	31

Page

Figure 25. Double mass curve of measured runoff plotted against computed runoff for North Fork Sun River near Augusta, Mont. 32
26. Relationship of effective annual precipitation to annual runoff of Marias River near Shelby, Mont. 33
27. Double mass curve of measured runoff plotted against computed runoff for Marias River near Shelby, Mont. 34
28. Relationship of effective annual precipitation to annual runoff of Judith River near Utica, Mont. 35
29. Double mass curve of measured runoff plotted against computed runoff for Judith River near Utica, Mont. 36
30. Relationship of effective annual precipitation to annual runoff of Musselshell River at Harlowton, Mont. 37
31. Double mass curve of measured runoff plotted against computed runoff for Musselshell River at Harlowton, Mont. 38
32. Relationship of effective annual precipitation to annual runoff of Yellowstone River at Corwin Springs, Mont. 39
33. Double mass curve of measured runoff plotted against computed runoff for Yellowstone River at Corwin Springs, Mont. 40
34. Relationship of effective annual precipitation to annual runoff of Bighorn River at Thermopolis, Wyo. 41
35. Double mass curve of measured runoff plotted against computed runoff for Bighorn River at Thermopolis, Wyo. 42
36. Relationship of effective annual precipitation to annual runoff of Powder River at Arvada, Wyo.. 43
37. Double mass curve of measured runoff plotted against computed runoff for Powder River at Arvada, Wyo. 44
38. Relationship of effective annual precipitation to annual runoff of Little Missouri River near Alzada, Mont. 45
39. Double mass curve of measured runoff plotted against computed runoff for Little Missouri River near Alzada, Mont. 46
40. Relationship of effective annual precipitation to annual runoff of Cannonball River at Breien, N. Dak. 47
41. Double mass curve of measured runoff plotted against computed runoff for Cannonball River at Breien, N. Dak. 48
42. Relationship of effective annual precipitation to annual runoff of Moreau River at Promise, S. Dak. 49
43. Double mass curve of measured runoff plotted against computed runoff for Moreau River at Promise, S. Dak. 50
44. Relationship of effective annual precipitation to annual runoff of Cheyenne River near Wasta, S. Dak. 51
45. Double mass curve of measured runoff plotted against computed runoff for Cheyenne River near Wasta, S. Dak. 52
46. Relationship of effective annual precipitation to annual runoff of Rapid Creek at Big Bend, S. Dak. 53
47. Double mass curve of measured runoff plotted against computed runoff for Rapid Creek at Big Bend, S. Dak. 54
48. Relationship of effective annual precipitation to annual runoff of Belle Fourche River, near Belle Fourche, S. Dak. 55
49. Double mass curve of measured runoff plotted against computed runoff for Belle Fourche River near Belle Fourche, S. Dak. 56
50. Relationship of effective annual precipitation to annual runoff of Bad River near Fort Pierre, S. Dak. 57
51. Double mass curve of measured runoff plotted against computed runoff for Bad River near Fort Pierre, S. Dak. 58
52. Relationship of effective annual precipitation to annual runoff of White River near Oacoma, S. Dak. 59
53. Double mass curve of measured runoff plotted against computed runoff for White River near Oacoma, S. Dak. 60
54. Relationship of effective annual precipitation to annual runoff of Niobrara River at Dunlap, Nebr. 61
55. Double mass curve of measured runoff plotted against computed runoff for Niobrara River at Dunlap, Nebr. 62
56. Relationship of effective annual precipitation to annual runoff of James River near Scotland, S. Dak. 63
57. Double mass curve of measured runoff plotted against computed runoff for James River near Scotland, S. Dak. 64
58. Relationship of effective annual precipitation to annual runoff of Big Sioux River at Akron, Ia. .. 65
59. Double mass curve of measured runoff plotted against computed runoff for Big Sioux River at Akron, Ia. 66
60. Relationship of effective annual precipitation to annual runoff of North Platte River at Saratoga, Wyo. 67

Page

Figure 61. Double mass curve of measured runoff plotted against computed runoff for North Platte River at Saratoga, Wyo. ... 68
62. Relationship of effective annual precipitation to annual runoff of North Fork South Platte River at South Platte, Colo. ... 69
63. Double mass curve of measured runoff plotted against computed runoff for North Fork South Platte River at South Platte, Colo. ... 70
64. Relationship of effective annual precipitation to annual runoff of Clear Creek near Golden, Colo. ... 71
65. Double mass curve of measured runoff plotted against computed runoff for Clear Creek near Golden, Colo. ... 72
66. Relationship of effective annual precipitation to annual runoff of Thompson River (below powerhouse) near Drake, Colo. ... 73
67. Double mass curve of measured runoff plotted against computed runoff for Thompson River (below powerhouse) near Drake, Colo. ... 74
68. Relationship of effective annual precipitation to annual runoff of Cache la Poudre River at mouth of canyon, near Fort Collins, Colo. ... 75
69. Double mass curve of measured runoff plotted against computed runoff for Cache la Poudre River at mouth of canyon, near Fort Collins, Colo. ... 76
70. Relationship of effective annual precipitation to annual runoff of Loup River at (near) Columbus, Nebr. ... 77
71. Double mass curve of measured runoff plotted against computed runoff for Loup River at (near) Columbus, Nebr. ... 78
72. Relationship of effective annual precipitation to annual runoff of Elkhorn River at Waterloo, Nebr. ... 79
73. Double mass curve of measured runoff plotted against computed runoff for Elkhorn River at Waterloo, Nebr. ... 80
74. Relationship of effective annual precipitation to annual runoff of Nishnabotna River above Hamburg, Ia. ... 81
75. Double mass curve of measured runoff plotted against computed runoff for Nishnabotna River above Hamburg, Ia. ... 82
76. Relationship of effective annual precipitation to annual runoff of Nodaway River near Burlington Junction, Mo. ... 83
77. Double mass curve of measured runoff plotted against computed runoff for Nodaway River near Burlington Junction, Mo. ... 84
78. Relationship of effective annual precipitation to annual runoff of Platte River near Agency, Mo. . 85
79. Double mass curve of measured runoff plotted against computed runoff for Platte River near Agency, Mo. ... 86
80. Relationship of effective annual precipitation to annual runoff of Arikaree River at Haigler, Nebr. ... 87
81. Double mass curve of measured runoff plotted against computed runoff for Arikaree River at Haigler, Nebr. ... 88
82. Relationship of effective annual precipitation to annual runoff of Smoky Hill River at Ellsworth, Kans. ... 89
83. Double mass curve of measured runoff plotted against computed runoff for Smoky Hill River at Ellsworth, Kans. ... 90
84. Relationship of effective annual precipitation to annual runoff of Saline River at Tescott, Kans. . 91
85. Double mass curve of measured runoff plotted against computed runoff for Saline River at Tescott, Kans. ... 92
86. Relationship of effective annual precipitation to annual runoff of Big Blue River at Randolph, Kans. ... 93
87. Double mass curve of measured runoff plotted against computed runoff for Big Blue River at Randolph, Kans. ... 94
88. Relationship of effective annual precipitation to annual runoff of Grand River near Gallatin, Mo. 95
89. Double mass curve of measured runoff plotted against computed runoff for Grand River near Gallatin, Mo. ... 96
90. Relationship of effective annual precipitation to annual runoff of Sac River near Stockton, Mo. . 97
91. Double mass curve of measured runoff plotted against computed runoff for Sac River near Stockton, Mo. ... 98
92. Relationship of effective annual precipitation to annual runoff of Gasconade River near Waynesville, Mo. ... 99
93. Double mass curve of measured runoff plotted against computed runoff for Gasconade River near Waynesville, Mo. ... 100
94. Relationship of effective annual precipitation to annual runoff of St. Mary River near Kimball, Alberta ... 101
95. Double mass curve of measured runoff plotted against computed runoff for St. Mary River near Kimball, Alberta ... 102
96. Relationship of effective annual precipitation to annual runoff of Neosho River near Parsons, Kans. ... 103

Page

Figure 97. Double mass curve of measured runoff plotted against computed runoff for Neosho River near Parsons, Kans. 104
98. Residual mass curves for Beaverhead River at Barratts, Mont. 107
99. Comparison of computed long-term effective precipitation with measured runoff of Beaverhead River Basin 107
100. Decline of base flow during drought years as shown by Big Spring Creek near Lewistown, Mont. 108
101. Determination of limiting annual water loss for Nodaway River Basin above Burlington Junction, Mo. 109
102. Relationship of winter precipitation to annual precipitation in Colorado, Wyoming, and Montana 110
103. Variation of limiting annual water loss with altitude 111
104. Limiting annual water loss in the Missouri River Basin 112

TABLES

Table 1. Distribution of annual precipitation by decades for the months October to March and June to August 17
2. Tributary basins studied for trends in the precipitation-runoff relationship 105

ABSTRACT

This report presents a study of trends in climate and in the relationship between precipitation and runoff in the Missouri River Basin for the period of available records. Long-term trends in annual precipitation are generally downward (or show a decline in precipitation) in the States of Montana, North Dakota, South Dakota, Nebraska, and Kansas, but seem to be indeterminate in the remainder of the basin. Long-term trends in mean annual temperature are generally upward (or show an increase in average temperature) for the entire basin. For the relatively short period of record available for study, trends in the precipitation-runoff relationship are found to exist for some basins draining the mountain ranges beginning usually about 1930, and indicate decreasing runoff yields under constant precipitation. The trends in the precipitation-runoff relationship are shown to be the result of concurrent trends in either or both temperature and groundwater outflow. A map of limiting annual water loss in the Missouri Basin is presented in this report.

INTRODUCTION

The existence of a basin-wide, long-term trend in annual precipitation indicating a continual decline in future precipitation would be a serious threat to agriculture. A widespread trend in the relationship between precipitation and runoff indicating a gradual decline in future runoff yields under equal precipitation would take out of production many irrigated acres in the basin.

The Missouri Basin is shaped like a parallelogram with its major axis lying in a northwest-southeast direction. Along the western edge are the mountains of the Continental Divide; in Wyoming and Montana outlying mountain ranges lie roughly parallel to the Divide. Climate varies from arid in intermontane valleys of Wyoming to humid in Missouri. The high-altitude regions of the mountain ranges in the basin have a very different climate from that of the flat plains immediately adjacent; annual precipitation often exceeds 50 inches on the mountain peaks compared with annual totals of less than 10 inches in the plains. Mean annual temperature ranges, north to south, from 40 to 56 degrees over the Great Plains, and decreases with altitude in the mountains according to a definite lapse rate for each locale. Because of the large areal extent of the Missouri Basin and of the range of climate, a satisfactory study of precipitation-runoff trends requires detailed investigation of many tributary basins.

A detailed discussion of the hydrologic factors influencing annual runoff is beyond the scope of this study. One of the best concise reviews of the variables entering the runoff equation is contained in a recent publication of the Geological Survey.[1] The results of the study of trends in the precipitation-runoff relationship are explained in this report by citing the changes in climatic and cultural conditions that may have caused the observed trends.

This report was compiled as part of the program of the Interior Department for development of the Missouri River Basin, by the staff of the Lincoln Regional Field Office, Special Reports and Investigations Section of the Surface Water Branch, U. S. Geological Survey, J. V. B. Wells, Chief.

W. B. Langbein furnished valuable advice and constructive criticism on the method used in showing the trends in the precipitation-runoff relationship.

PRECIPITATION

Precipitation may be considered the starting point for studies of runoff. A study of the time trend of annual precipitation is a prerequisite to the study of trends in the precipitation - runoff relationship. In a subsequent section of this report the effect of long - term declining precipitation on ground water contributions to current runoff is discussed. The study of trends of annual precipitation was made with graphs of precipitation at selected long-term

1 Langbein, W. B., and others, Annual runoff in the United States: U.S. Geol. Survey Circ. 52, 1949.

weather stations to give a representative coverage for the basin. There are only a few long-term weather stations available in the western half of the basin; in the eastern half of the basin the available long-term weather stations are more numerous. Figures 1 to 7 show the plots of the 10-year centered moving averages at the selected stations for the period of continuous record ending in 1948. A computed trend line was drawn through each plot. The trend line has a slightly different position from one computed using original unaveraged figures. Note the general decline in the basin precipitation during the decade 1930-40.

The trend lines, only, have been plotted on a map (see fig. 8) to show a composite picture of the trends in annual precipitation for the entire Missouri Basin. Figure 8 indicates that there is a general downward trend in annual precipitation in the Great Plains but that there are mixed trends in humid Missouri and in areas in or adjacent to mountain ranges. The area extending in a north-south direction across the basin between the meridians of 96 and 100 degrees longitude has had a greater decline in annual precipitation than any other part of the basin.

In general, climatic trends over long periods appear to follow a consistent worldwide pattern. Matthes[2] has shown that glacial evidence indicates uniform long-term trends in world climate. Assuming that, over long periods of time, there is good correlation between precipitation trends in the world, a comparative study of the precipitation trends at a Missouri Basin station with a long period of record and like trends at a station, located elsewhere, with much longer record may indicate possible trends in the Missouri Basin for a much longer period.

Milan, Italy, has the longest published record,[3] continuous 1768-1936, of annual precipitation for any weather station in the world. Figure 9 is a plot of 10-year centered moving average annual precipitation at Milan, Italy. For comparison with records in the Missouri Basin, the Milan record has been broken at the year 1833, and divided into two parts, so that the latter period, 1833 to end of record, will approximate the longest period of precipitation record in the Missouri Basin. Both the Milan record and Missouri Basin records show downward trends for the period 1833 to the present. However, the trend for the Milan record before 1833 is upward, compensating for the later downward trend, and making the entire period at Milan show one significant level trend. It is apparent that the general downward trend of precipitation in the Missouri Basin reflects the period of record available.

Variation of Precipitation Distribution Within the Year

Annual precipitation is not only variable as to the total occurring in each year, but is also variable with respect to the percentage of the annual total distributed to each month. Large changes in the distribution of the annual precipitation to the individual months have an important effect on the annual runoff produced, because an inch of precipitation in April will usually produce more runoff than the same quantity precipitated with equal intensity in July. Changes in the distribution of the annual precipitation such that a greater-than-normal percentage falls in the summer months of higher evapotranspiration demand usually result in annual runoff less than normal for the corresponding annual precipitation.

Figure 10 shows graphically the average monthly distribution in percent of annual total by decades, from 1881 to 1940, for six weather stations in or adjacent to the basin. Table 1 is a list of the percentages of the annual total precipitated in the six months October to March, and the percentage of the annual total precipitated in the three months June to August averaged by decades.

No consistent variation appears to exist for the stations used, and the average distribution percentages by decades vary only a minor amount from the average for the period 1881-1940. The percentage distribution within individual years, of course, varies widely from the long-term average. Apparently, there is no significant trend in the seasonal distribution of the total annual precipitation.

Areal Variation of Precipitation

Precipitation measured at a single point is not a precise measure of the precipitation of the surrounding area. The accuracy with which point precipitation represents the precipitation on the surrounding area varies from poor for individual storms to good for annual values. The degree of correlation found to exist between annual precipitation measured at two points indicates how well the annual precipitation measured at the one point represents the precipitation at the other. To define the areal variation in representativeness of point-measured precipitation, a key station was selected for the particular area under study, and correlations were made between precipitation measured at the key station and that measured at surrounding stations. The results are graphically portrayed on a map of the basin (see fig. 11) on which correlation roses are shown for the key stations, Great Falls, Mont., Bismarck, N. Dak., Cheyenne, Wyo., Omaha, Nebr., and Kansas City, Mo. The correlations are based on annual-precipitation values for the period 1920-48.

It is surprising to note how well the precipitation at Great Falls and Bismarck represents the precipitation for surrounding areas, compared with the results obtained at Omaha and Kansas City. The elongation of the correlation roses in particular directions is probably intimately associated with mean annual storm paths. Note that the correlation roses are not extended beyond the Continental Divide at Cheyenne and Great Falls; this was not done because of the lack of precipitation records at or near the Continental Divide. Actually there is an apparent continuation of the correlation in the area west of the mountains. The correlation roses show indirectly the optimum spacing of precipitation gages to obtain the same

2 Matthes, F. E., Hydrology (edited by O. E. Meinzer), Glaciers, pp. 149-219, 1949.

3 Clayton, H. H., World Weather Records, Smithsonian Misc. Colls., vols. 79, 90, and 105, 1944.

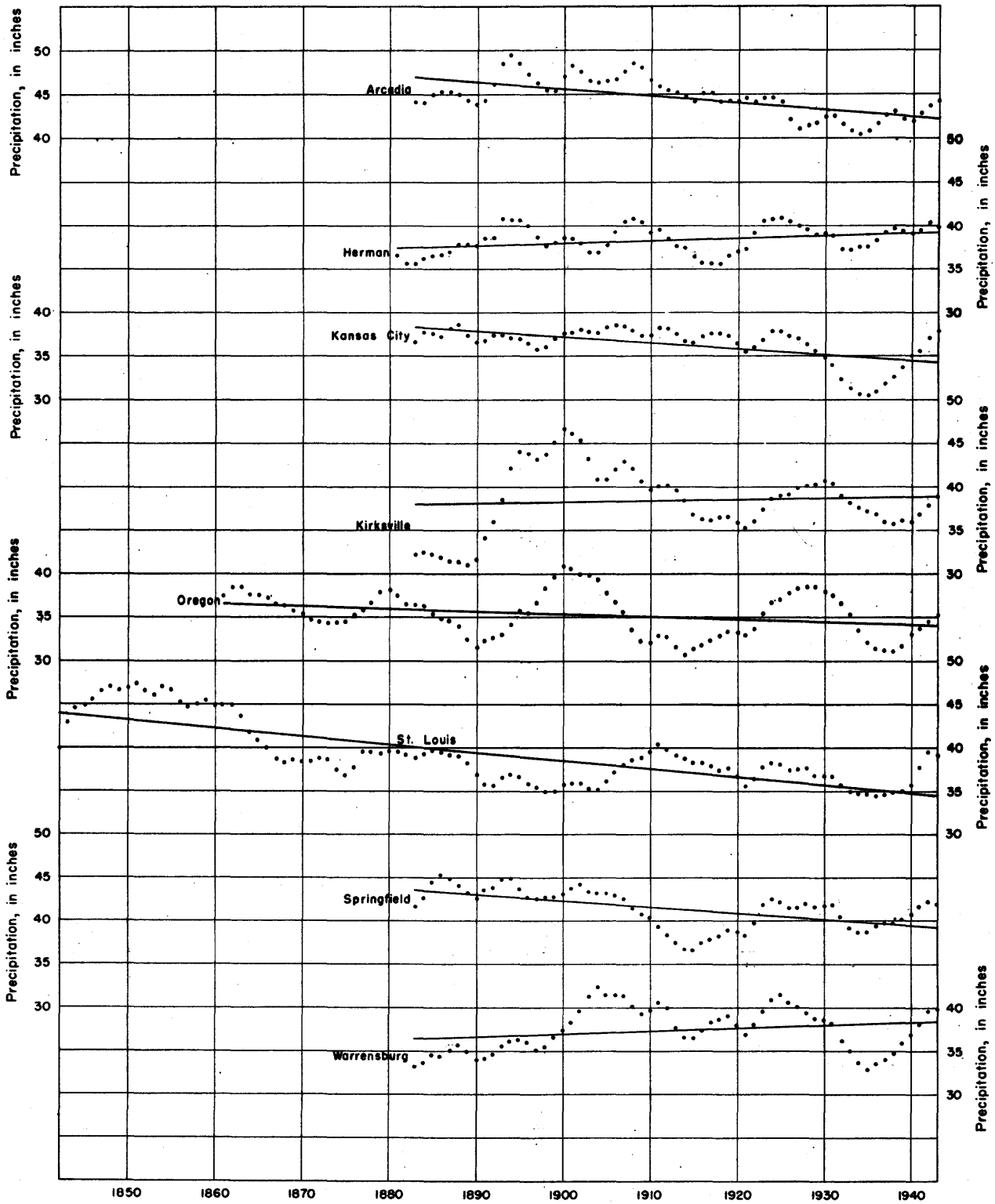

Figure 1. — Plots of 10-year centered moving average annual precipitation with computed trend lines for selected weather stations in Missouri.

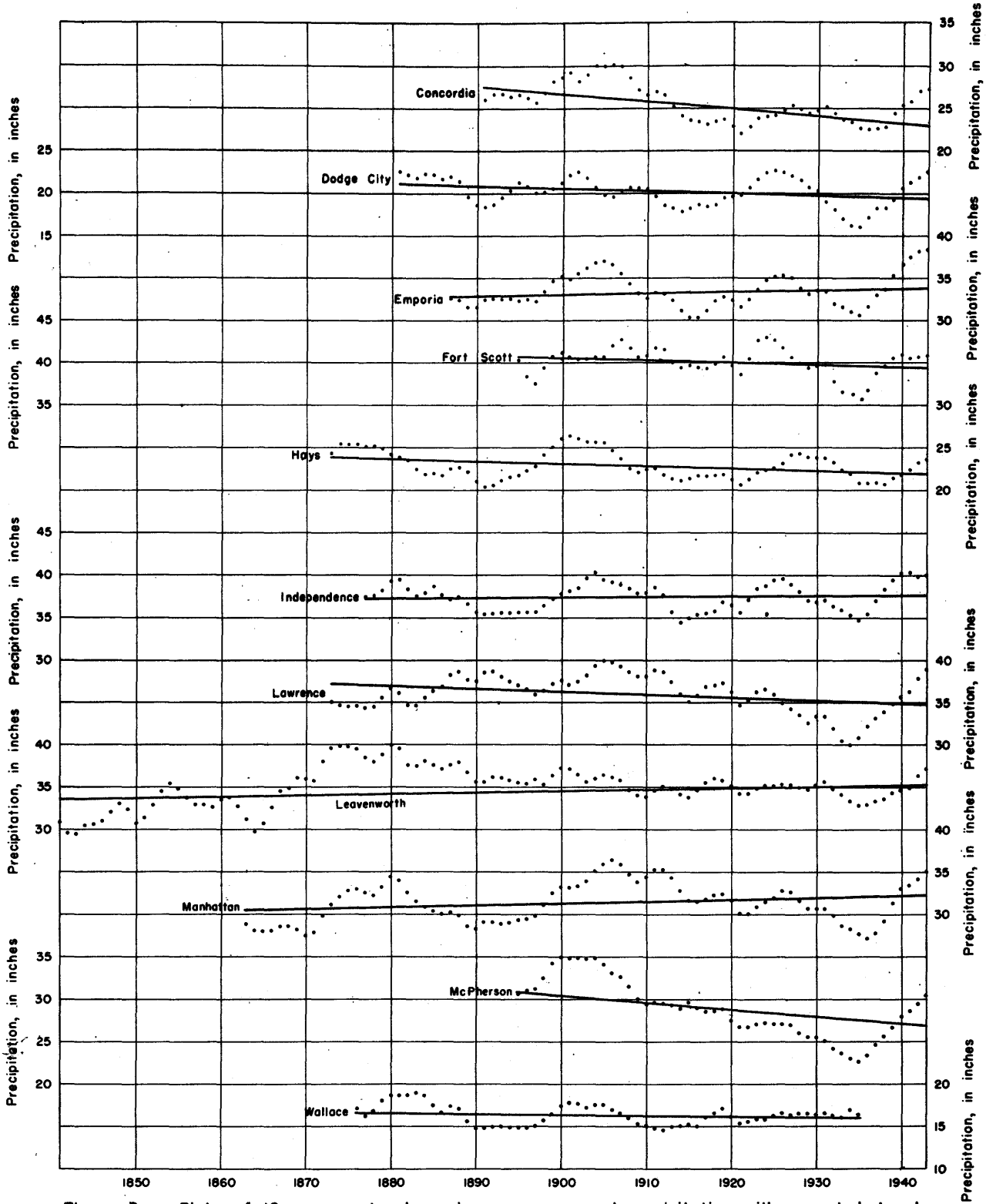

Figure 2. —Plots of 10-year centered moving average annual precipitation with computed trend lines for selected weather stations in Kansas.

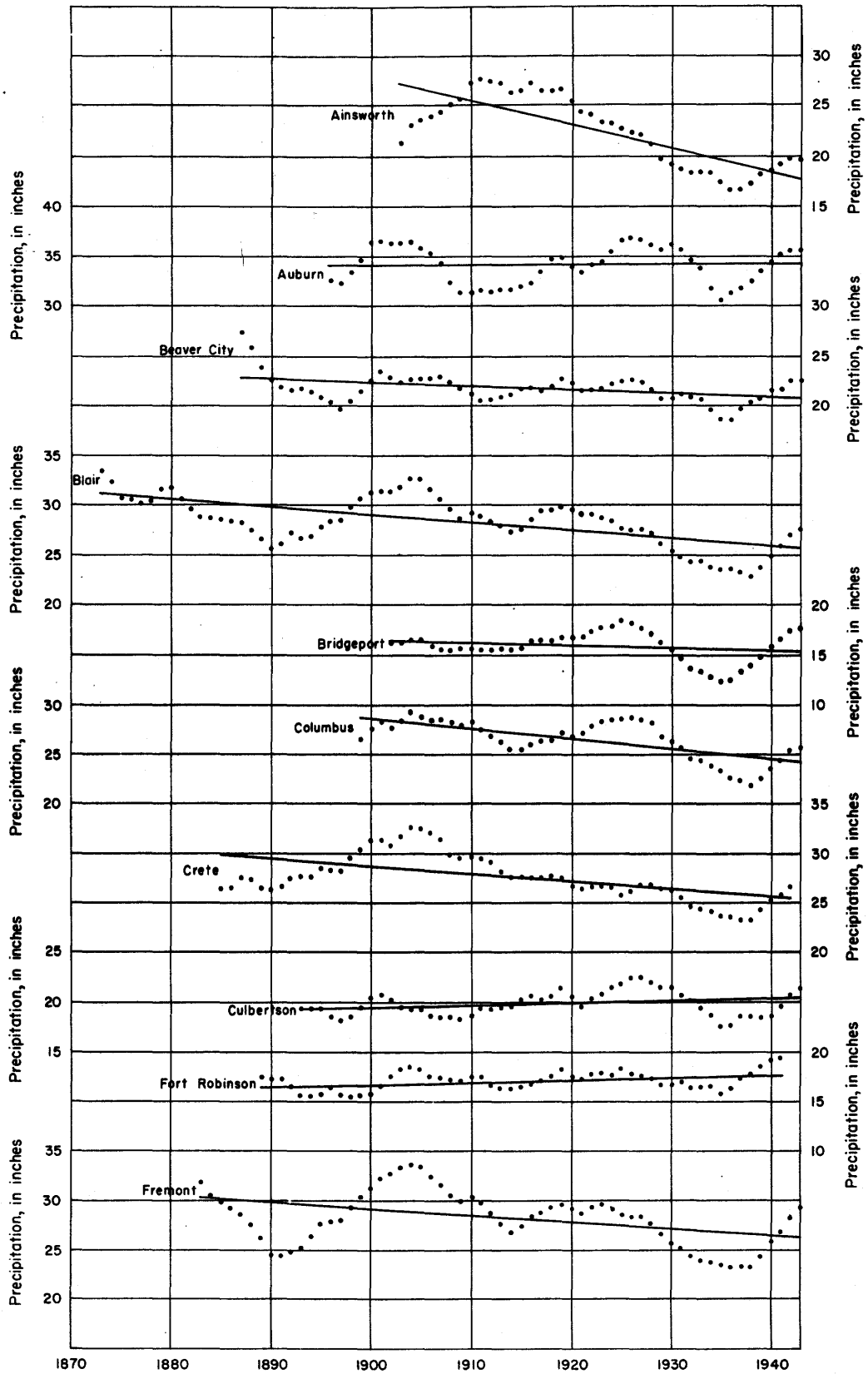

Figure 3.—Plots of 10-year centered moving average annual precipitation with computed trend lines for selected weather stations in Nebraska (Continued on fig. 4).

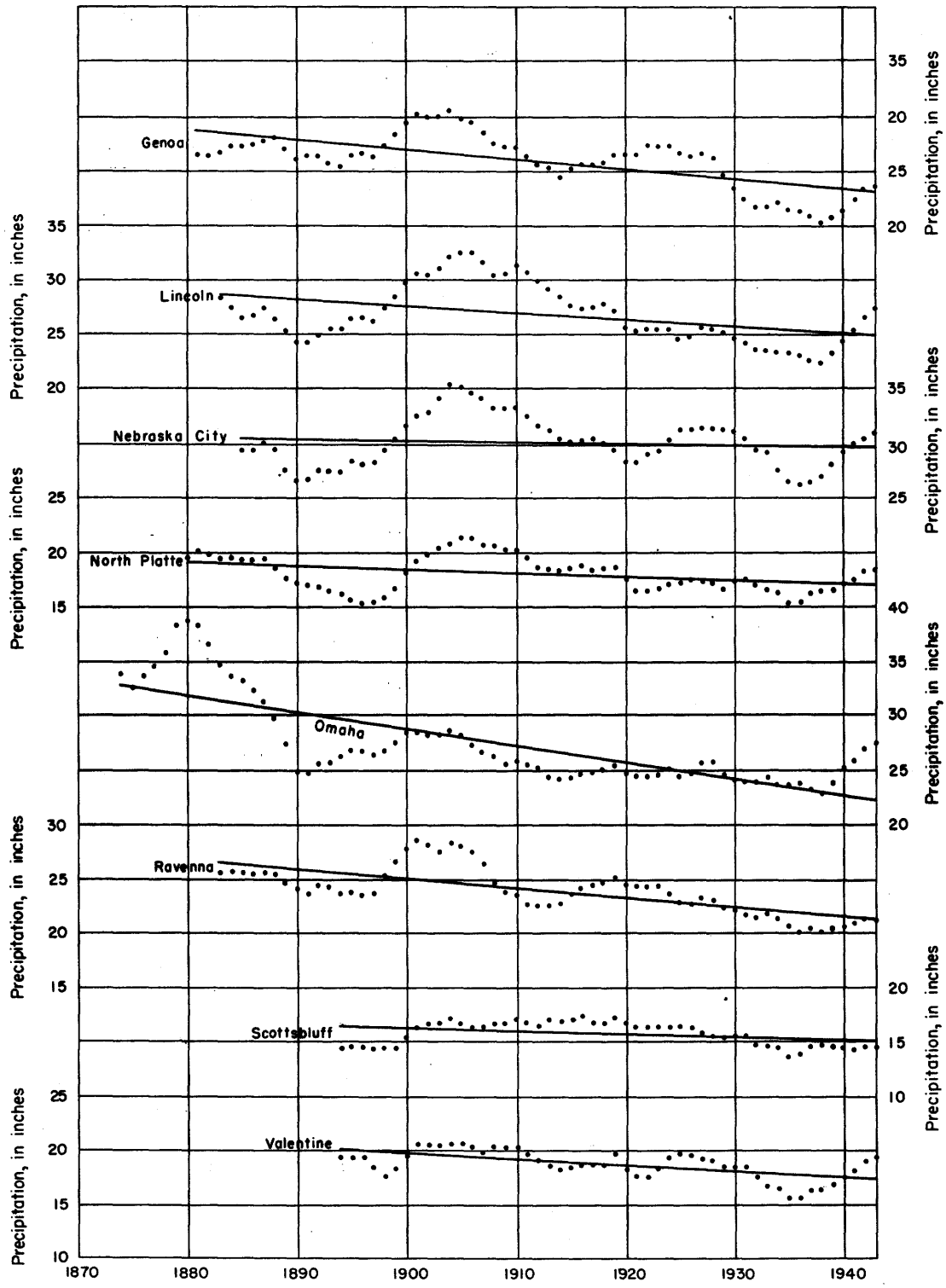

Figure 4.— Plots of 10-year centered moving average annual precipitation with computed trend lines for selected weather stations in Nebraska (Continued from fig. 3).

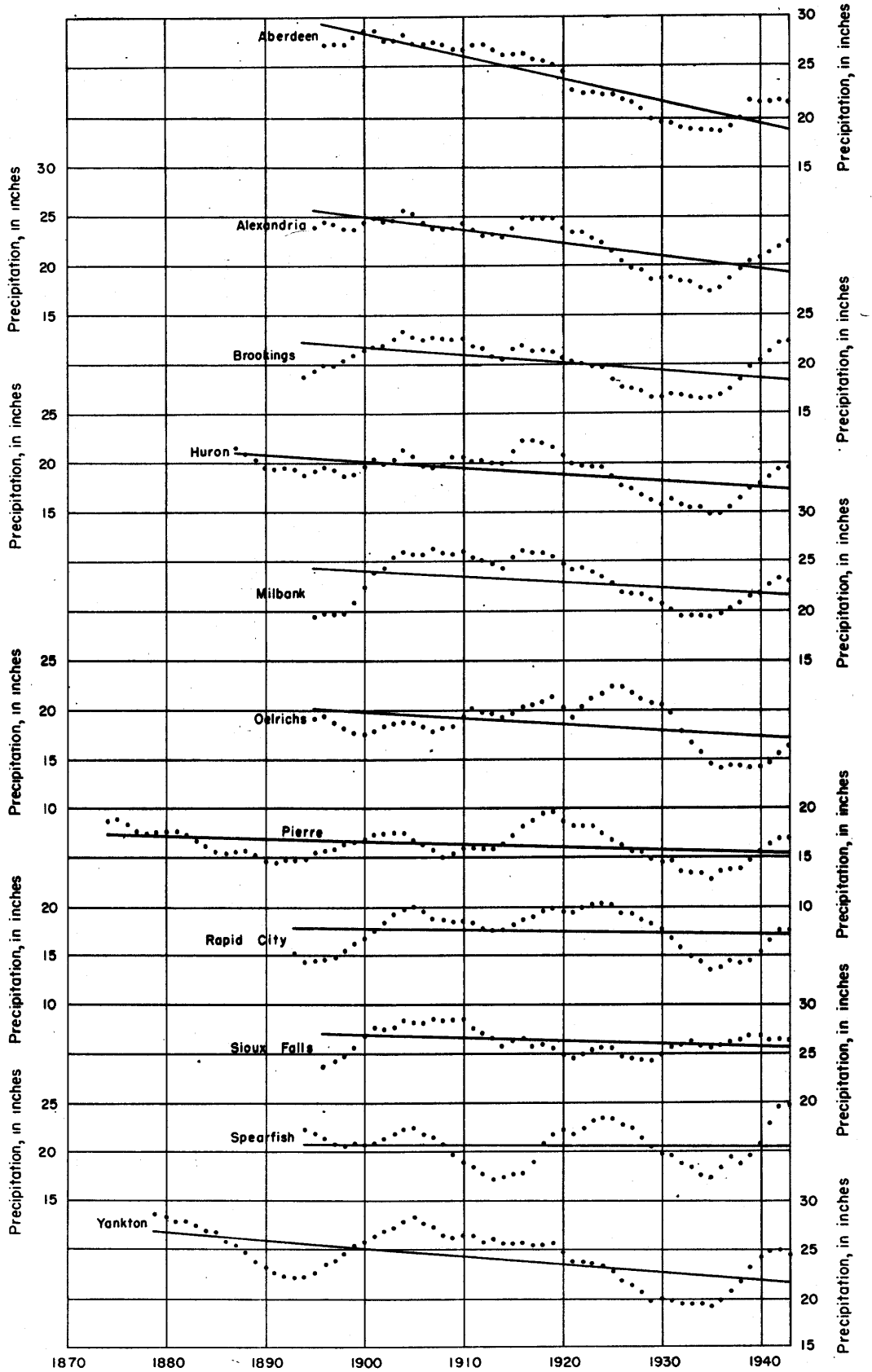

Figure 5.—Plot of 10-year centered moving average annual precipitation with computed trend lines for selected weather stations in South Dakota.

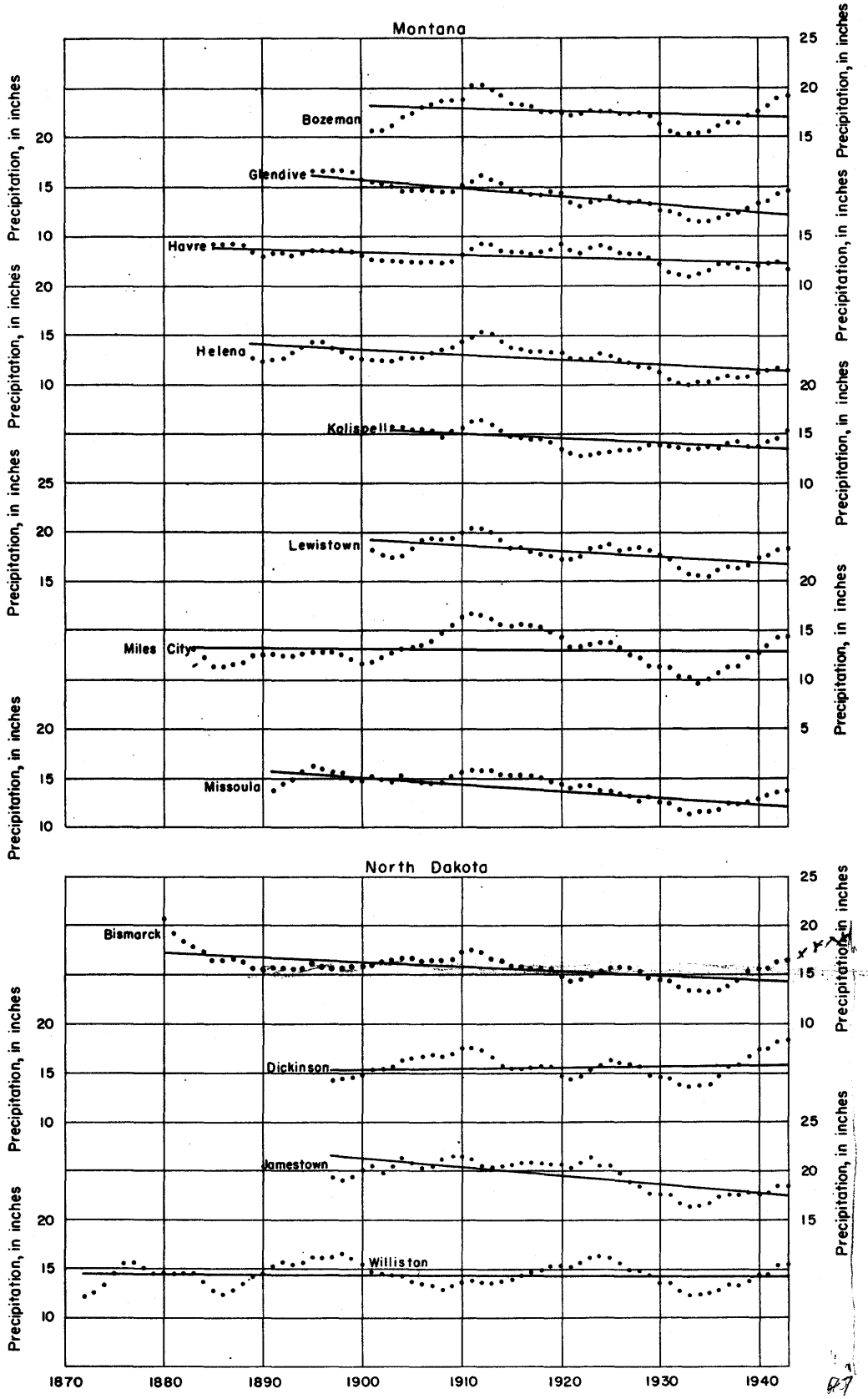

Figure 6.—Plots of 10-year centered moving average annual precipitation with computed trend lines for selected weather stations in Montana and North Dakota.

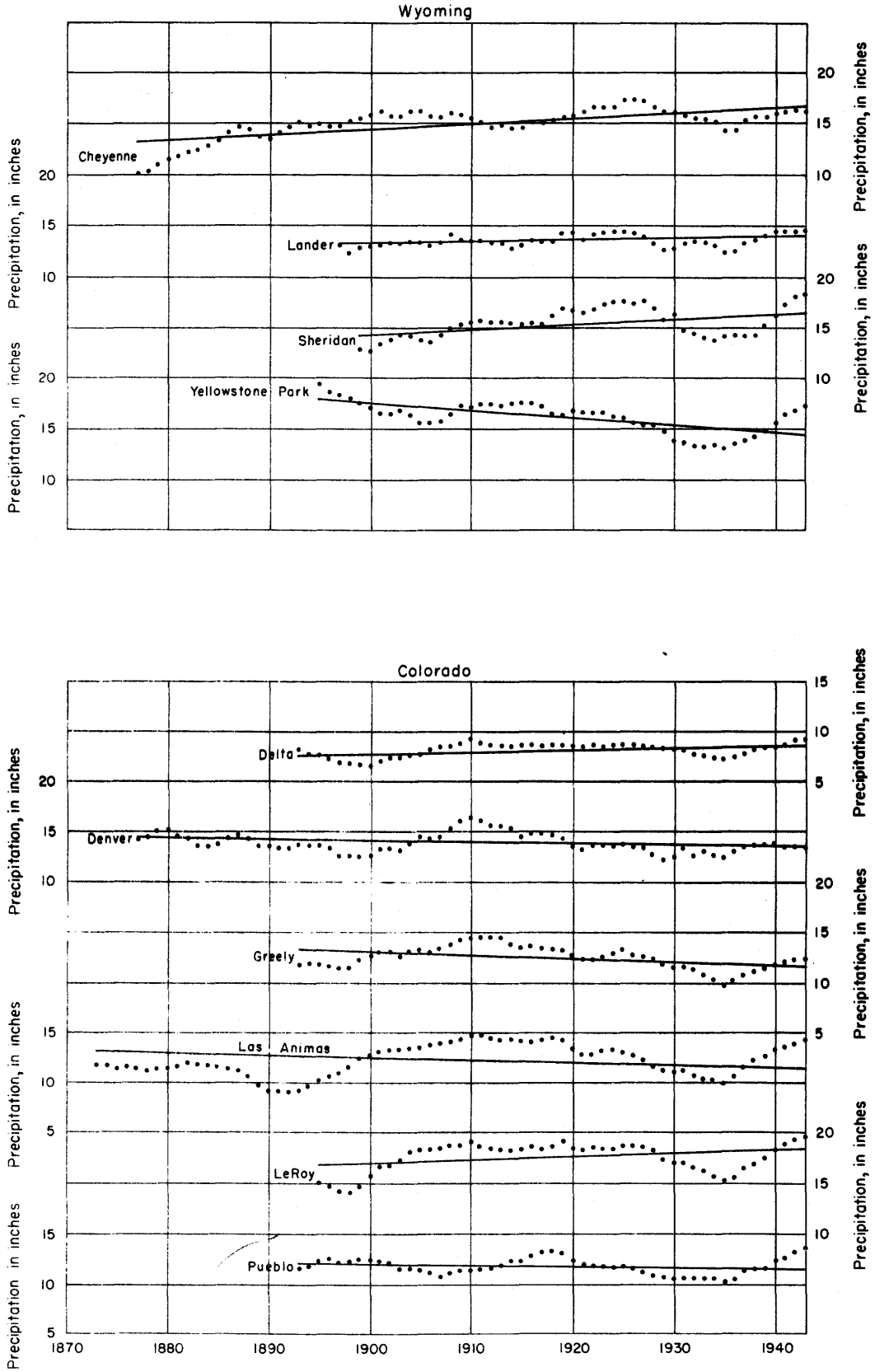

Figure 7. — Plots of 10-year centered moving average annual precipitation with computed trend lines for selected weather stations in Colorado and Wyoming.

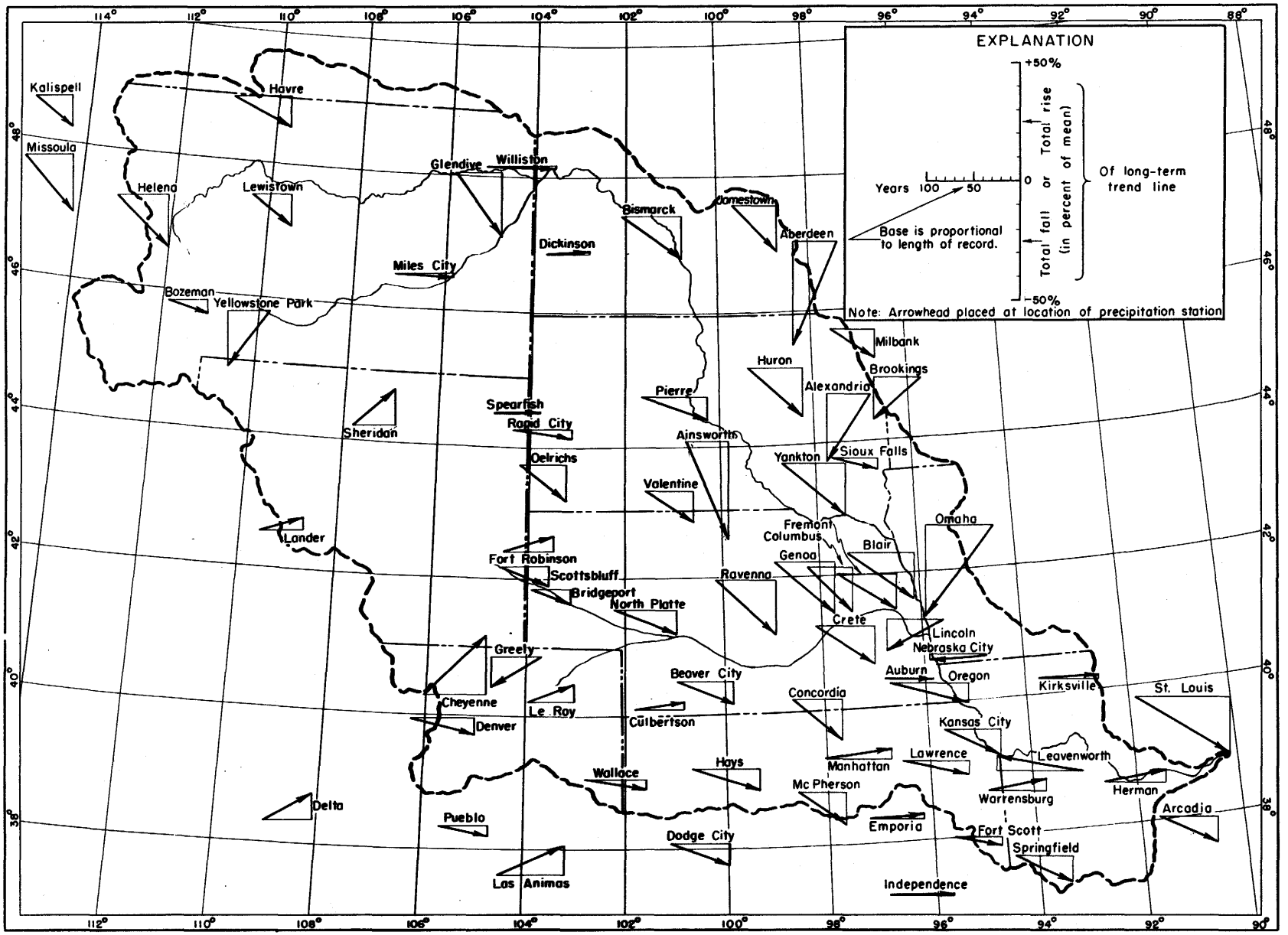

Figure 8. — Long-term trends in annual precipitation in the Missouri River Basin.

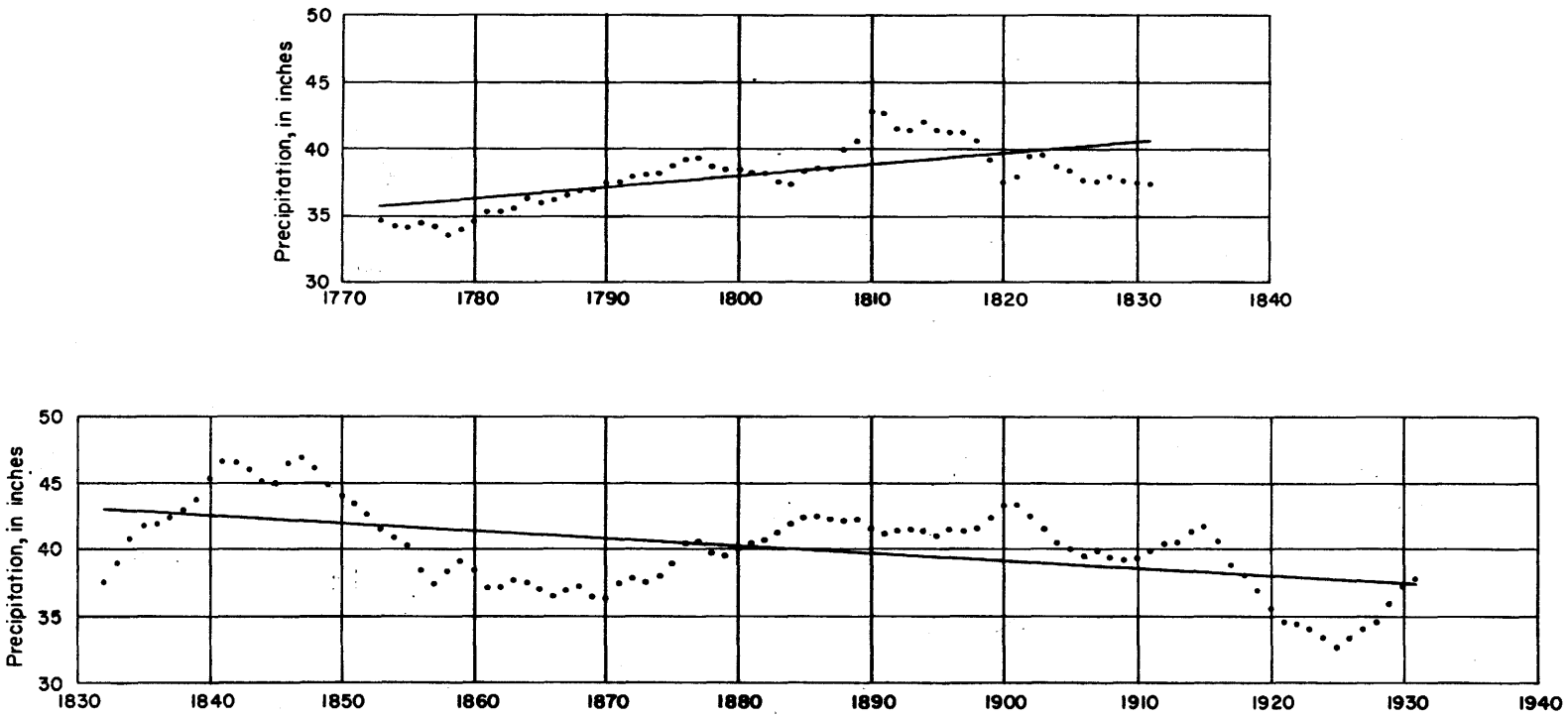

Figure 9.—Plot of 10-year centered moving average annual precipitation with computed trend lines for two periods at Milan, Italy.

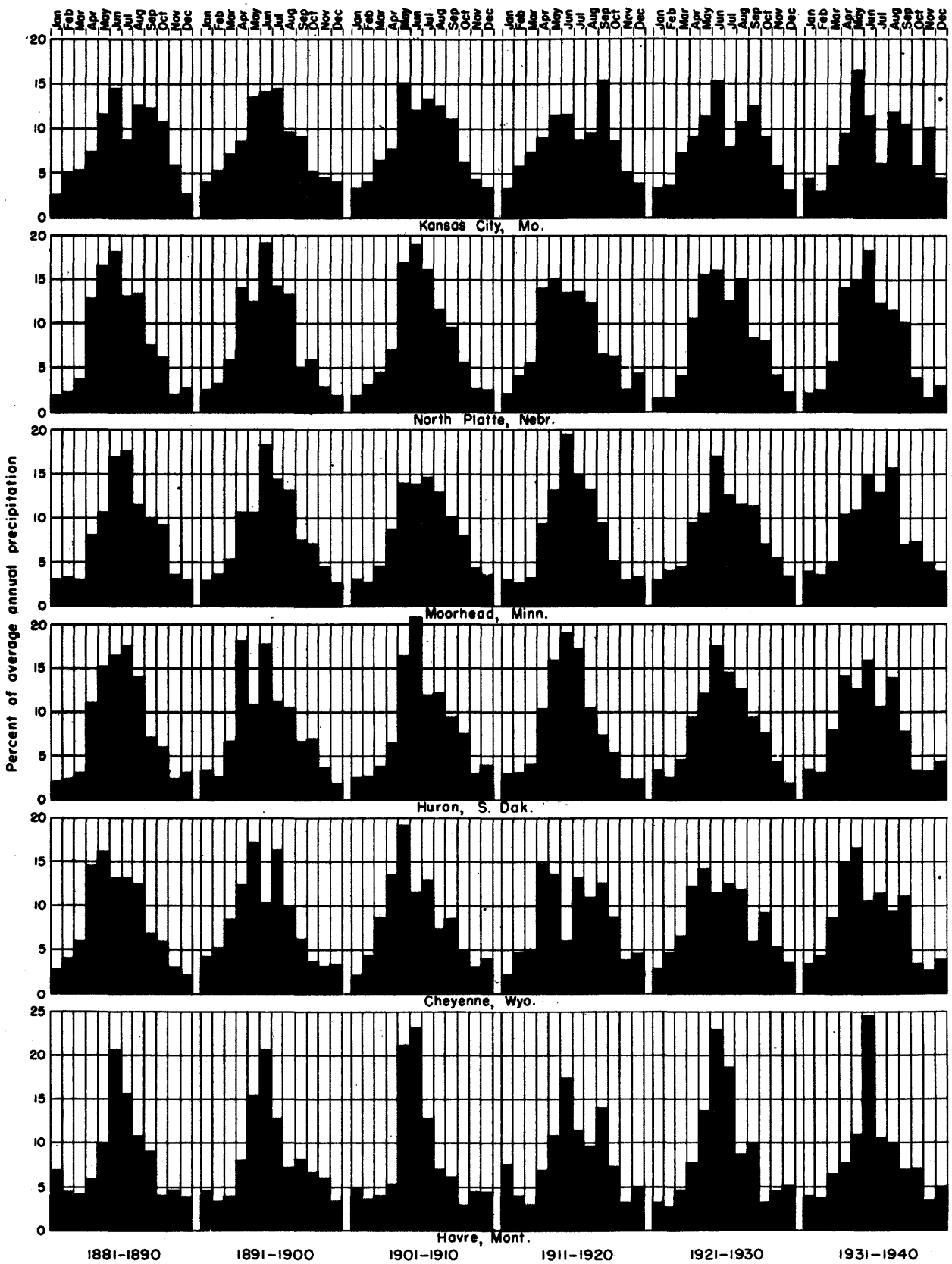

Figure 10.—Average monthly distribution of annual precipitation by decades for selected weather stations.

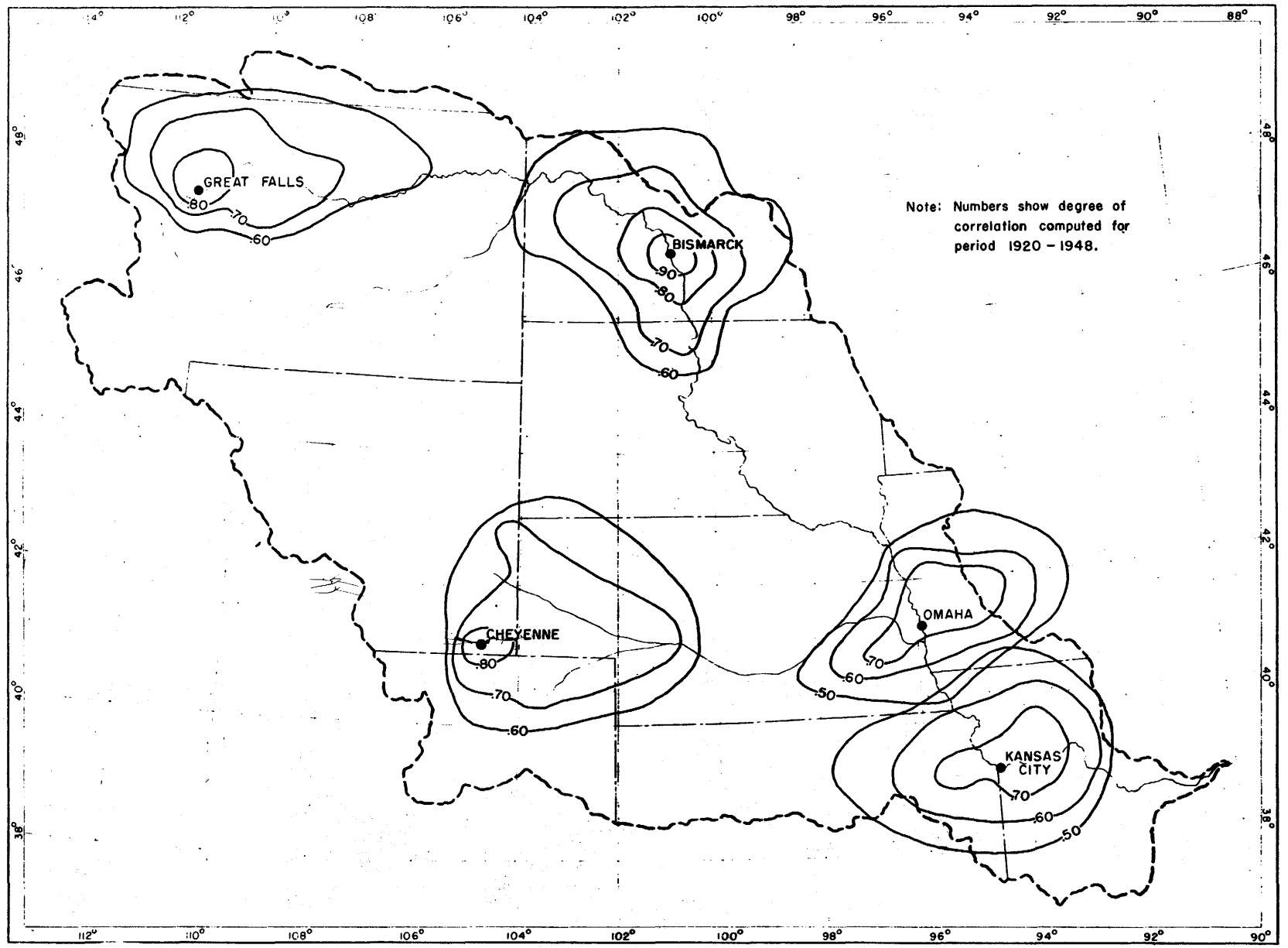

Figure 11.—Roses showing correlation of annual precipitation between selected weather stations and surrounding stations.

Table 1. —Distribution of annual precipitation by decades for the months October to March and June to August

Station	1881-1940 (percent)	1881-90 (percent)	1891-1900 (percent)	1901-10 (percent)	1911-20 (percent)	1921-30 (percent)	1931-40 (percent)
October to March							
Kansas City	32	32	30	28	34	33	34
North Platte	21	19	22	20	25	22	19
Moorhead	25	25	26	26	20	27	28
Huron	22	19	25	23	20	24	25
Cheyenne	28	24	28	27	29	32	26
Havre	27	28	28	24	30	23	29
June to August							
Kansas City	34	36	38	38	30	34	29
North Platte	44	45	47	47	39	44	42
Moorhead	44	46	46	41	48	41	44
Huron	44	48	39	45	46	45	40
Cheyenne	34	39	36	32	30	36	32
Havre	43	47	41	43	39	45	45

relative accuracy of computed basin-average precipitation in drainage areas of identical shape and size in different geographic locations within the basin. It would be necessary to have precipitation stations more closely spaced near Omaha than near Bismarck to obtain the same accuracy of basin-average annual precipitation.

TEMPERATURE TRENDS

Figure 12 shows the long-term temperature trends found at selected stations in the basin. The trend lines are fitted to 10-year centered moving average plots of the mean annual temperature. The trend seems to be generally upward with the strongest upward tendency occurring in the Great Plains and arid intermontane valleys. The upward temperature trend is very likely associated with the downward trend in precipitation. Figure 13 shows computed regression lines between annual precipitation and mean annual temperature at selected long-term weather stations in or near the basin. Temperature was arbitrarily selected as the independent variable. The regression lines show a wide variation in slope throughout the basin, ranging from practically none at Williston, N. Dak., to a maximum 10-inch decrease in annual precipitation for an 8-degree rise in mean annual temperature at Omaha, Nebr. Correlation between mean annual temperature and annual precipitation is low for the basin; at Omaha 0.35 was the coefficient of correlation computed. Plotting points for individual years at Omaha have been shown to portray the wide scatter indicative of the practical absence of relationship. On the basis of the temperature trend to date and the relationship of annual temperature and annual precipitation, an assumption might be made that our climate will gradually become warmer and drier in the future. However, such an assumption would be groundless; our future climate cannot be accurately forecast on the basis of past performance.

TRENDS IN THE PRECIPITATION-RUNOFF RELATIONSHIP

A long-term upward or downward trend in the relation of annual precipitation and annual runoff in any portion of the Missouri Basin would be of general interest. As plans for further utilization of surface waters for irrigation are carried out, the existence of a long-term downward trend--that is, declining runoff yield under constant precipitation--in the relationship of precipitation to runoff would become especially serious in those regions now supplied with barely sufficient water. Essentially, the investigations contained in this section were designed to determine whether equal yields of runoff resulted from identical annual precipitation at the beginning and end of the period of runoff record. If the study indicated a trend in the relationship for a particular tributary basin, further investigations were made to determine what changes in climatic or cultural conditions may have caused the trend.

Unfortunately, neither the precipitation nor runoff records available for the study of trends in the precipitation-runoff relationship are of ideal length or character. In the basin, runoff records of long duration are few. The number of gaging stations in operation prior to 1930 is hardly sufficient to define the variation of average annual runoff with geographic location. The runoff records used in the study have been tabulated from the published annual discharges corrected, where appropriate, for reductions in stream flow through irrigation. Some discharge records of long duration cannot be converted into usable runoff records because of uncertain amounts used for irrigation. Equally serious limitations apply to the precipitation records. In some basins enough weather stations were not available to allow computation of a reliable basin average annual precipitation. In tributary basins deriving their water from the high mountain ranges, the distribution of precipitation gages was also poor; almost all records were

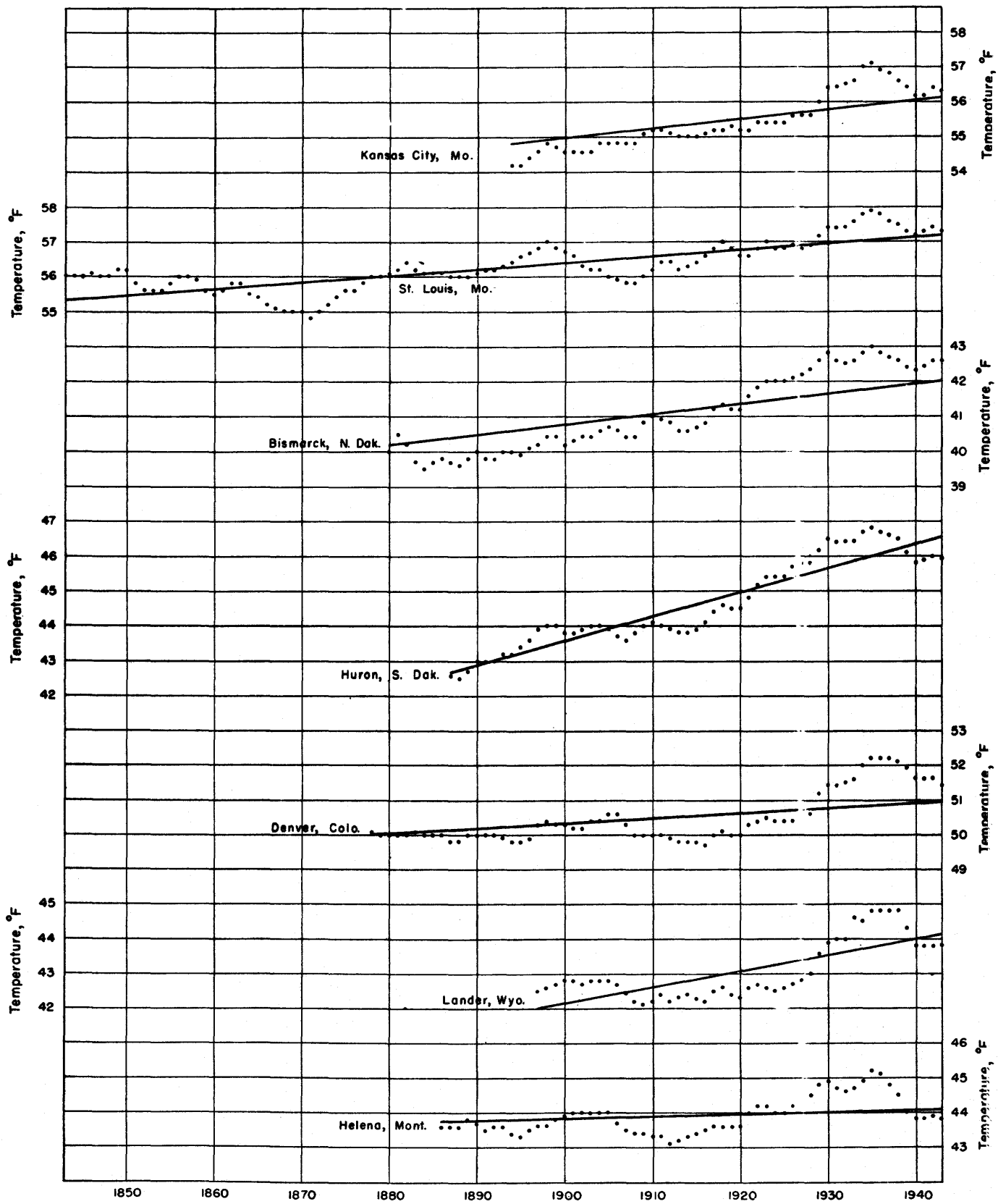

Figure 12.—Plots of 10-year centered moving average annual mean temperature with computed trend lines for selected weather stations.

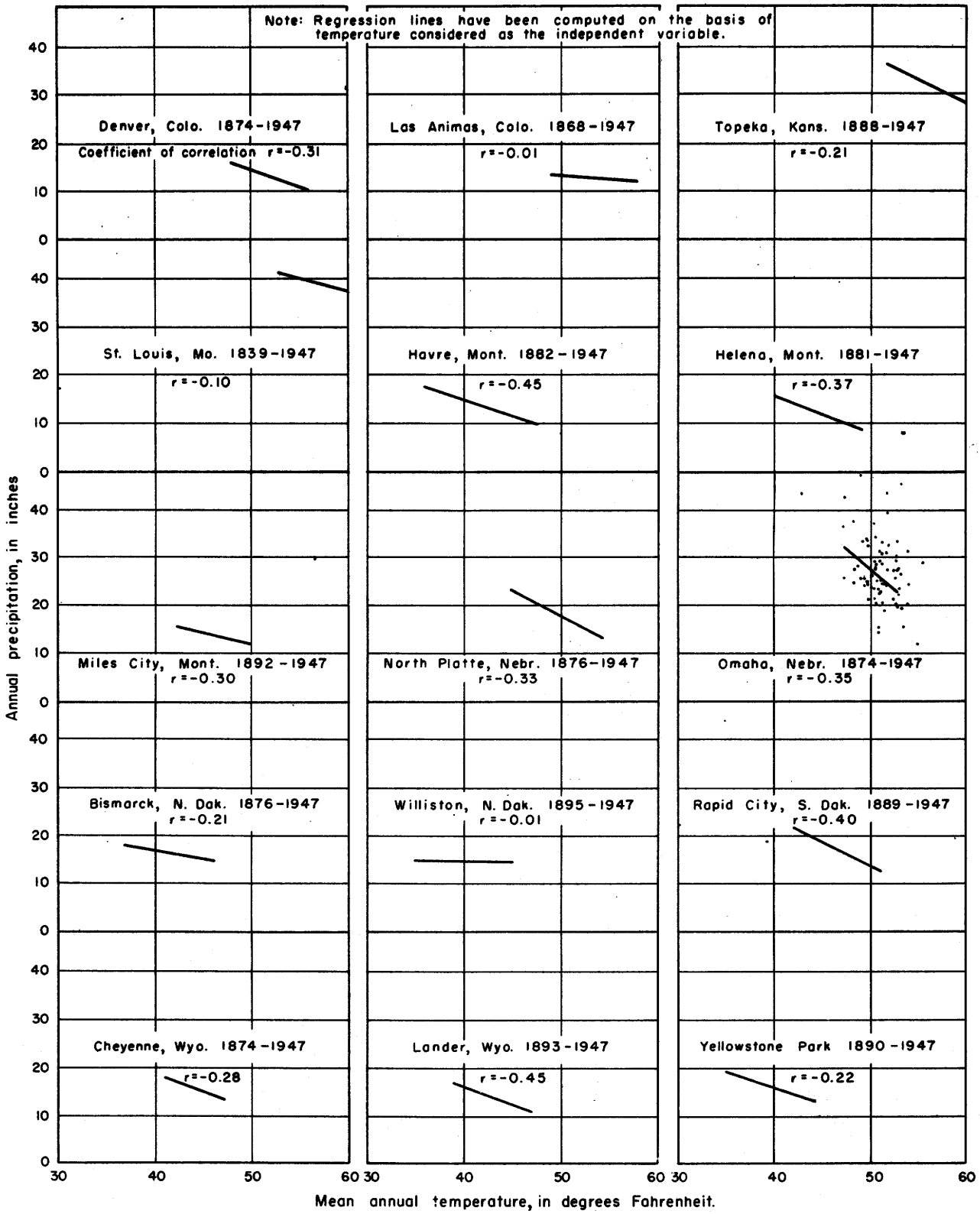

Figure 13.—Relationship of annual precipitation to mean annual temperature at selected weather stations.

collected at points on the valley floor or at points on the flat plains relatively distant from the mountains. It has been common practice to assume that the intrarelationship of the amounts of annual precipitation, occurring in the same basin at high altitudes and at the low altitudes of the weather stations, is such that although a true basin-average precipitation cannot be computed, the average computed from available low-altitude weather stations accurately represents a constant relationship to the true basin-average precipitation. Recently, several storage-type precipitation gages have been established at points along the Continental Divide; after these stations have been operated for a period of several years the assumed constancy of the relationship between high altitude and low altitude precipitation may be tested.

The method used in this report for the study of trends in the relationship of precipitation and runoff is based on a graphical comparison of two variables. This plot, called the double mass curve, is constructed by plotting corresponding cumulative totals of measured annual runoff against computed annual runoff. The resulting double mass curve closely approximates a straight line if there is no change in the relationship between the two variables. If there is a change in the relationship between the two variables, the double mass curve will show the time of occurrence and magnitude of the change by an abrupt change of slope.

Because annual runoff is a function of annual precipitation minus annual losses, it is necessary to use a synthetic quantity computed on the basis of the precipitation and roughly equivalent to measured runoff in the construction of the double mass curve. Briefly summarized, the procedure used for all tributary basins in this report was: preparation of a curve showing the average relationship between precipitation and runoff; listing of synthetic runoff values taken from that curve; and study of consistency of of computed runoff and measured runoff via double mass curve.

The details of procedure are best shown by the study made on the Osage River Basin above the Geological Survey gage at Bagnell, Mo. Definitions of the algebraic terms used are:

- P - precipitation
- P_e - effective basin-average annual precipitation, computed from formula, $P_e = aP_o + bP_1$
- P_o - current year, basin-average precipitation
- P_1 - first antecedent year, basin-average precipitation
- a, b - constants such that sum of "a" plus "b" equals unity
- R - current-year measured runoff
- R_c - current-year computed runoff

The values of "a" and "b" are determined by successive trial correlations so that the resulting values of P_e correlate best with the corresponding values of R. For the Osage Basin P_e was found equal to $0.8\,P_o + 0.2\,P_1$. The individual year values of P_e and R were used to define a curve of relationship as shown on figure 14. The values of synthetic runoff, R_c, were picked from this curve, entering with the known values of P_e. Cumulative values of R and R_c were then plotted to show a double mass curve (see fig. 15). This plot shows no trend in the precipitation-runoff relationship in the Osage Basin. Shown at the top of figure 14 is a residual mass curve for the Osage Basin. The residual mass curve is constructed by plotting the cumulative $R-R_c$ values against time. The residual mass curve is related to the double mass curve as follows: the changes in relationship between R and R_c (and hence between P and R) are magnified and the maximum or minimum point is equivalent to the break in slope of the double mass curve.

The procedure, as described above, was used on all the tributary basins studied for trends in the precipitation-runoff relationship. Figures 16 to 97 show the precipitation-runoff relationship curves and the double mass curves for the studies. See figure 17, the double mass curve for Beaverhead River at Barratts, Mont., for an example of a basin in which a trend in the precipitation-runoff relationship was found. For that basin an almost uninterrupted decline in runoff relative to precipitation is indicated for the period since 1924.

Table 2 contains a list of the basins studied showing the period of record, standard error of estimated R_c, and indicated trends in the precipitation-runoff relationship. With the exception of the Niobrara Basin, all tributary basins that showed a trend in the precipitation-runoff relationship drain from mountainous or semimountainous country.

POSSIBLE EXPLANATION OF TRENDS

The following hydrologic factors have important effect on the precipitation-runoff relationship and may be responsible for the indicated trends:

- Climatic—temperature, seasonal distribution of precipitation, variations in orographic effect, and long-term variations in ground-water storage; and
- Cultural—forest denudation, farming and consumptive use.

In a preceding section upward temperature trends, with sharp increases during the decade 1930-40, were shown to be general for the basin. As most of the declining yield trends in the precipitation-runoff relationship started at approximately the same time as the rapid increase in temperature, it would be logical to ascribe part of the trend to temperature effect. However, if temperature increases were alone responsible, generally declining yields of runoff from equal precipitation should be the rule for the entire Missouri Basin, a condition that does not exist.

Seasonal variation of precipitation, discussed in a previous section, was shown to have remained relatively constant from 1880 to 1940 so the effect of this factor must be ruled out as a possible cause of the precipitation-runoff trends except in the mountain

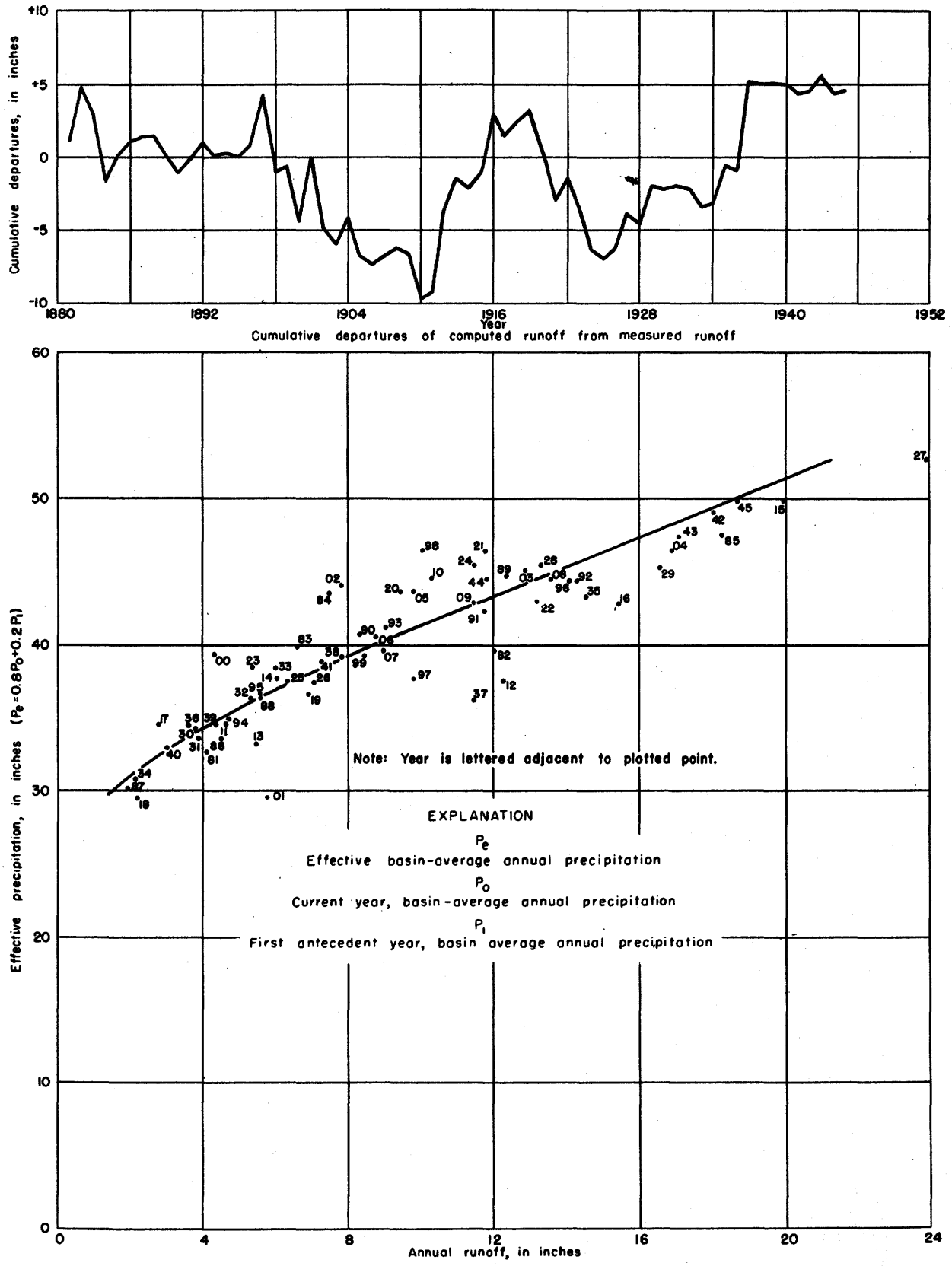

Figure 14. —Relationship of effective annual precipitation to annual runoff of Osage River near Bagnell, Mo.

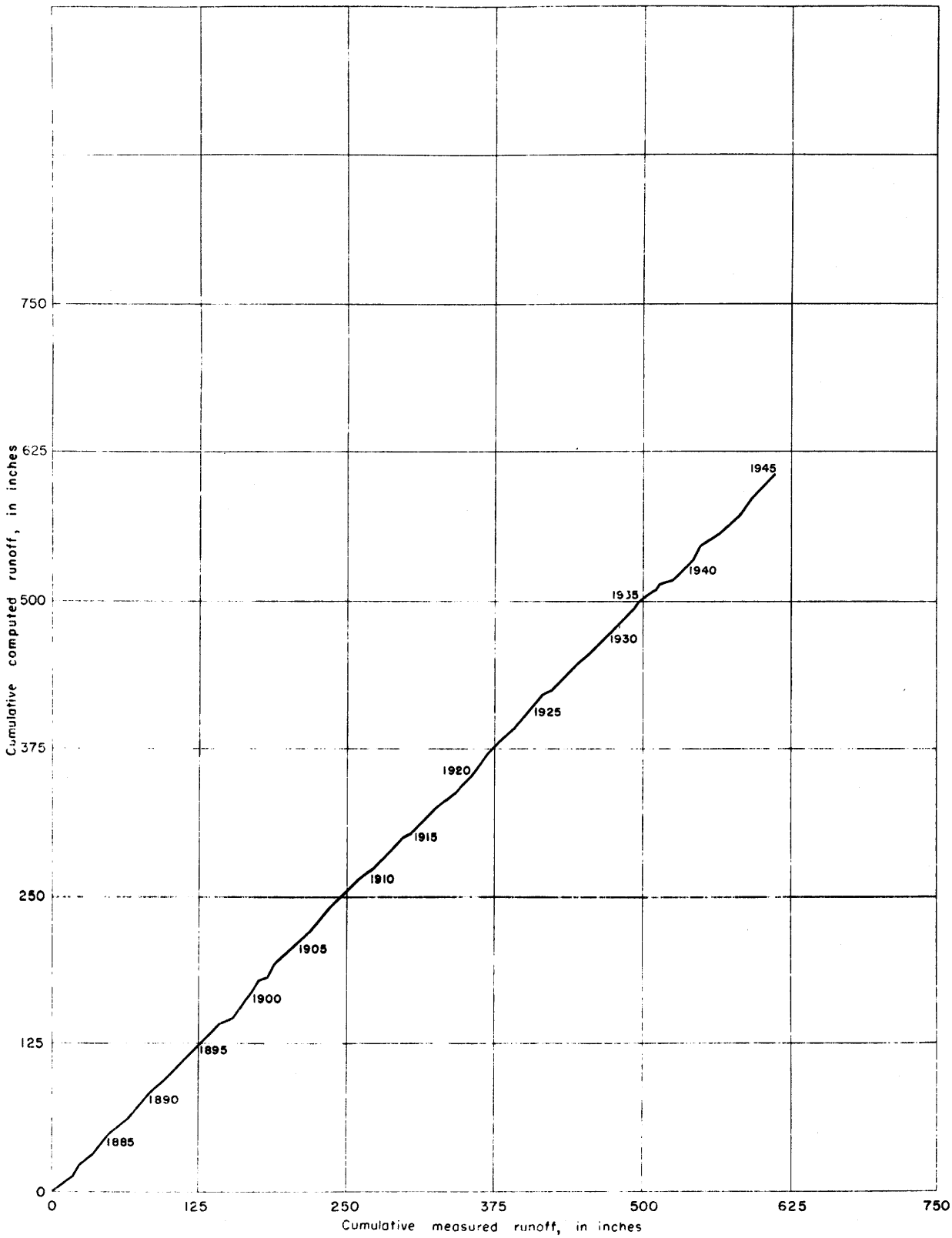

Figure 15. —Double mass curve of measured runoff plotted against computed runoff for Osage River near Bagnell, Mo.

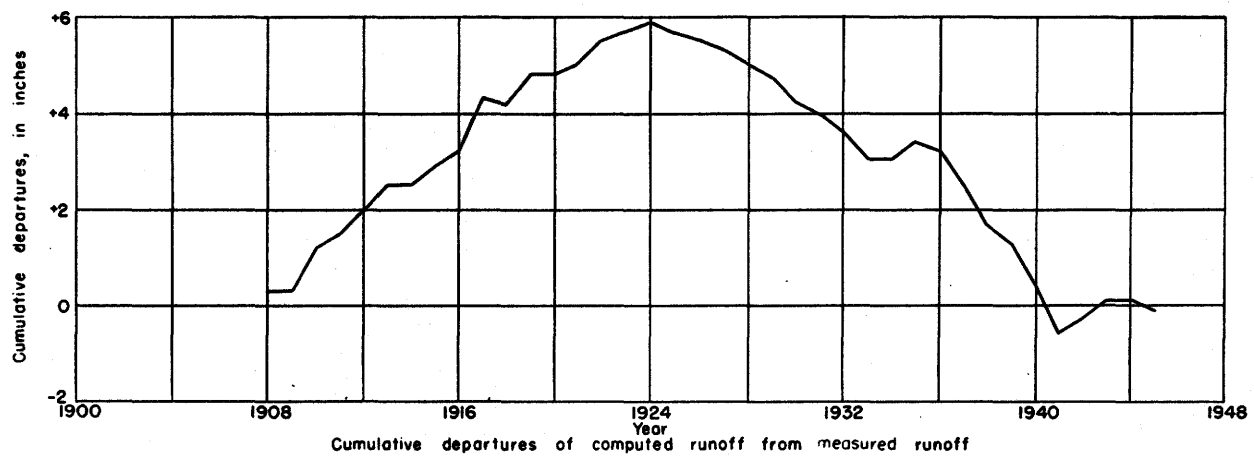

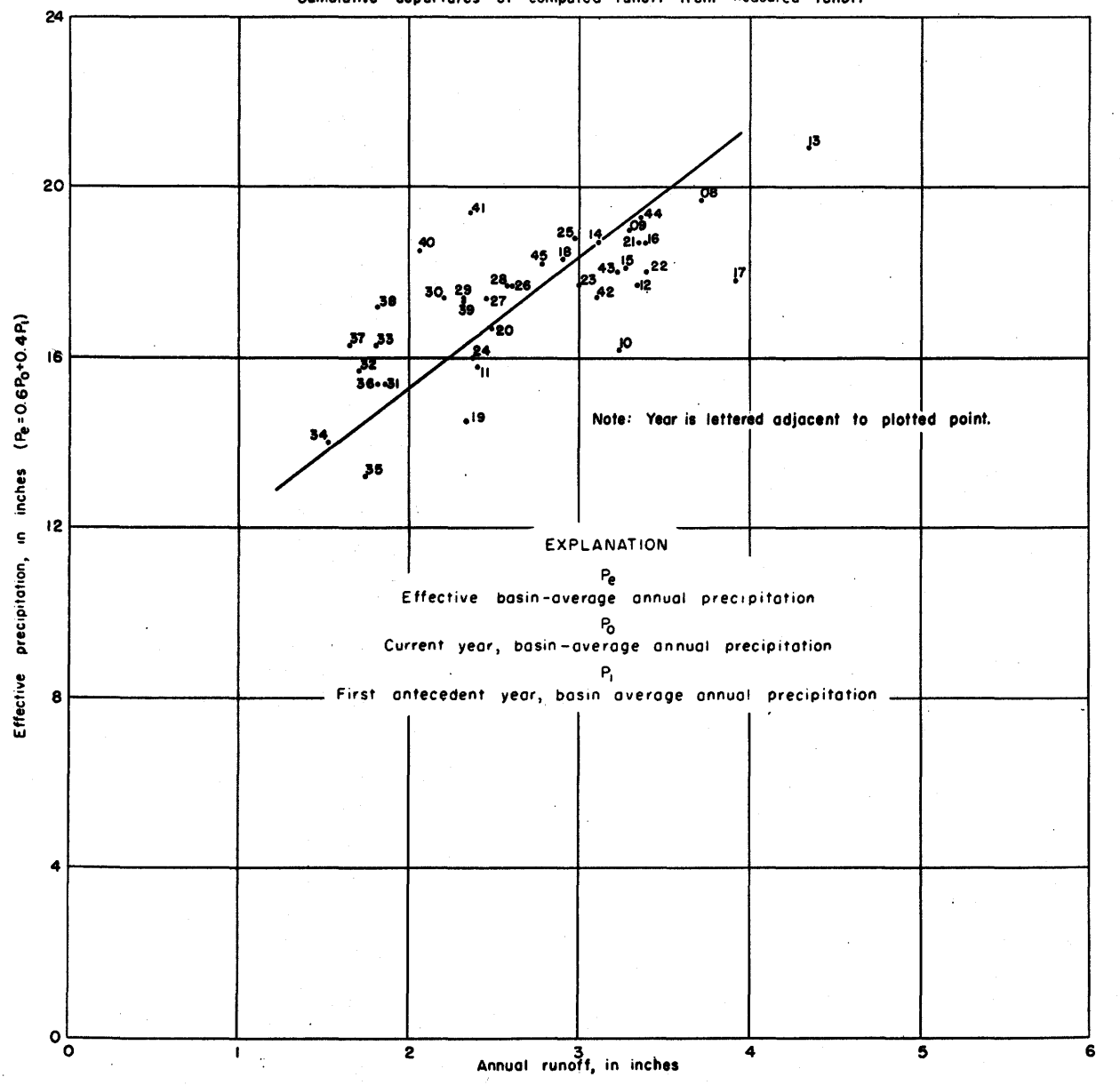

Figure 16. —Relationship of effective annual precipitation to annual runoff of Beaverhead River at Barratts, Mont.

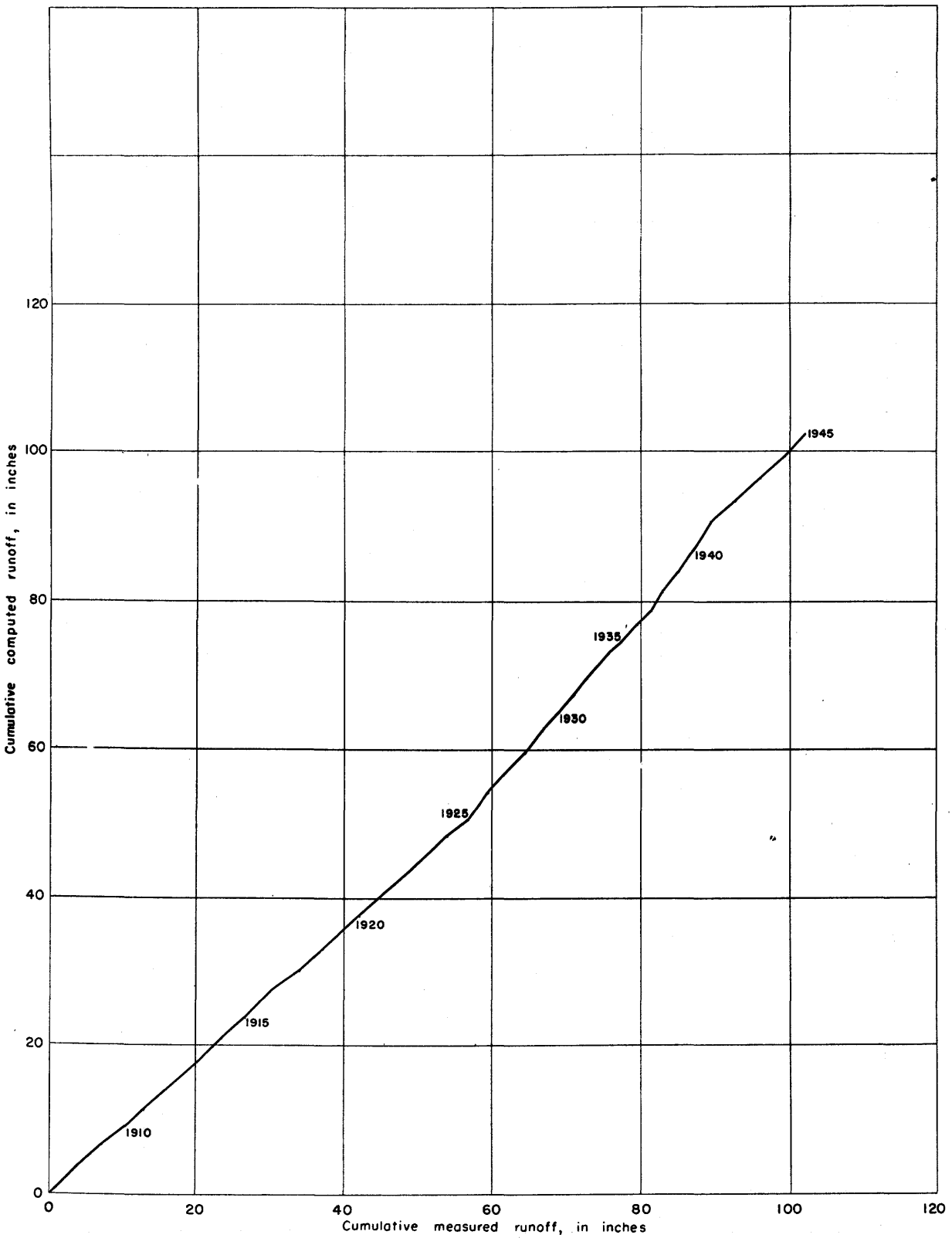

Figure 17. —Double mass curve of measured runoff plotted against computed runoff for Beaverhead River at Barratts, Mont.

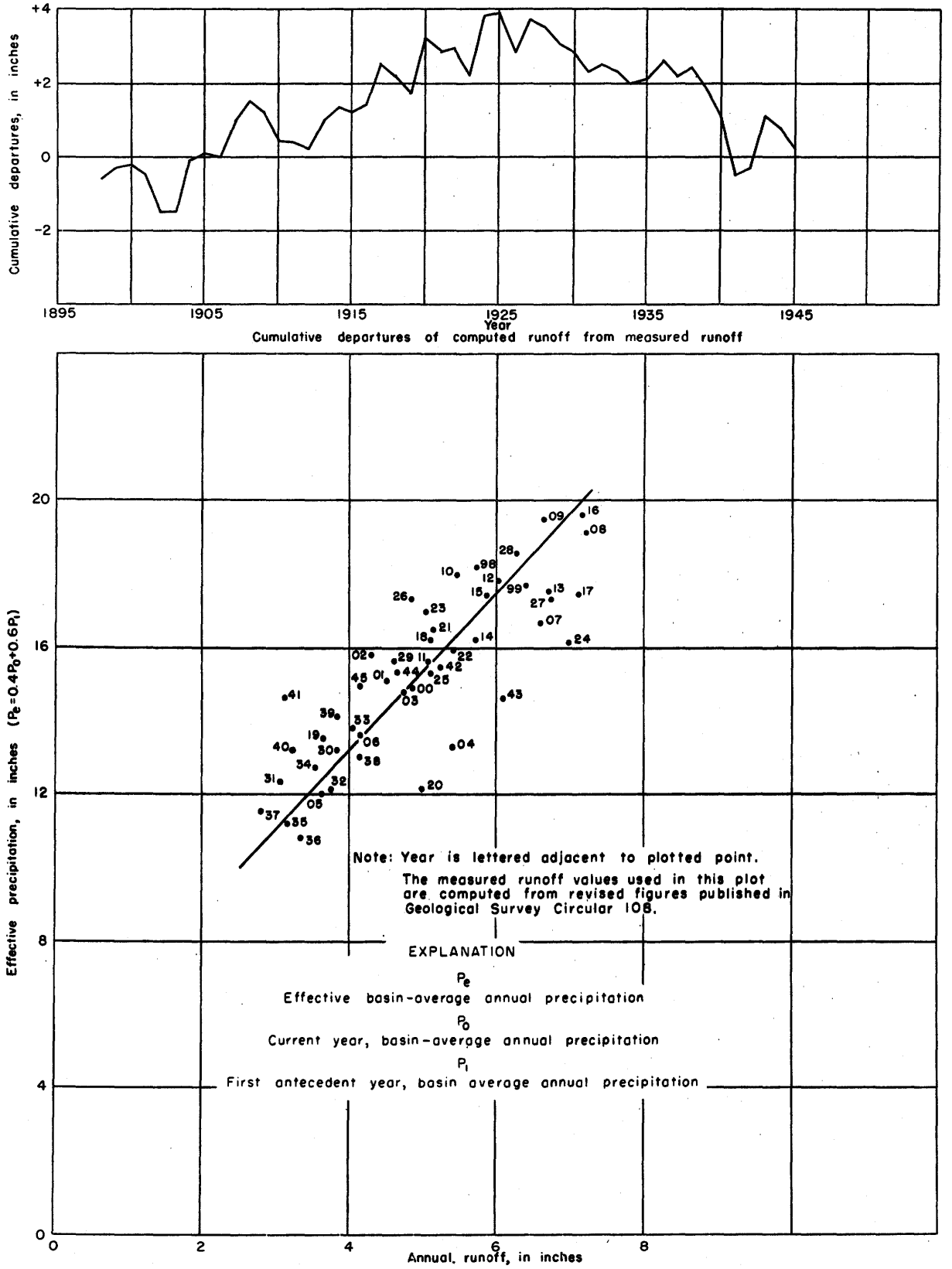

Figure 18. —Relationship of effective annual precipitation to annual runoff of Missouri River at Fort Benton, Mont.

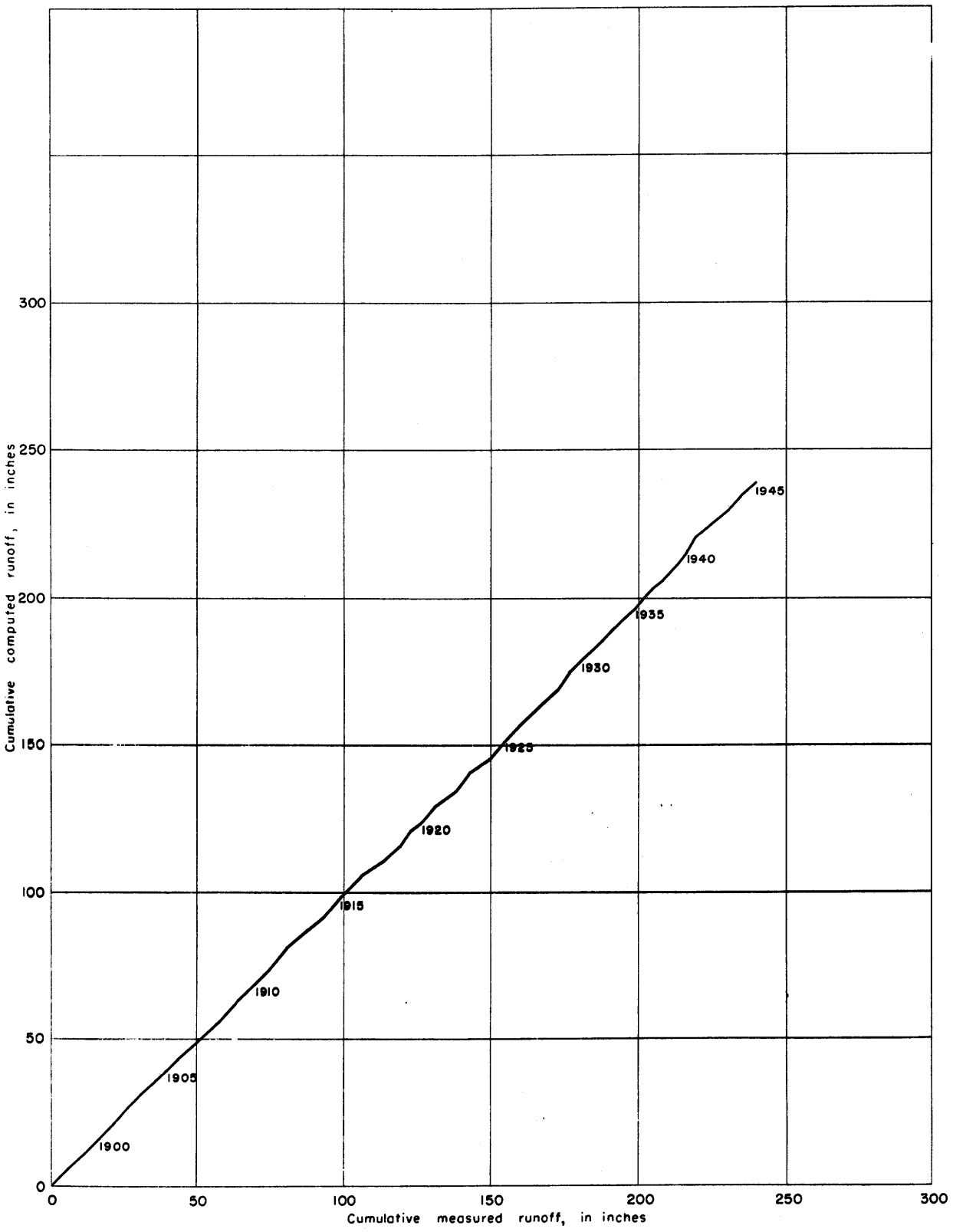

Figure 19.—Double mass curve of measured runoff plotted against computed runoff for Missouri River at Fort Benton, Mont.

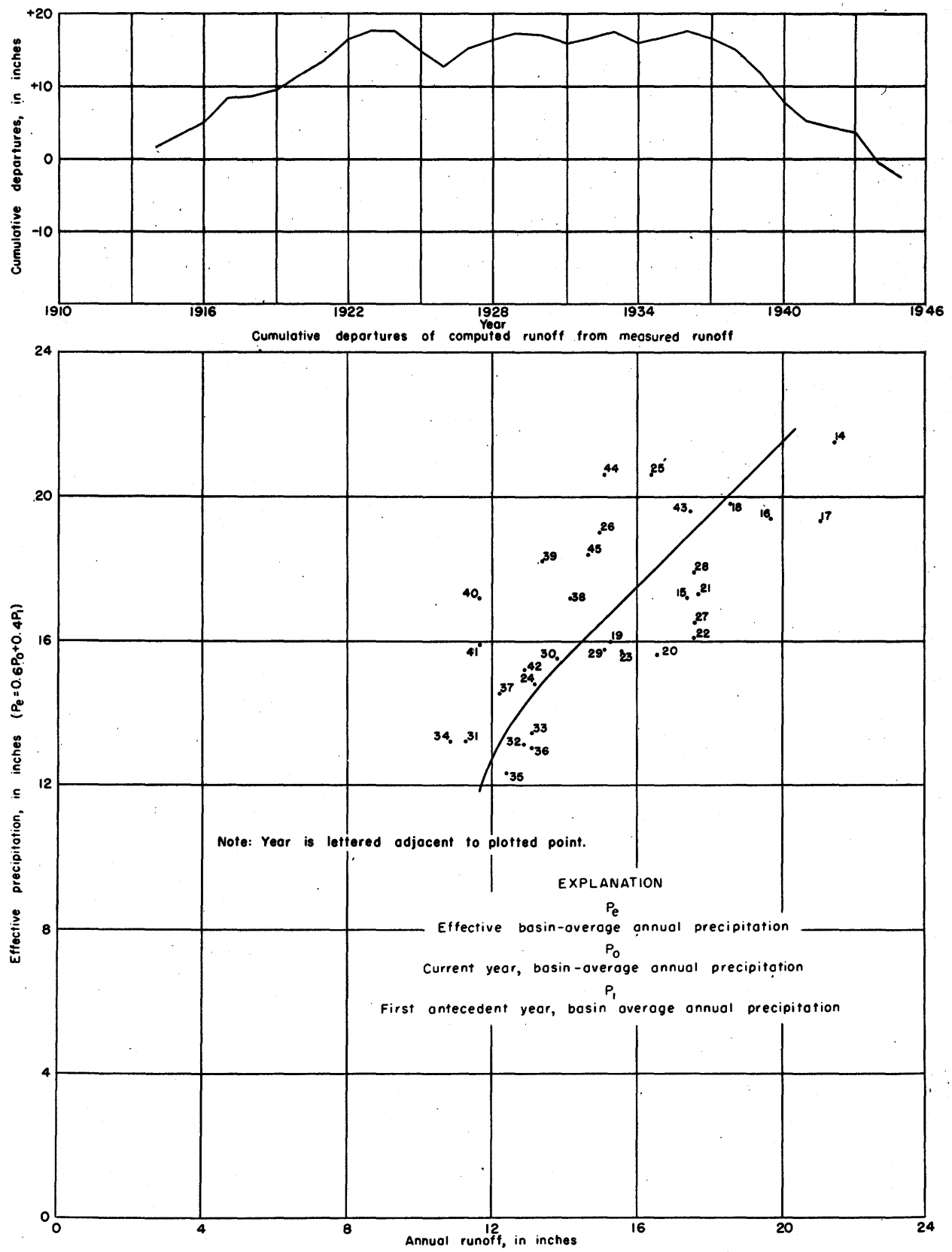

Figure 20.—Relationship of effective annual precipitation to annual runoff of Madison River near West Yellowstone, Mont.

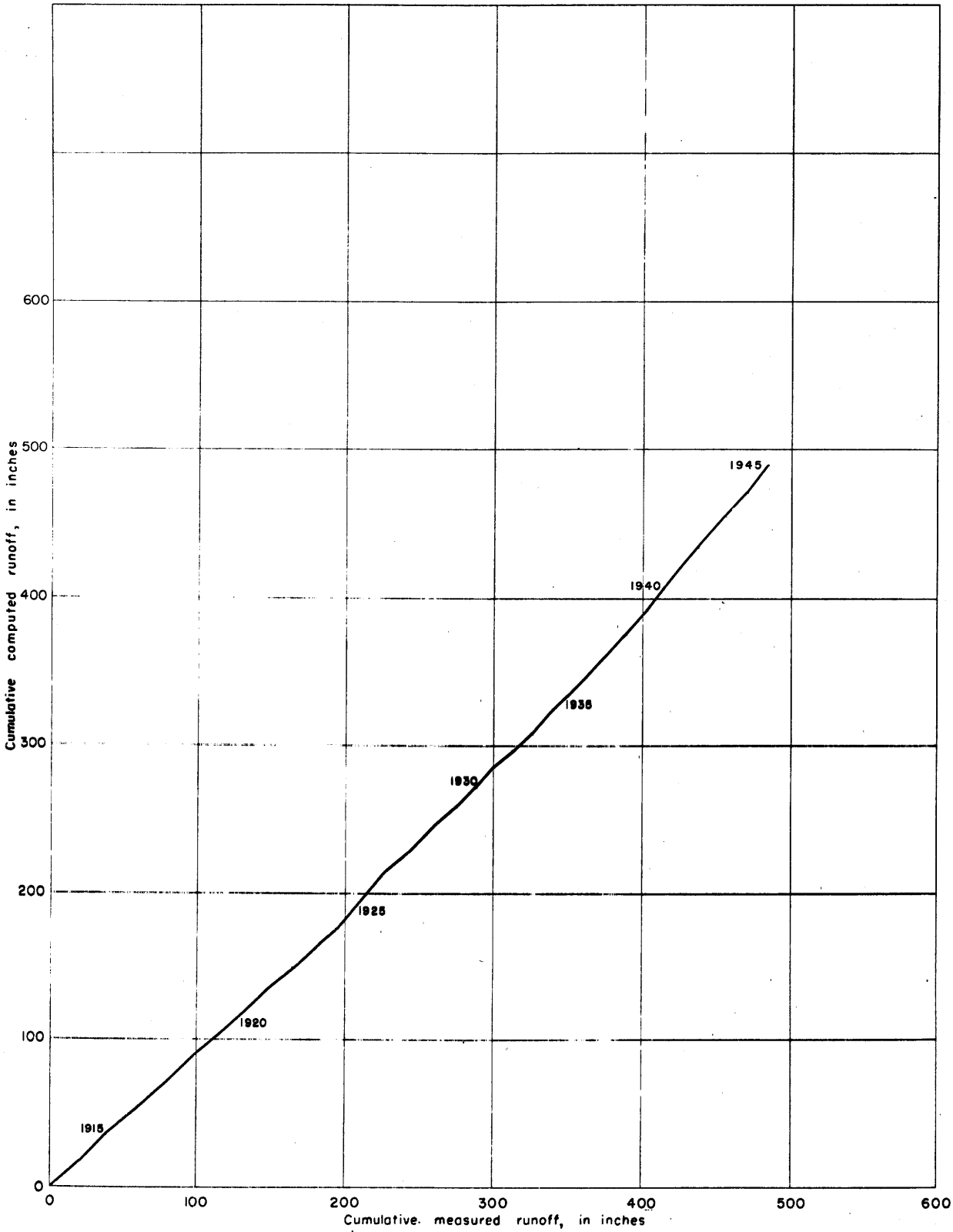

Figure 21.—Double mass curve of measured runoff plotted against computed runoff for Madison River near West Yellowstone, Mont.

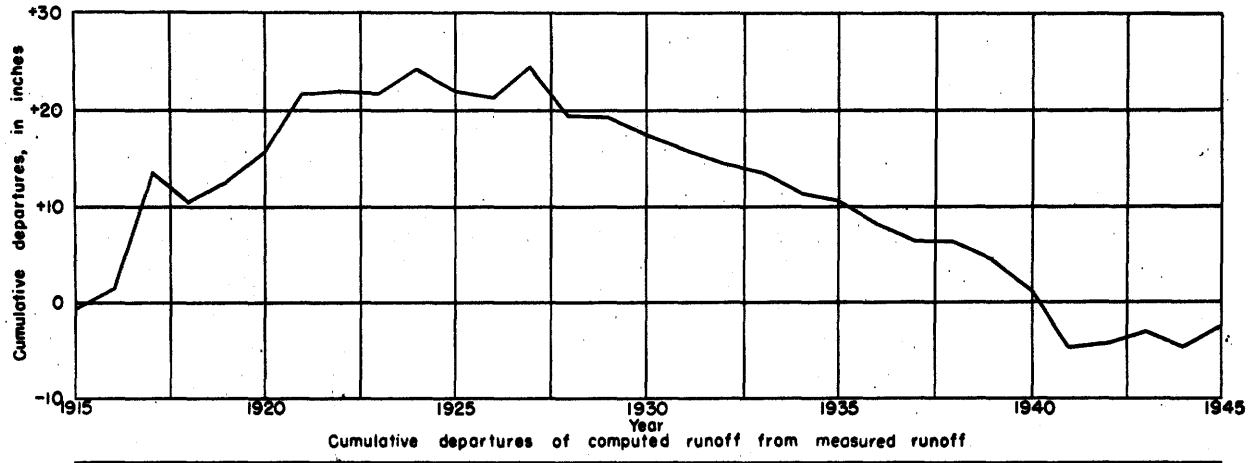

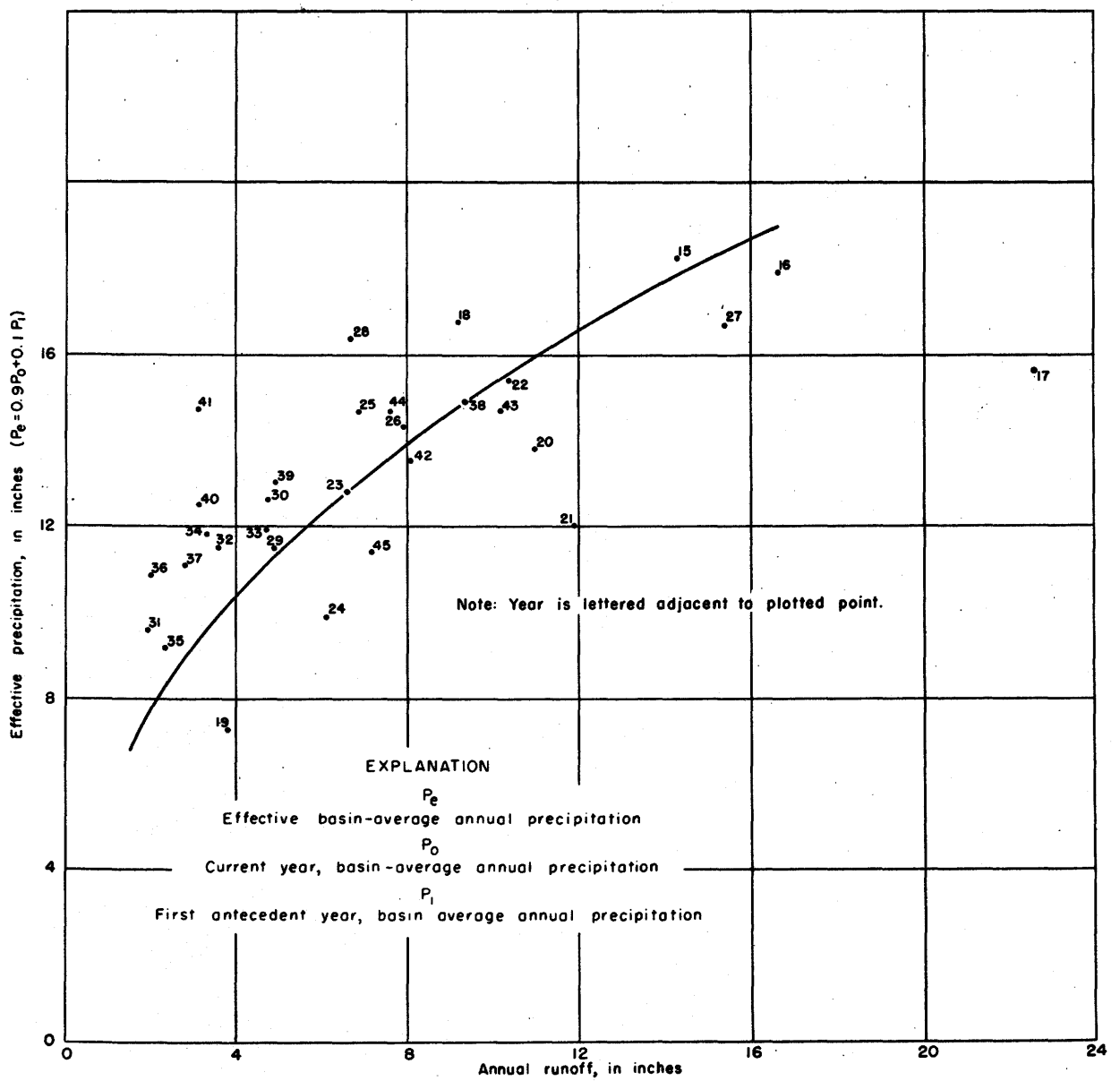

Figure 22.—Relationship of effective annual precipitation to annual runoff of Tenmile Creek near Rimini, Mont.

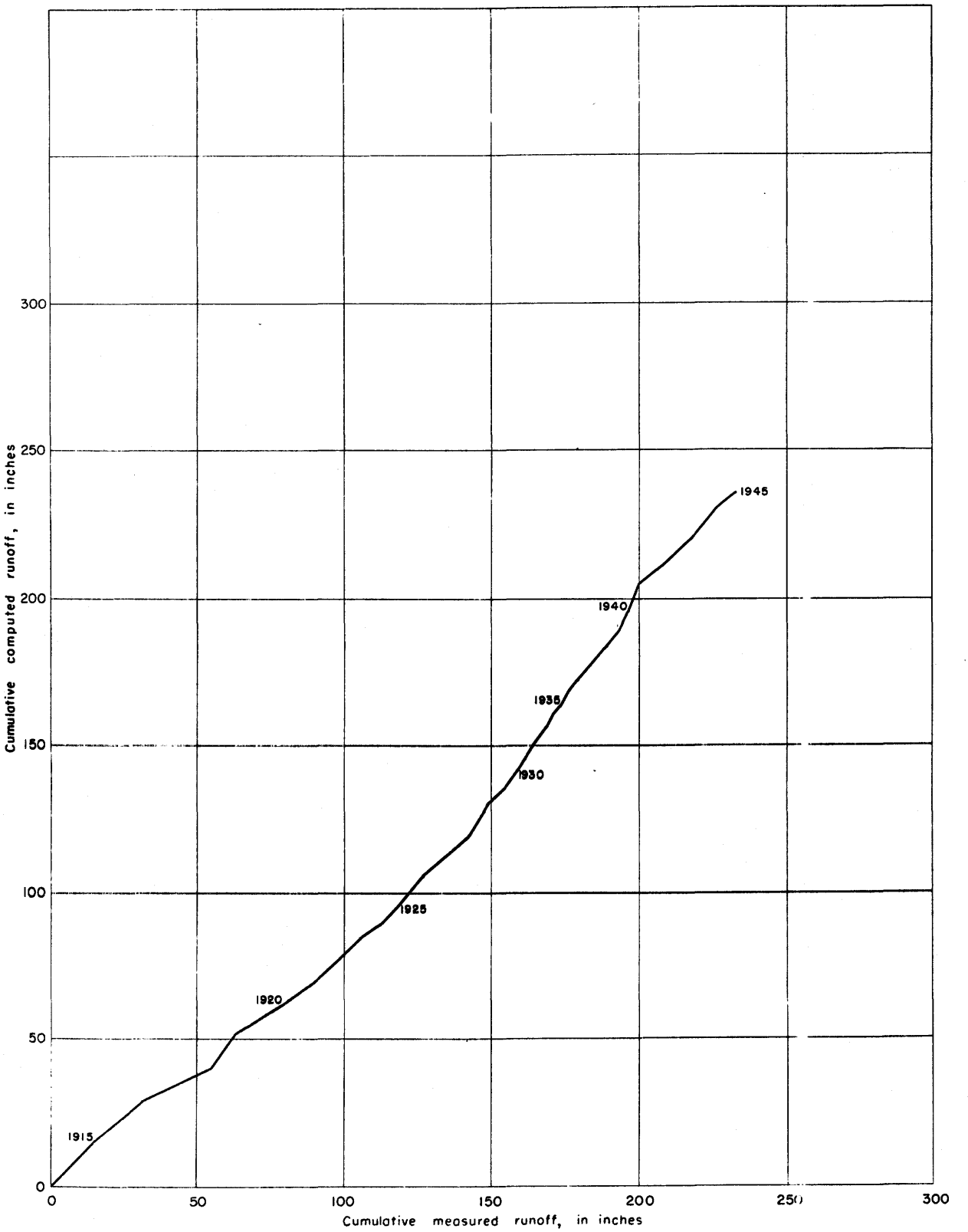

Figure 23.—Double mass curve of measured runoff plotted against computed runoff for Tenmile Creek near Rimini, Mont.

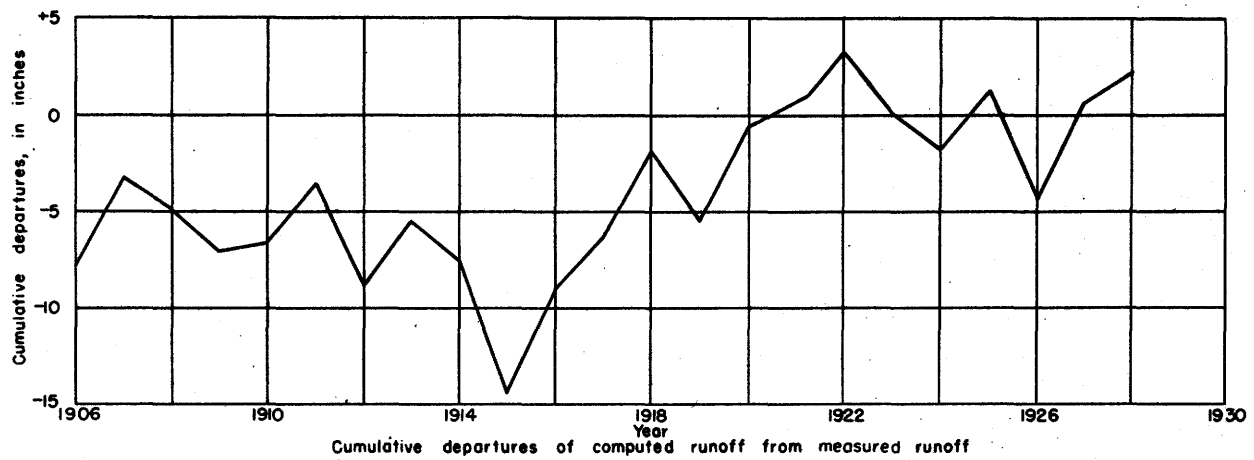

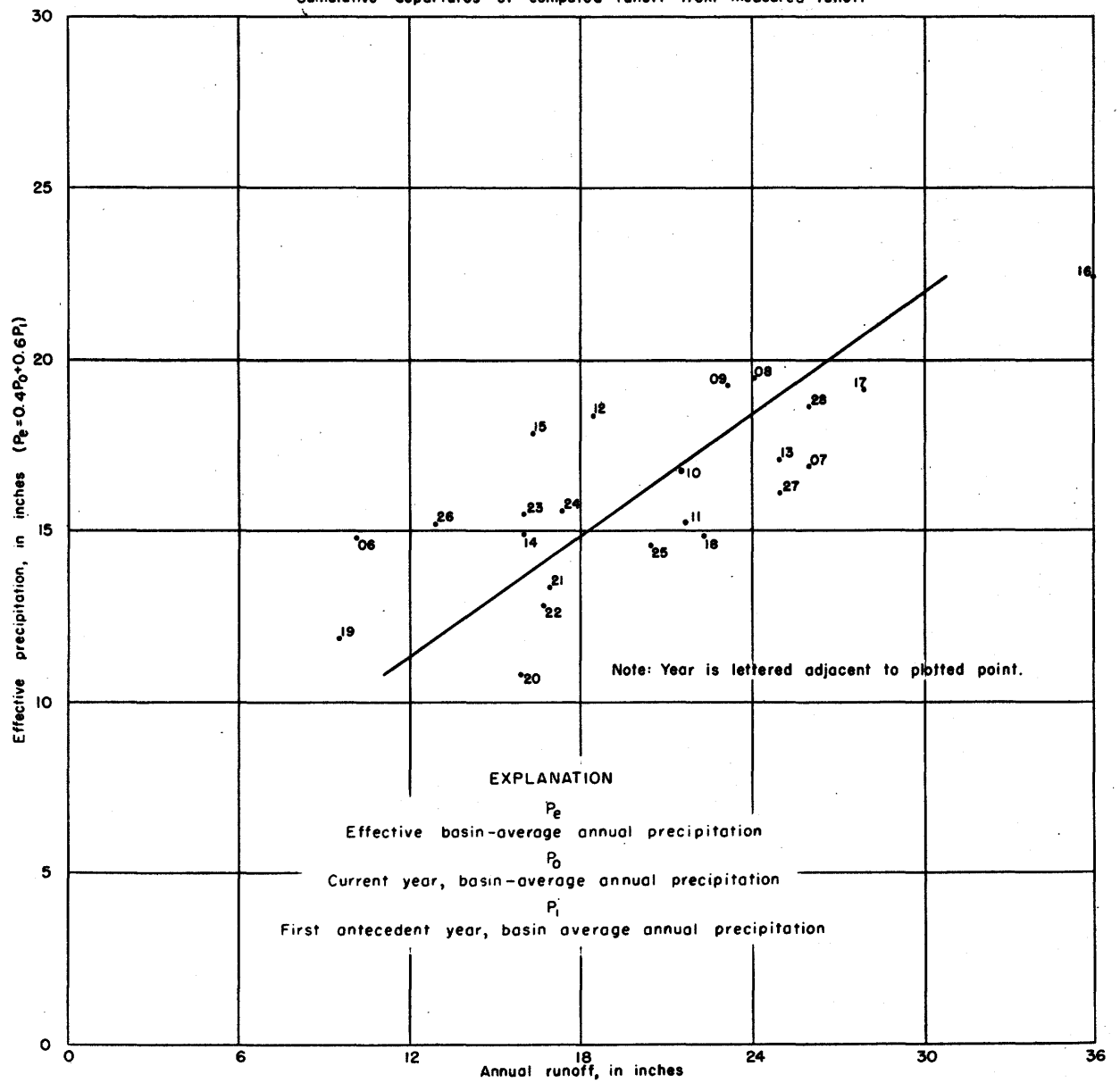

Figure 24.—Relationship of effective annual precipitation to annual runoff of North Fork Sun River near Augusta, Mont.

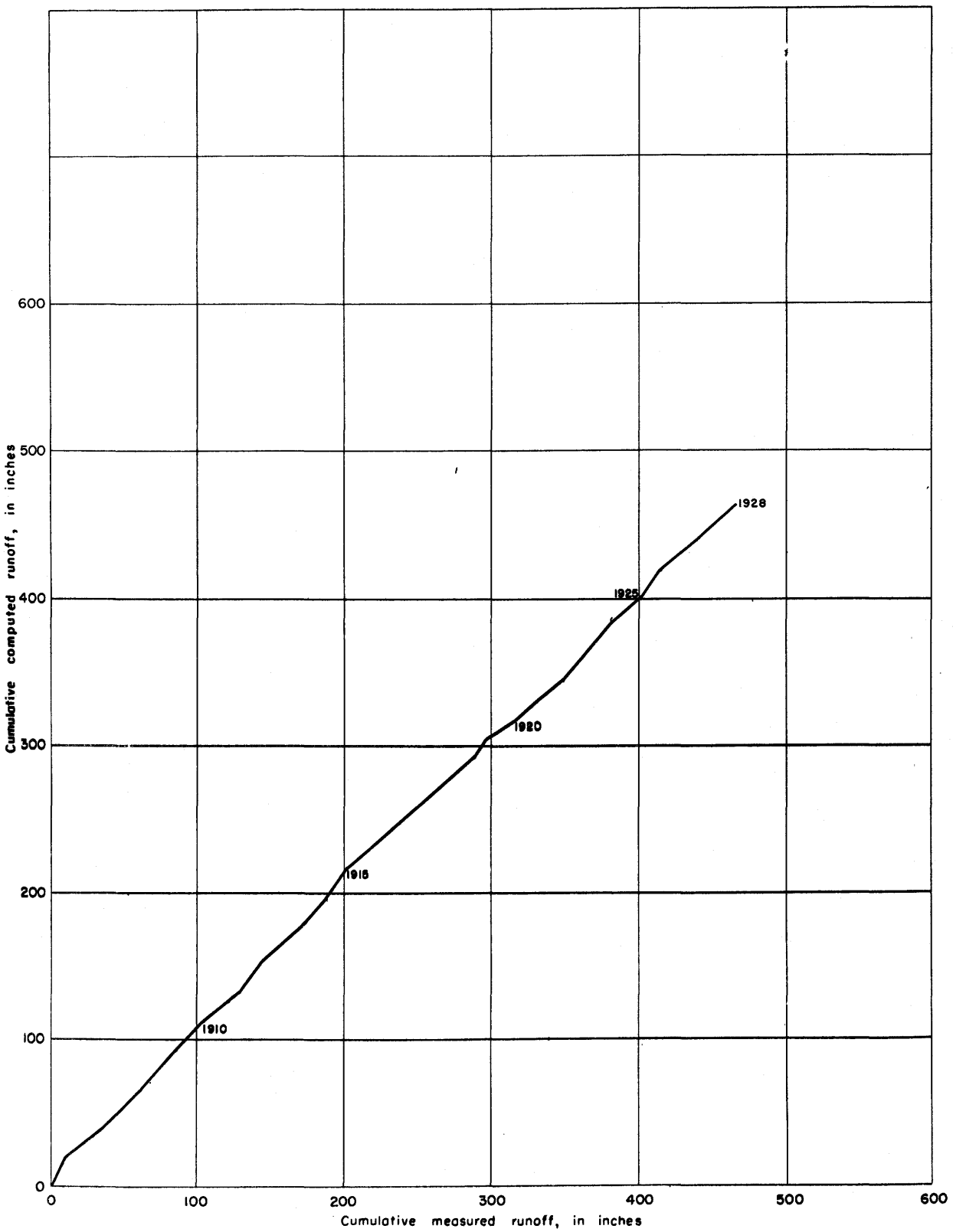

Figure 25.—Double mass curve of measured runoff plotted against computed runoff for North Fork Sun River near Augusta, Mont.

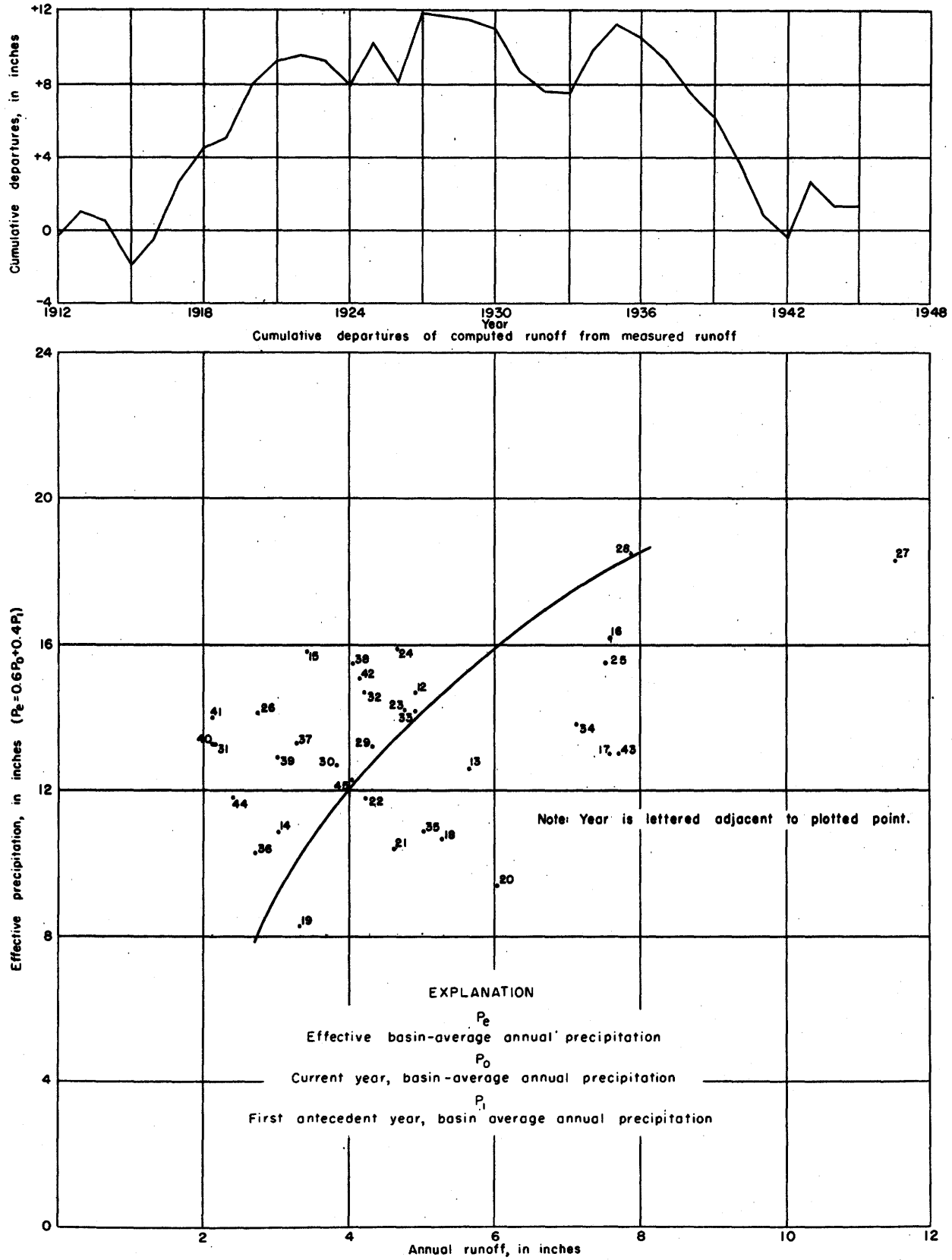

Figure 26.—Relationship of effective annual precipitation to annual runoff of Marias River near Shelby, Mont.

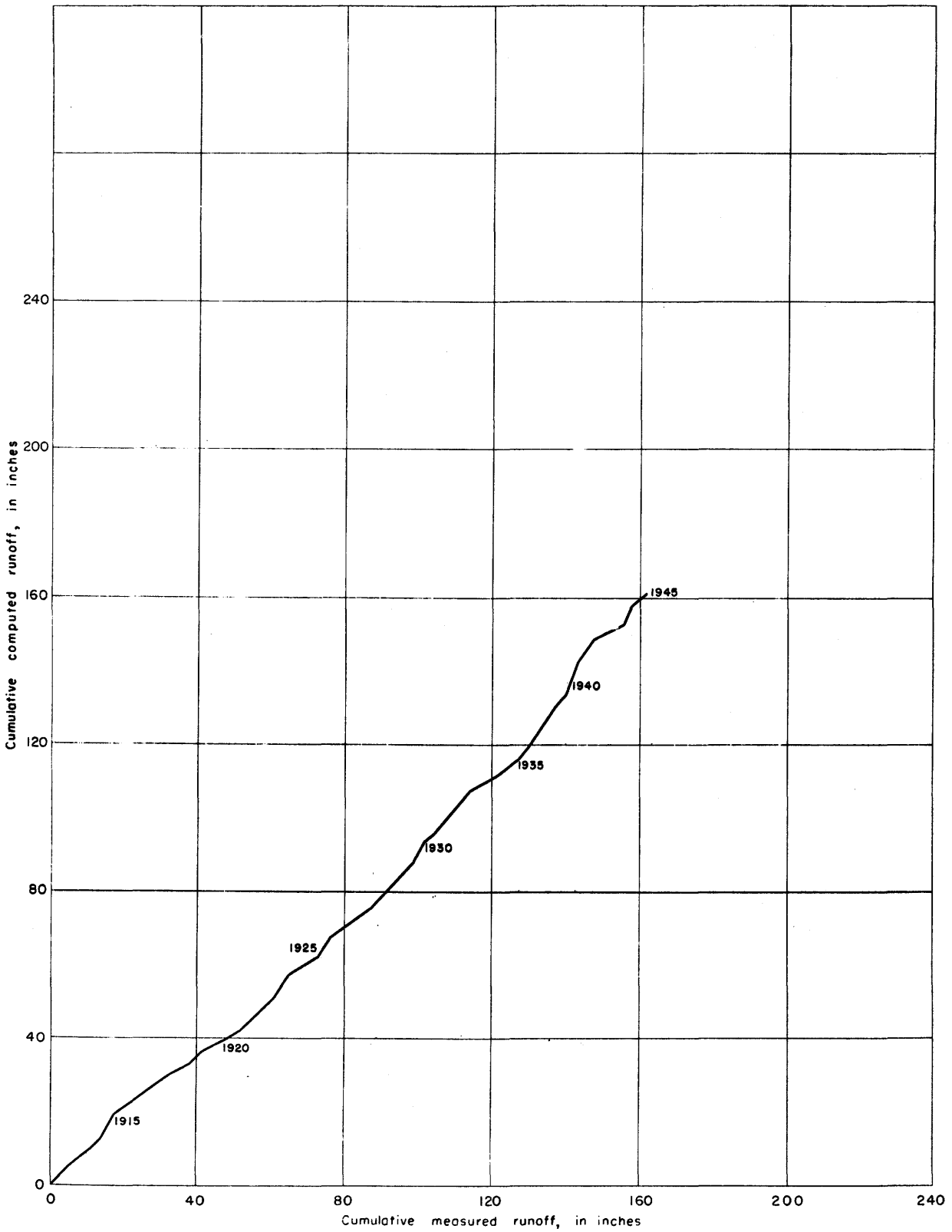

Figure 27.—Double mass curve of measured runoff plotted against computed runoff for Marias River near Shelby, Mont.

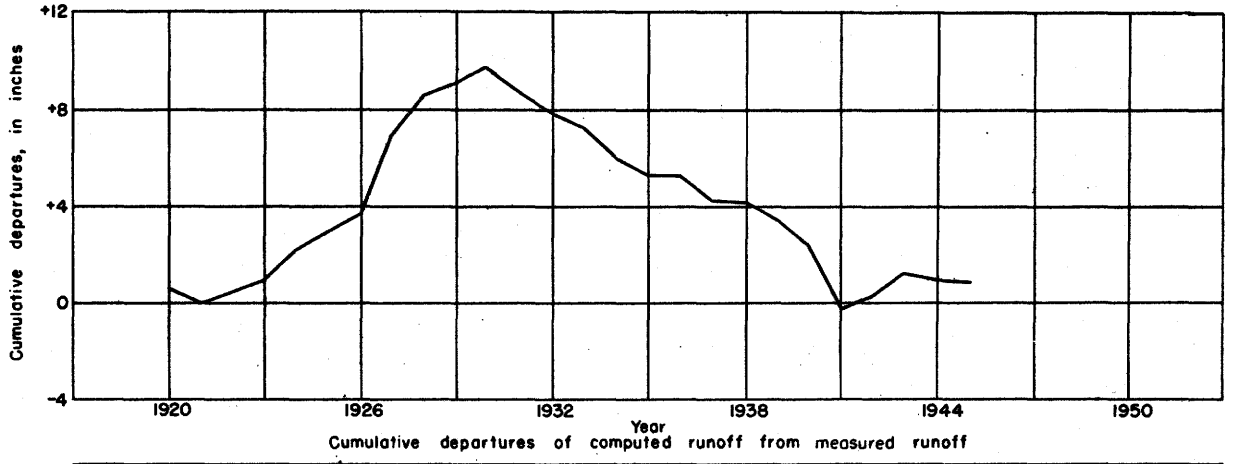

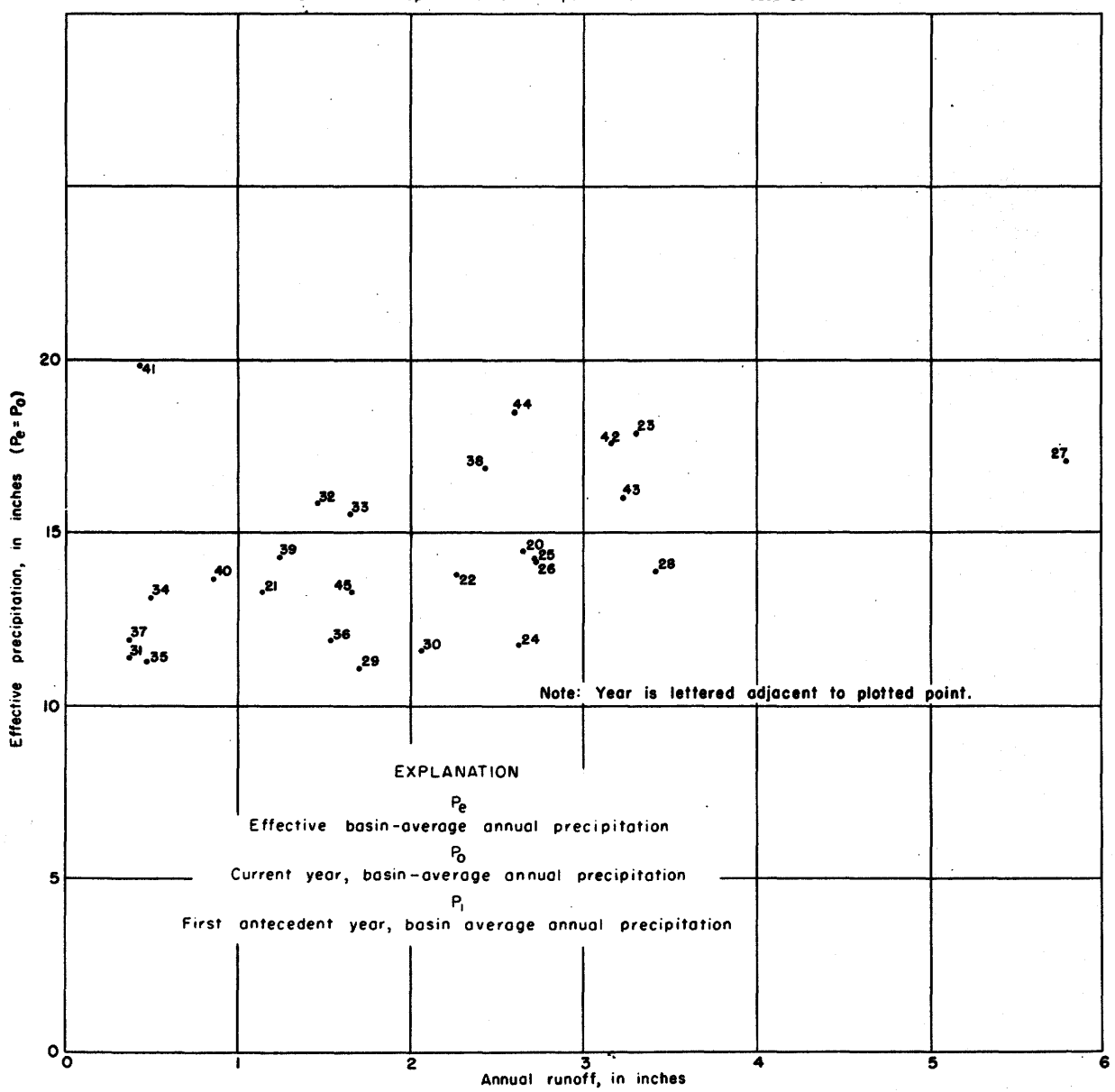

Figure 28.—Relationship of effective annual precipitation to annual runoff of Judith River near Utica, Mont.

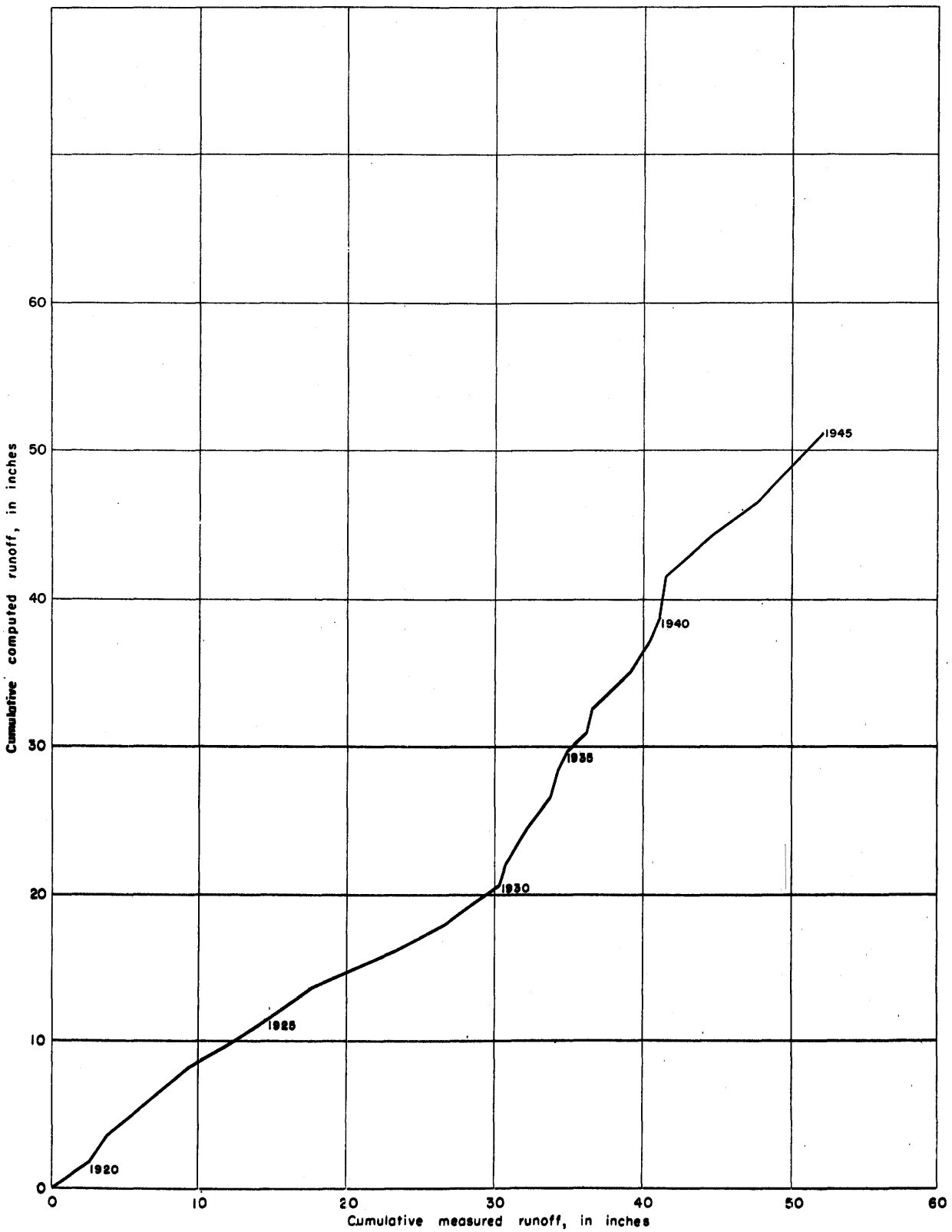

Figure 29.—Double mass curve of measured runoff plotted against computed runoff for Judith River near Utica, Mont.

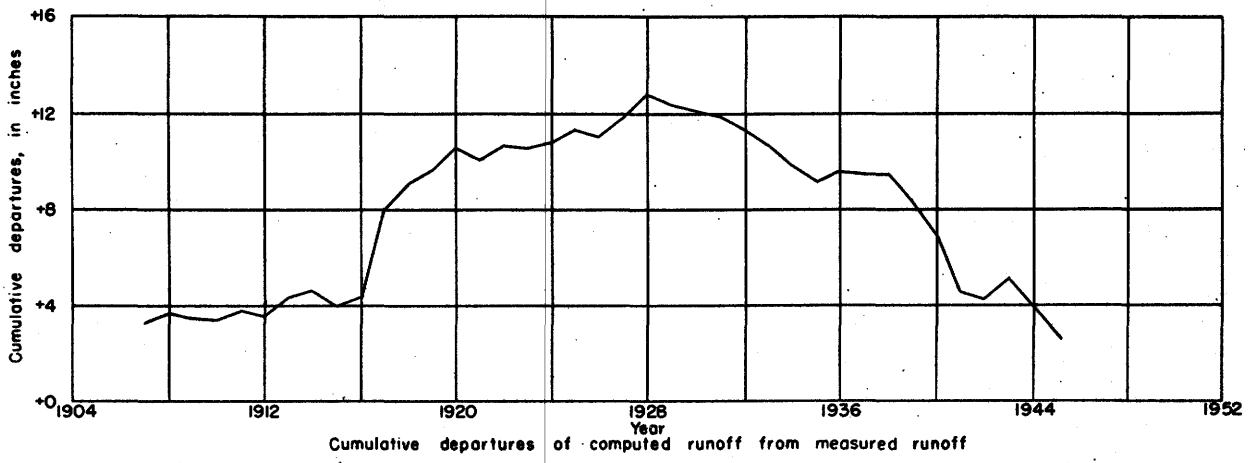

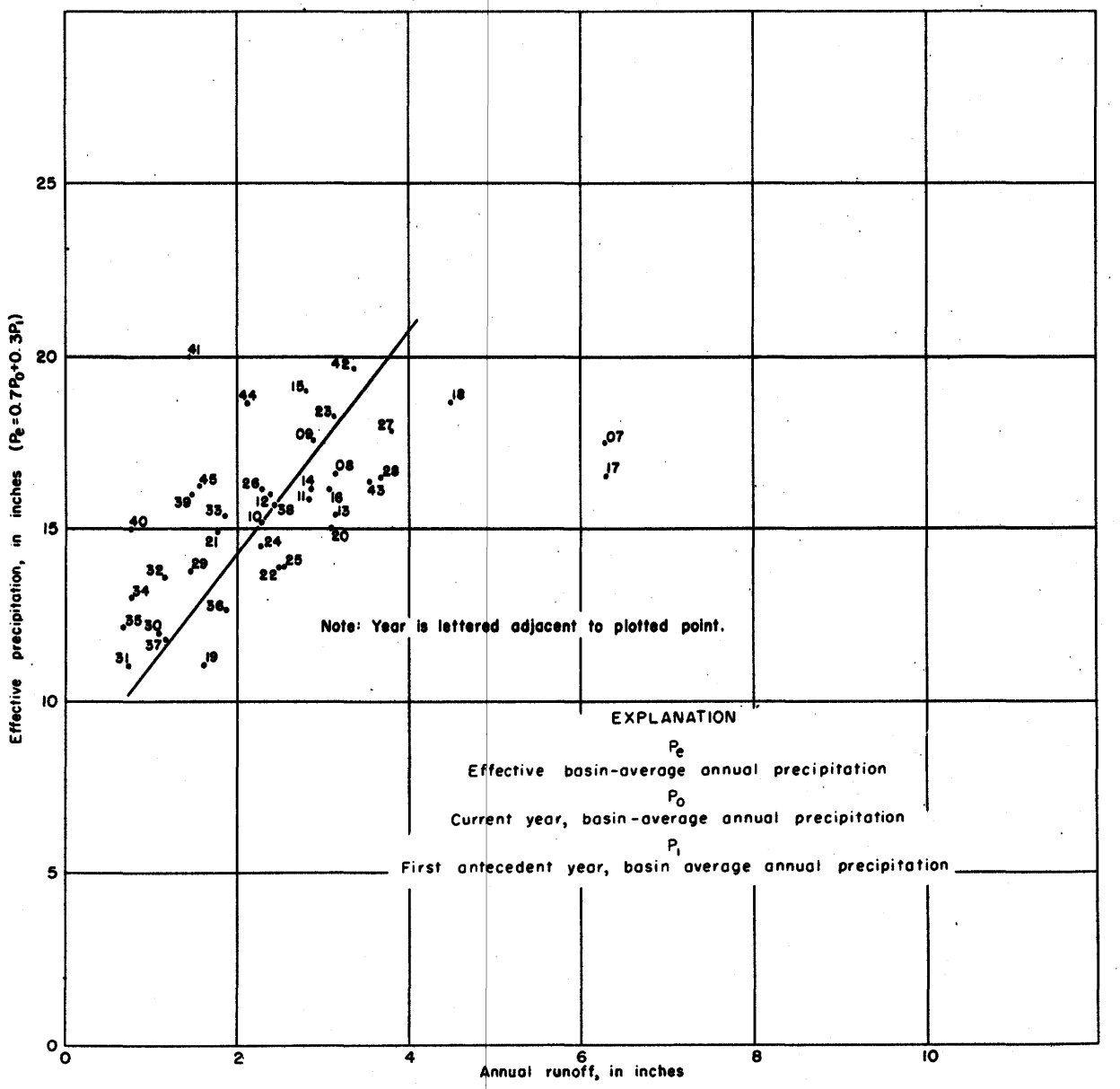

Figure 30.—Relationship of effective annual precipitation to annual runoff of Musselshell River at Harlowton, Mont.

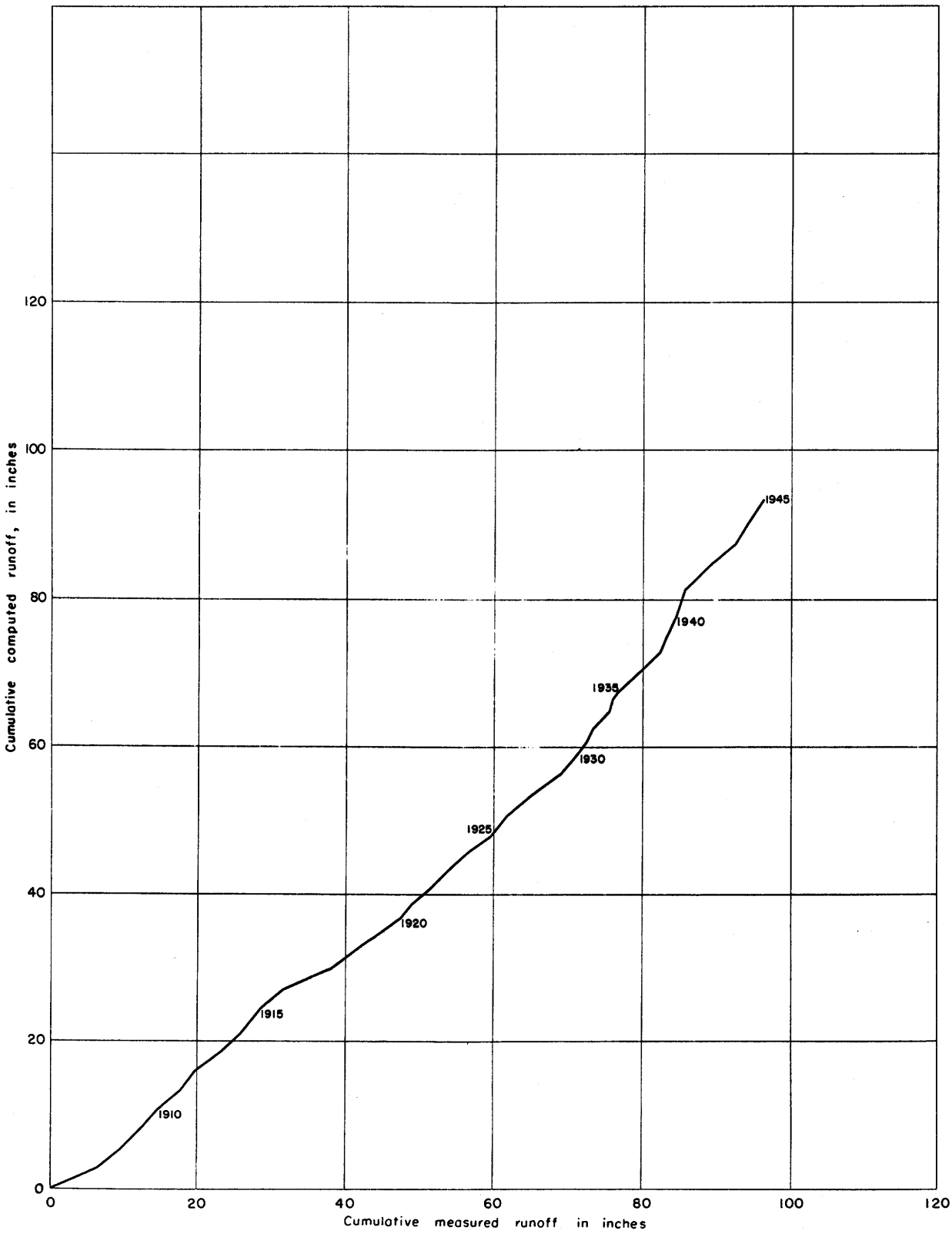

Figure 31.—Double mass curve of measured runoff plotted against computed runoff for Musselshell River at Harlowton, Mont.

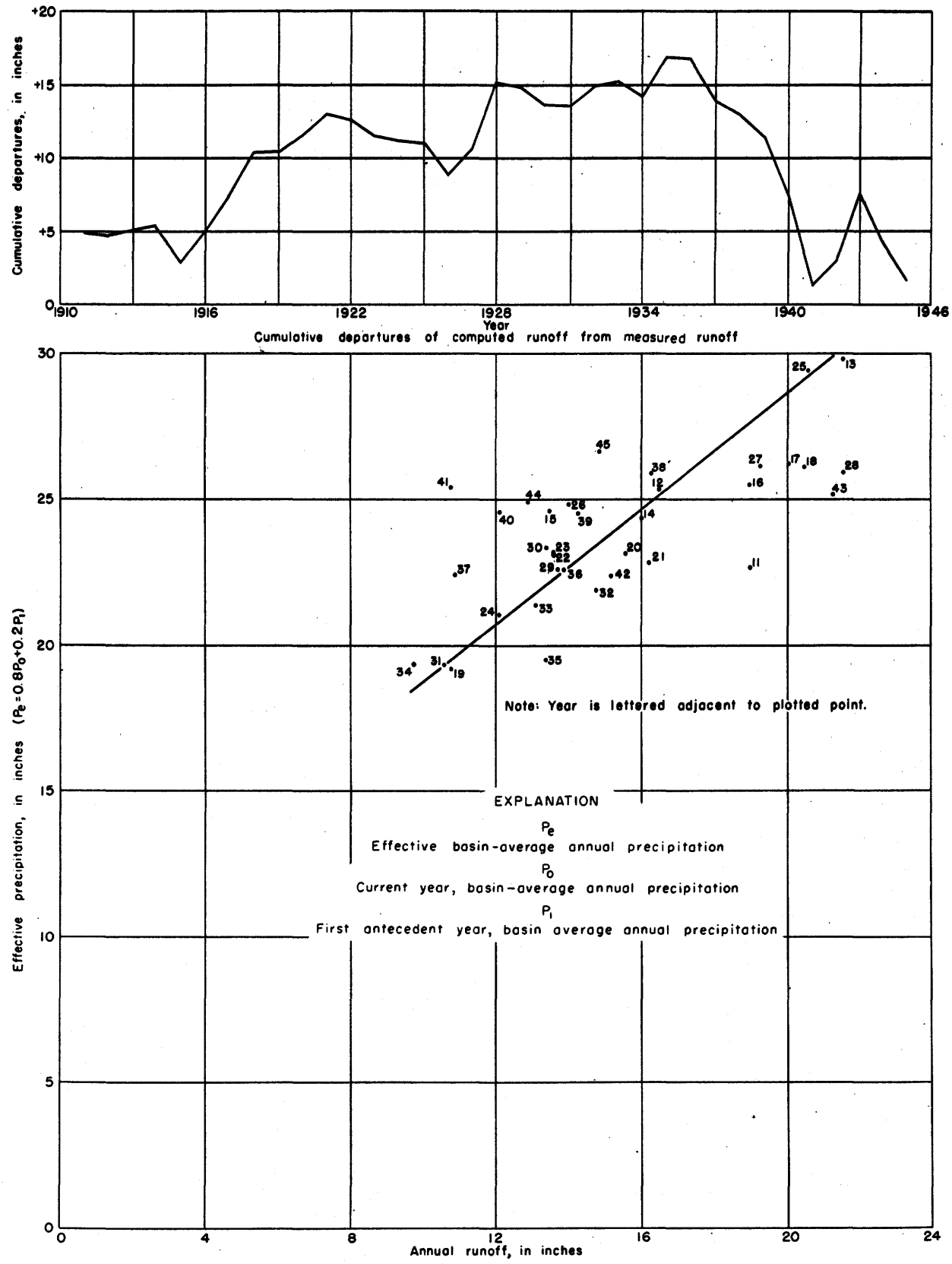

Figure 32.—Relationship of effective annual precipitation to annual runoff of Yellowstone River at Corwin Springs, Mont.

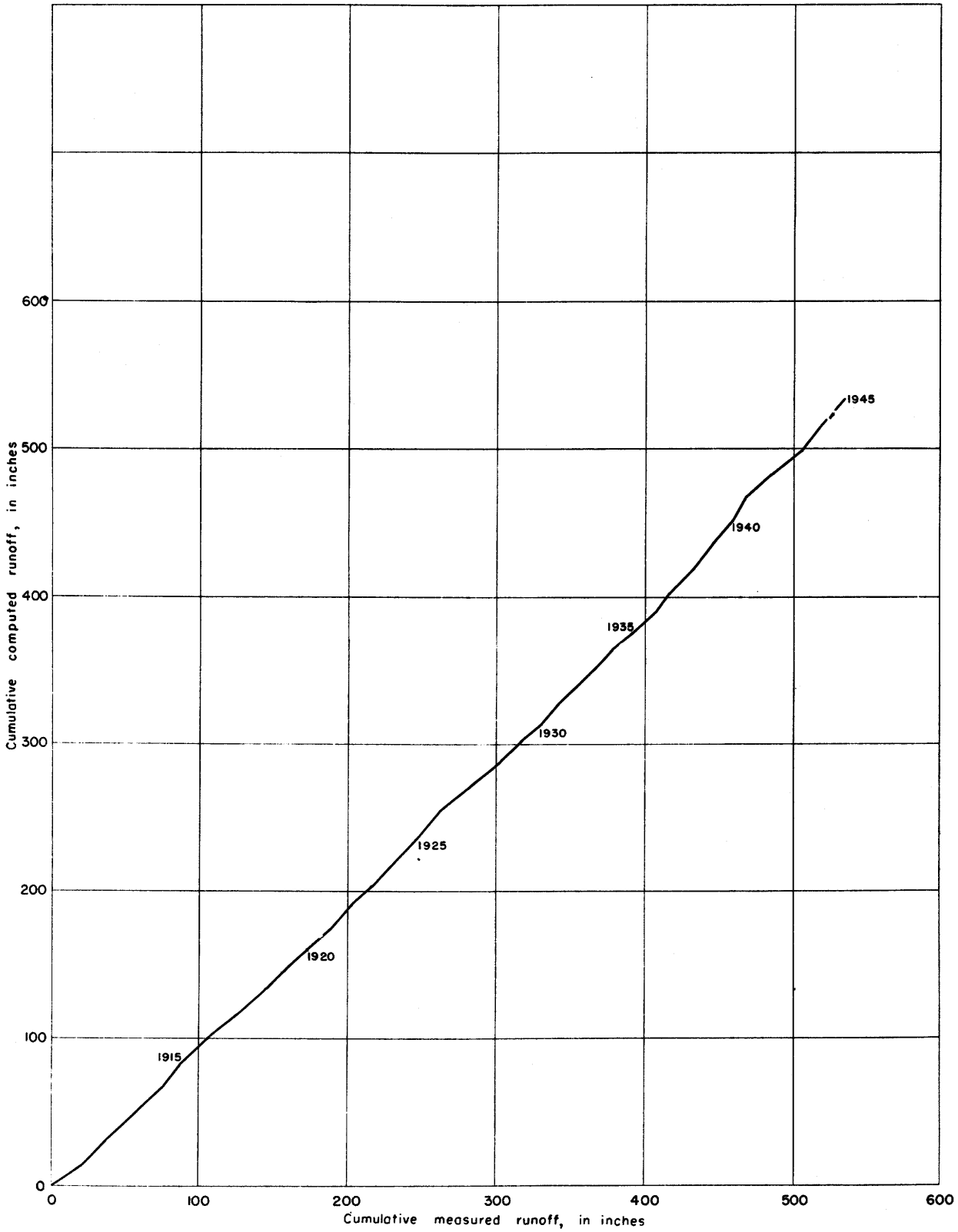

Figure 33.—Double mass curve of measured runoff plotted against computed runoff for Yellowstone River at Corwin Springs, Mont.

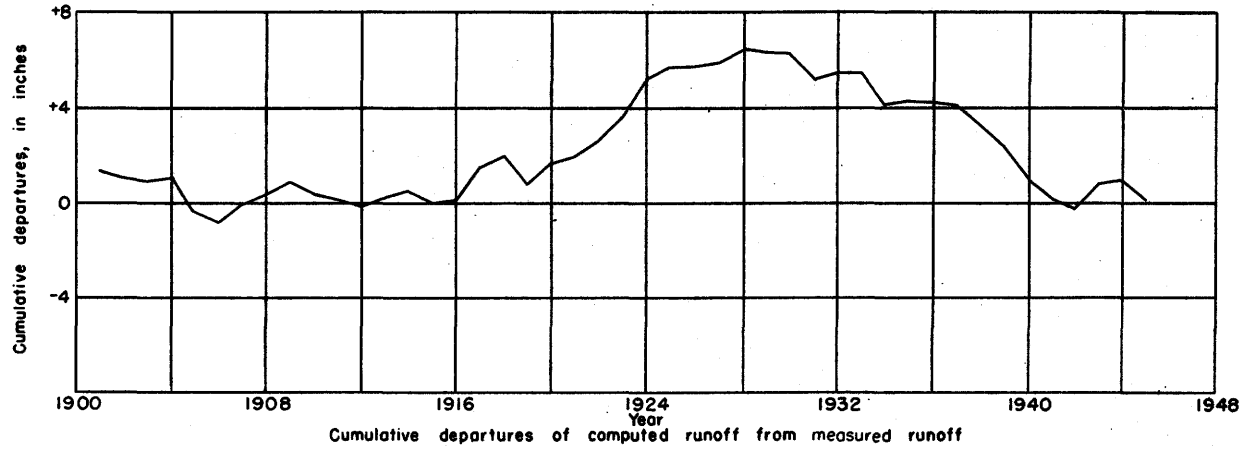

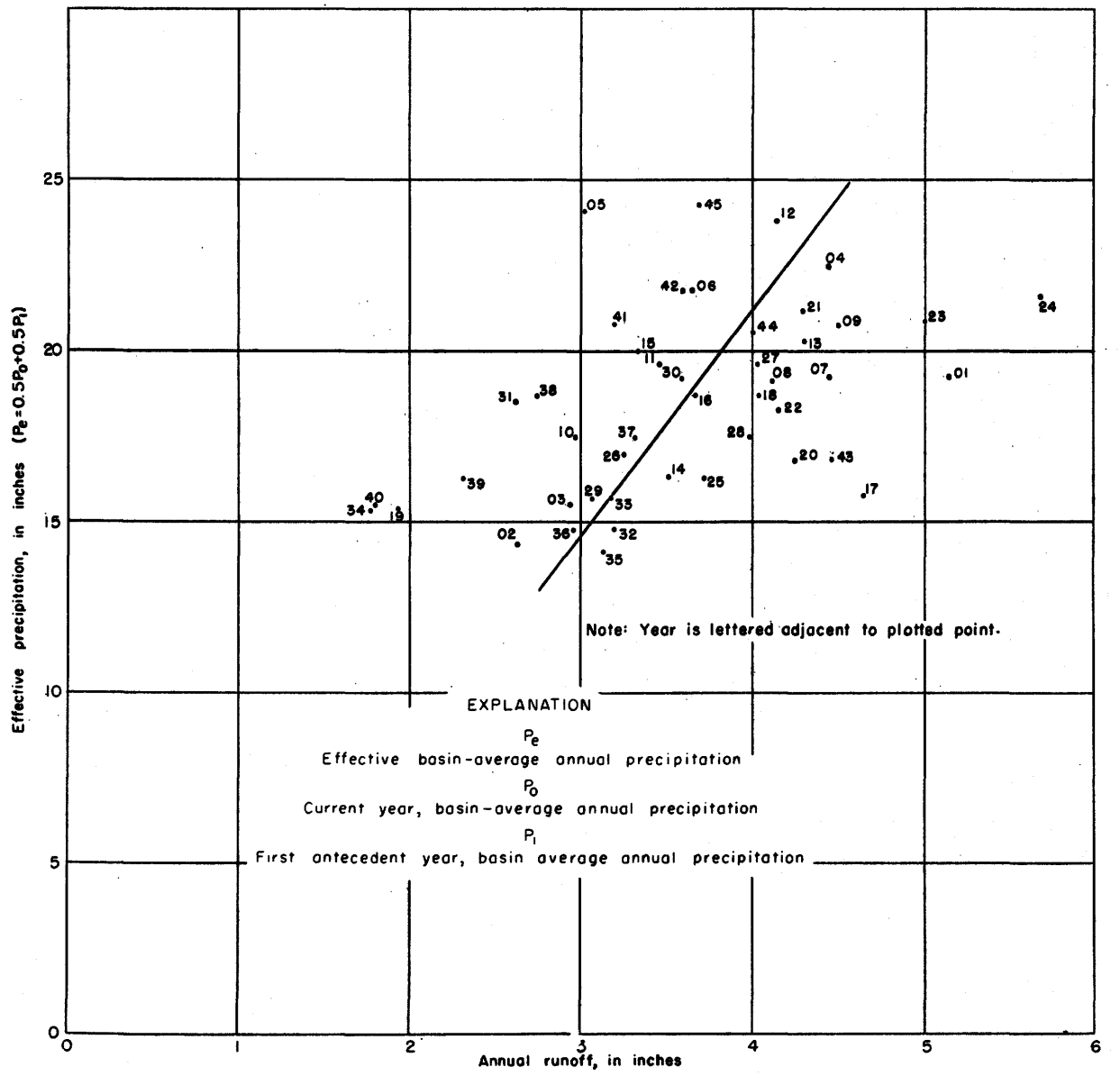

Figure 34.—Relationship of effective annual precipitation to annual runoff of Bighorn River at Thermopolis, Wyo.

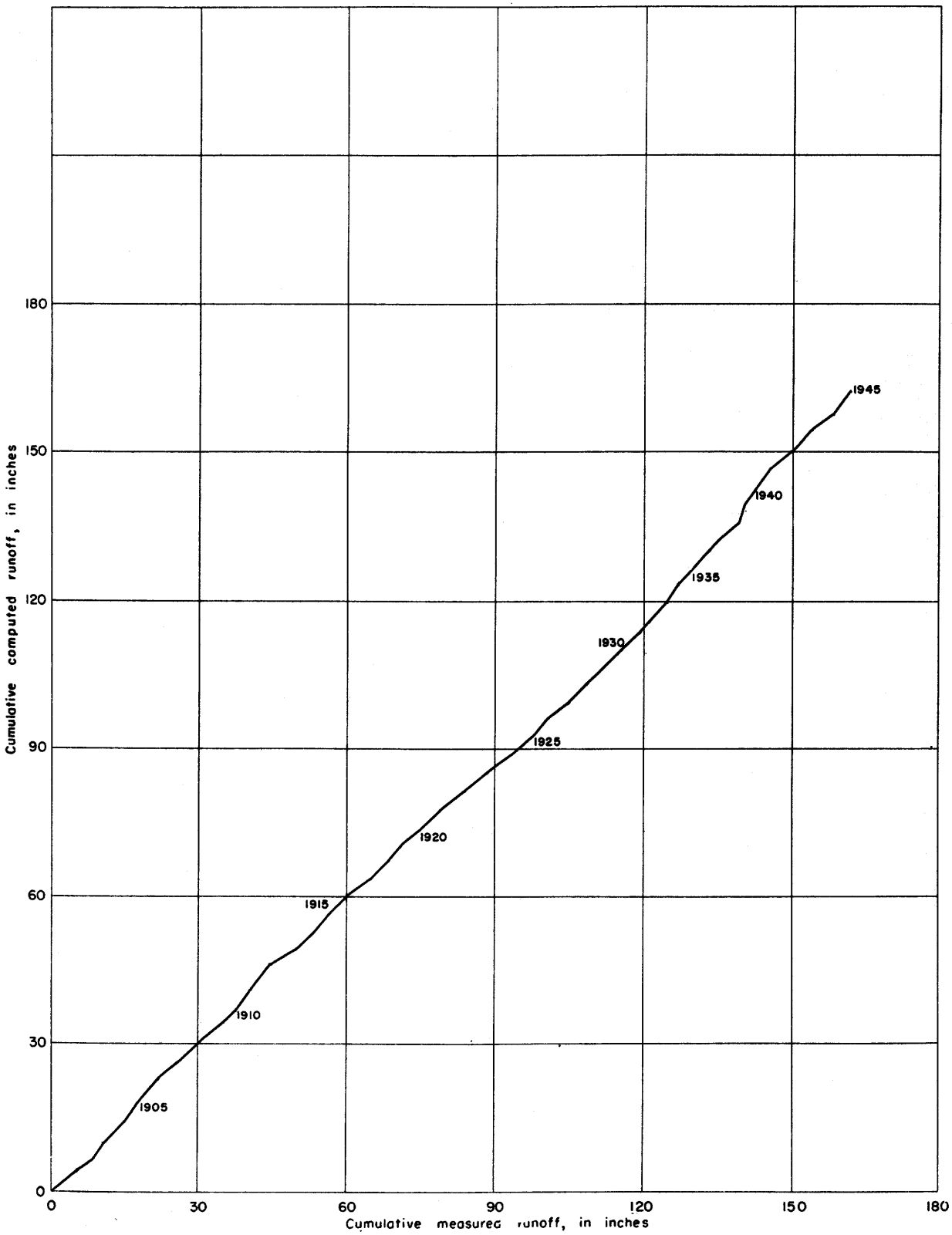

Figure 35.—Double mass curve of measured runoff plotted against computed runoff for Bighorn River at Thermopolis, Wyo.

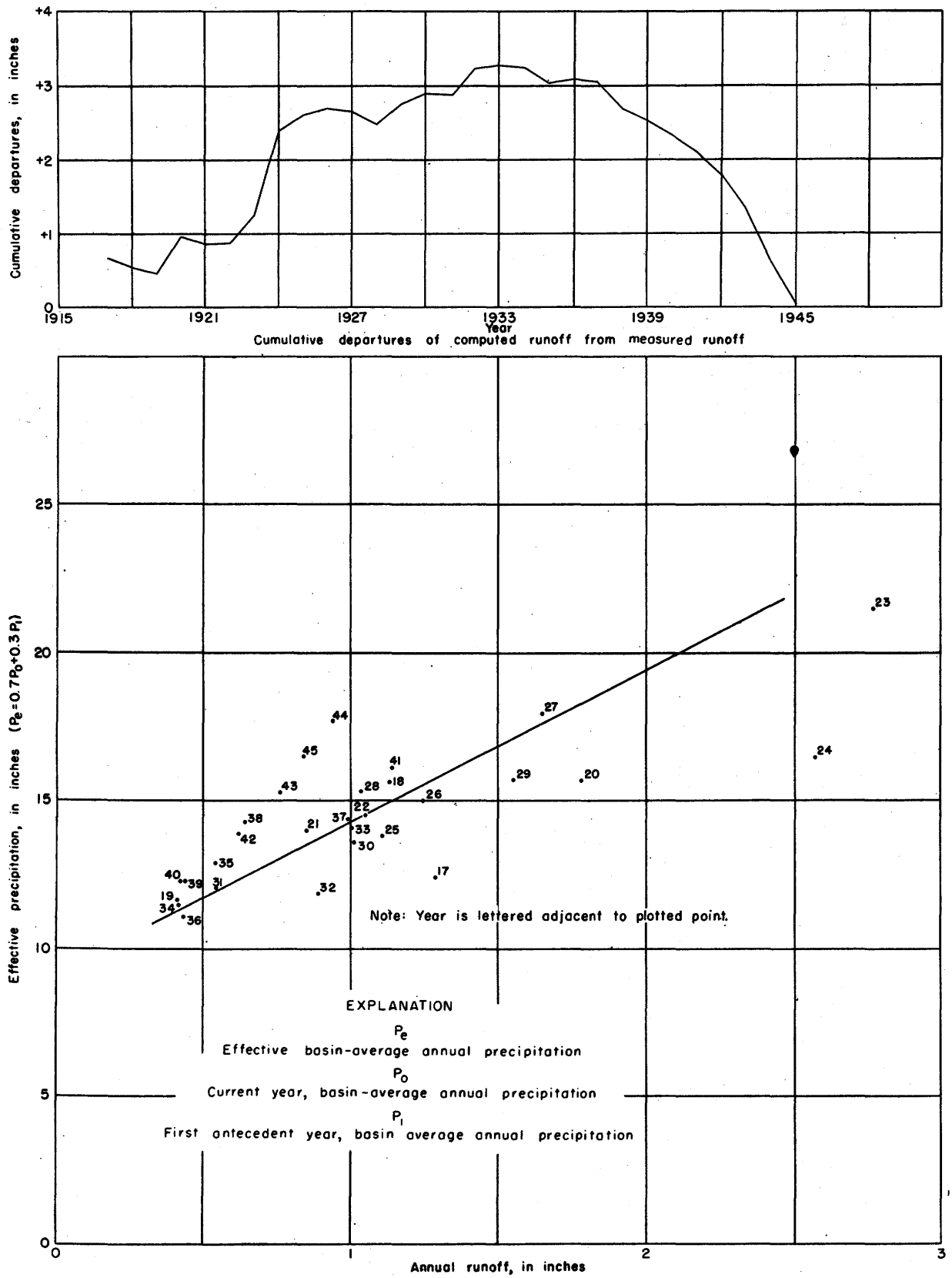

Figure 36.—Relationship of effective annual precipitation to annual runoff of Powder River at Arvada, Wyo.

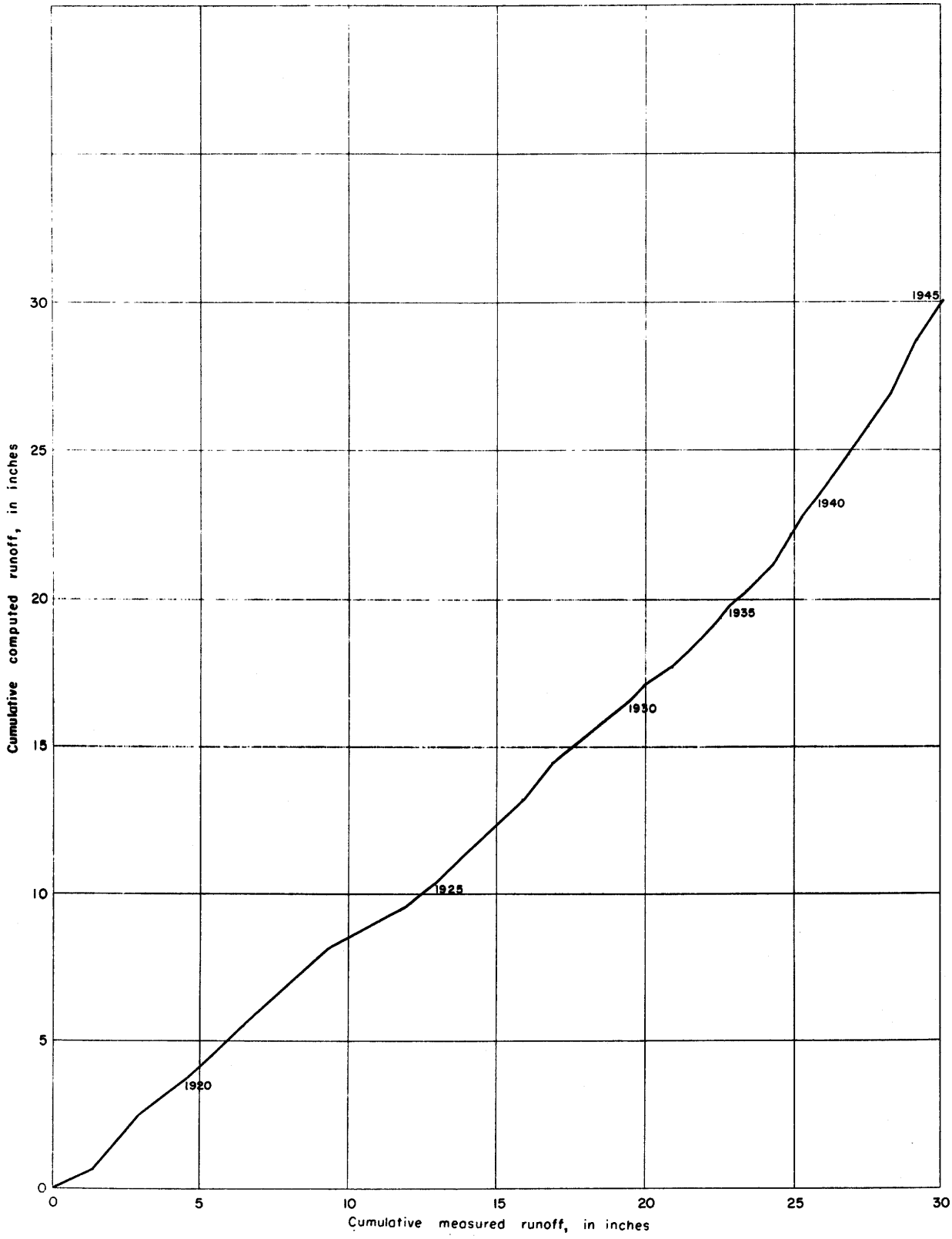

Figure 37.—Double mass curve of measured runoff plotted against computed runoff for Powder River at Arvada, Wyo.

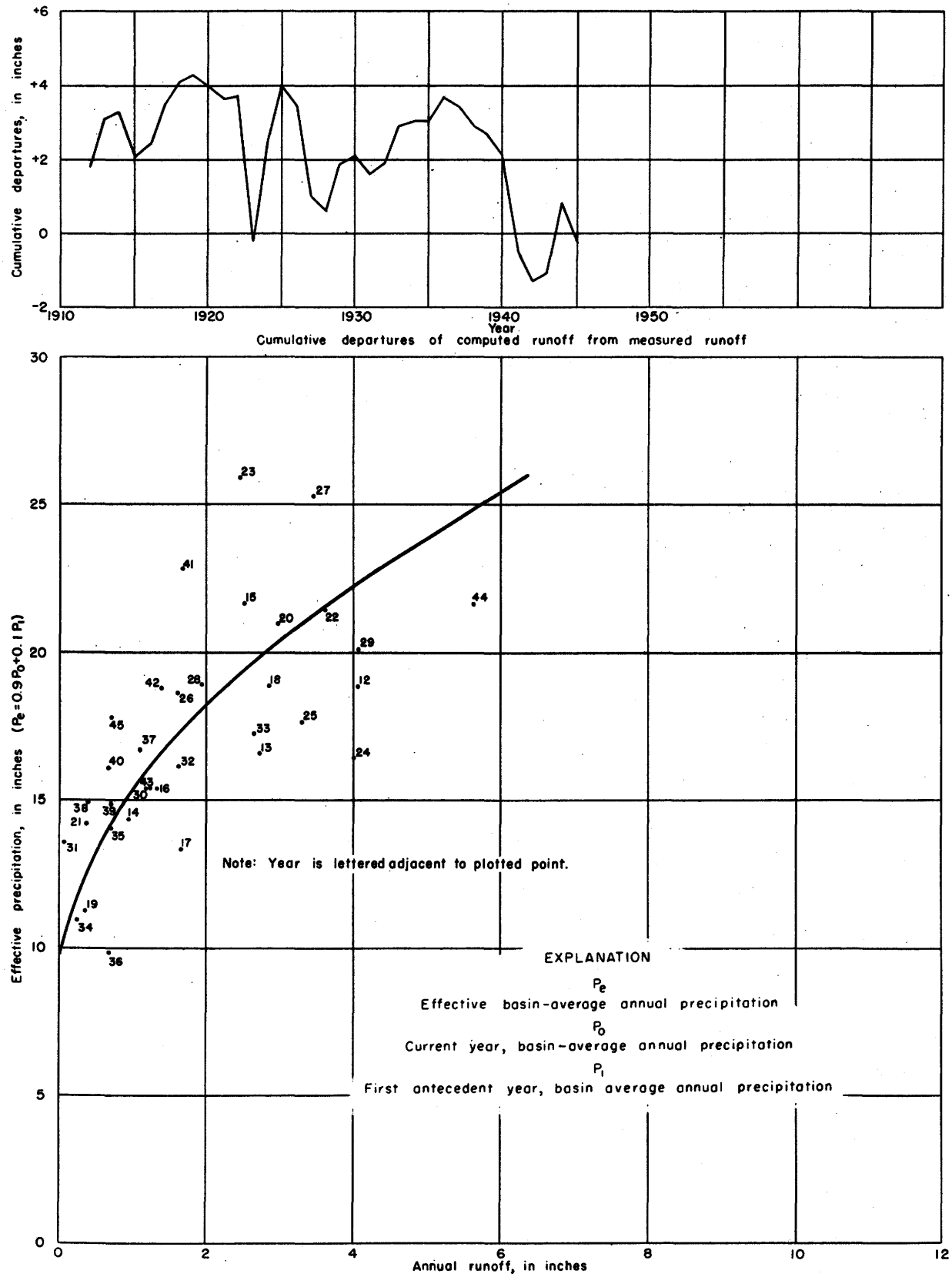

Figure 38.—Relationship of effective annual precipitation to annual runoff of Little Missouri River near Alzada, Mont.

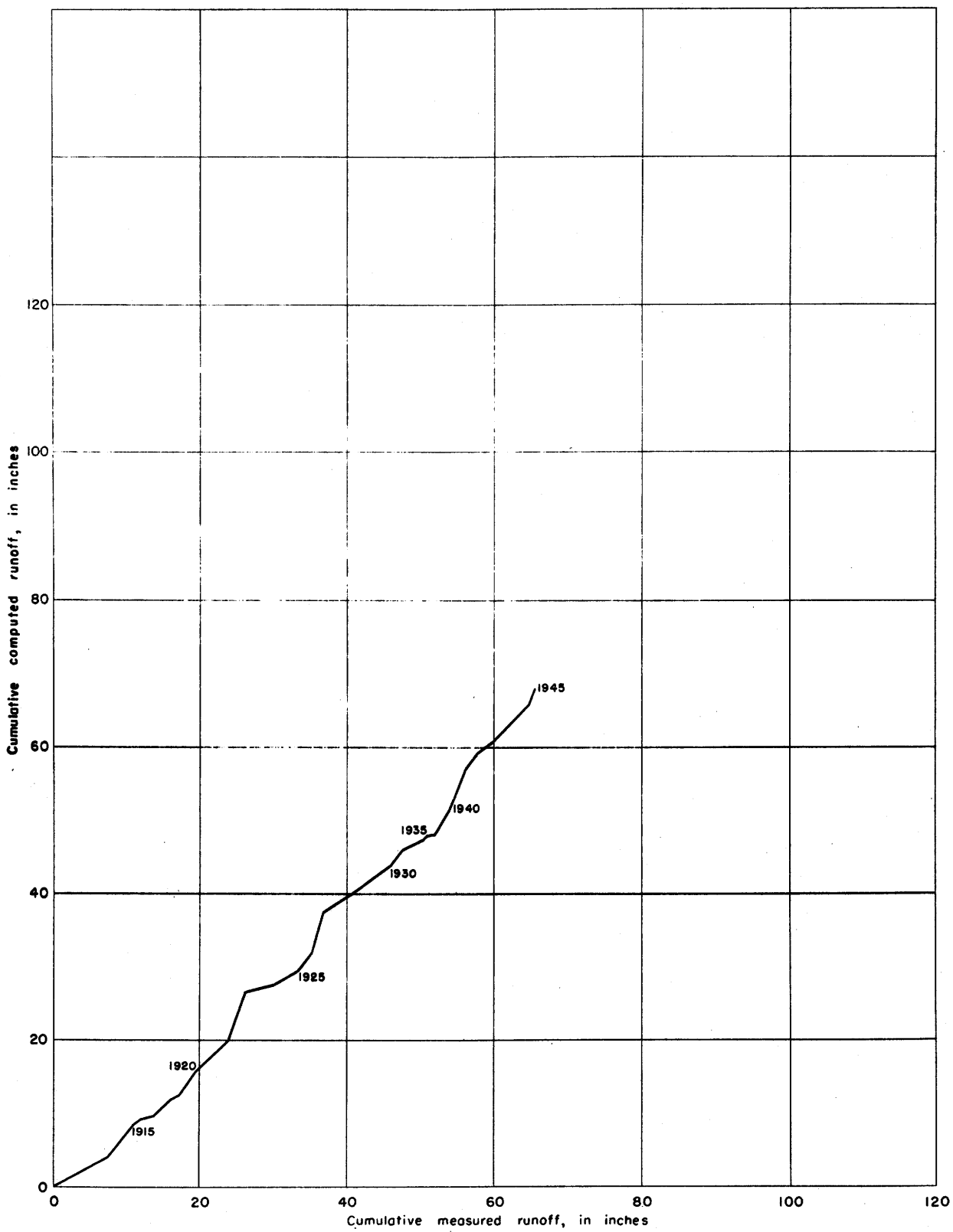

Figure 39.—Double mass curve of measured runoff plotted against computed runoff for Little Missouri River near Alzada, Mont.

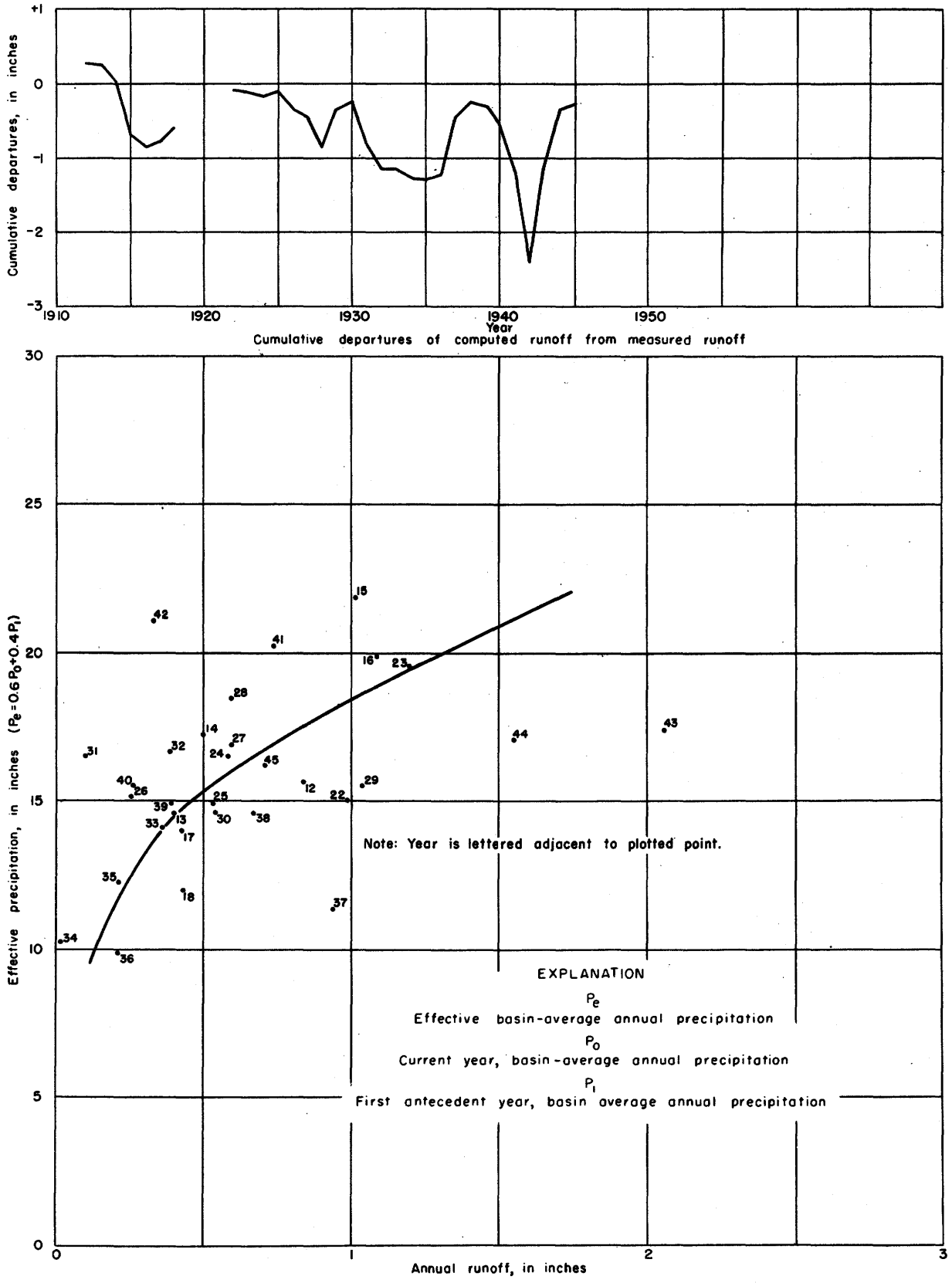

Figure 40.—Relationship of effective annual precipitation to annual runoff of Cannonball River at Breien, N. Dak.

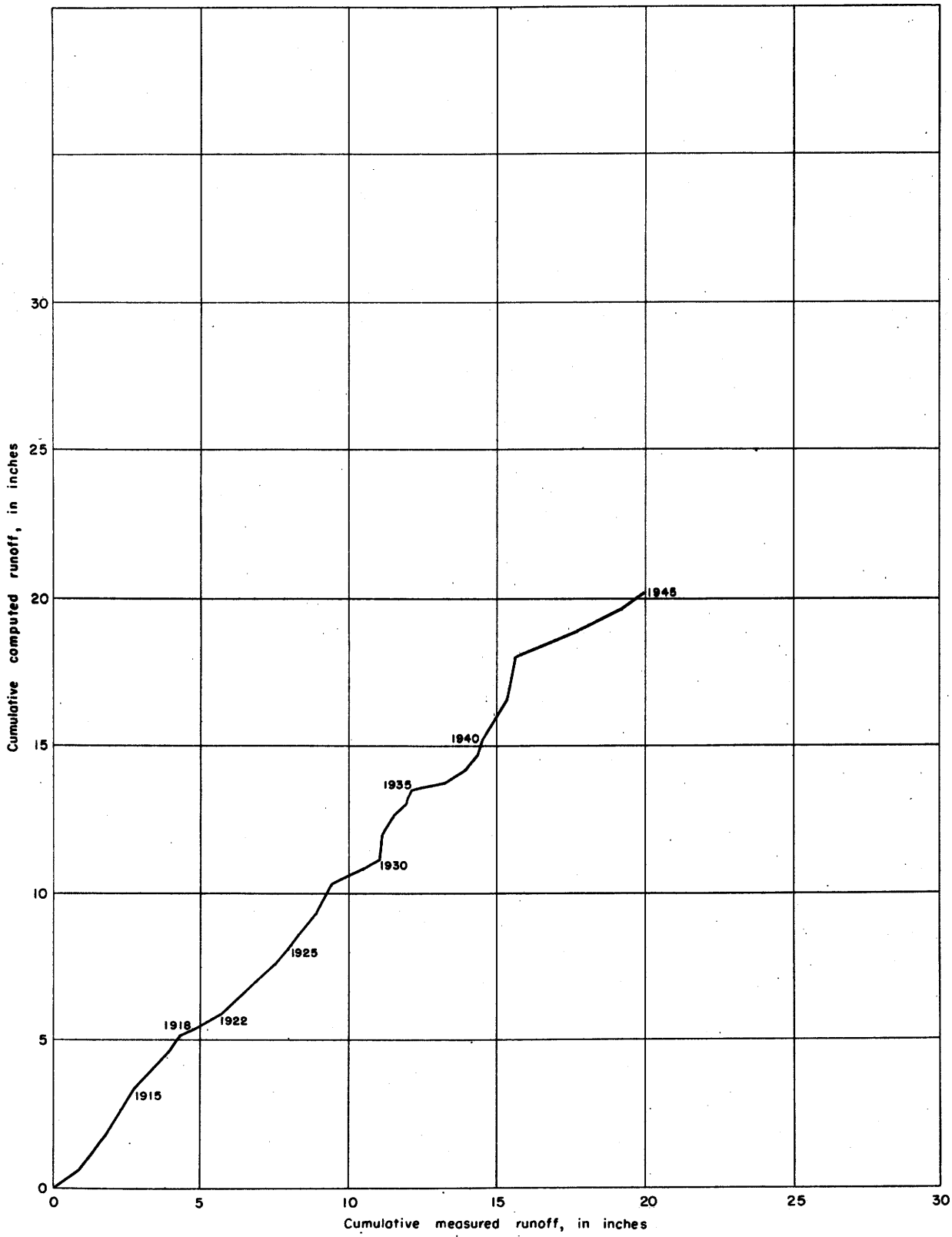

Figure 41.—Double mass curve of measured runoff plotted against computed runoff for Cannonball River at Breien, N. Dak.

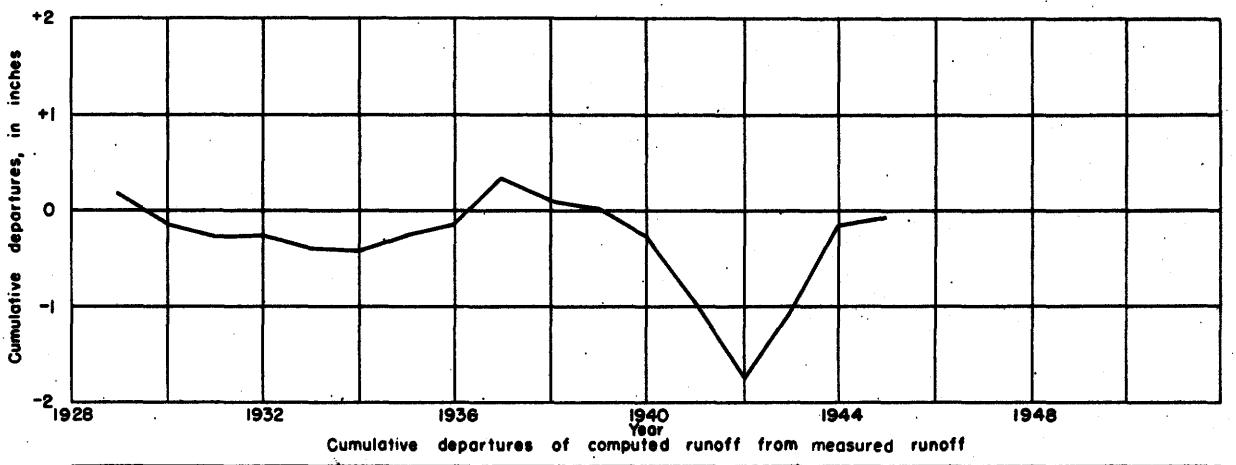

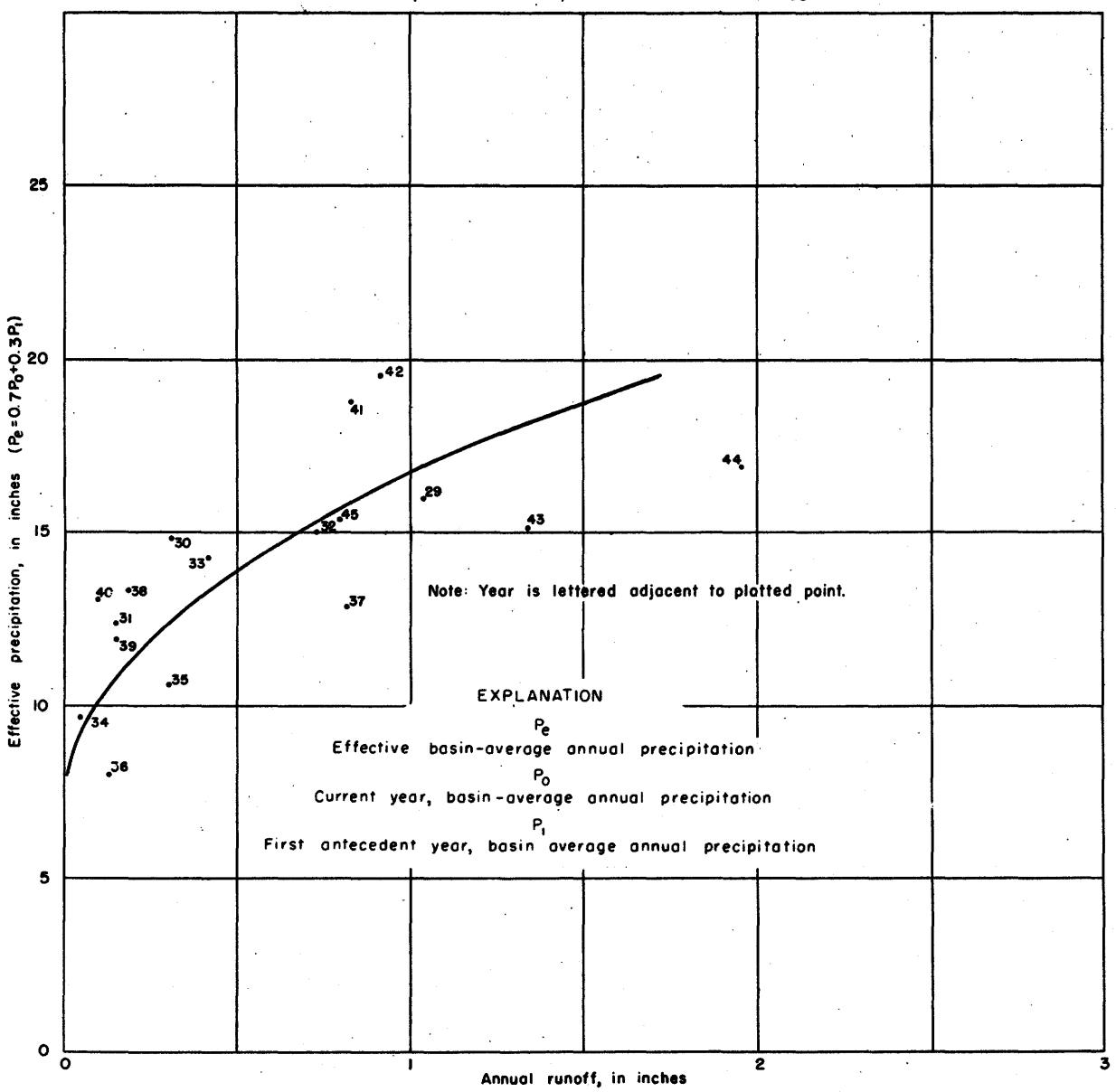

Figure 42.—Relationship of effective annual precipitation to annual runoff of Moreau River at Promise, S. Dak.

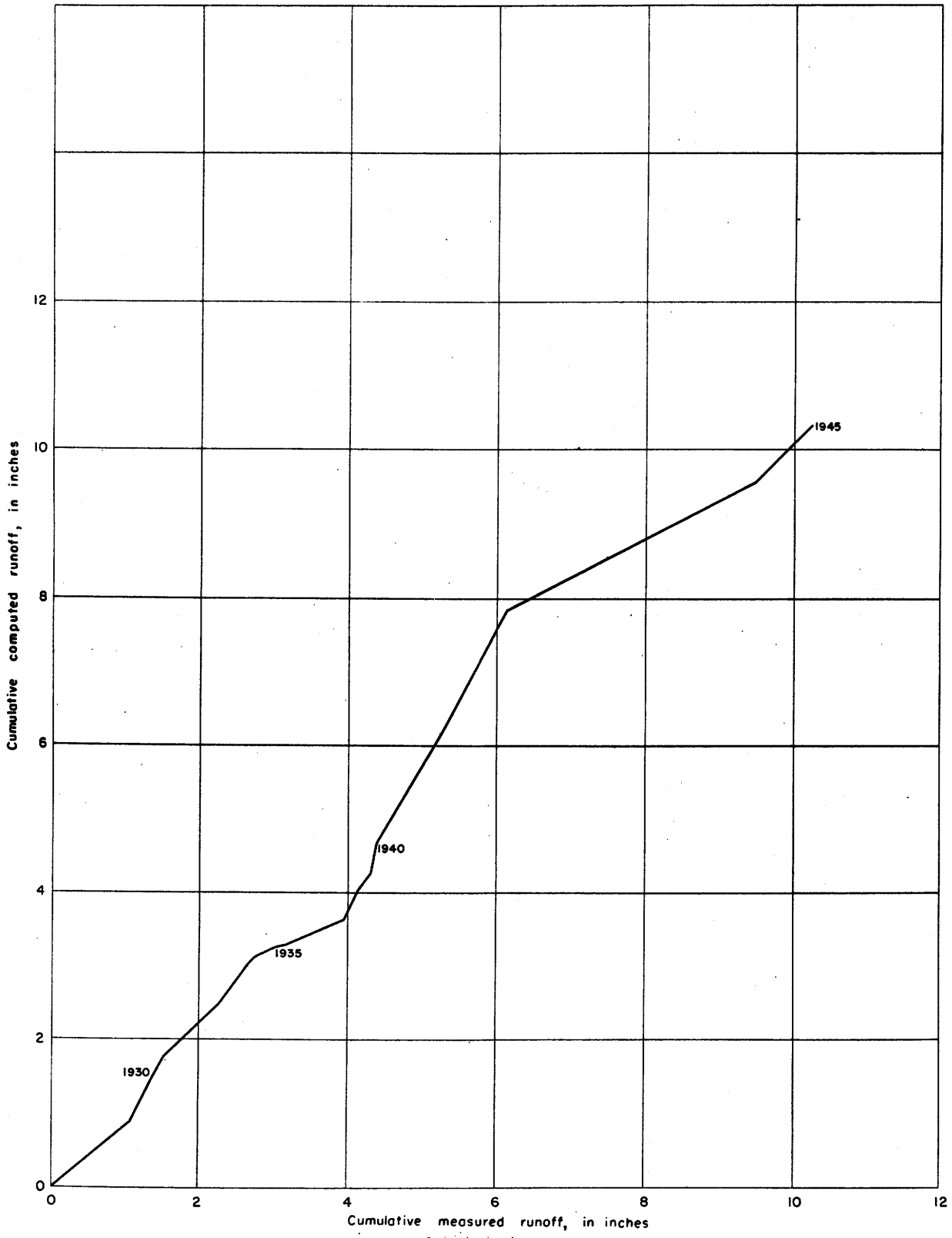

Figure 43.—Double mass curve of measured runoff plotted against computed runoff for Moreau River at Promise, S. Dak.

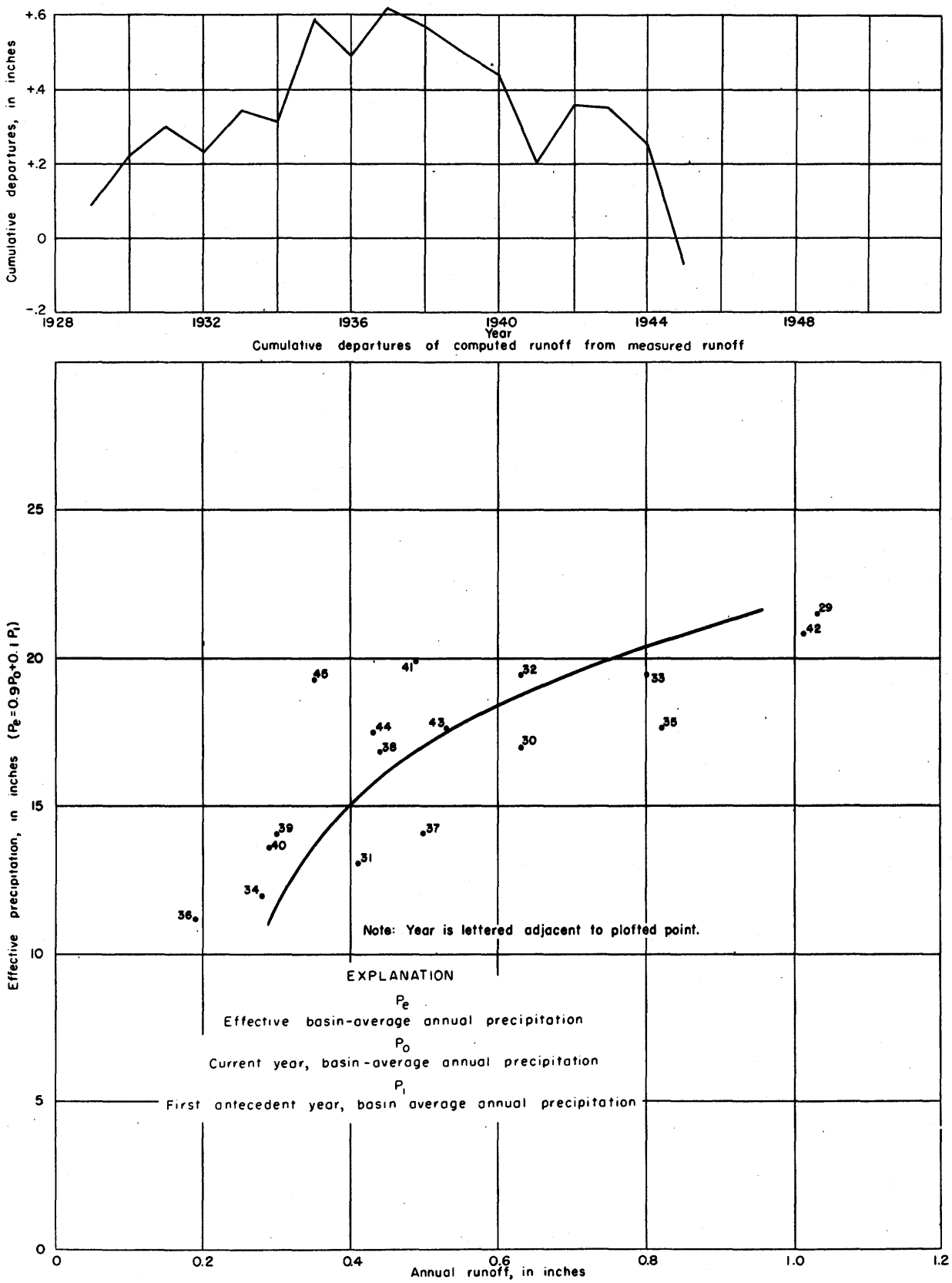

Figure 44.—Relationship of effective annual precipitation to annual runoff of Cheyenne River near Wasta, S. Dak.

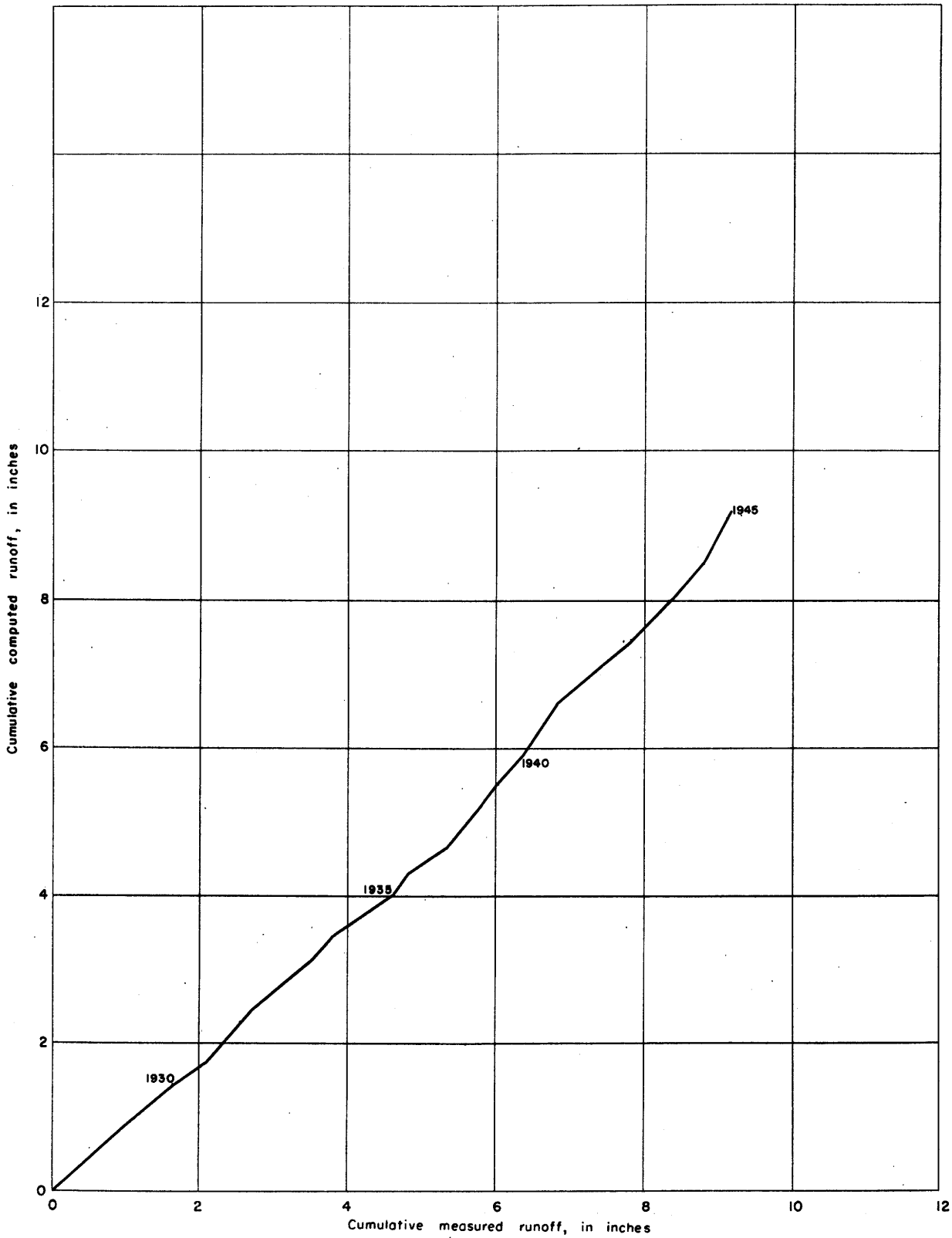

Figure 45.—Double mass curve of measured runoff plotted against computed runoff for Cheyenne River near Wasta, S. Dak.

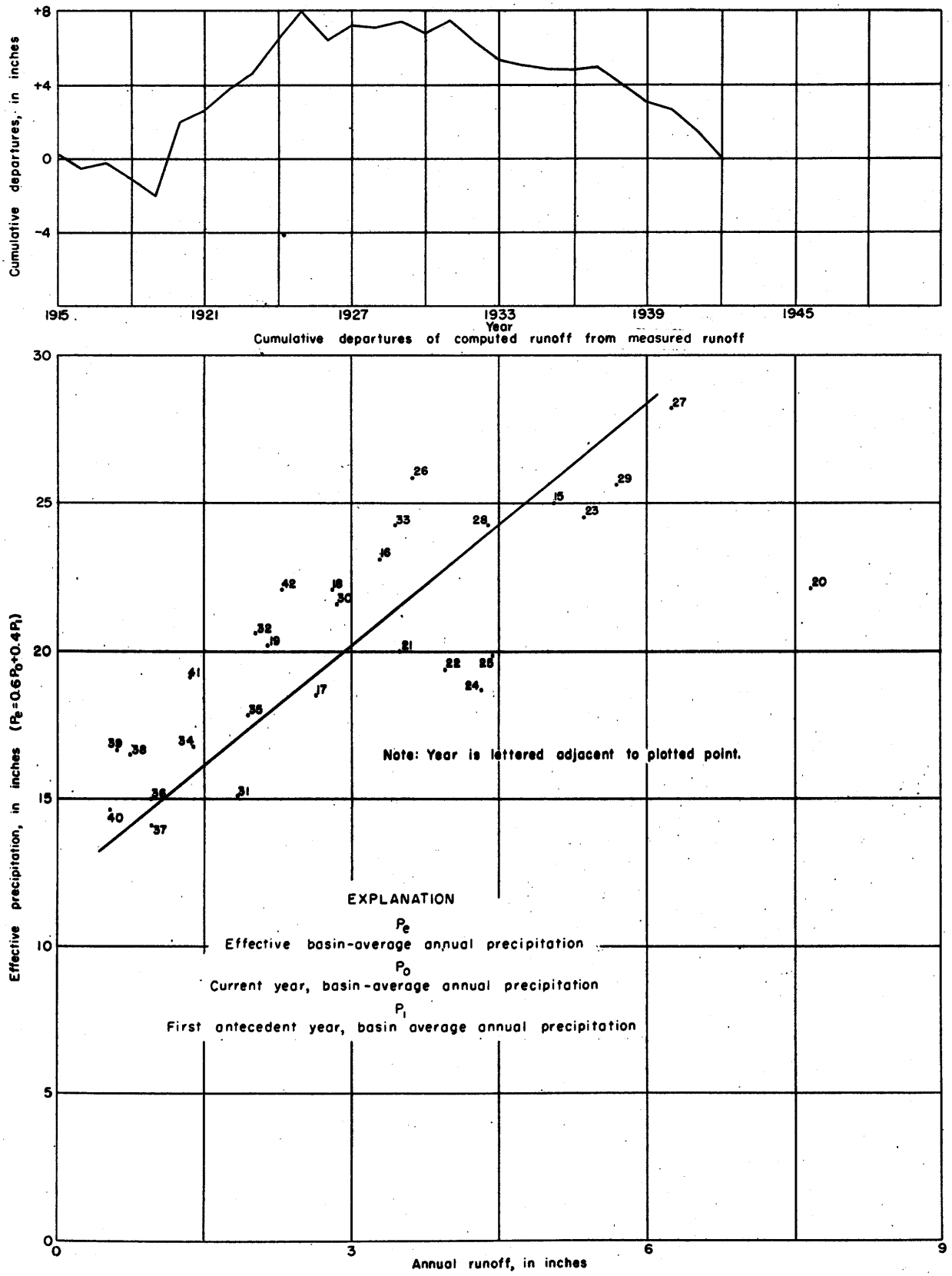

Figure 46.—Relationship of effective annual precipitation to annual runoff of Rapid Creek at Big Bend, S. Dak.

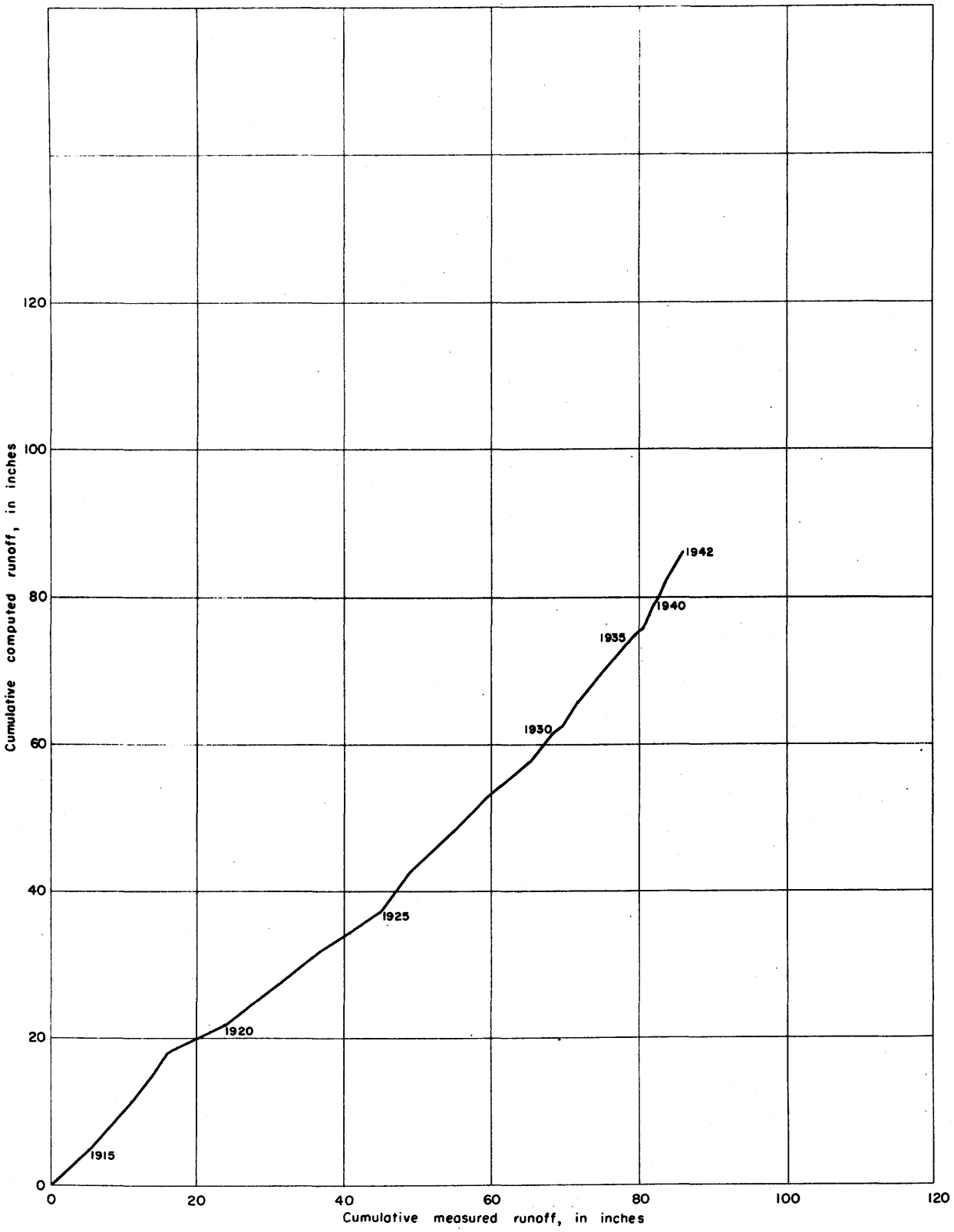

Figure 47. —Double mass curve of measured runoff plotted against computed runoff for Rapid Creek at Big Bend, S. Dak.

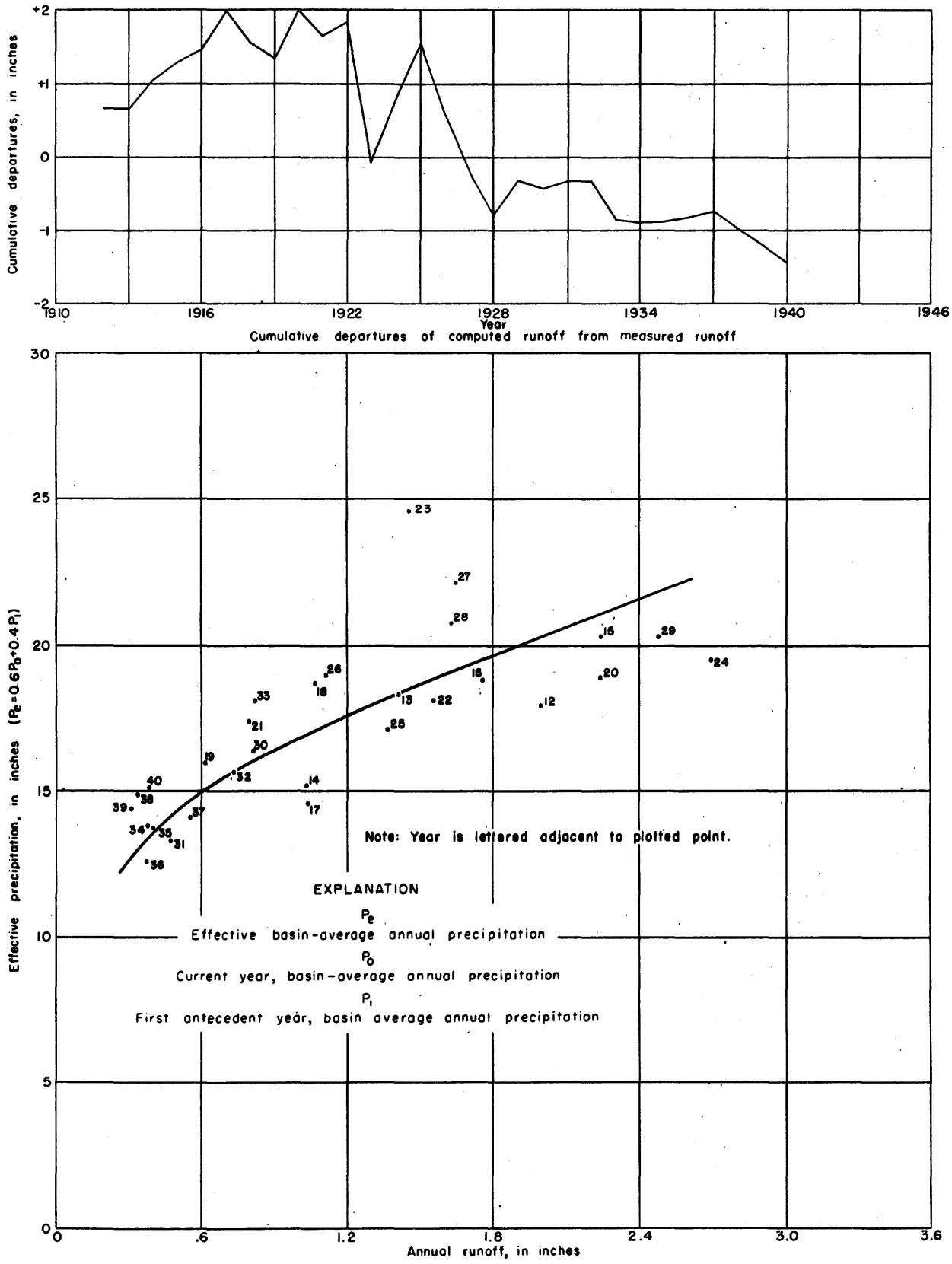

Figure 48.—Relationship of effective annual precipitation to annual runoff of Belle Fourche River, near Belle Fourche, S. Dak.

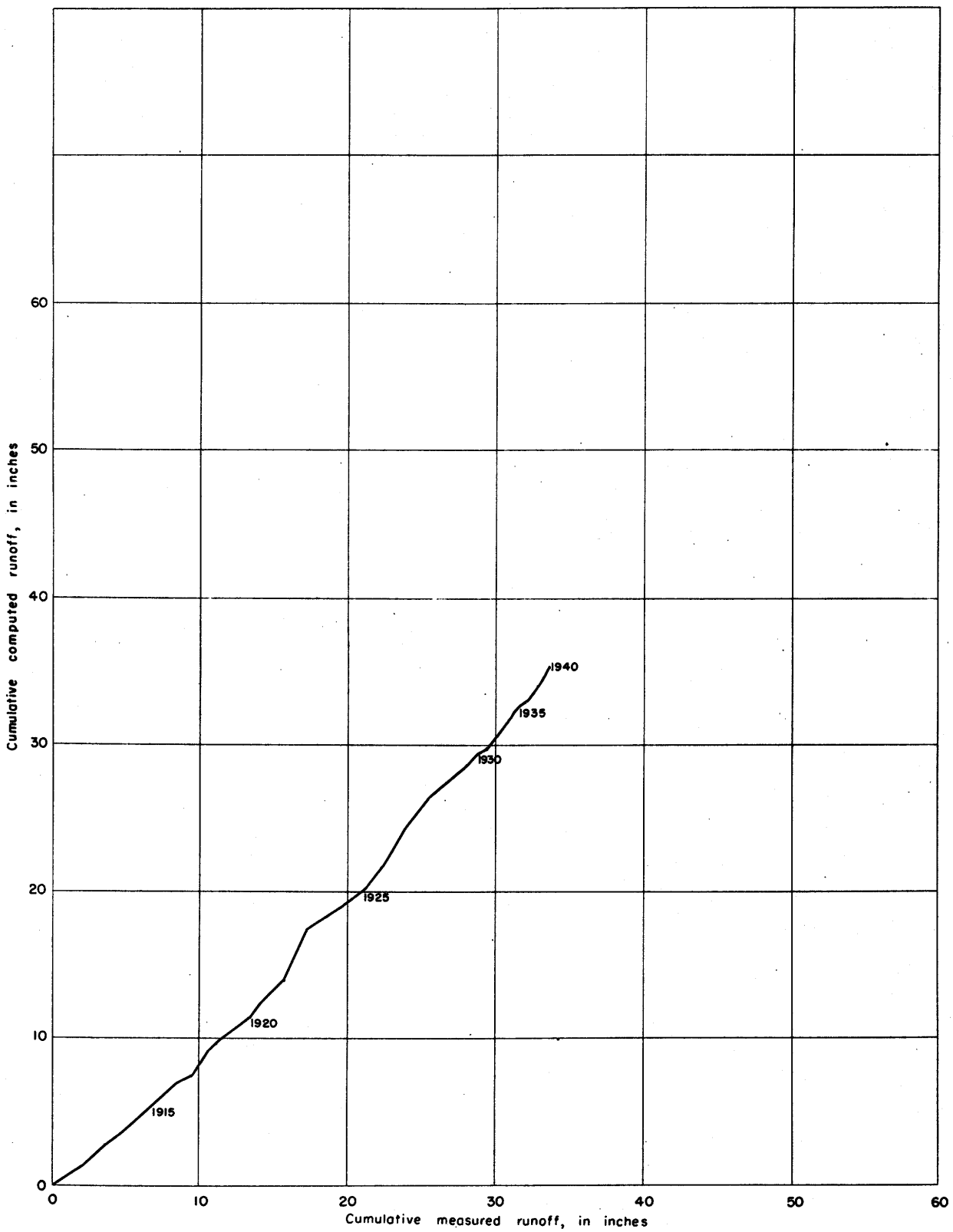

Figure 49.—Double mass curve of measured runoff plotted against computed runoff for Belle Fourche River near Belle Fourche, S. Dak.

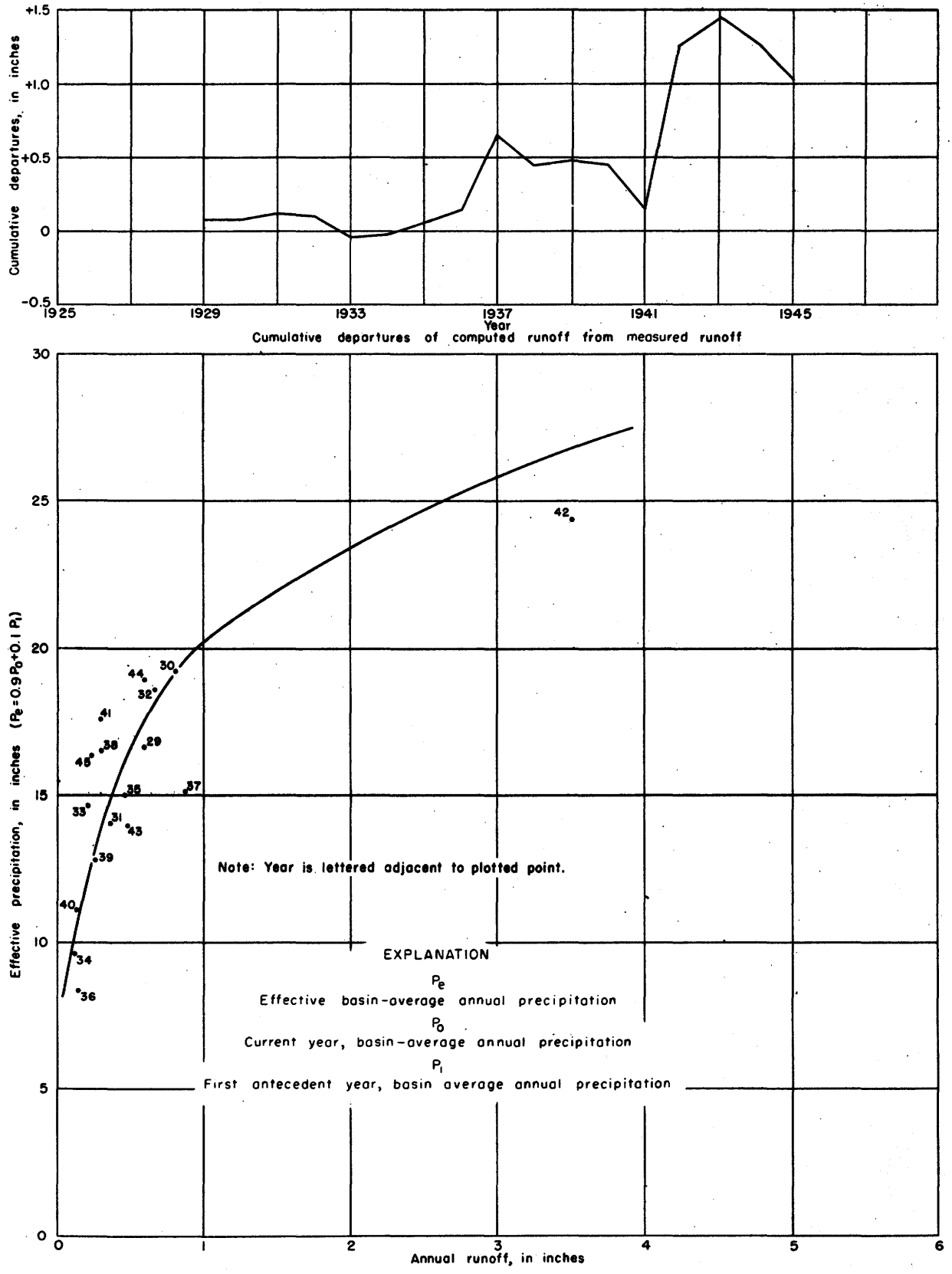

Figure 50.—Relationship of effective annual precipitation to annual runoff of Bad River near Fort Pierre, S. Dak.

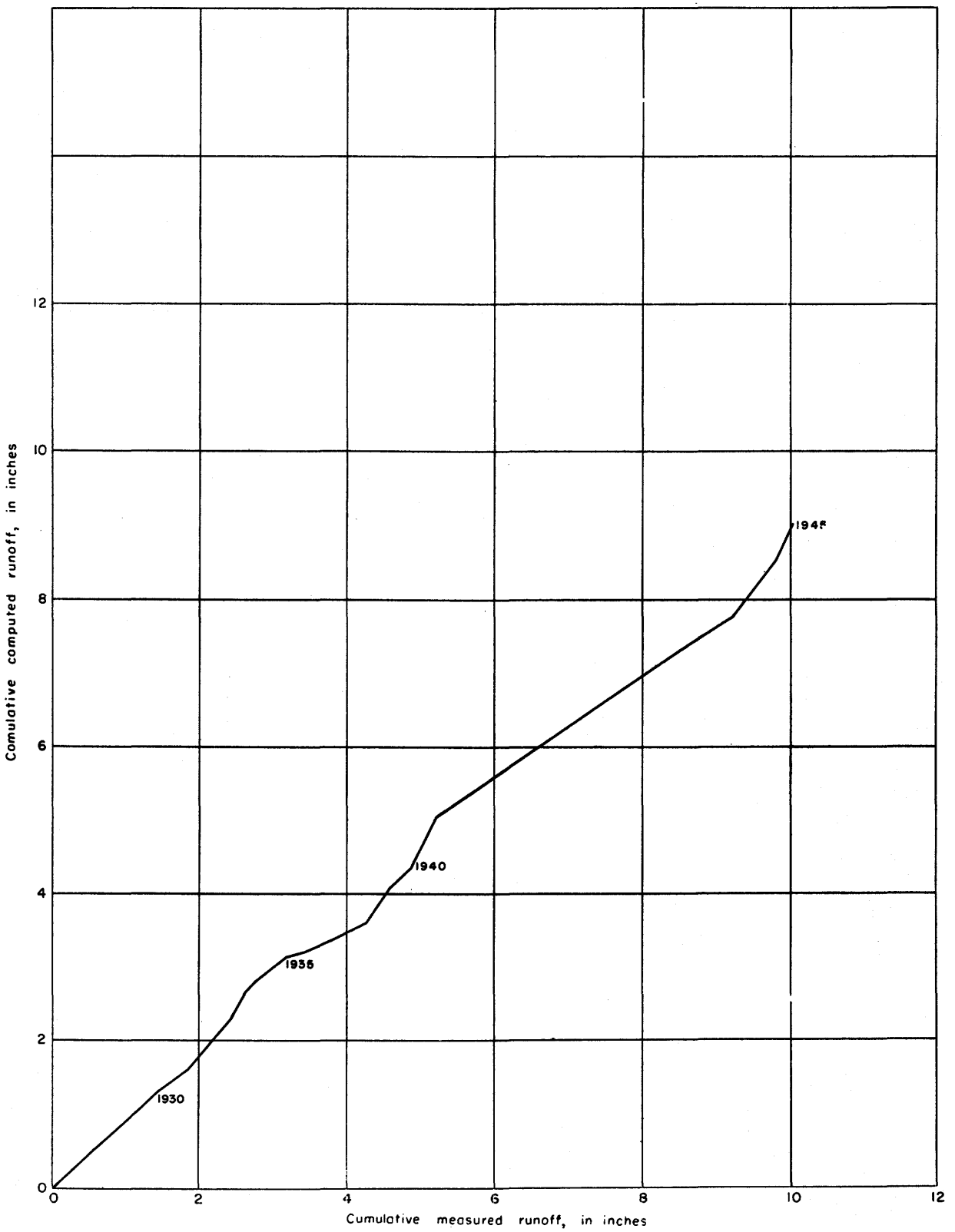

Figure 51.—Double mass curve of measured runoff plotted against computed runoff for Bad River near Fort Pierre, S. Dak.

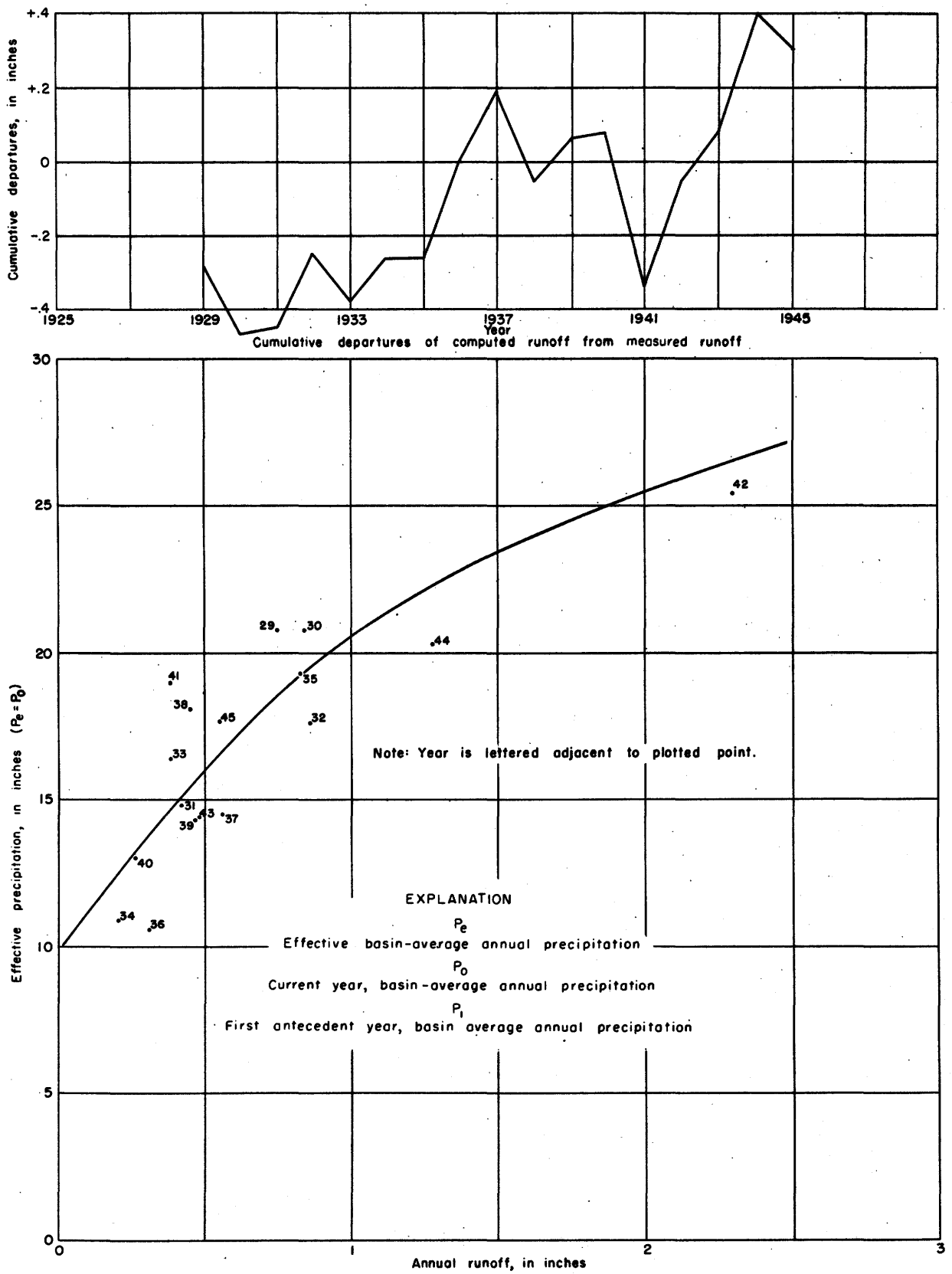

Figure 52.—Relationship of effective annual precipitation to annual runoff of White River near Oacoma, S. Dak.

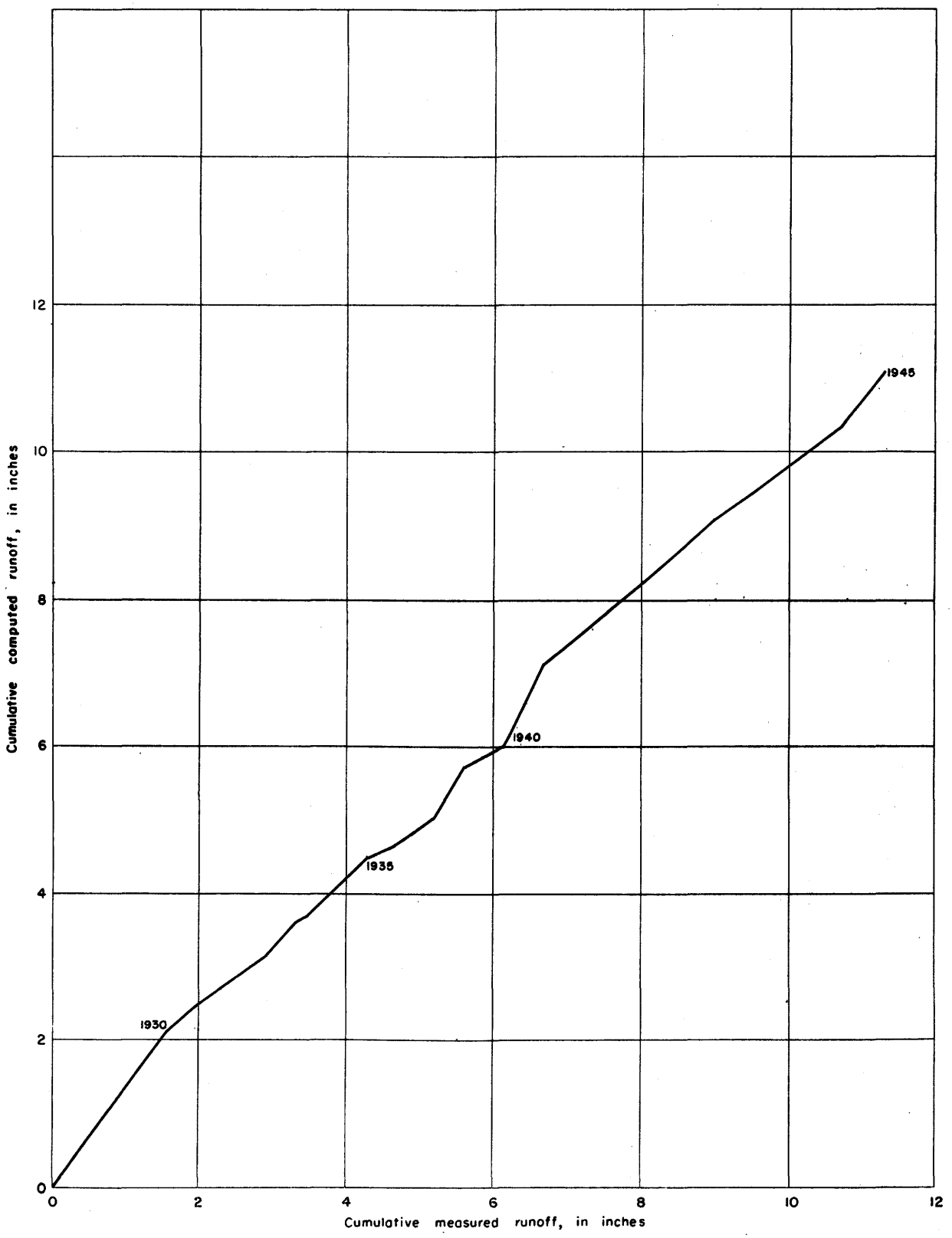

Figure 53.—Double mass curve of measured runoff plotted against computed runoff for White River near Oacoma, S. Dak.

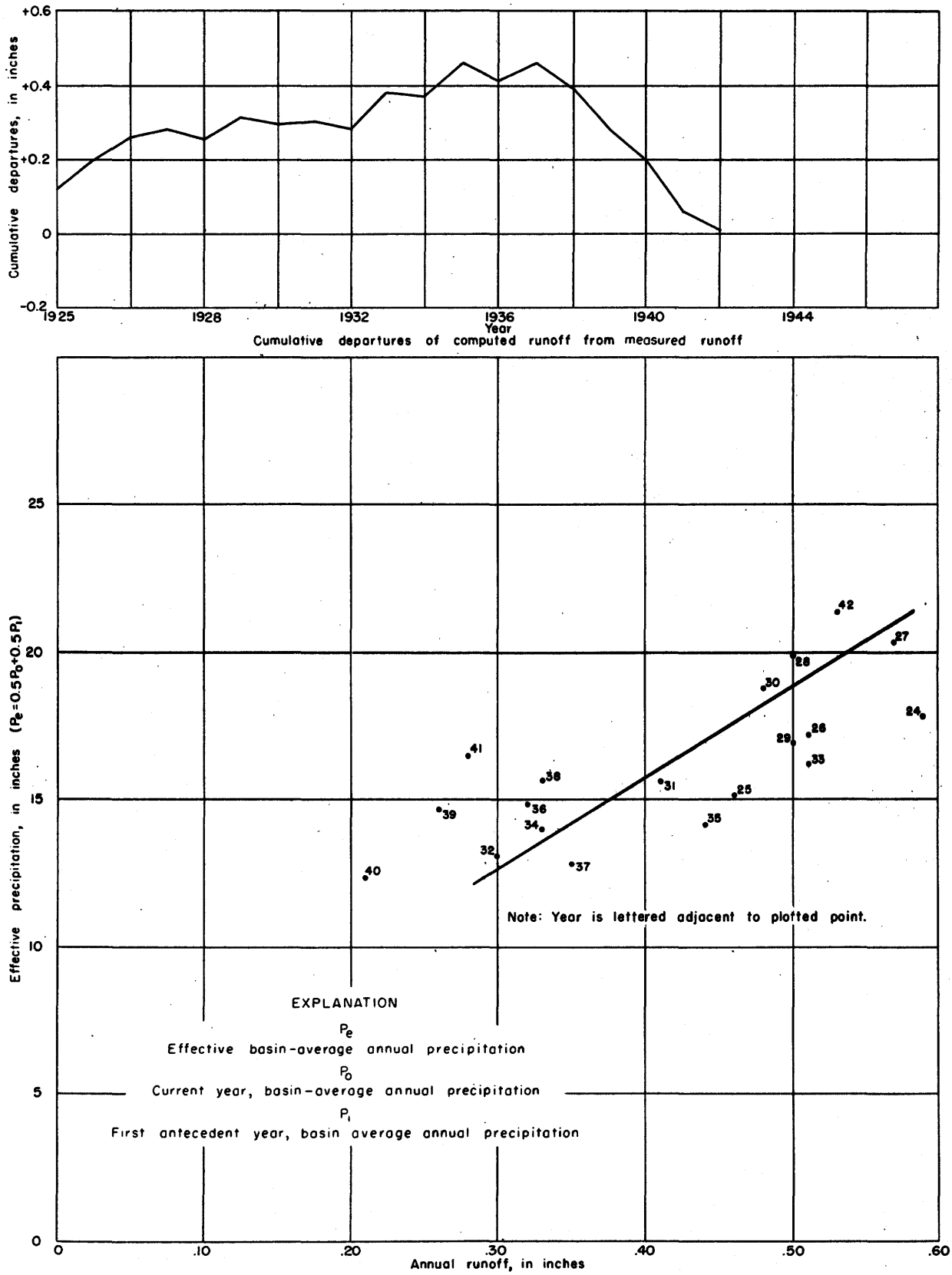

Figure 54.—Relationship of effective annual precipitation to annual runoff of Niobrara River at Dunlap, Nebr.

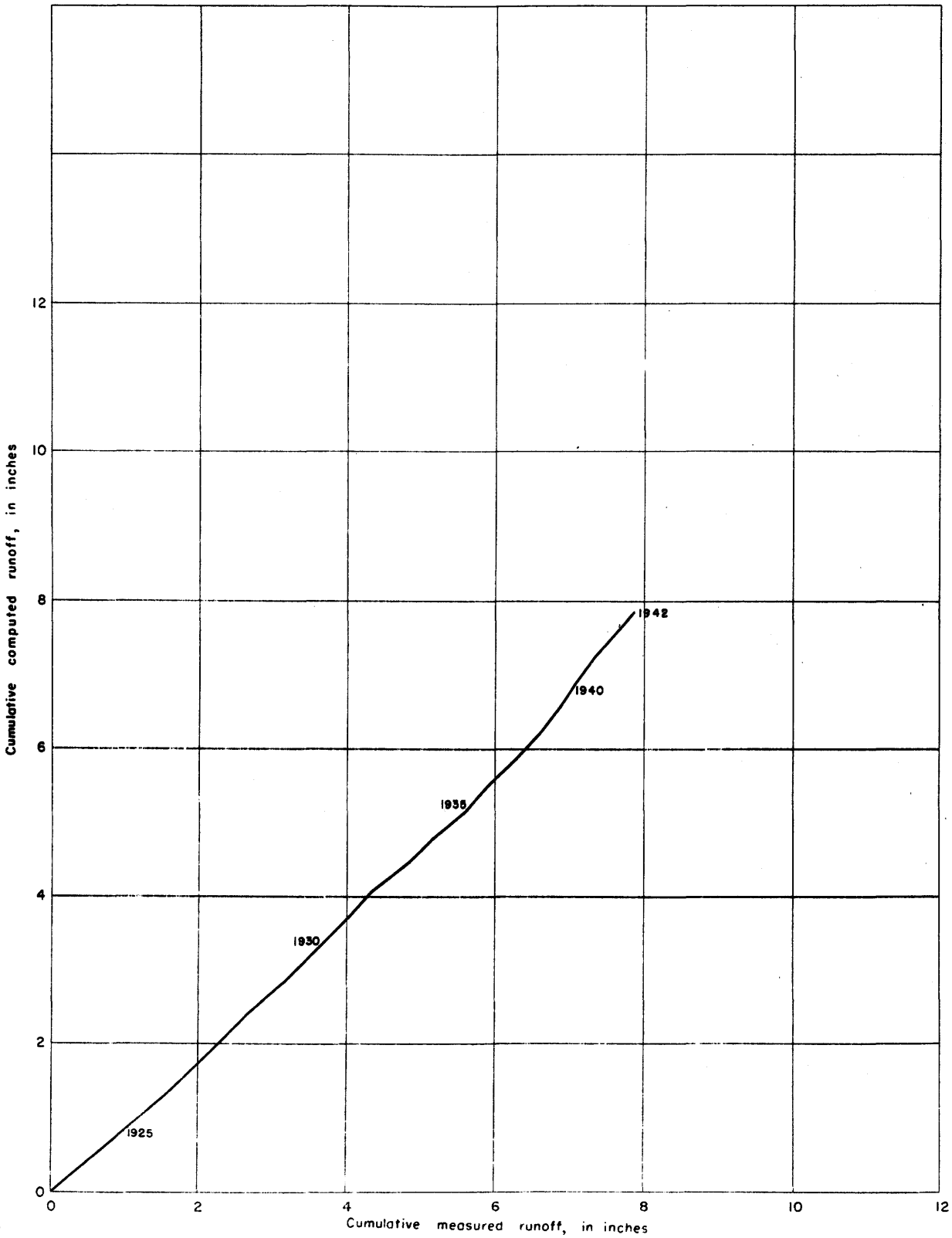

Figure 55.—Double mass curve of measured runoff plotted against computed runoff for Niobrara River at Dunlap, Nebr.

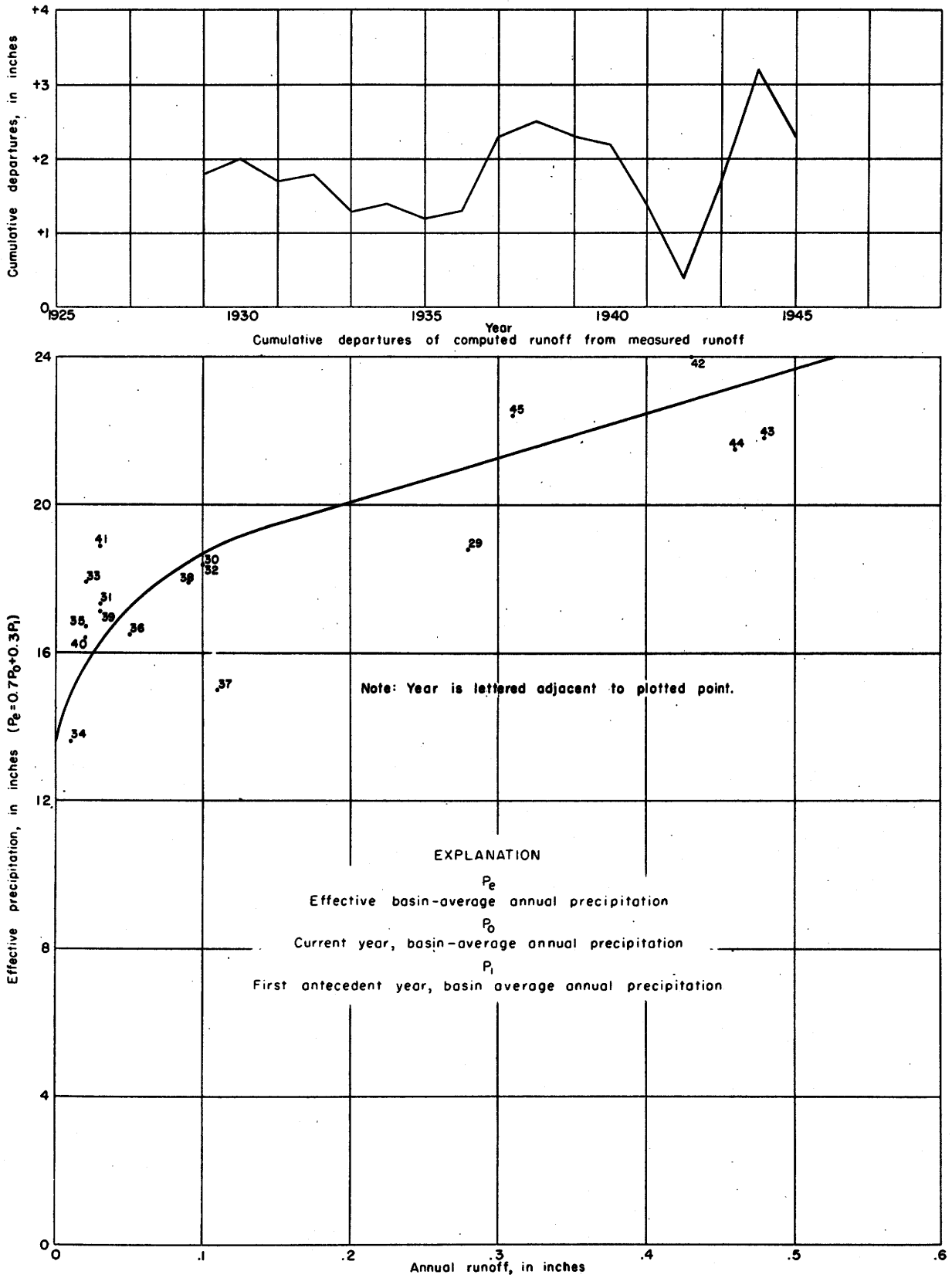

Figure 56.—Relationship of effective annual precipitation to annual runoff of James River near Scotland, S. Dak.

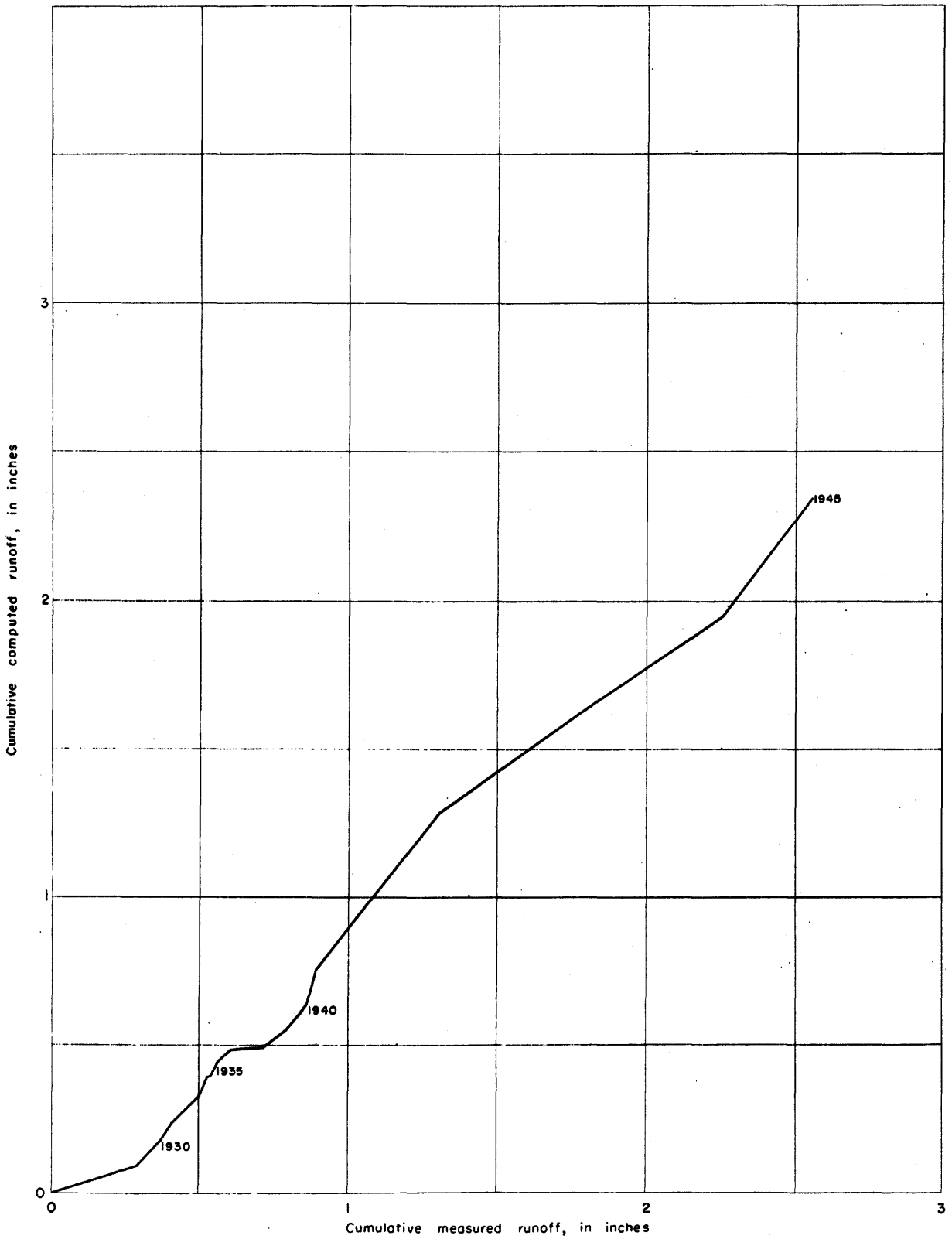

Figure 57.—Double mass curve of measured runoff plotted against computed runoff for James River near Scotland, S. Dak.

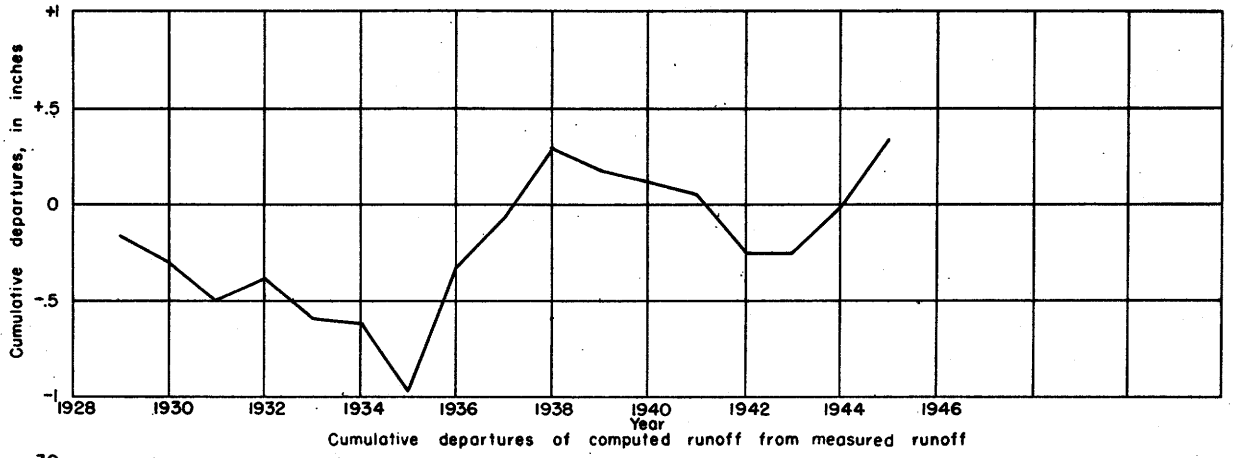

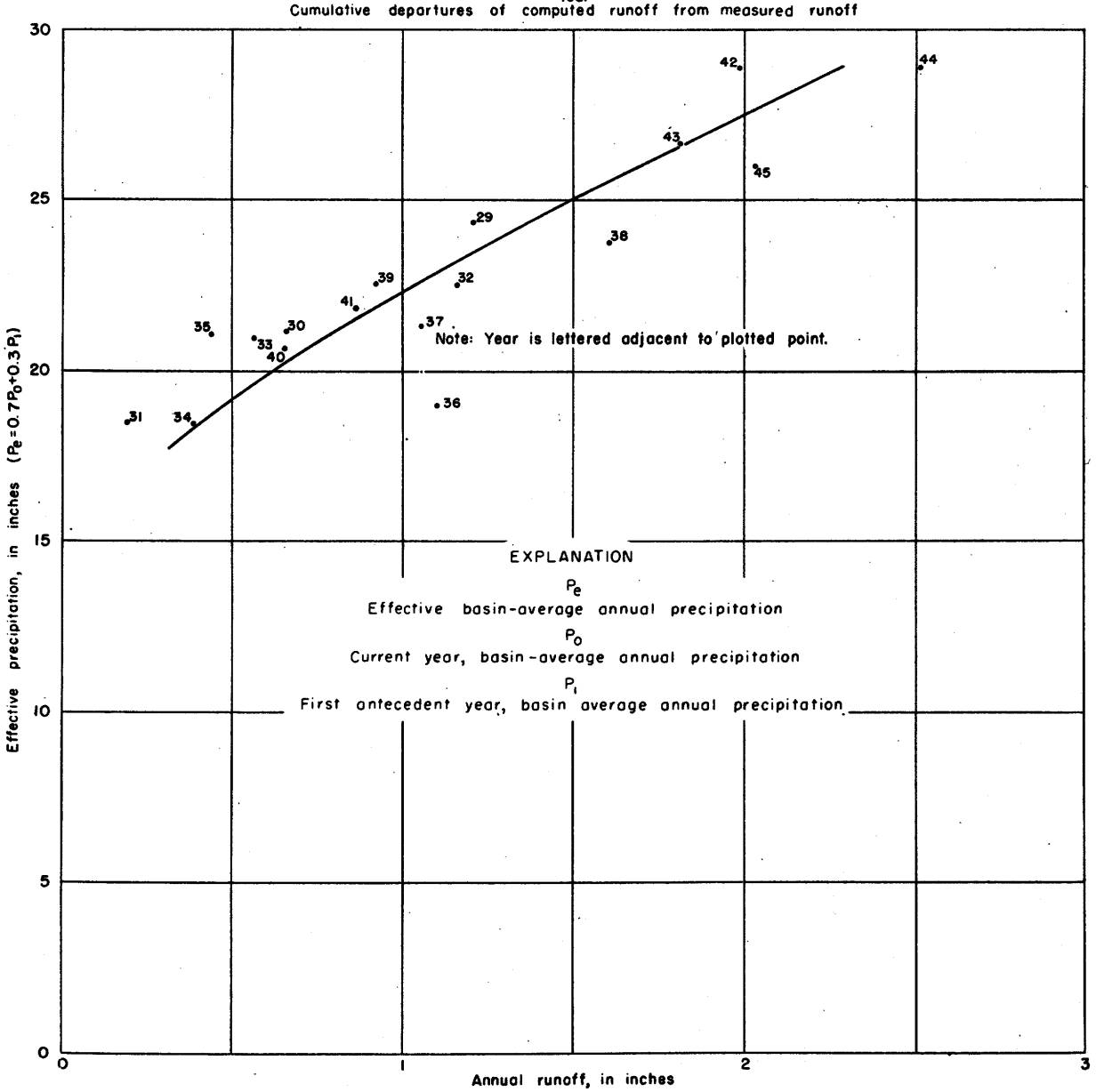

Figure 58. —Relationship of effective annual precipitation to annual runoff of Big Sioux River at Akron, Iowa.

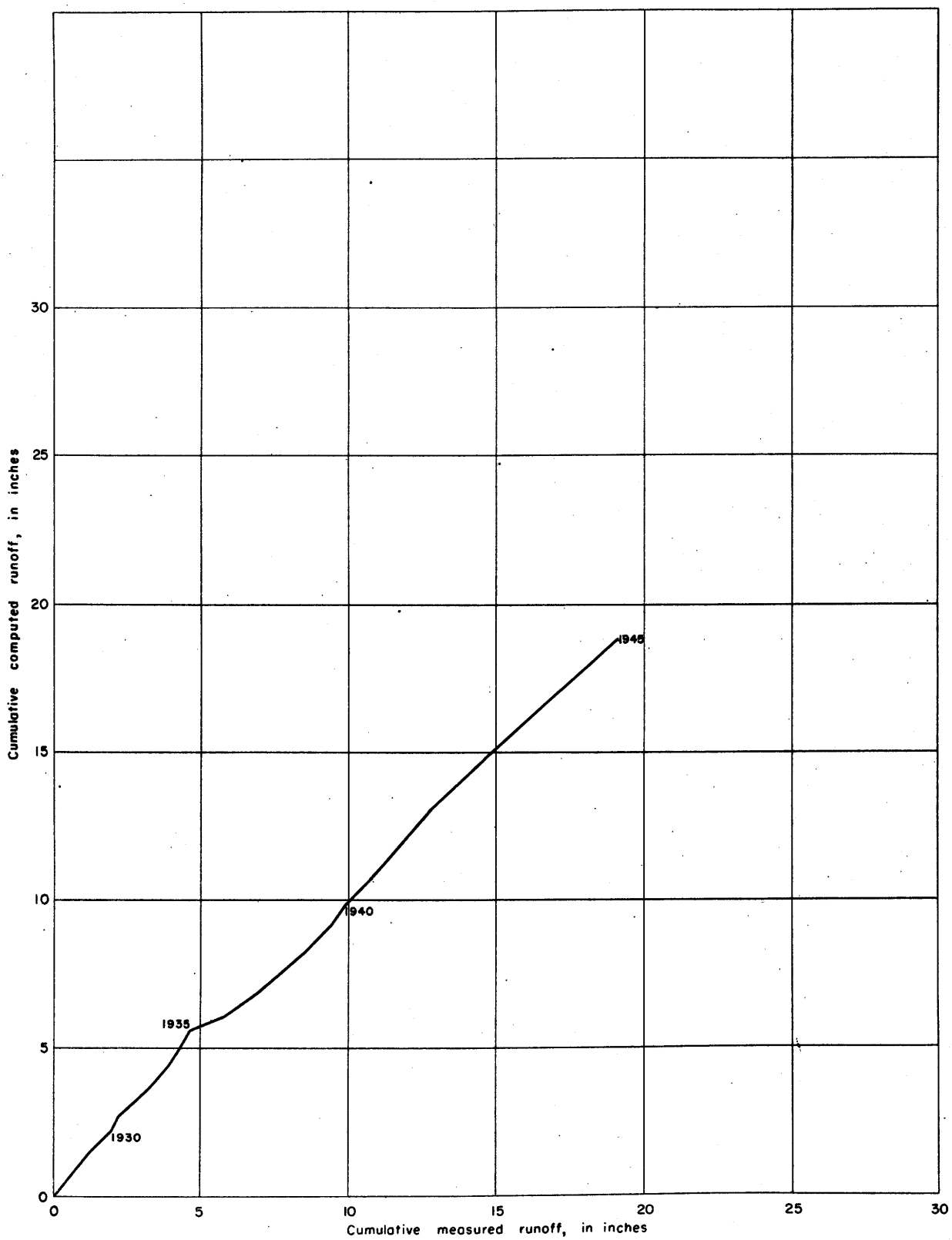

Figure 59.—Double mass curve of measured runoff plotted against computed runoff for Big Sioux River at Akron, Iowa.

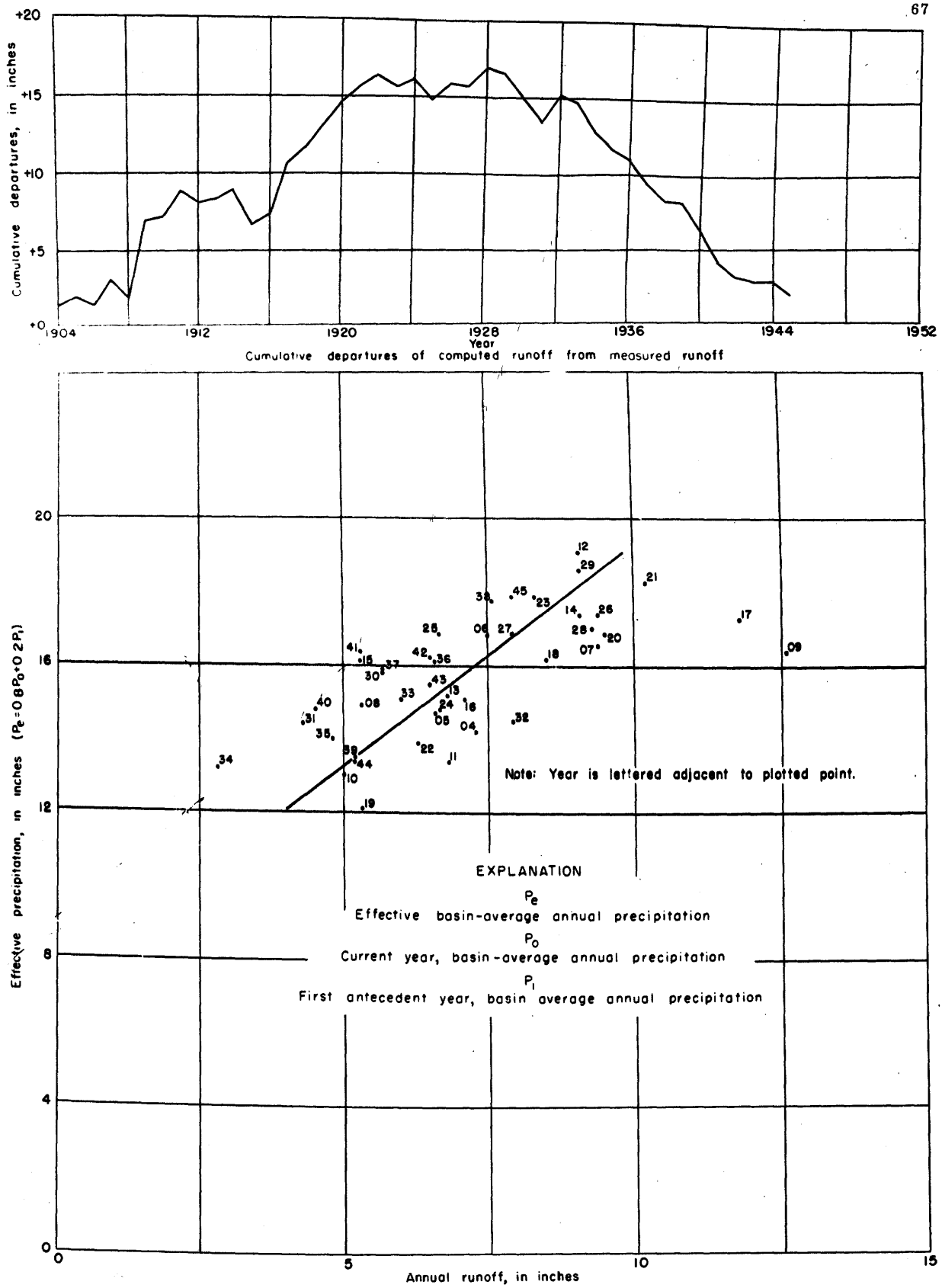

Figure 60. —Relationship of effective annual precipitation to annual runoff of North Platte River at Saratoga, Wyo.

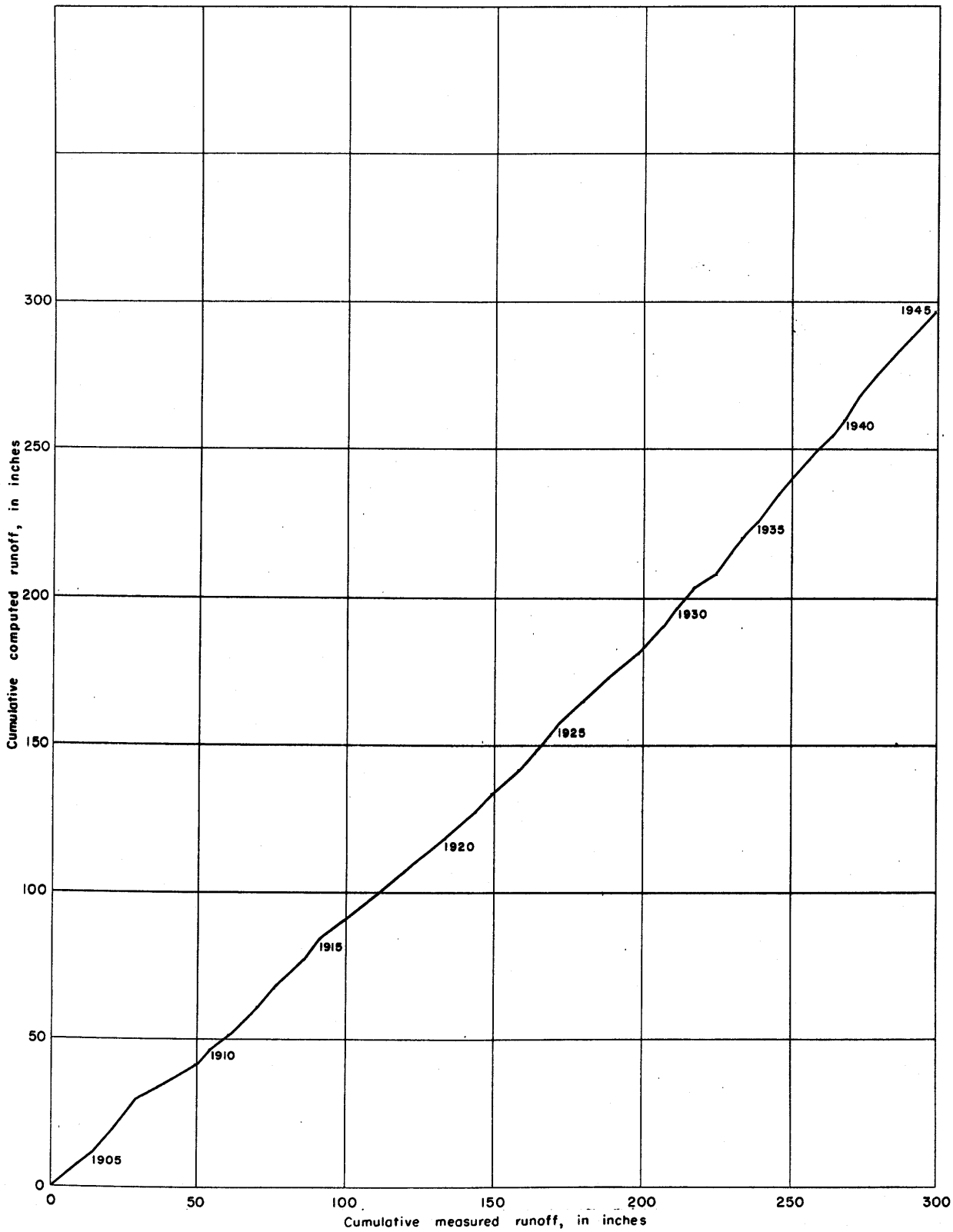

Figure 61.—Double mass curve of measured runoff plotted against computed runoff for North Platte River at Saratoga, Wyo.

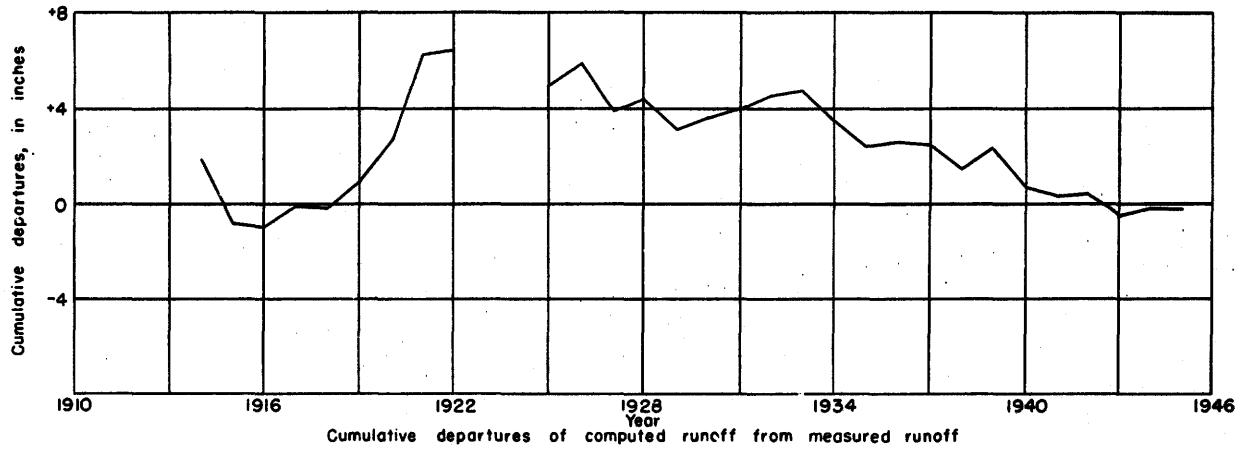

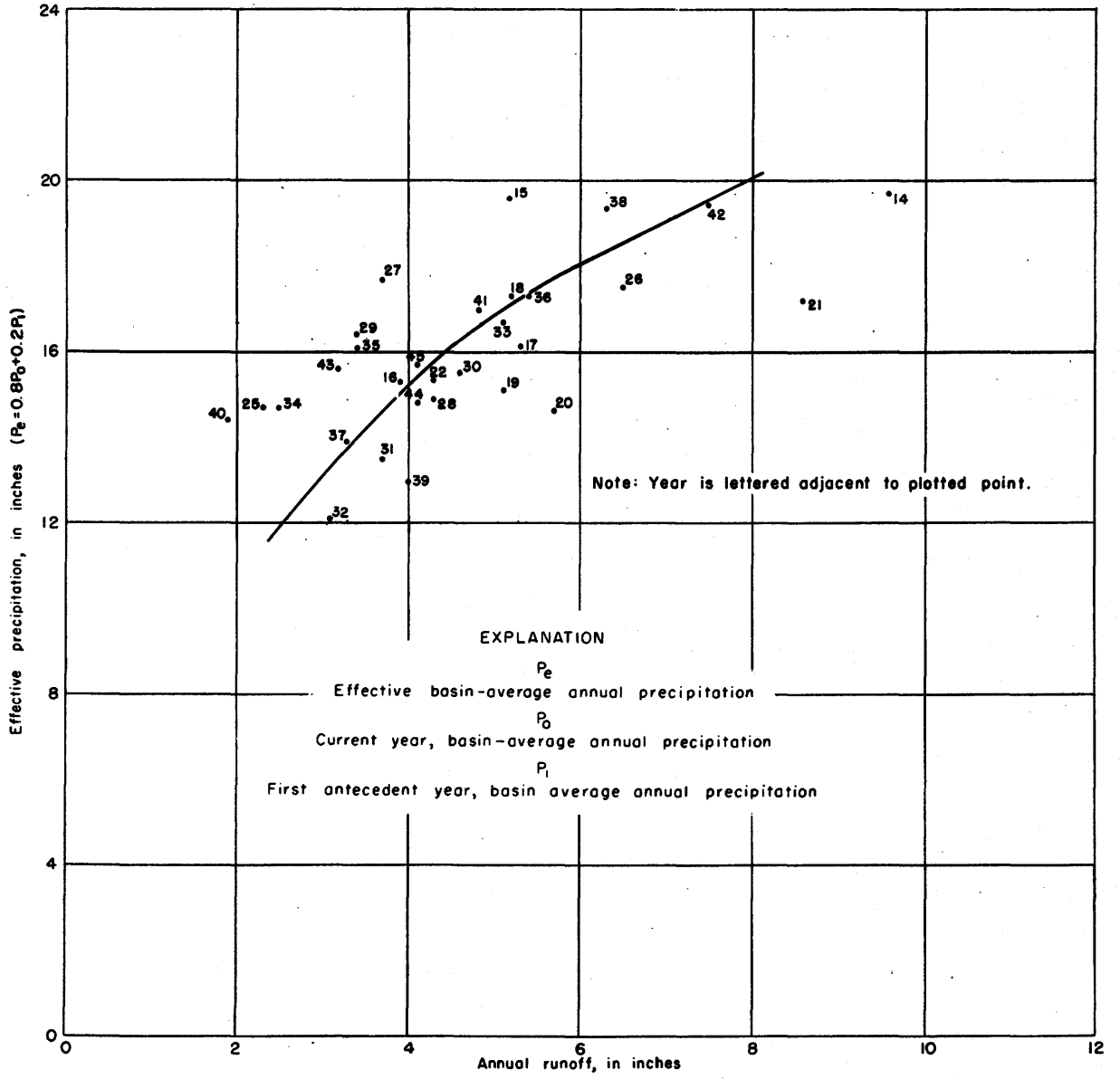

Figure 62. —Relationship of effective annual precipitation to annual runoff of North Fork South Platte River at South Platte, Colo.

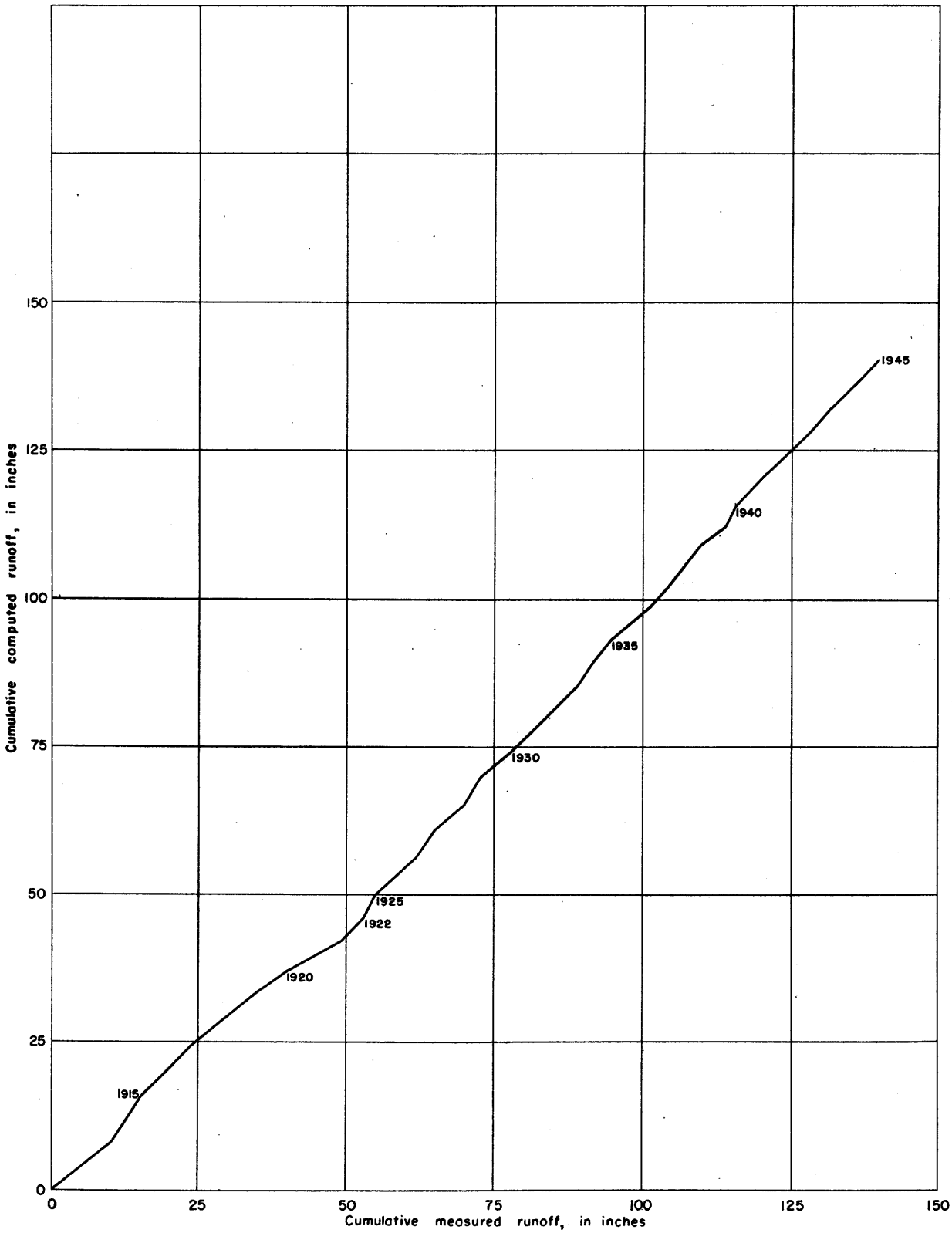

Figure 63. —Double mass curve of measured runoff plotted against computed runoff for North Fork South Platte River at South Platte, Colo.

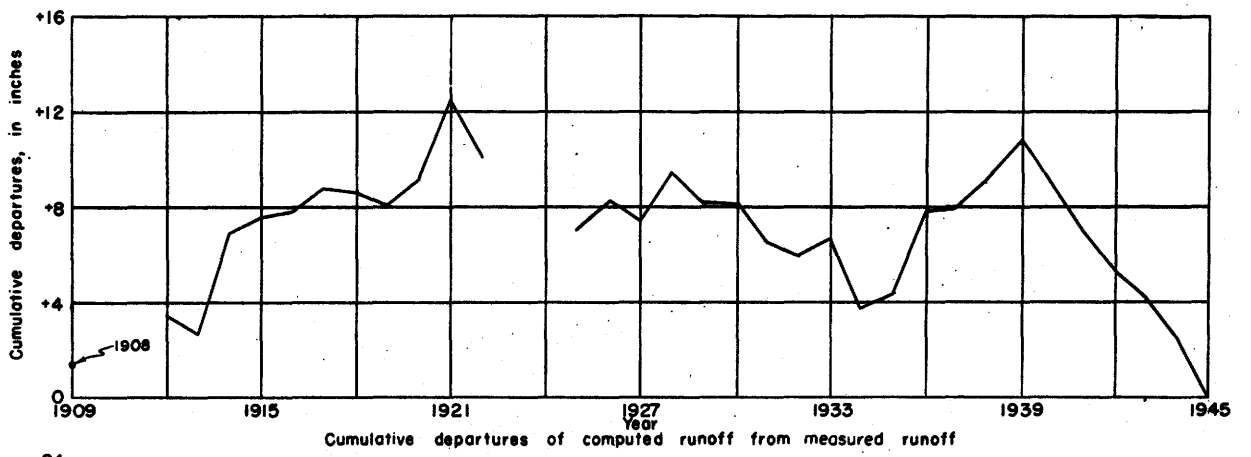

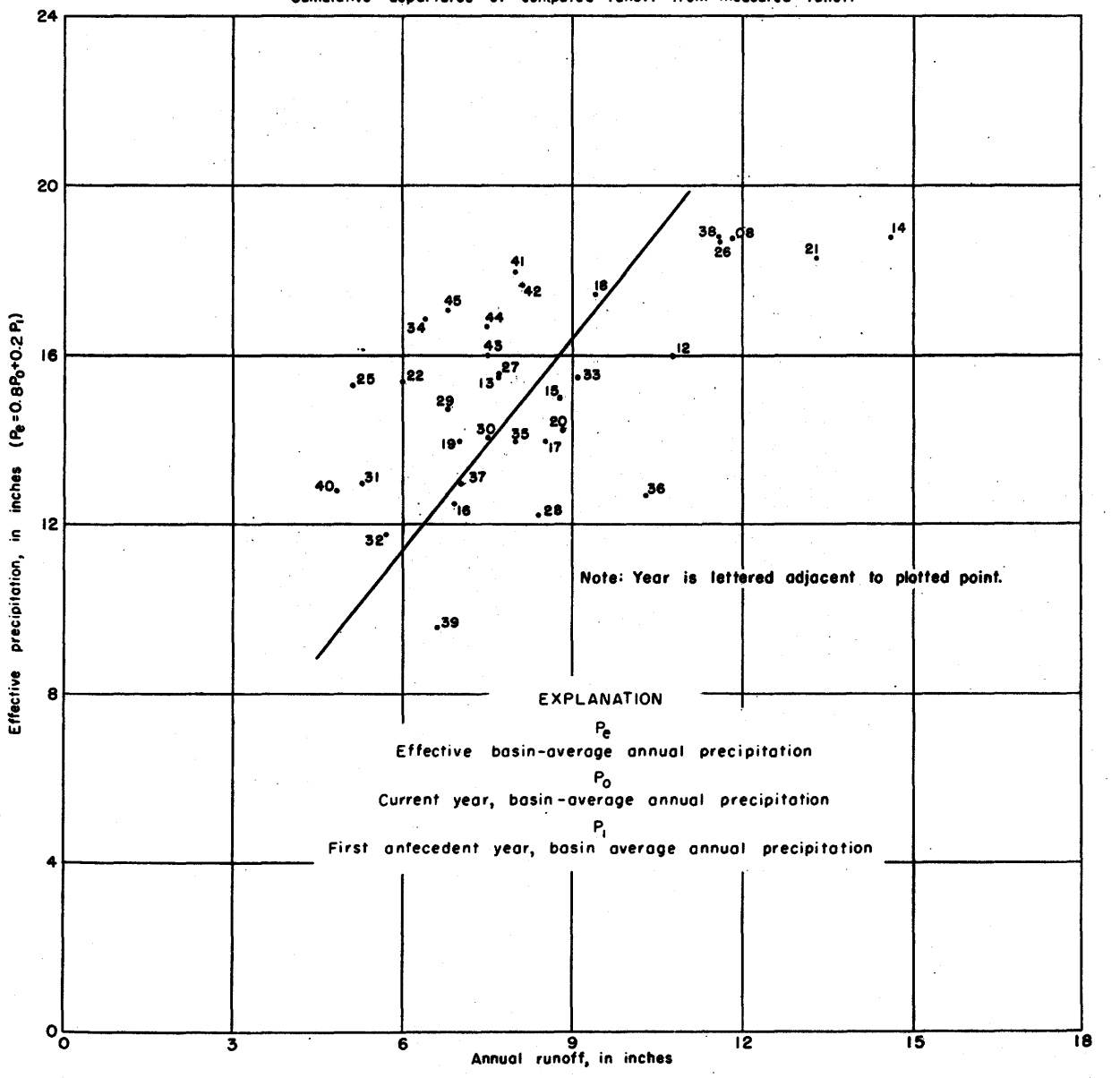

Figure 64. —Relationship of effective annual precipitation to annual runoff of Clear Creek near Golden, Colo.

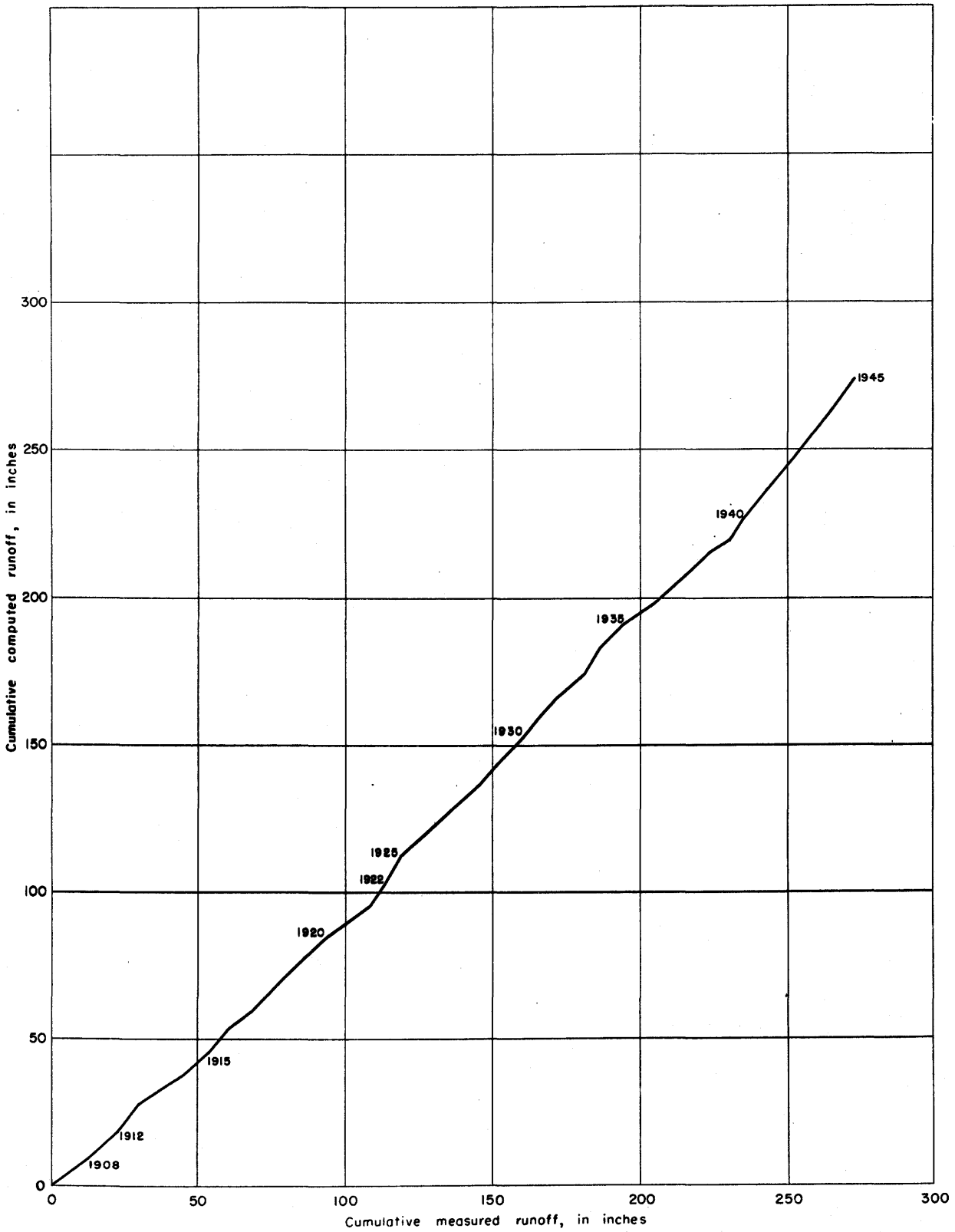

Figure 65. —Double mass curve of measured runoff plotted against computed runoff for Clear Creek near Golden, Colo.

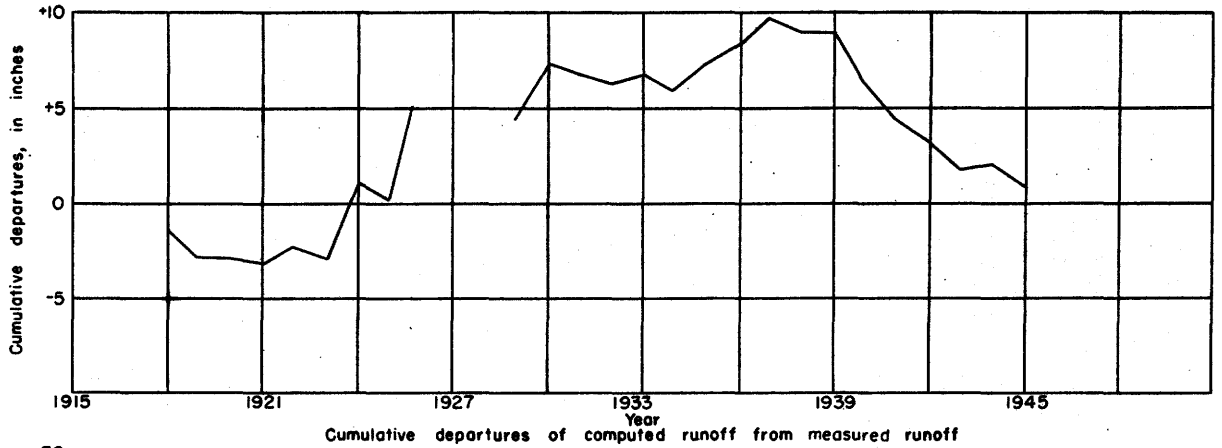

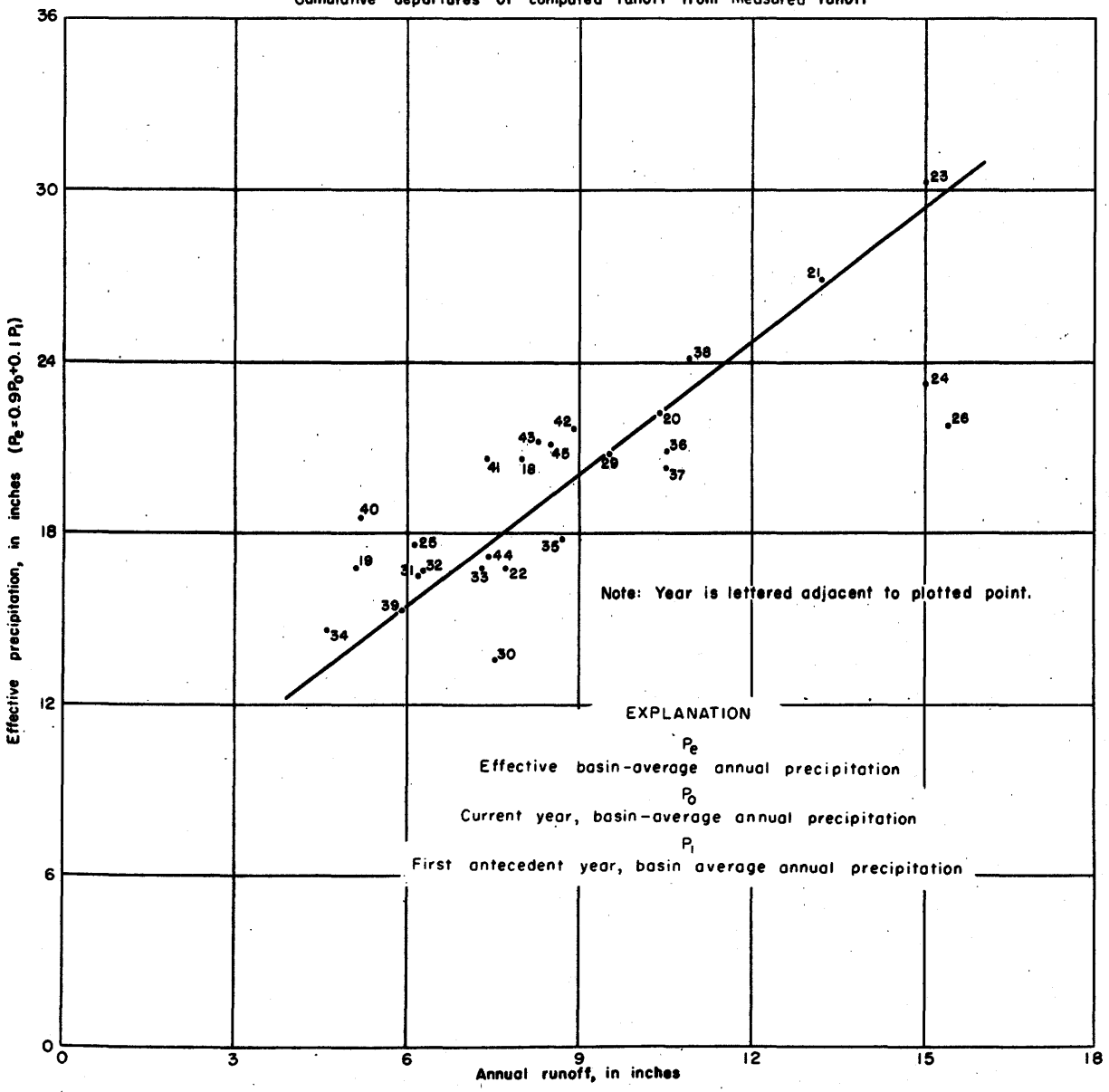

Figure 66. —Relationship of effective annual precipitation to annual runoff of Thompson River (below powerhouse) near Drake, Colo.

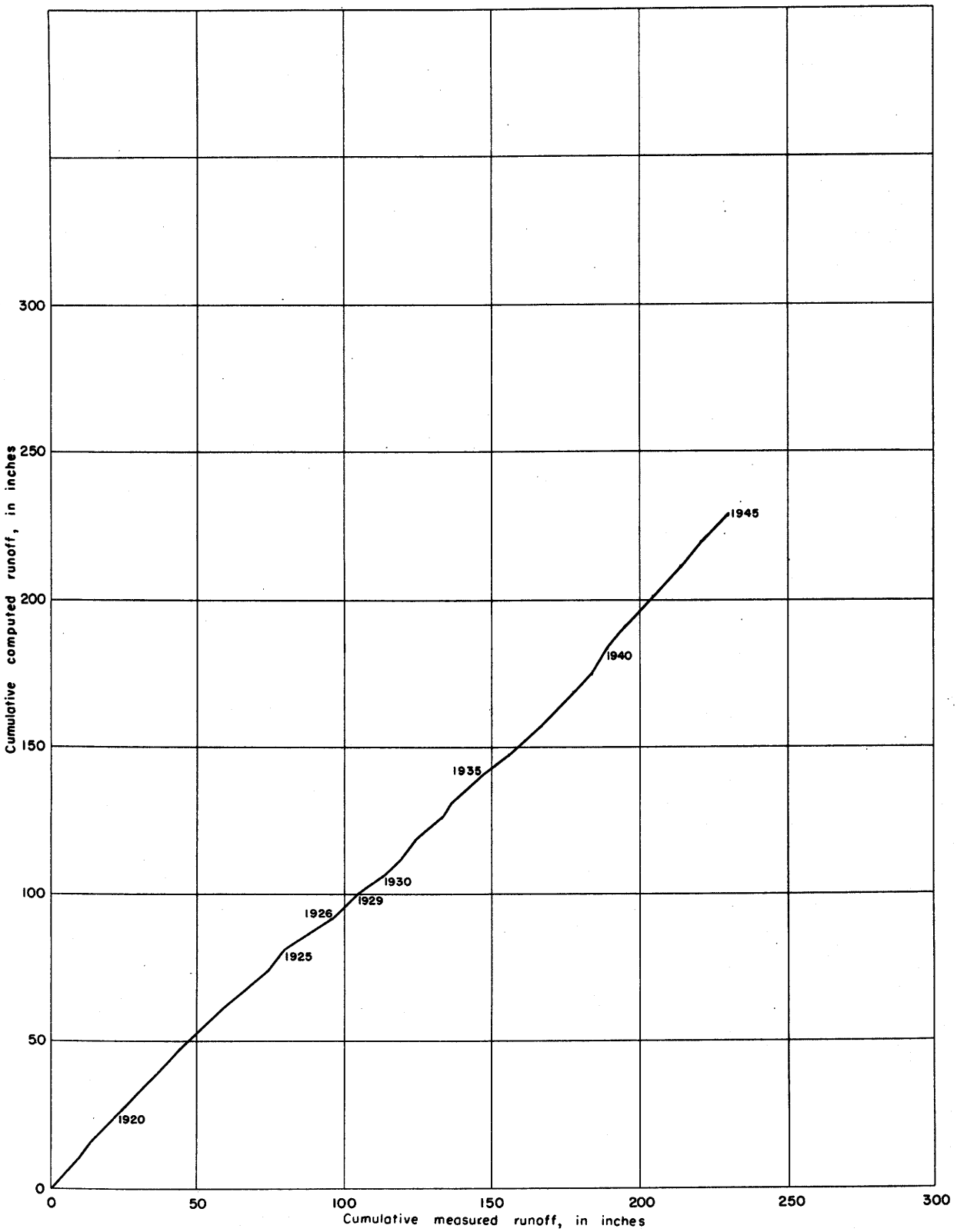

Figure 67.—Double mass curve of measured runoff plotted against computed runoff for Thompson River (below powerhouse) near Drake, Colo.

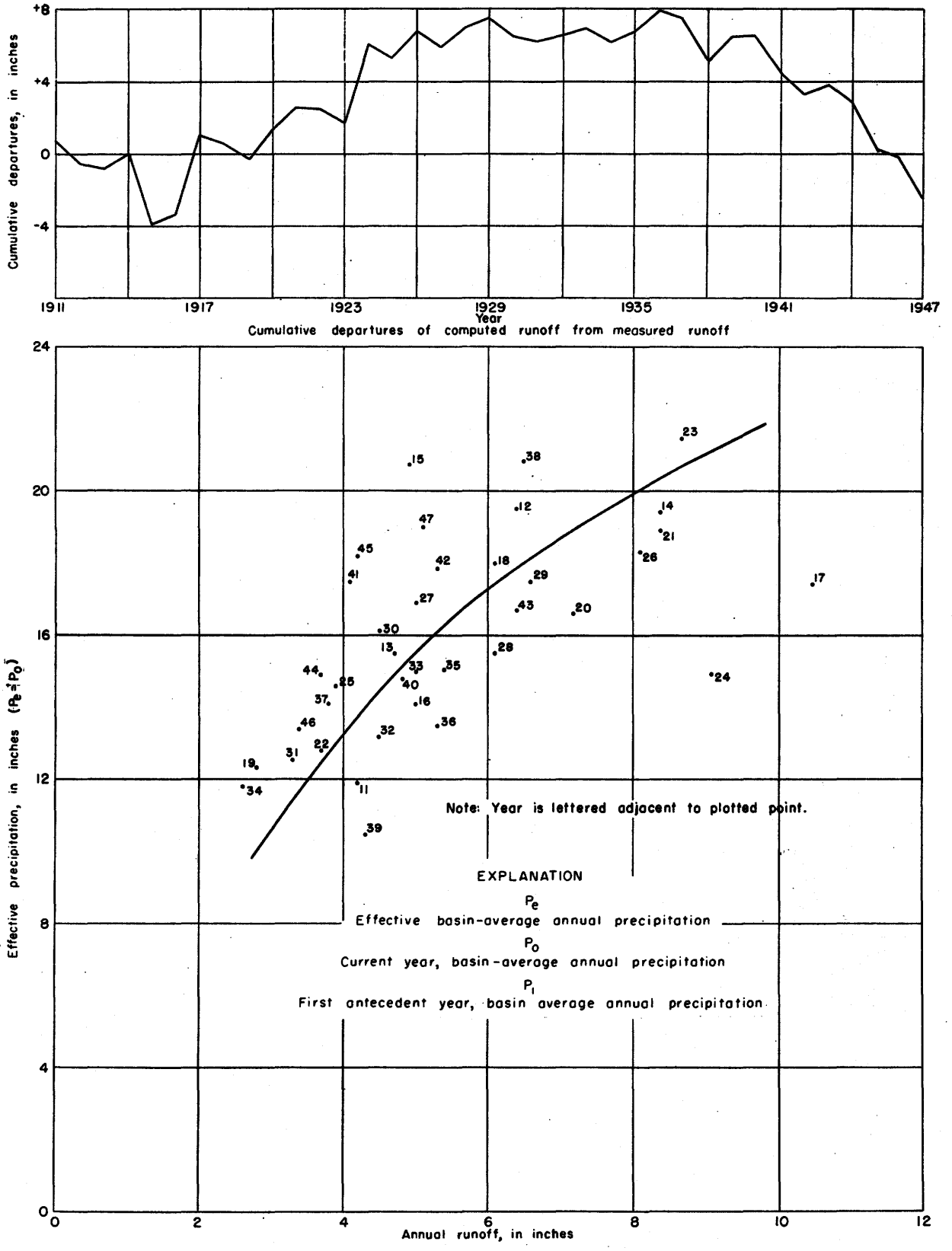

Figure 68.—Relationship of effective annual precipitation to annual runoff of Cache la Poudre River at mouth of canyon, near Fort Collins, Colo.

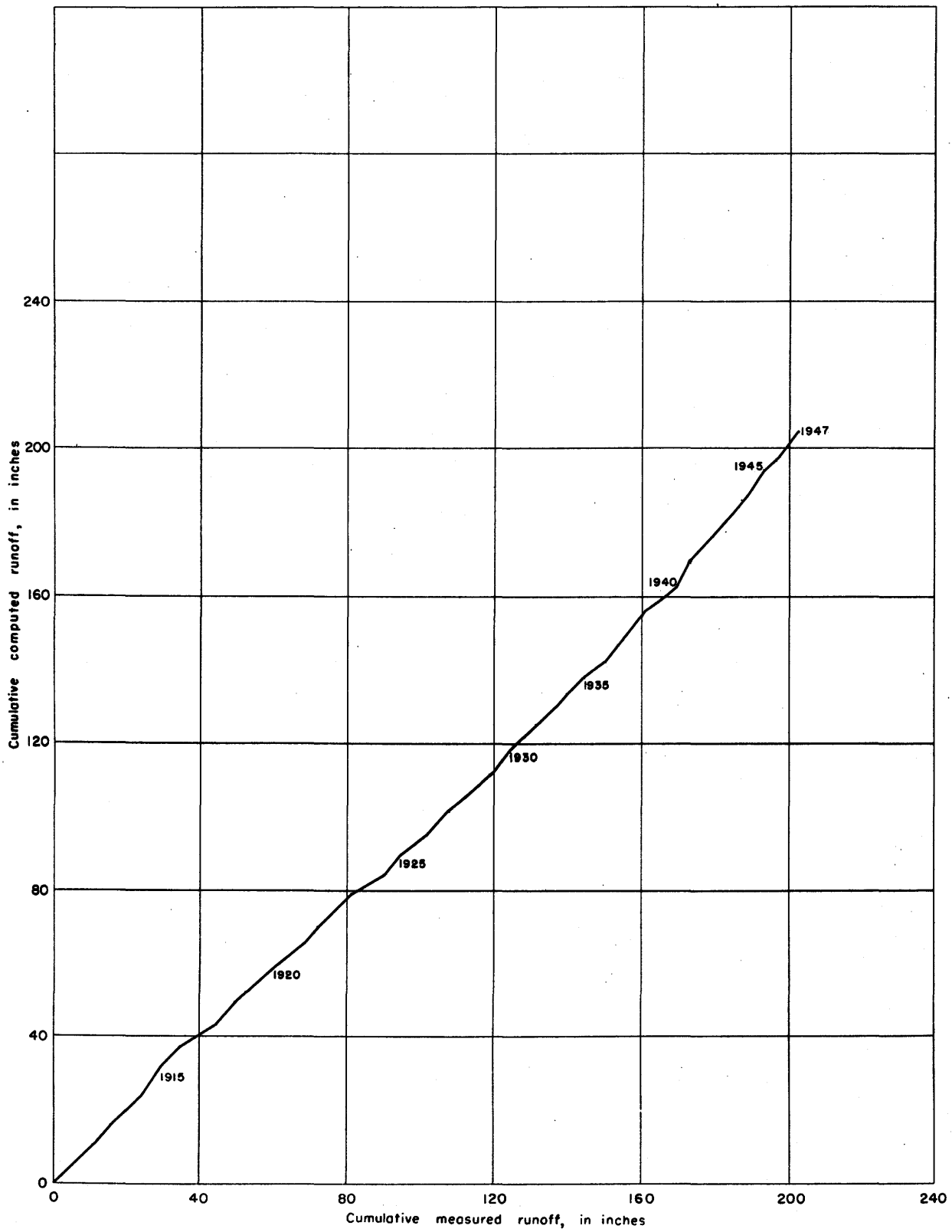

Figure 69.—Double mass curve of measured runoff plotted against computed runoff for Cache la Poudre River at mouth of canyon, near Fort Collins, Colo.

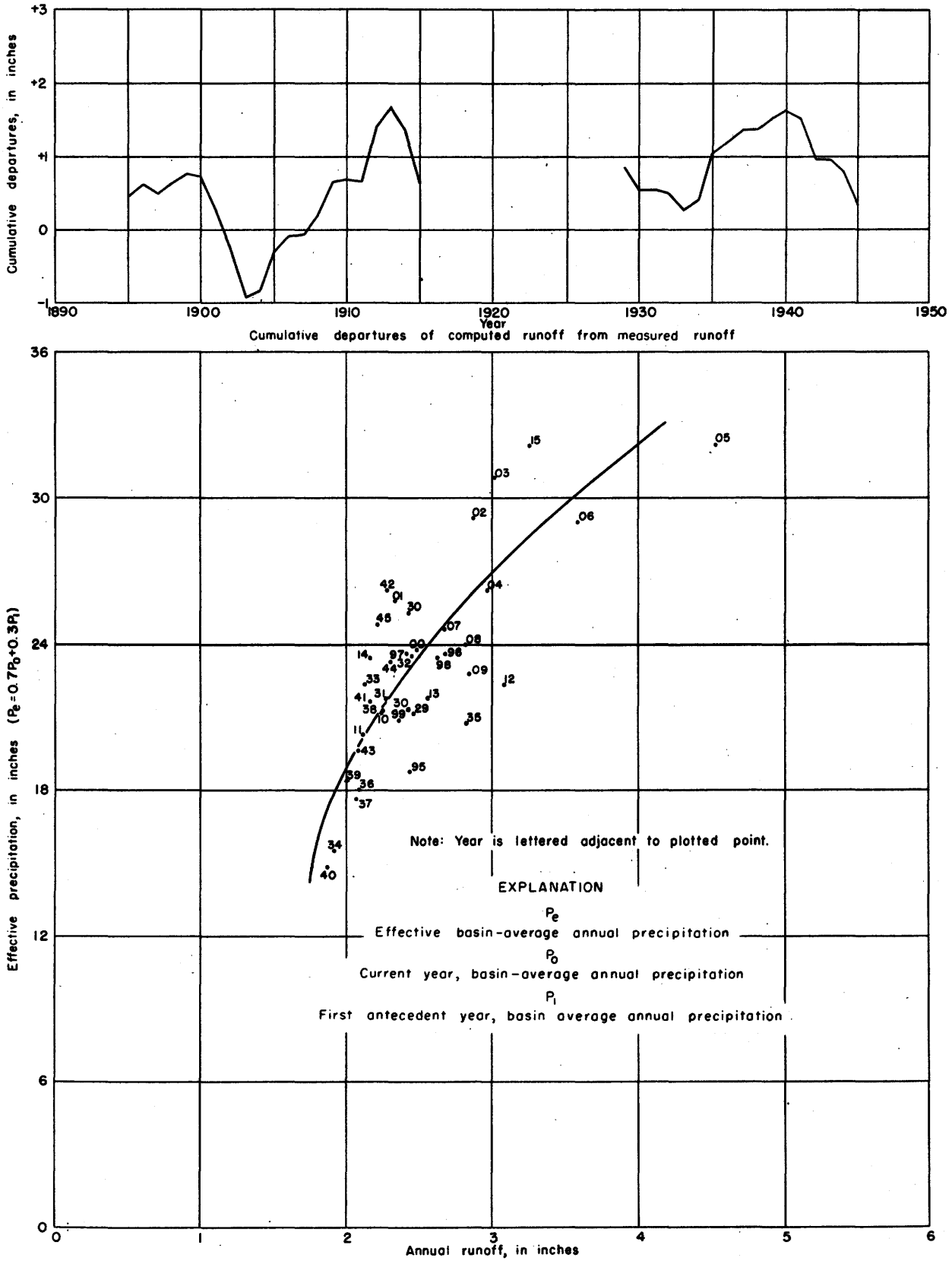

Figure 70. —Relationship of effective annual precipitation to annual runoff of Loup River at (near) Columbus, Nebr.

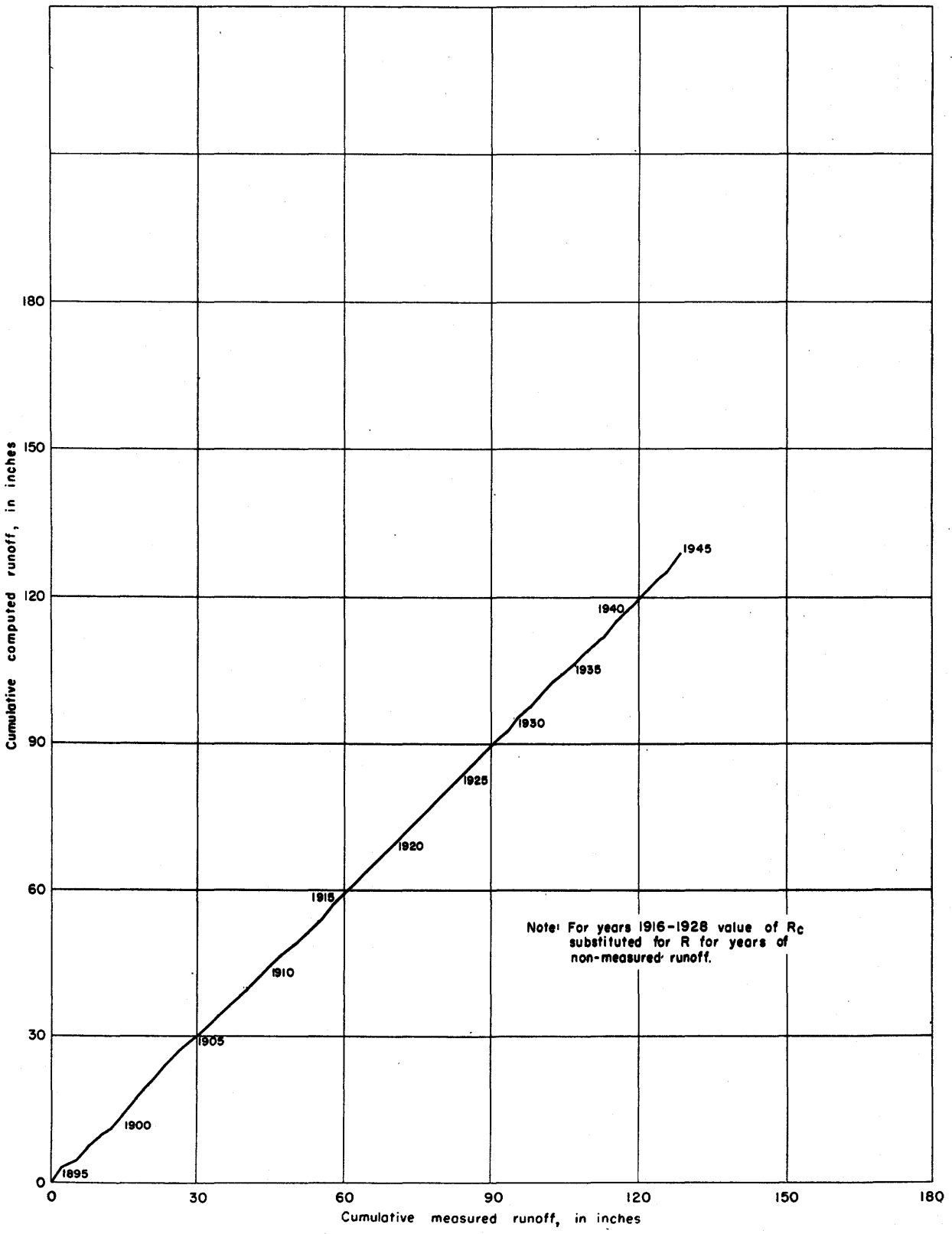

Figure 71. —Double mass curve of measured runoff plotted against computed runoff for Loup River at (near) Columbus, Nebr.

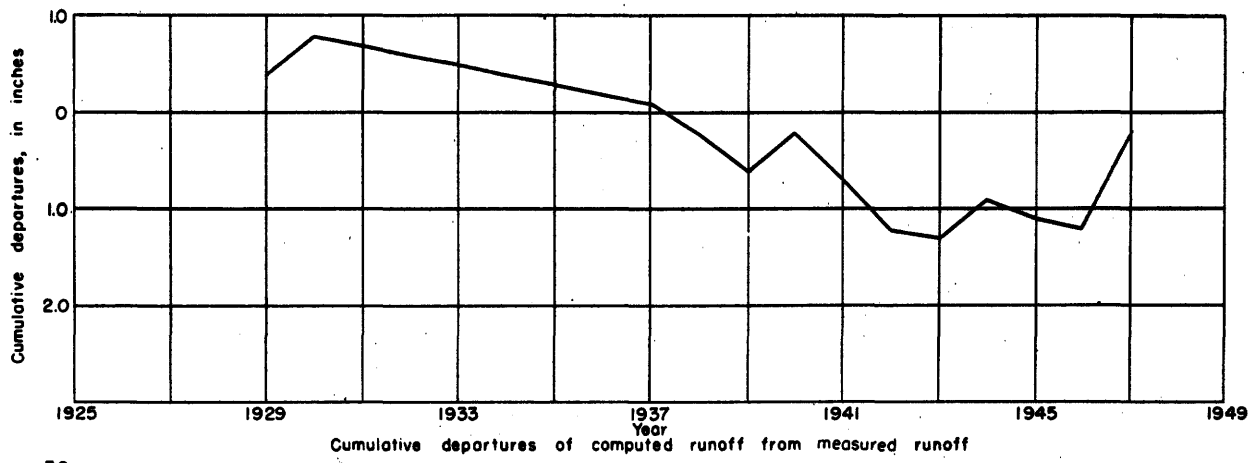

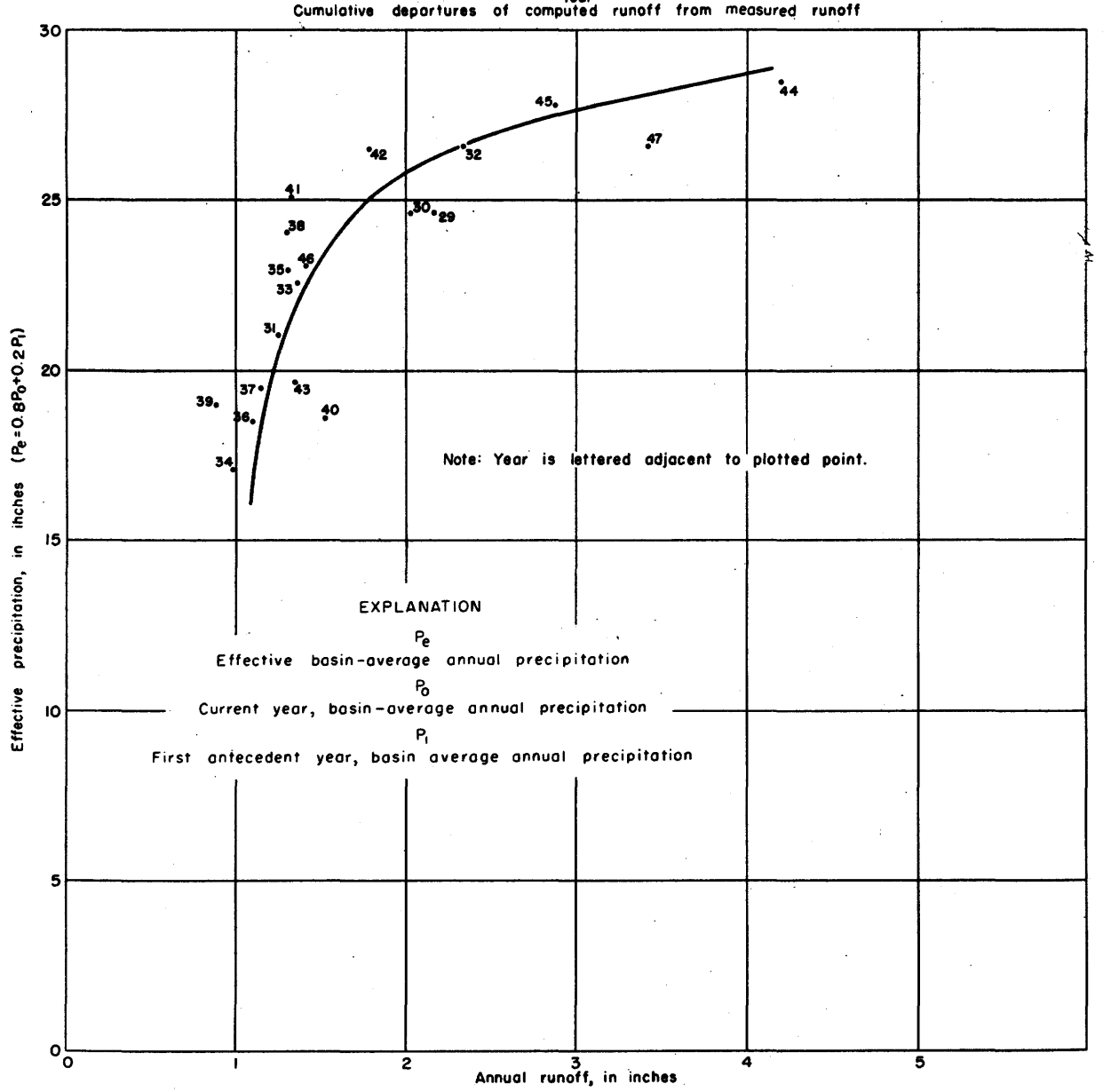

Figure 72. —Relationship of effective annual precipitation to annual runoff of Elkhorn River at Waterloo, Nebr.

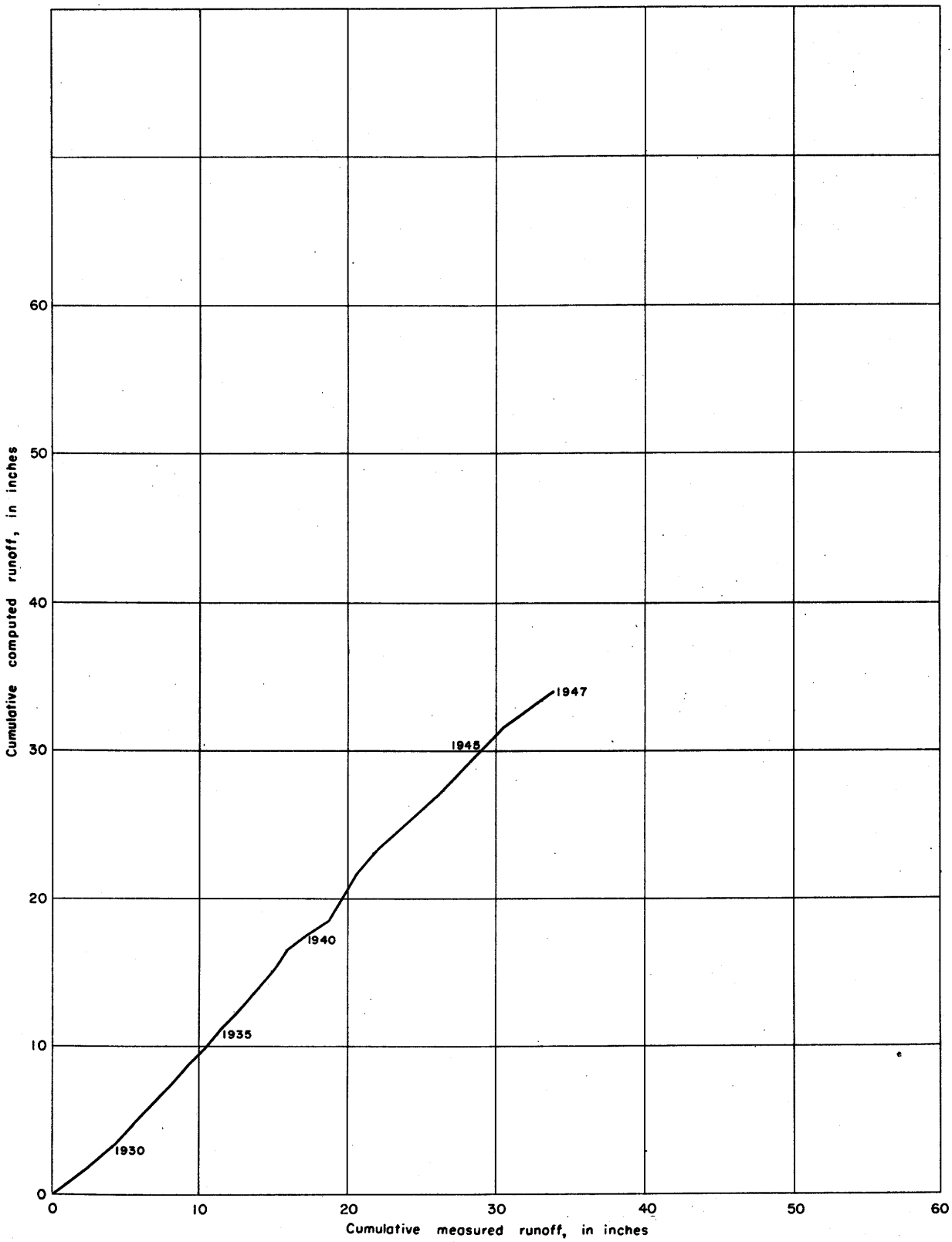

Figure 73.—Double mass curve of measured runoff plotted against computed runoff for Elkhorn River at Waterloo, Nebr.

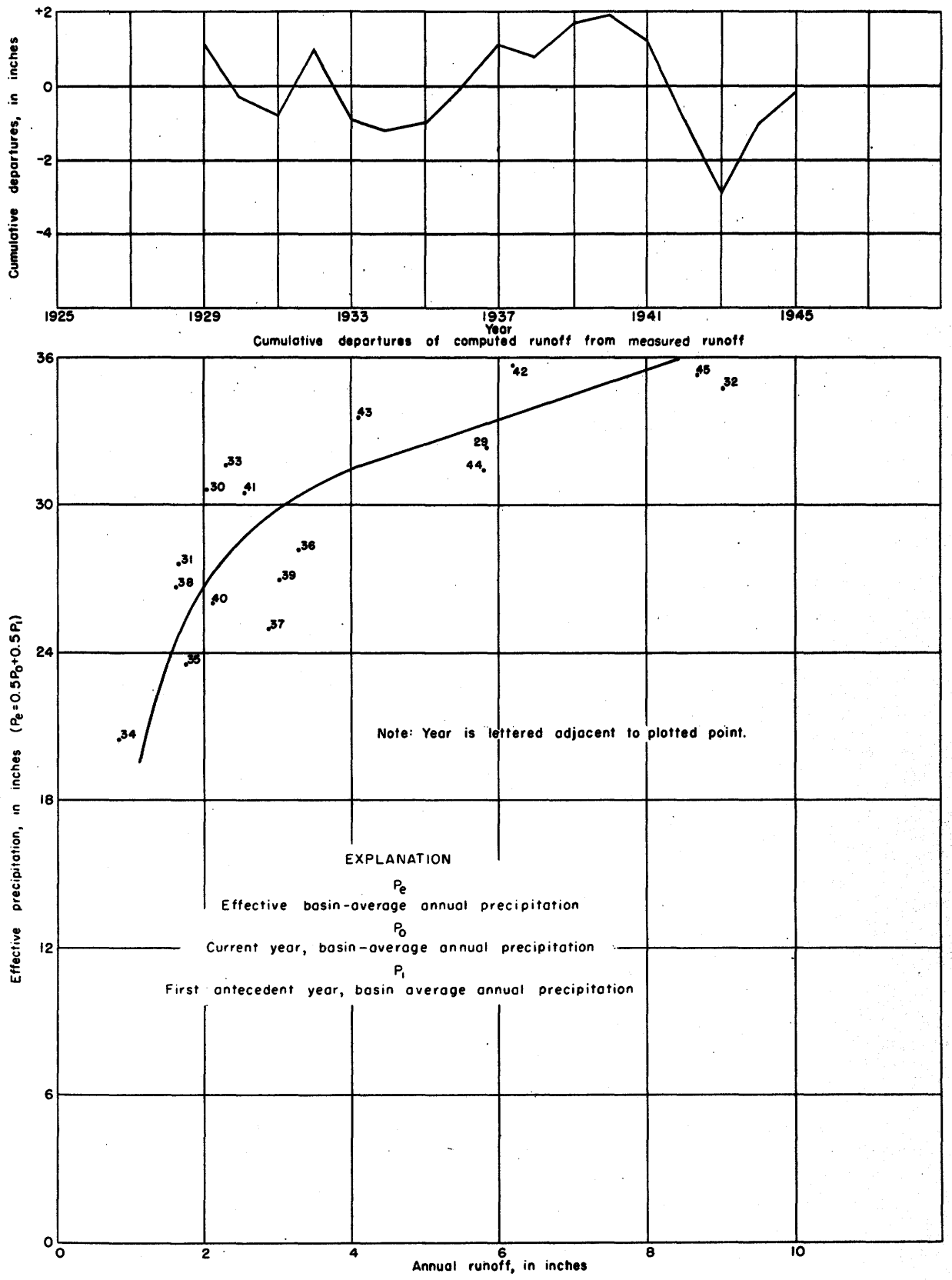

Figure 74.—Relationship of effective annual precipitation to annual runoff of Nishnabotna River above Hamburg, Iowa.

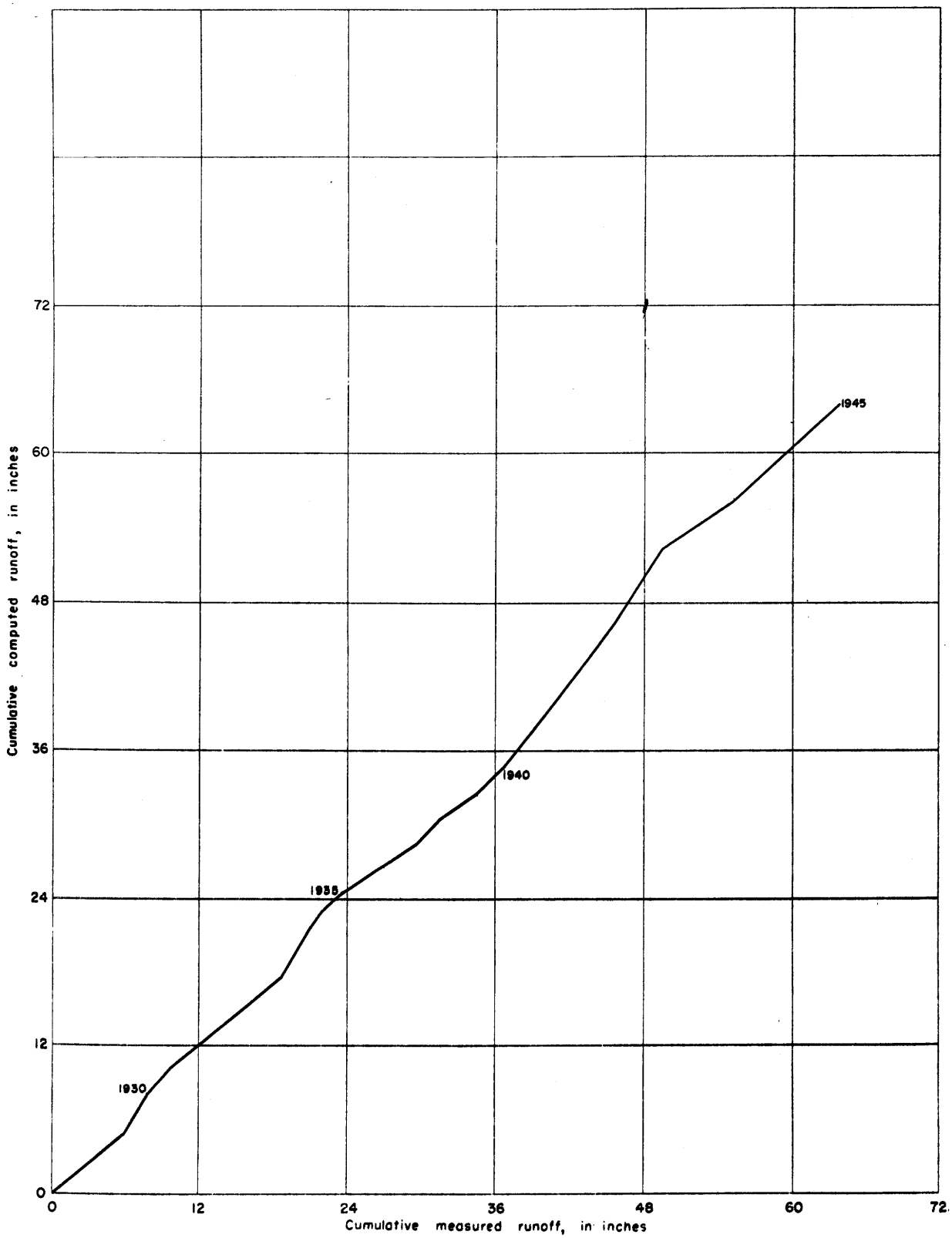

Figure 75. —Double mass curve of measured runoff plotted against computed runoff for Nishnabotna River above Hamburg, Iowa.

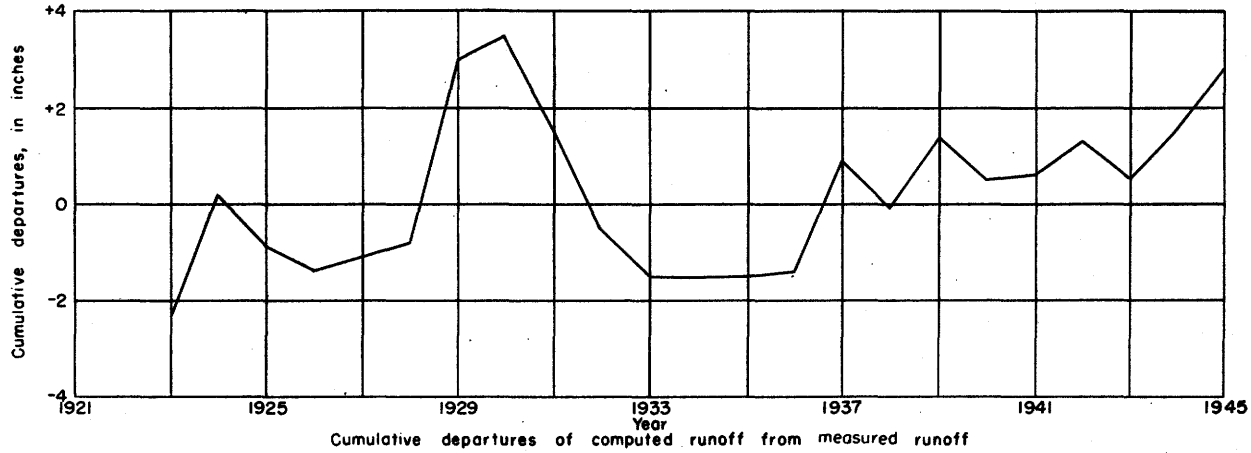

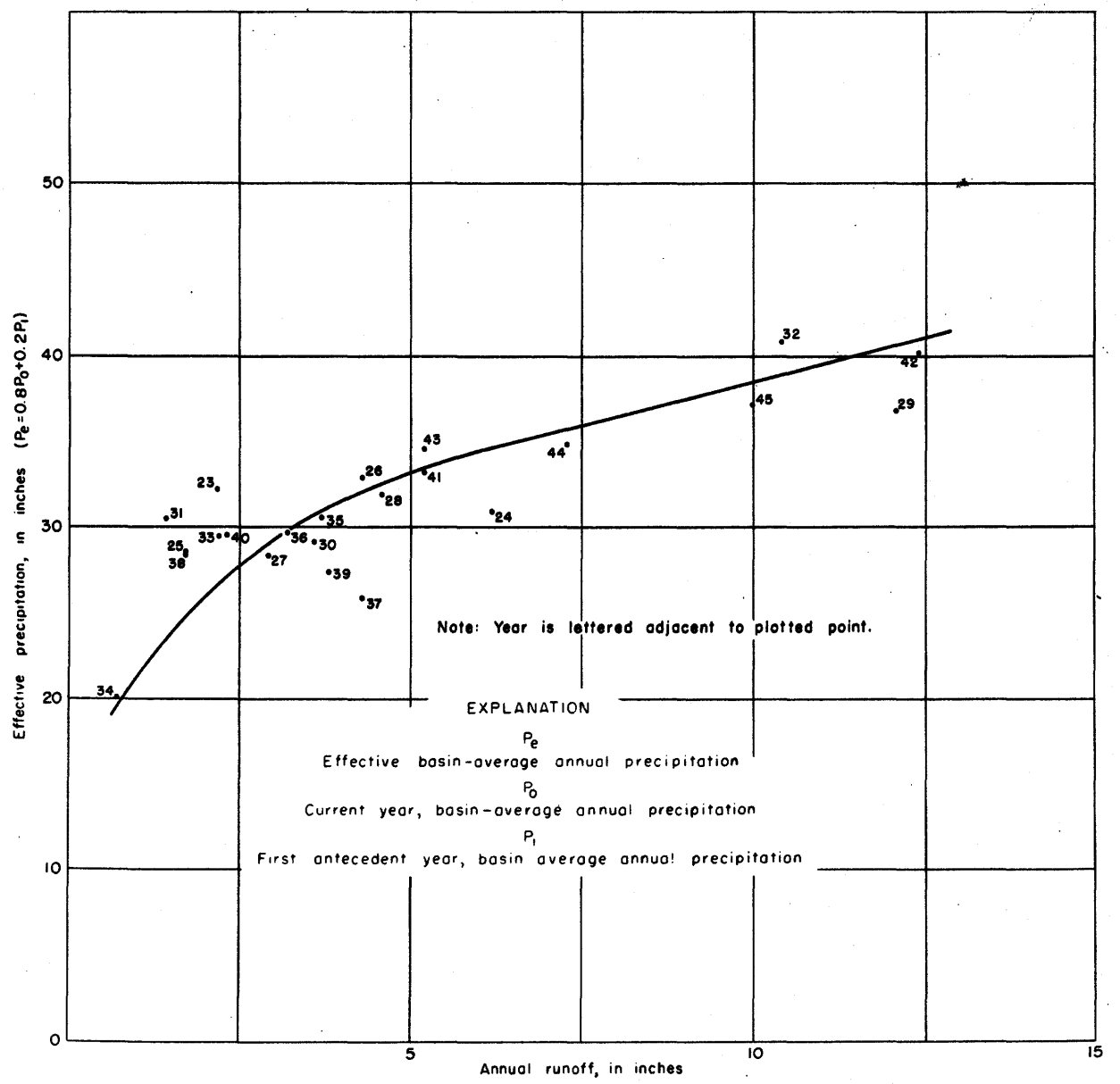

Figure 76. —Relationship of effective annual precipitation to annual runoff of Nodaway River near Burlington Junction, Mo.

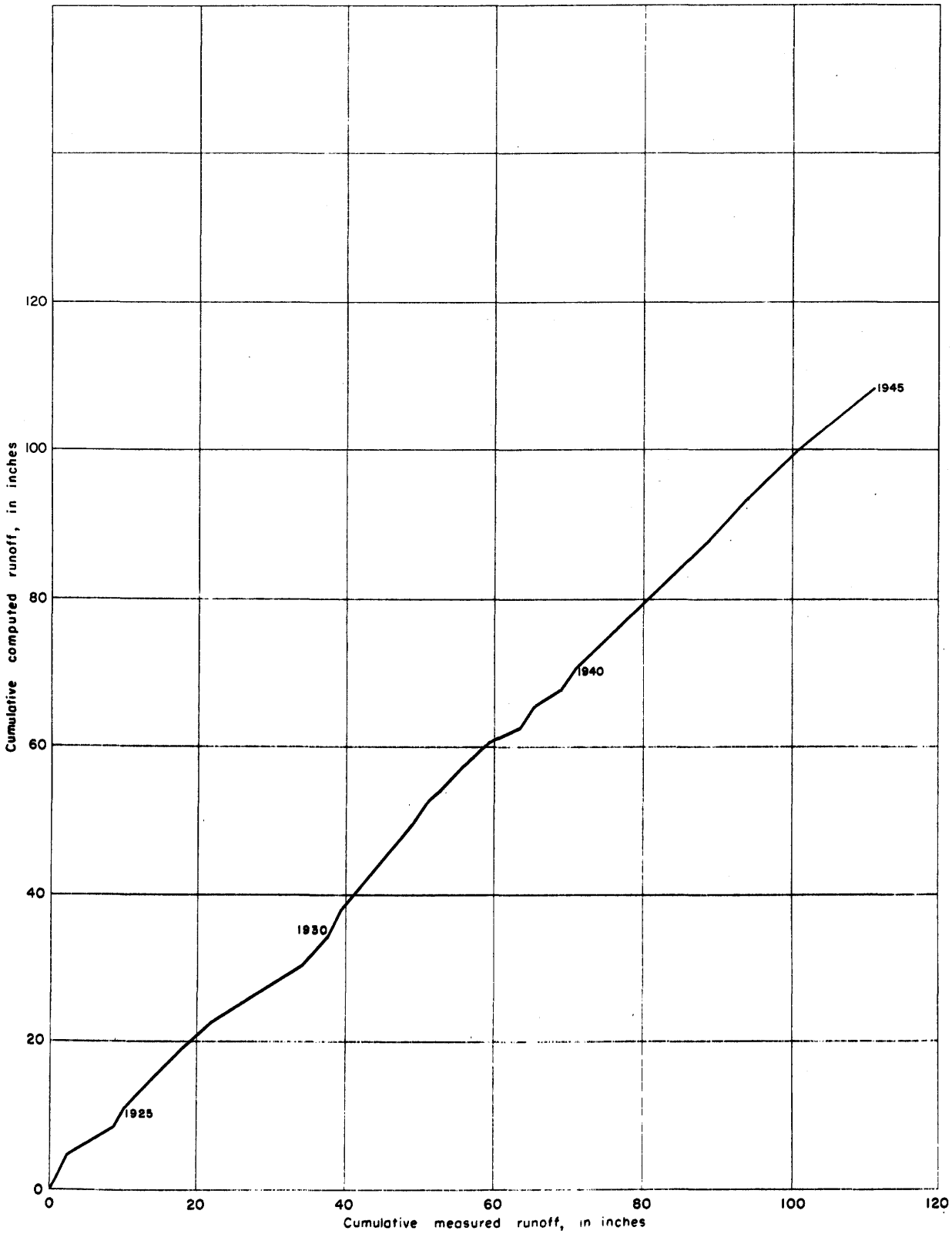

Figure 77. —Double mass curve of measured runoff plotted against computed runoff for Nodaway River near Burlington Junction, Mo.

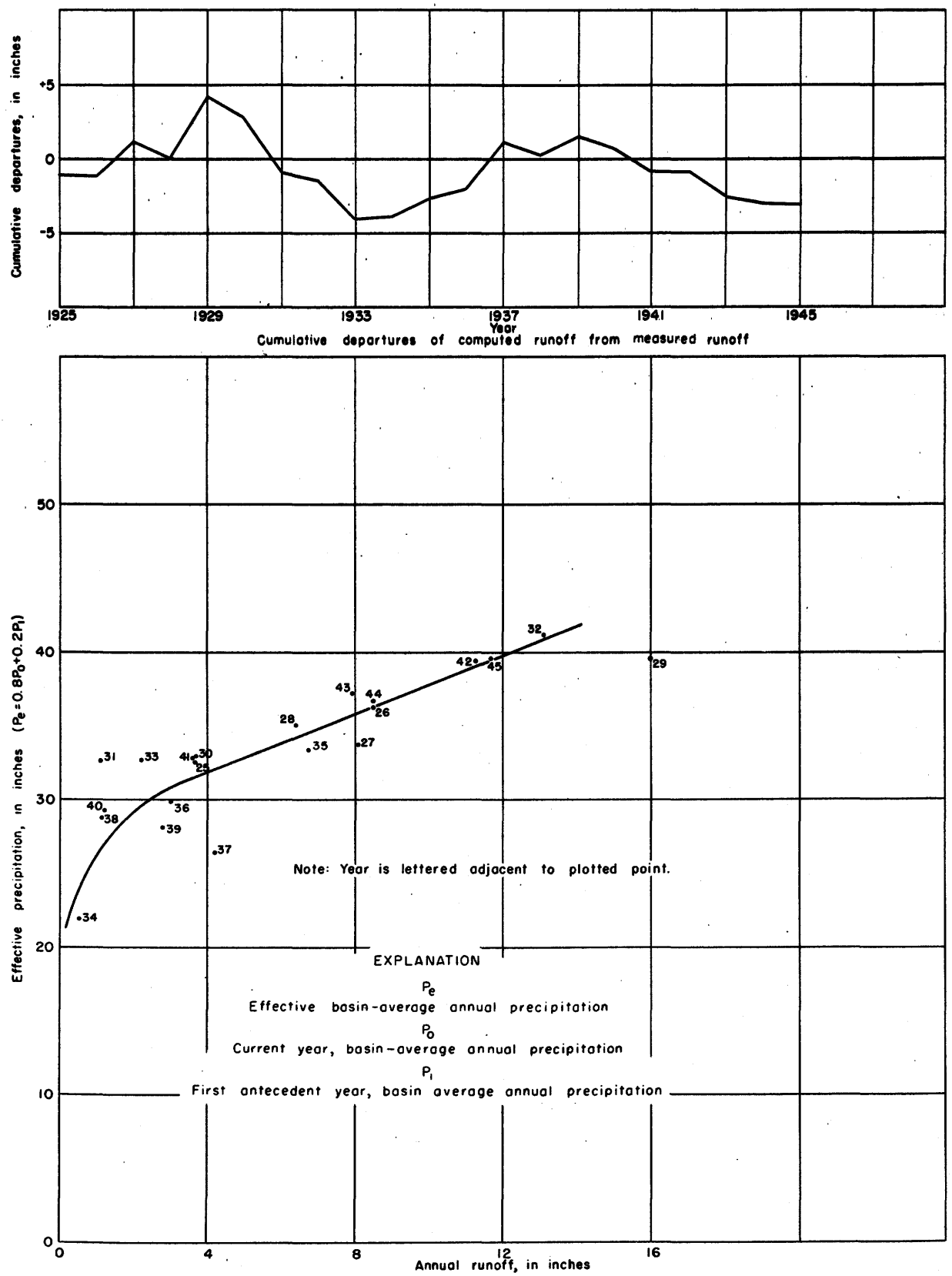

Figure 78.—Relationship of effective annual precipitation to annual runoff of Platte River near Agency, Mo.

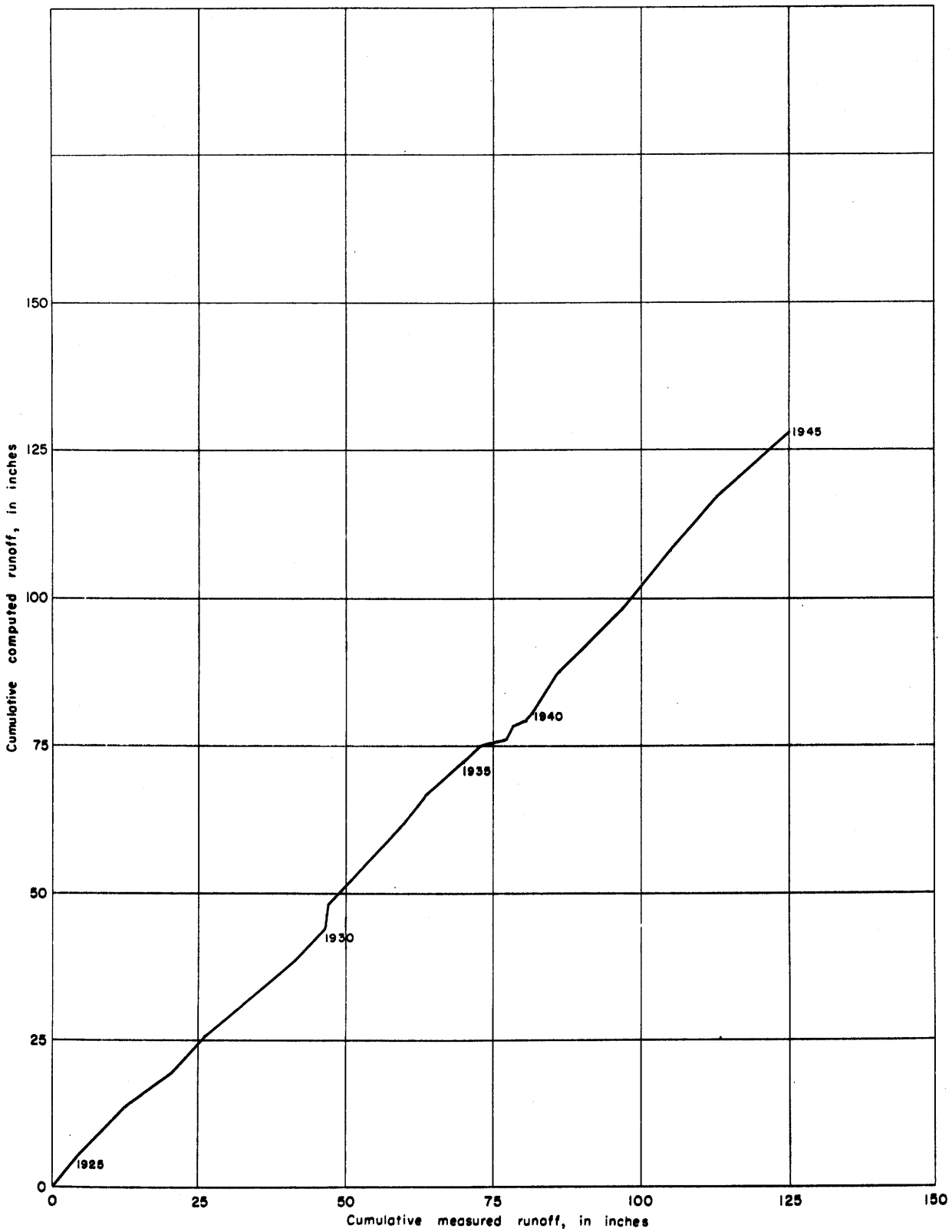

Figure 79. —Double mass curve of measured runoff plotted against computed runoff for Platte River near Agency, Mo.

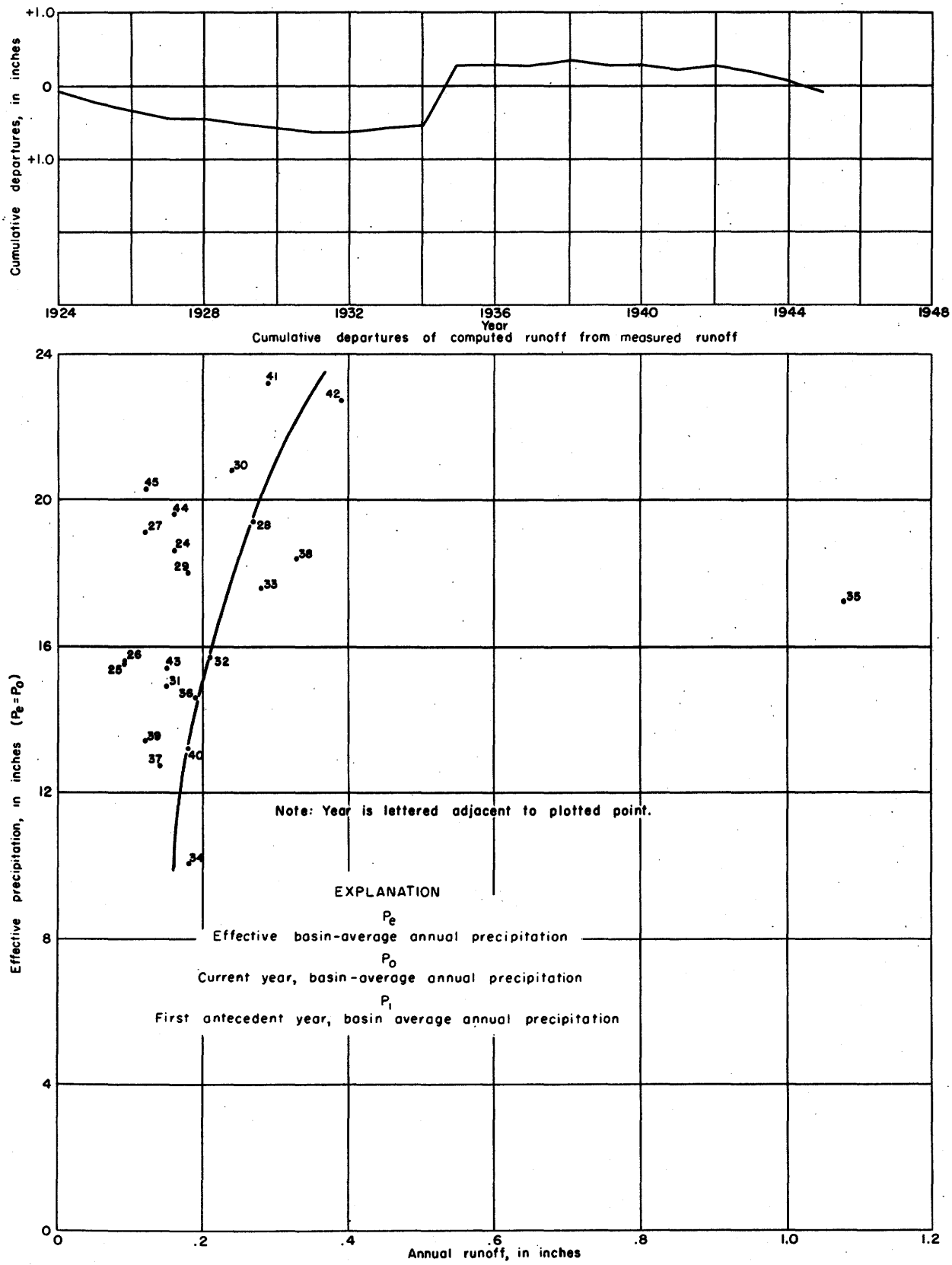

Figure 80. —Relationship of effective annual precipitation to annual runoff of Arikaree River at Haigler, Nebr.

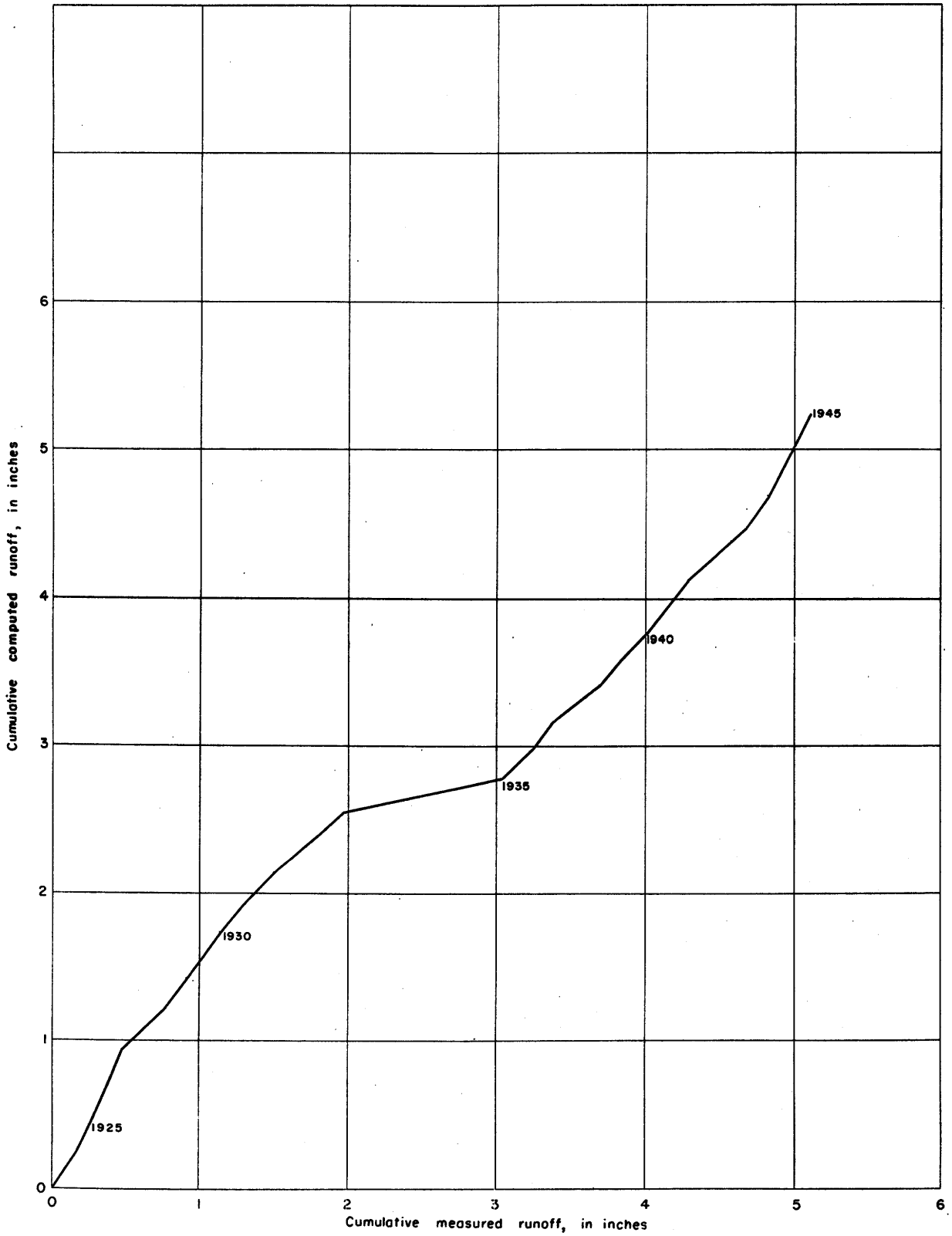

Figure 81.—Double mass curve of measured runoff plotted against computed runoff for Arikaree River at Haigler, Nebr.

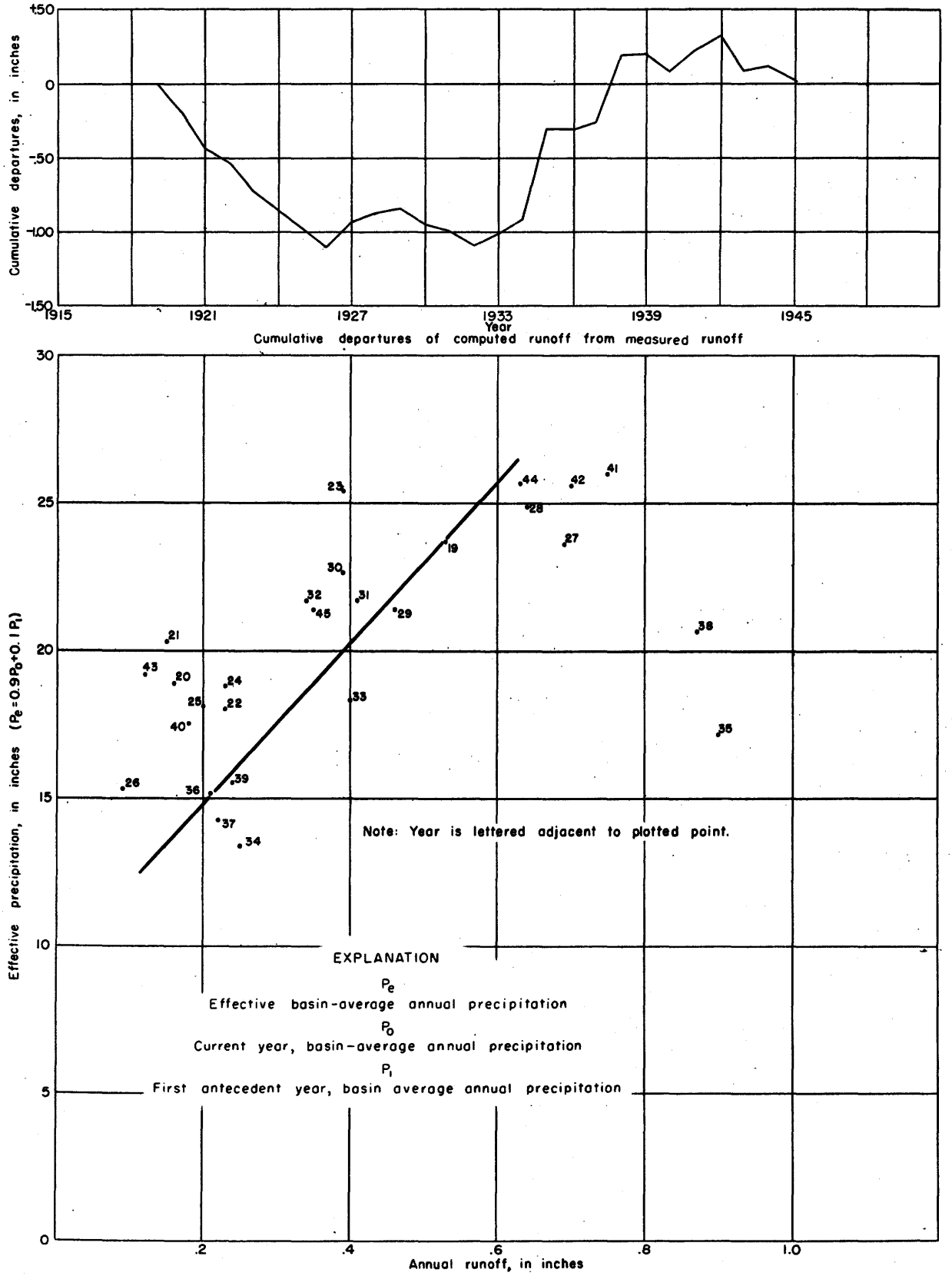

Figure 82.—Relationship of effective annual precipitation to annual runoff of Smoky Hill River at Ellsworth, Kans.

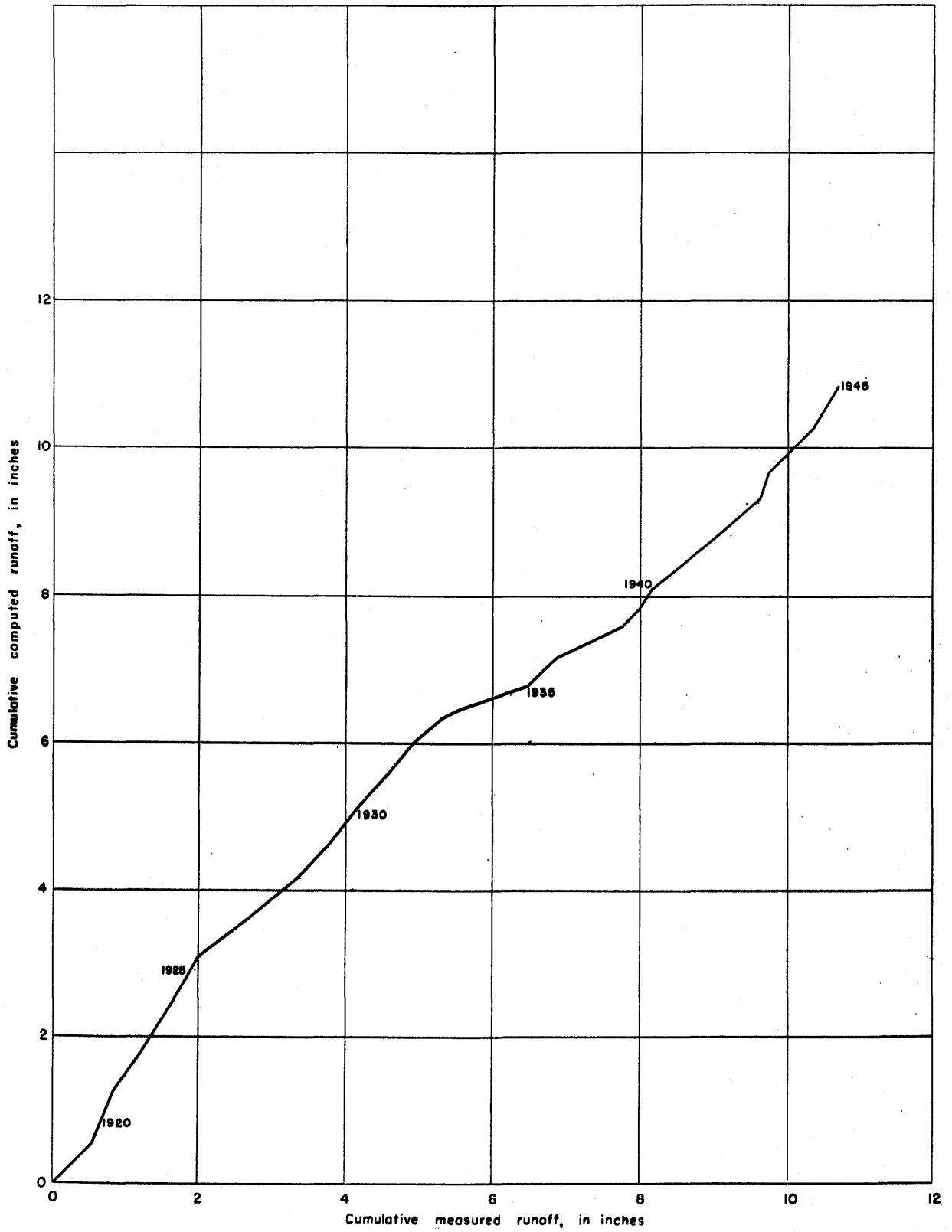

Figure 83.—Double mass curve of measured runoff plotted against computed runoff for Smoky Hill River at Ellsworth, Kans.

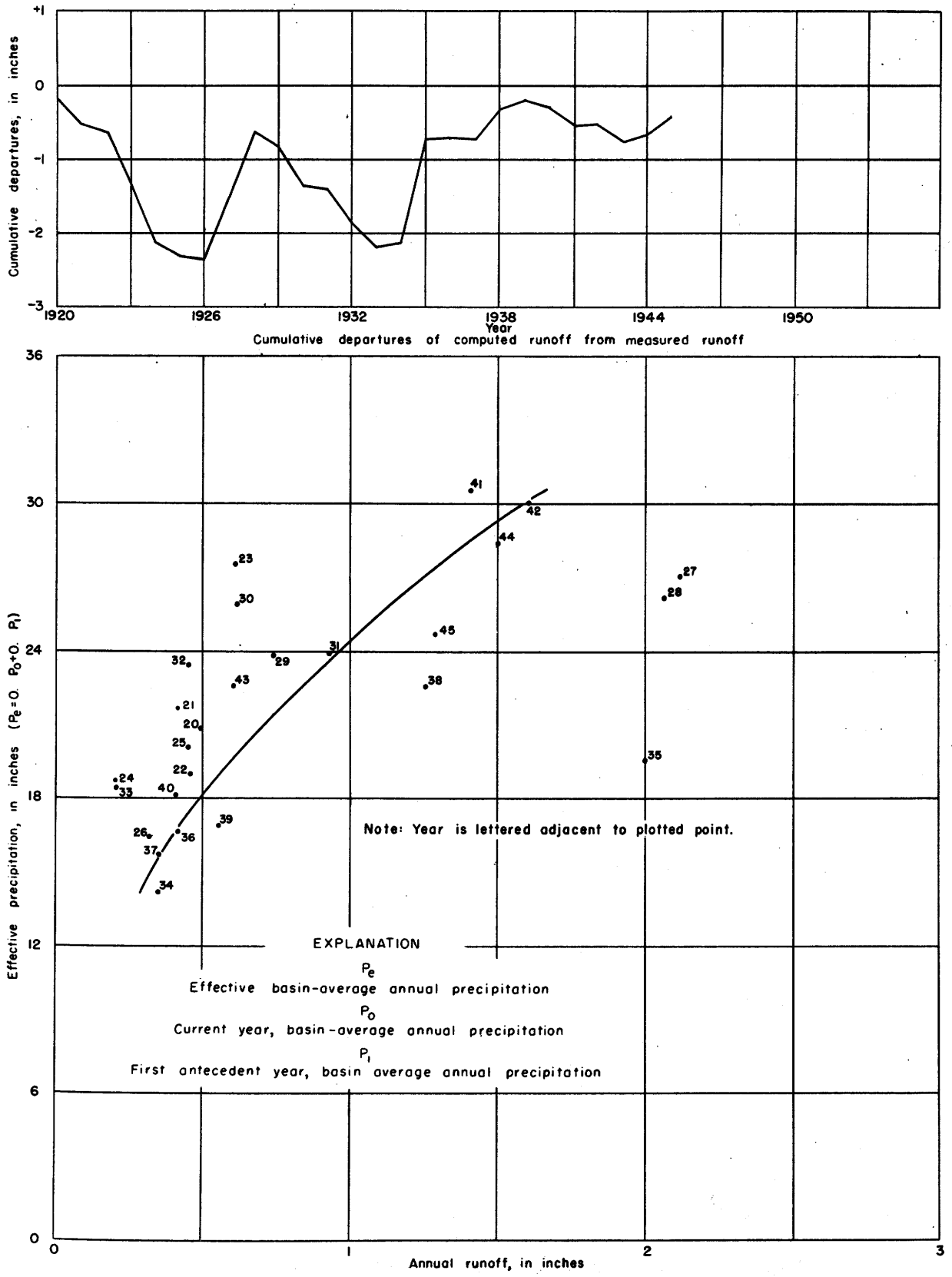

Figure 84. —Relationship of effective annual precipitation to annual runoff of Saline River at Tescott, Kans.

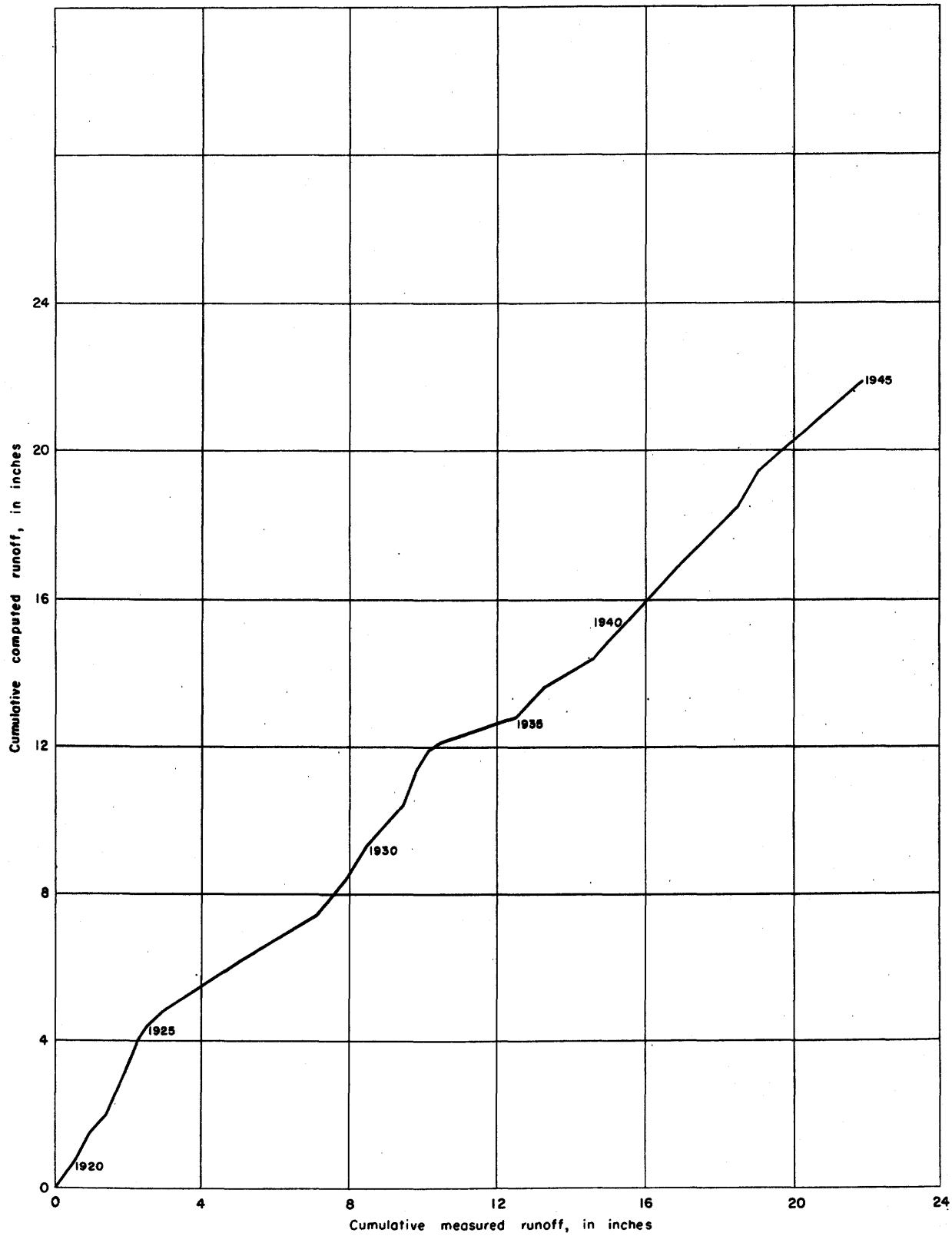

Figure 85. —Double mass curve of measured runoff plotted against computed runoff for Saline River at Tescott, Kans.

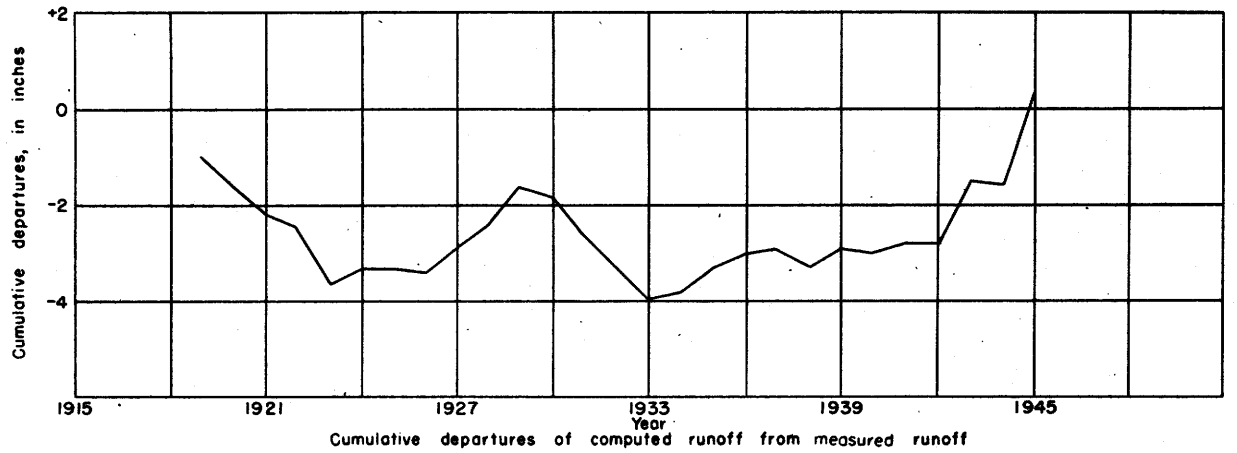

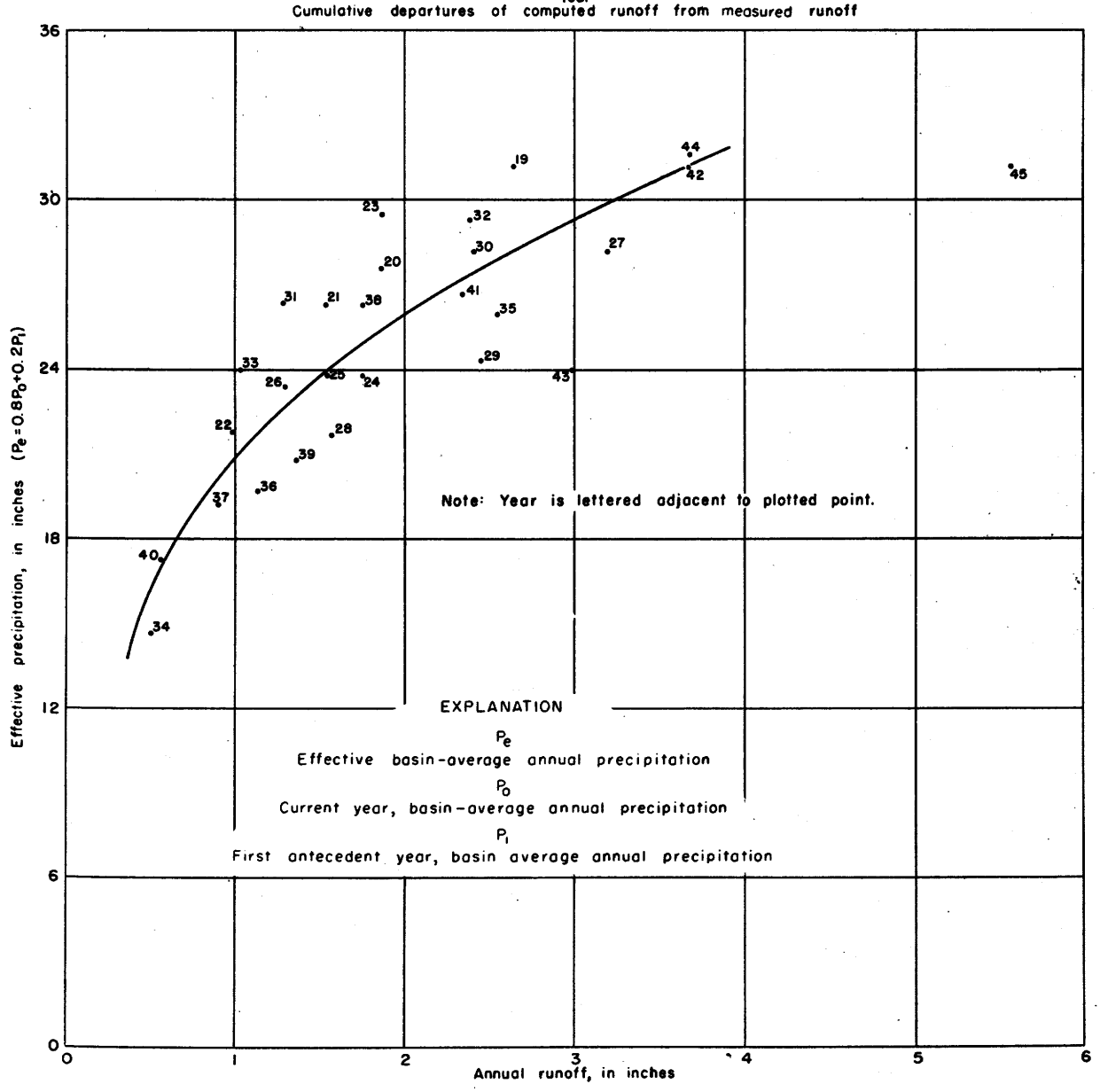

Figure 86.—Relationship of effective annual precipitation to annual runoff of Big Blue River at Randolph, Kans.

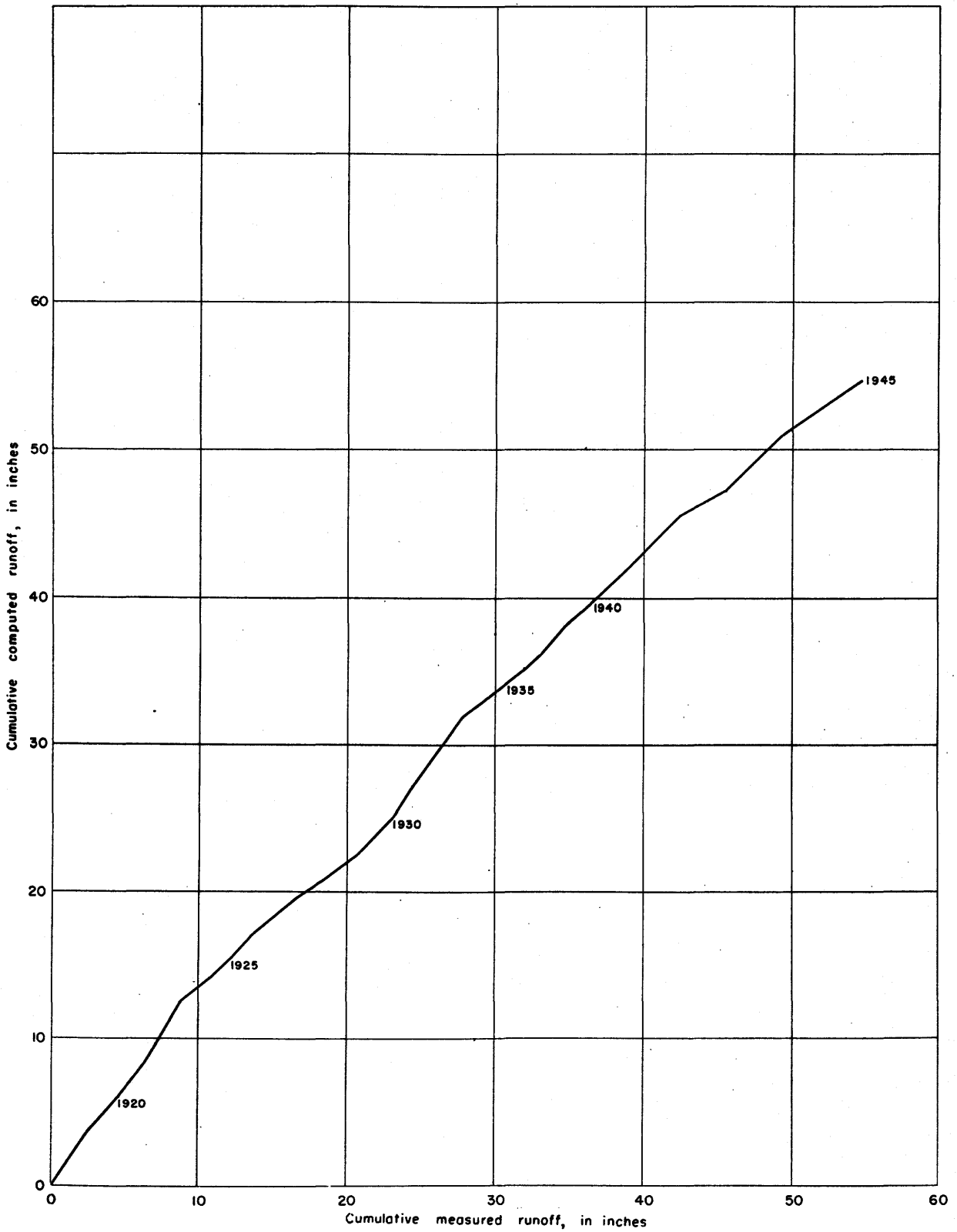

Figure 87.—Double mass curve of measured runoff plotted against computed runoff for Big Blue River at Randolph, Kans.

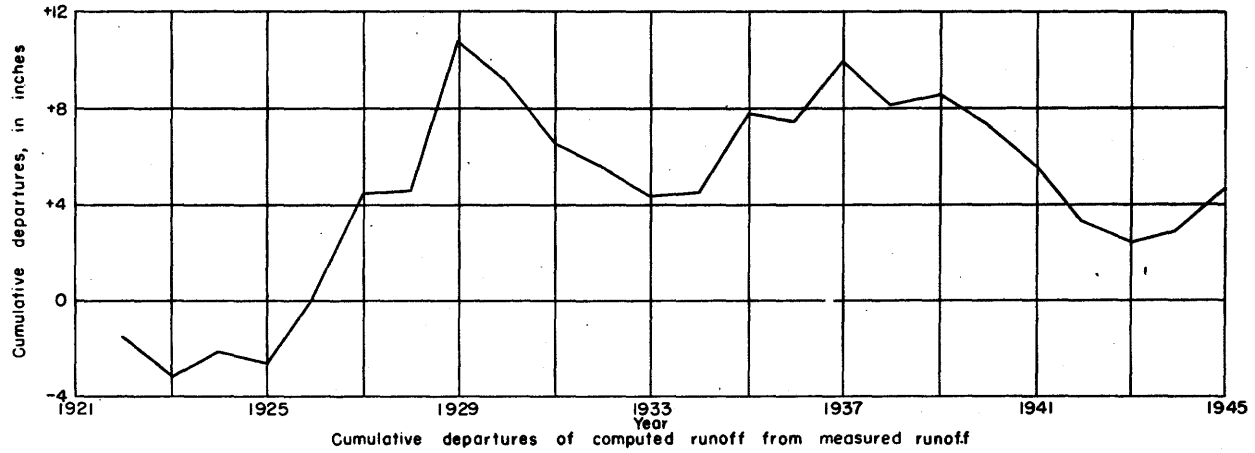

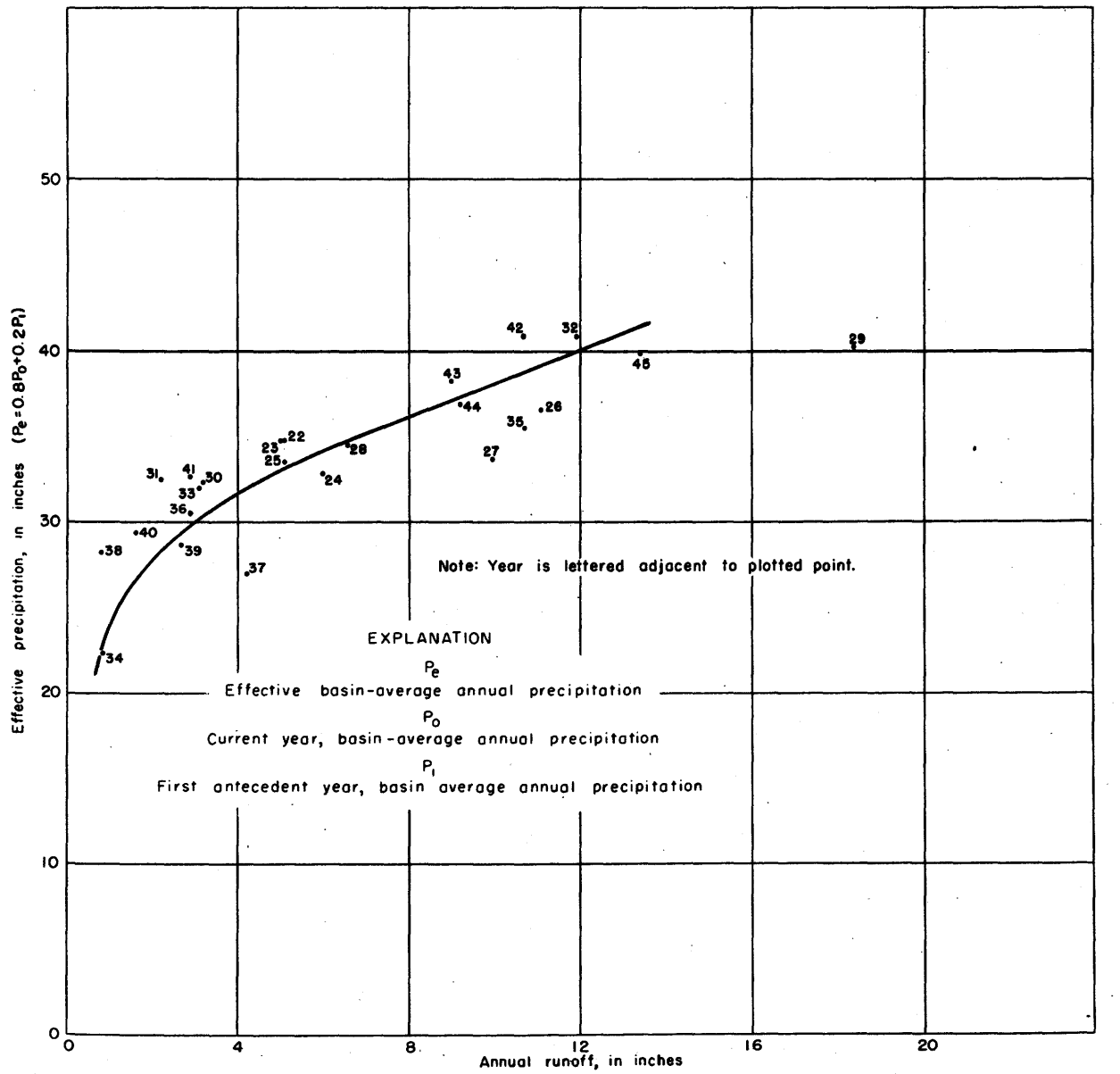

Figure 88. —Relationship of effective annual precipitation to annual runoff of Grand River near Gallatin, Mo.

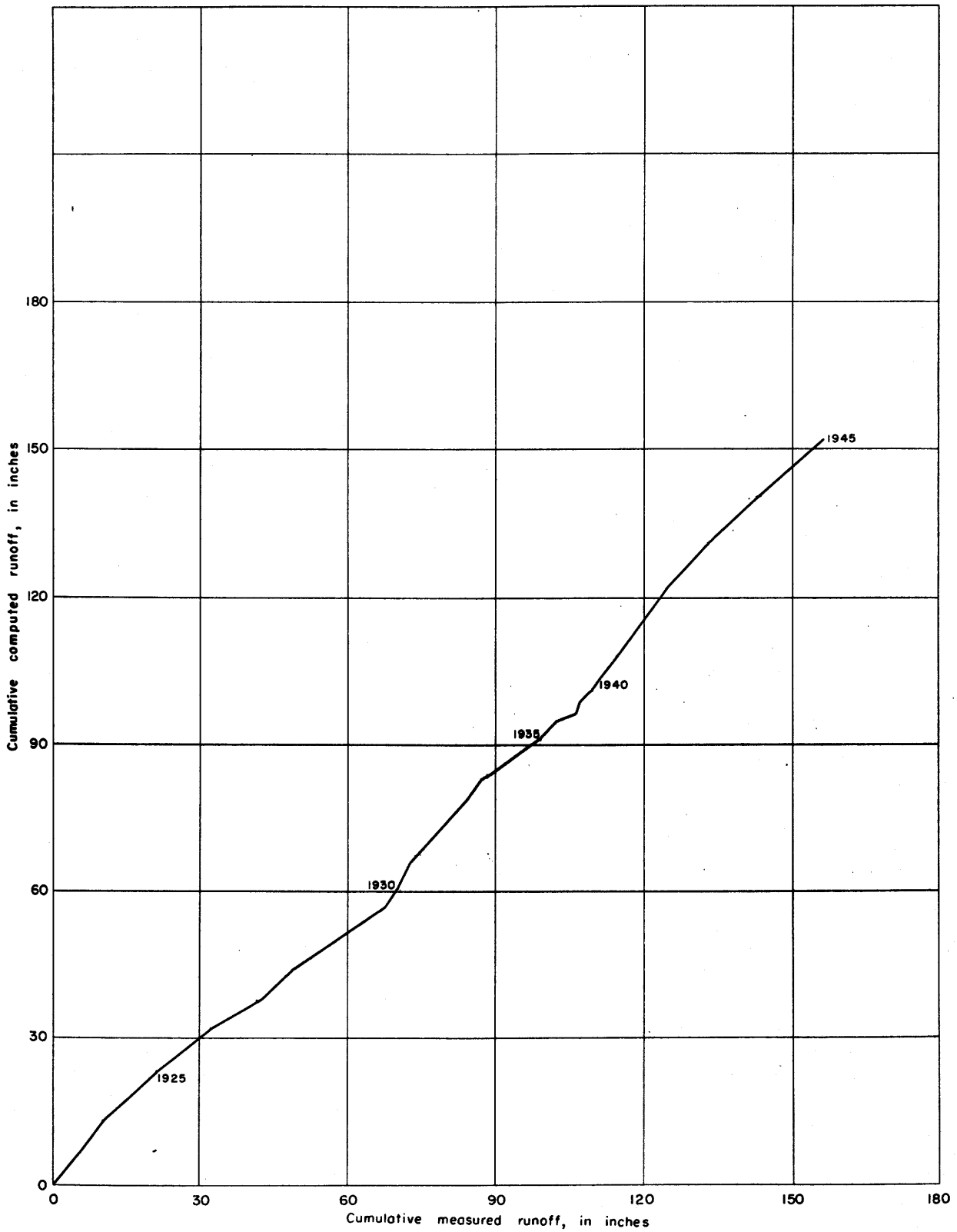

Figure 89. —Double mass curve of measured runoff plotted against computed runoff for Grand River near Gallatin, Mo.

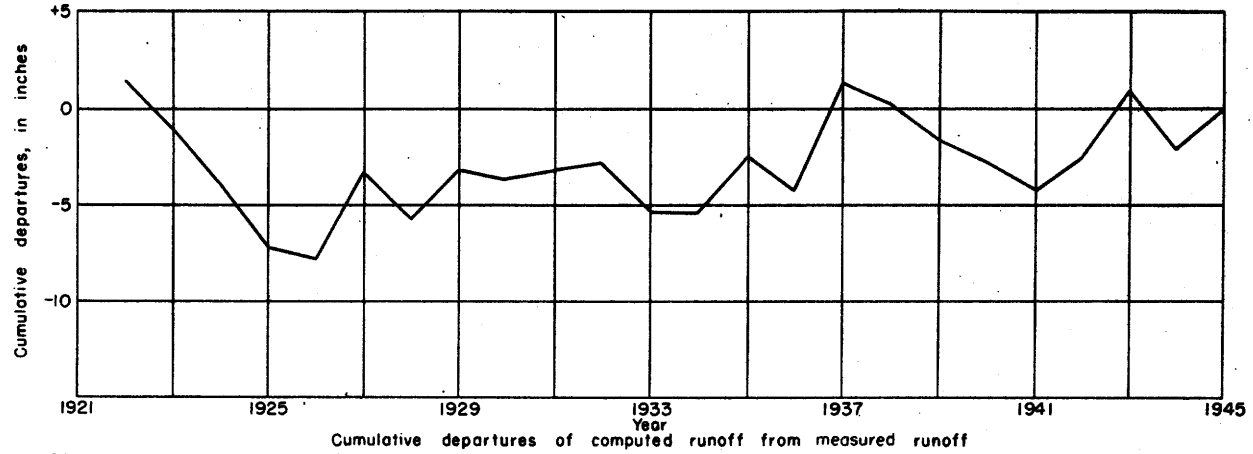

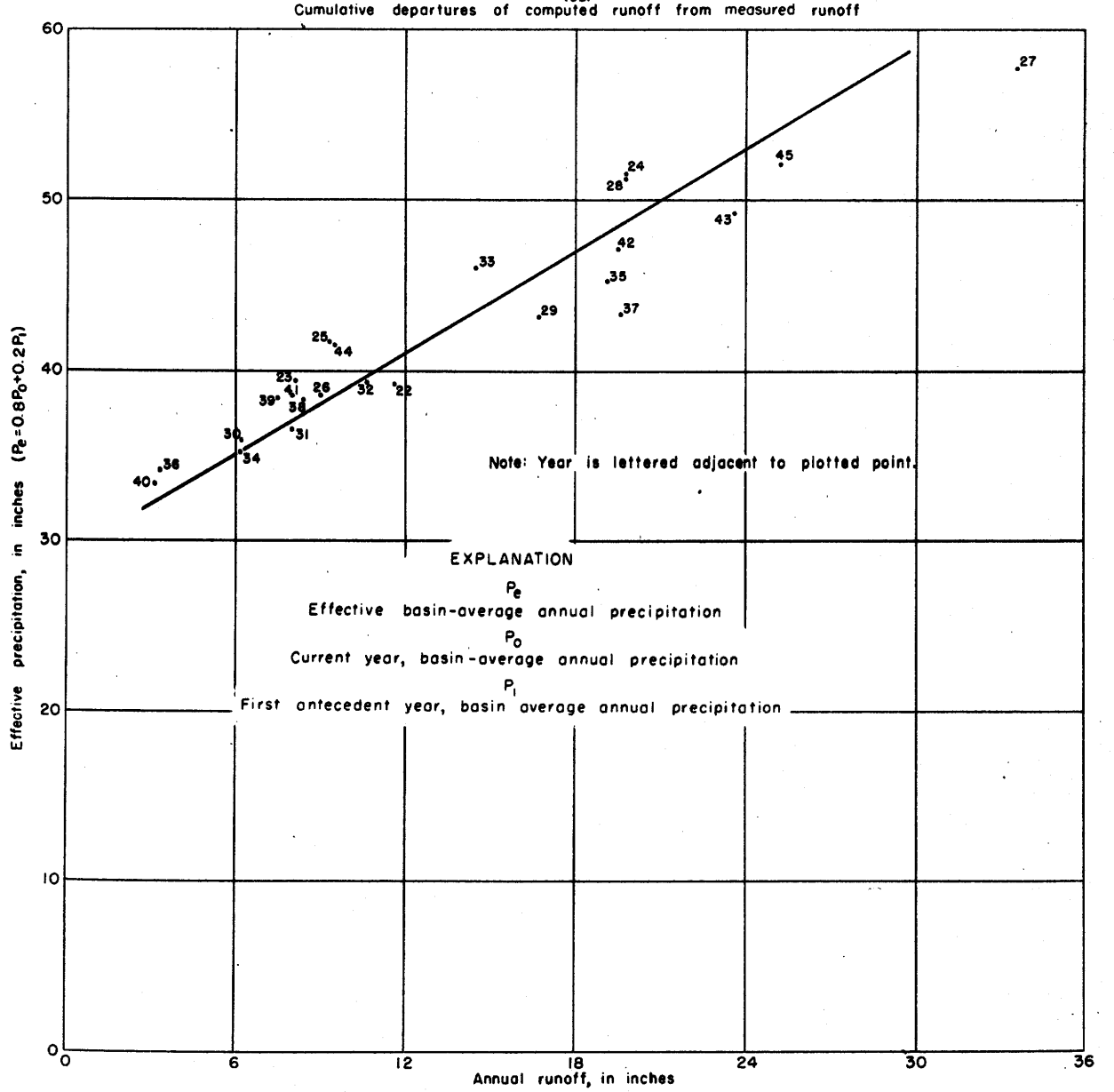

Figure 90.—Relationship of effective annual precipitation to annual runoff of Sac River near Stockton, Mo.

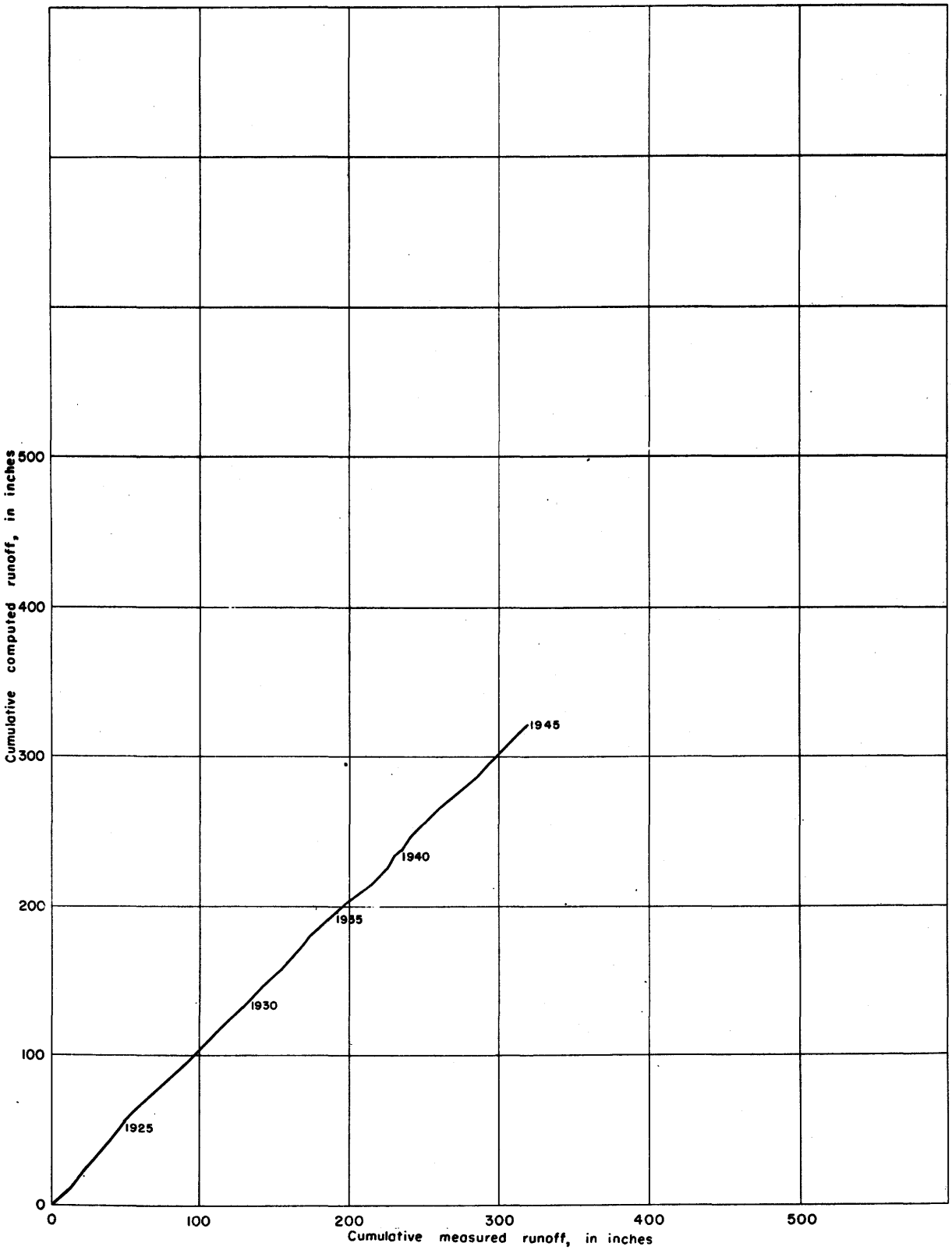

Figure 91. —Double mass curve of measured runoff plotted against computed runoff for Sac River near Stockton, Mo.

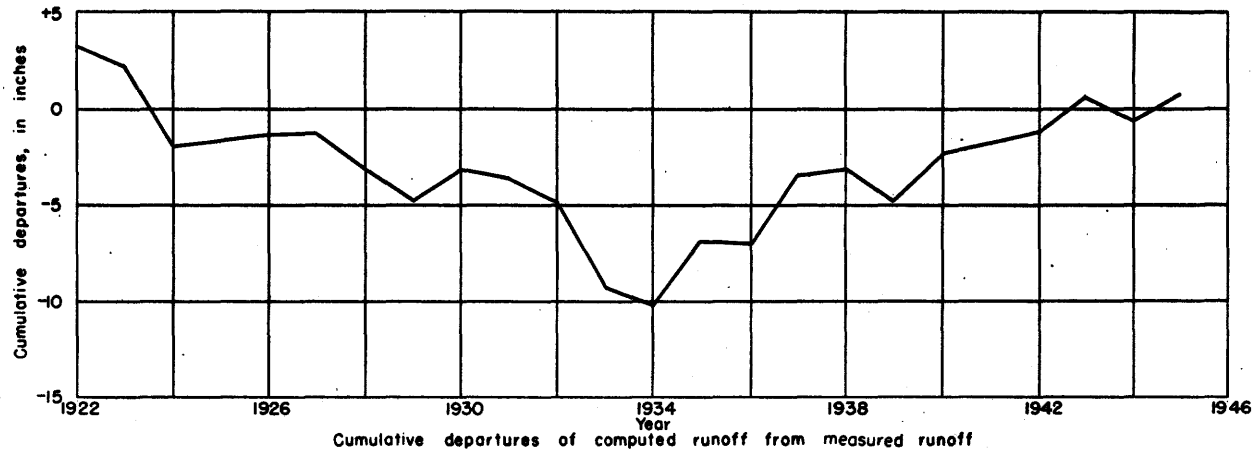

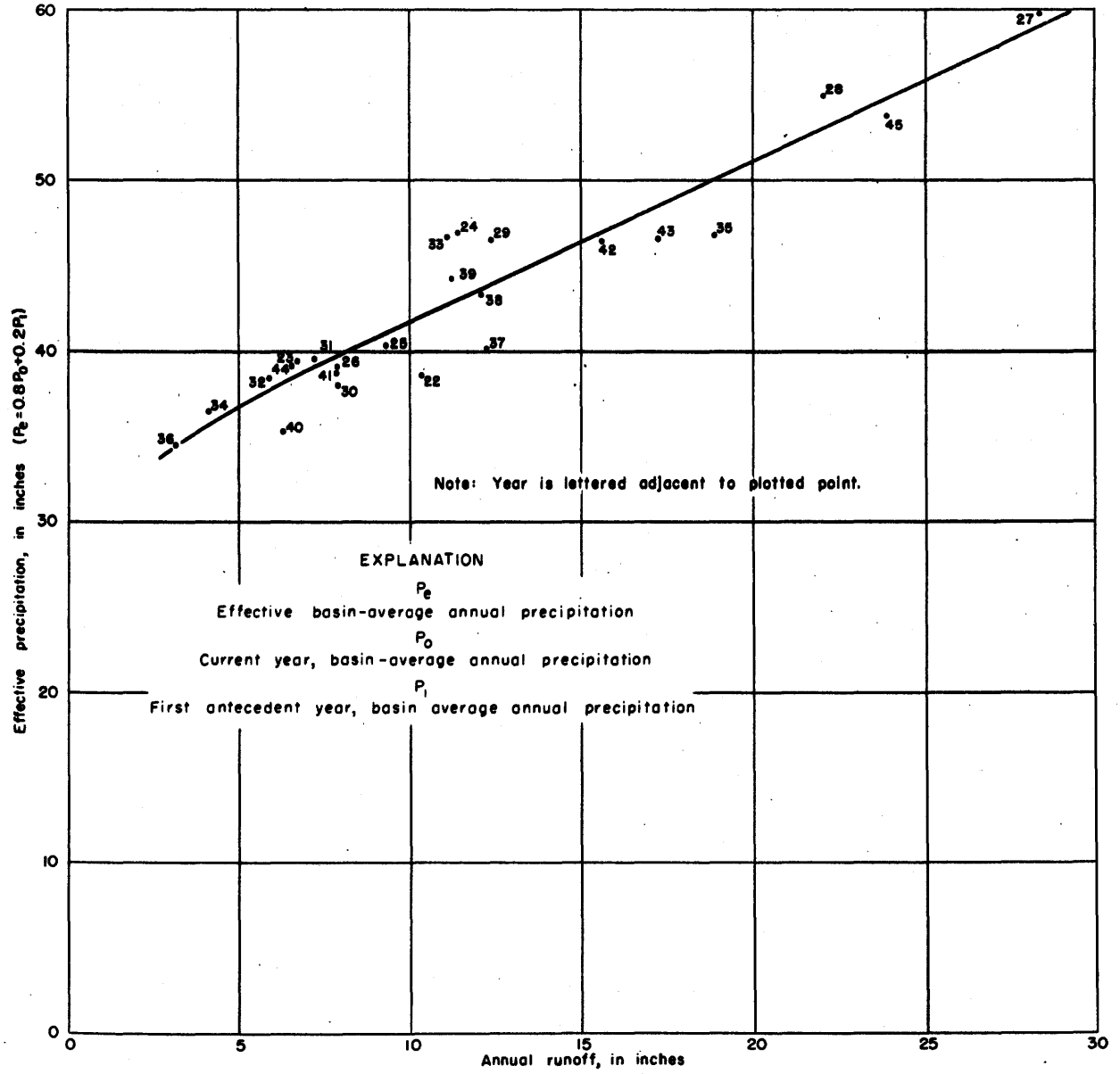

Figure 92. —Relationship of effective annual precipitation to annual runoff of Gasconade River near Waynesville, Mo.

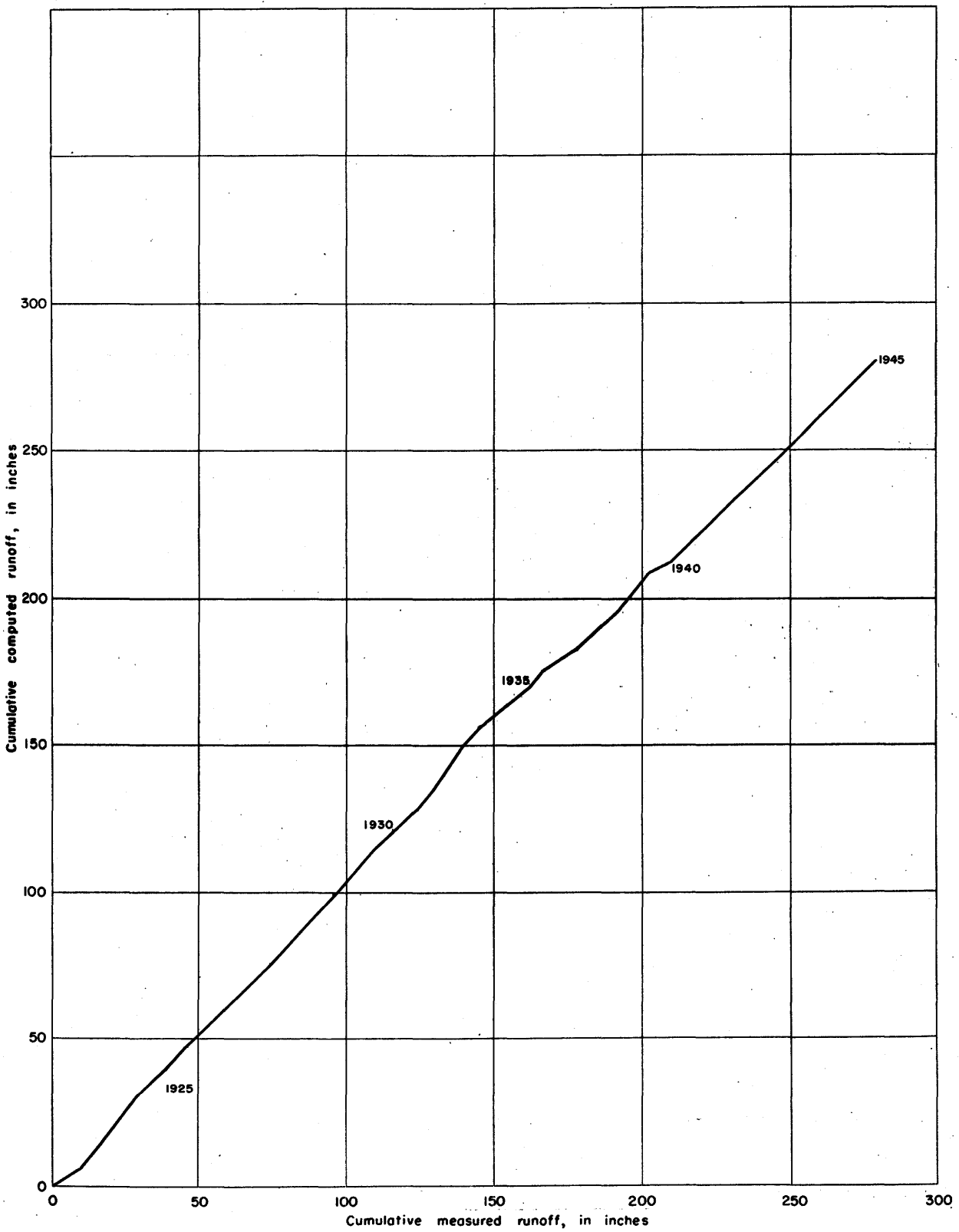

Figure 93. —Double mass curve of measured runoff plotted against computed runoff for Gasconade River near Waynesville, Mo.

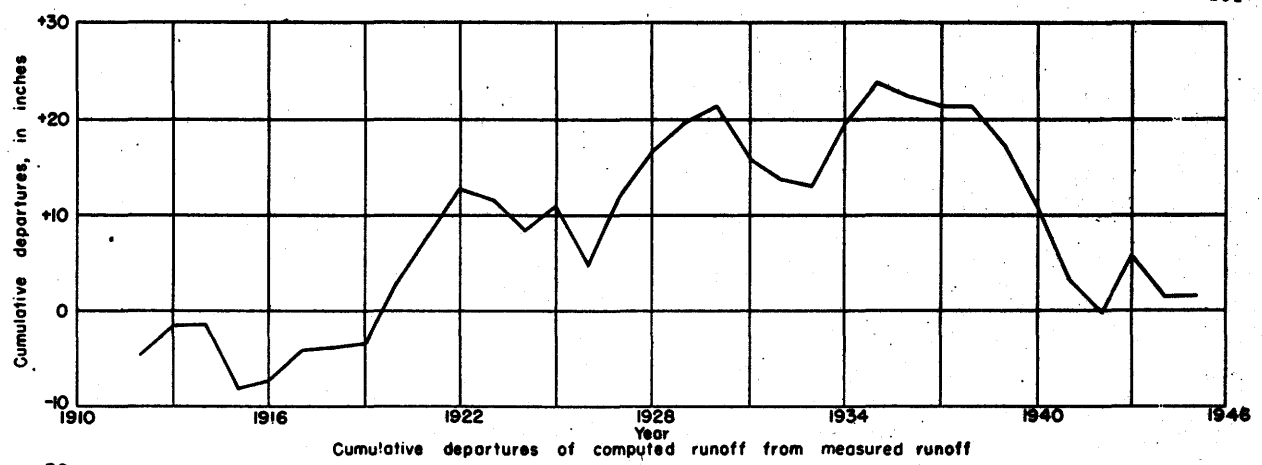

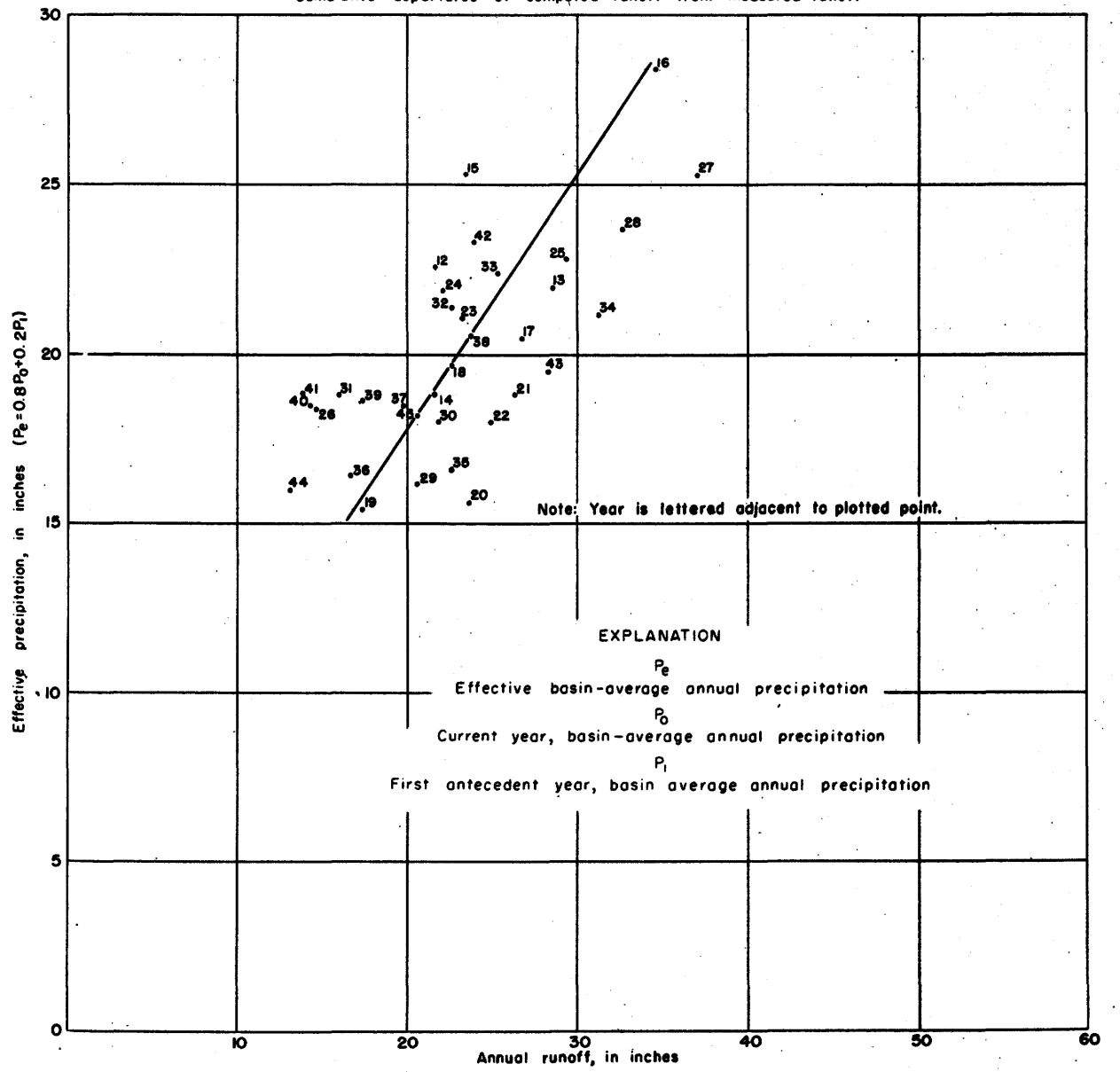

Figure 94.—Relationship of effective annual precipitation to annual runoff of St. Mary River near Kimball, Alberta.

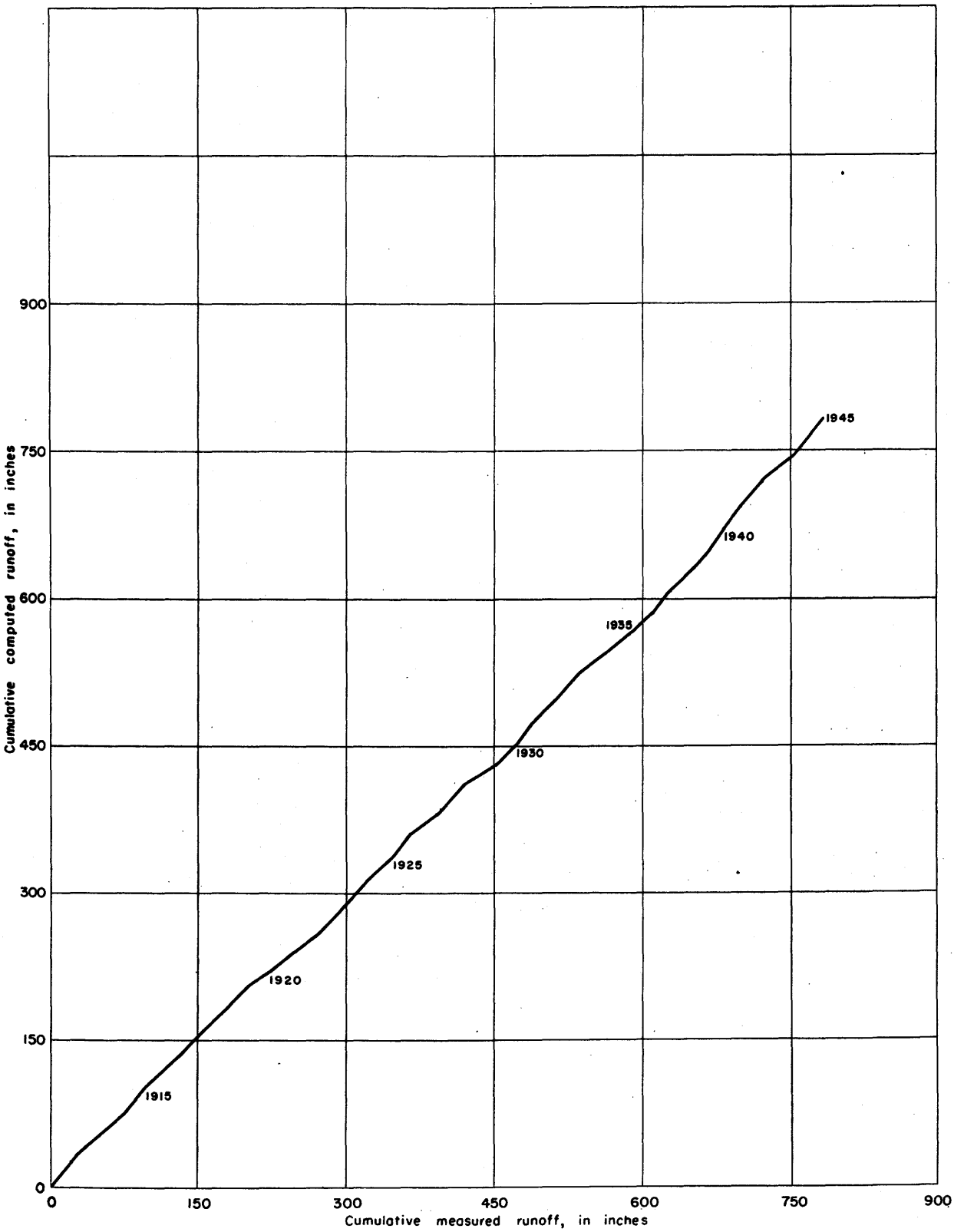

Figure 95.—Double mass curve of measured runoff plotted against computed runoff for St. Mary River near Kimball, Alberta.

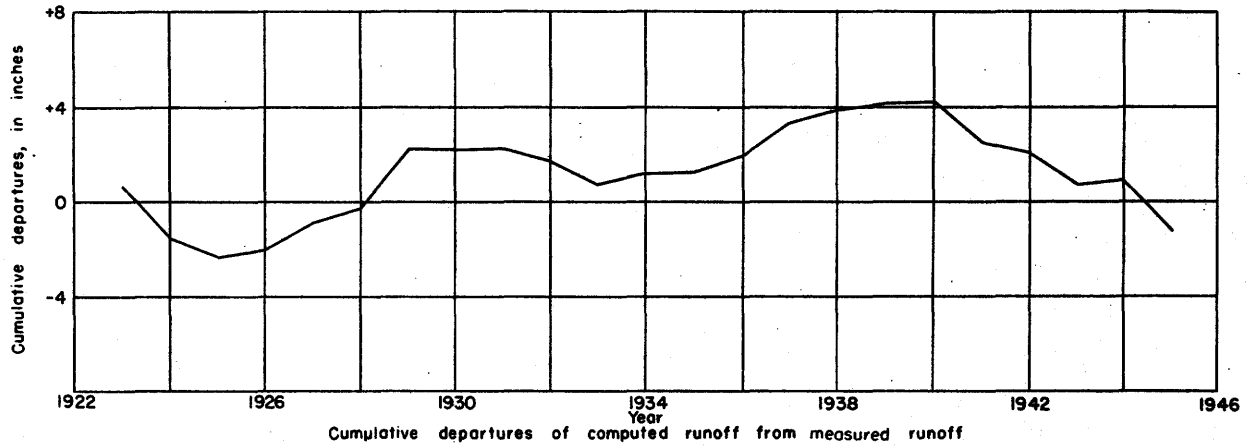

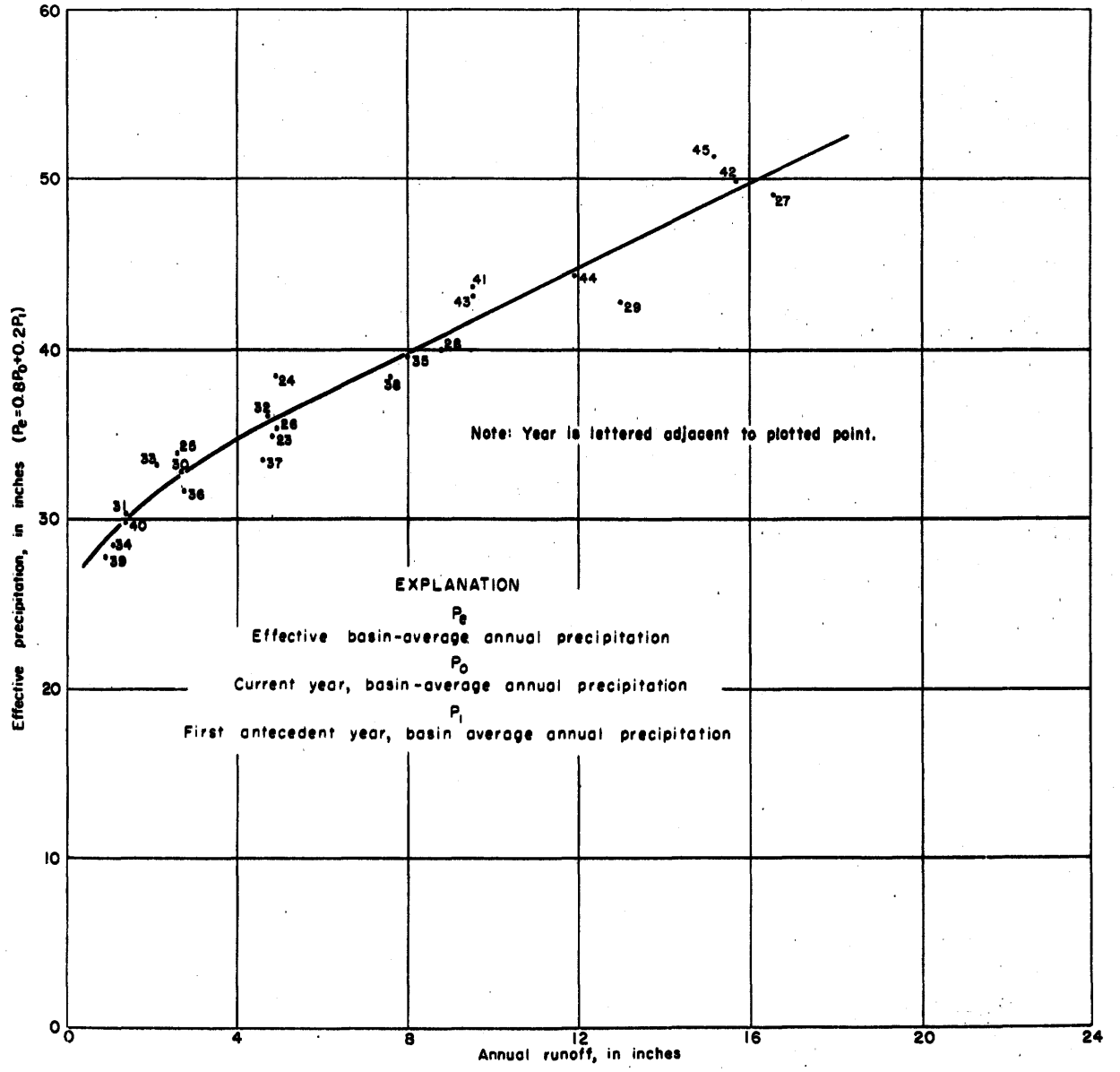

Figure 96.—Relationship of effective annual precipitation to annual runoff of Neosho River near Parsons, Kans.

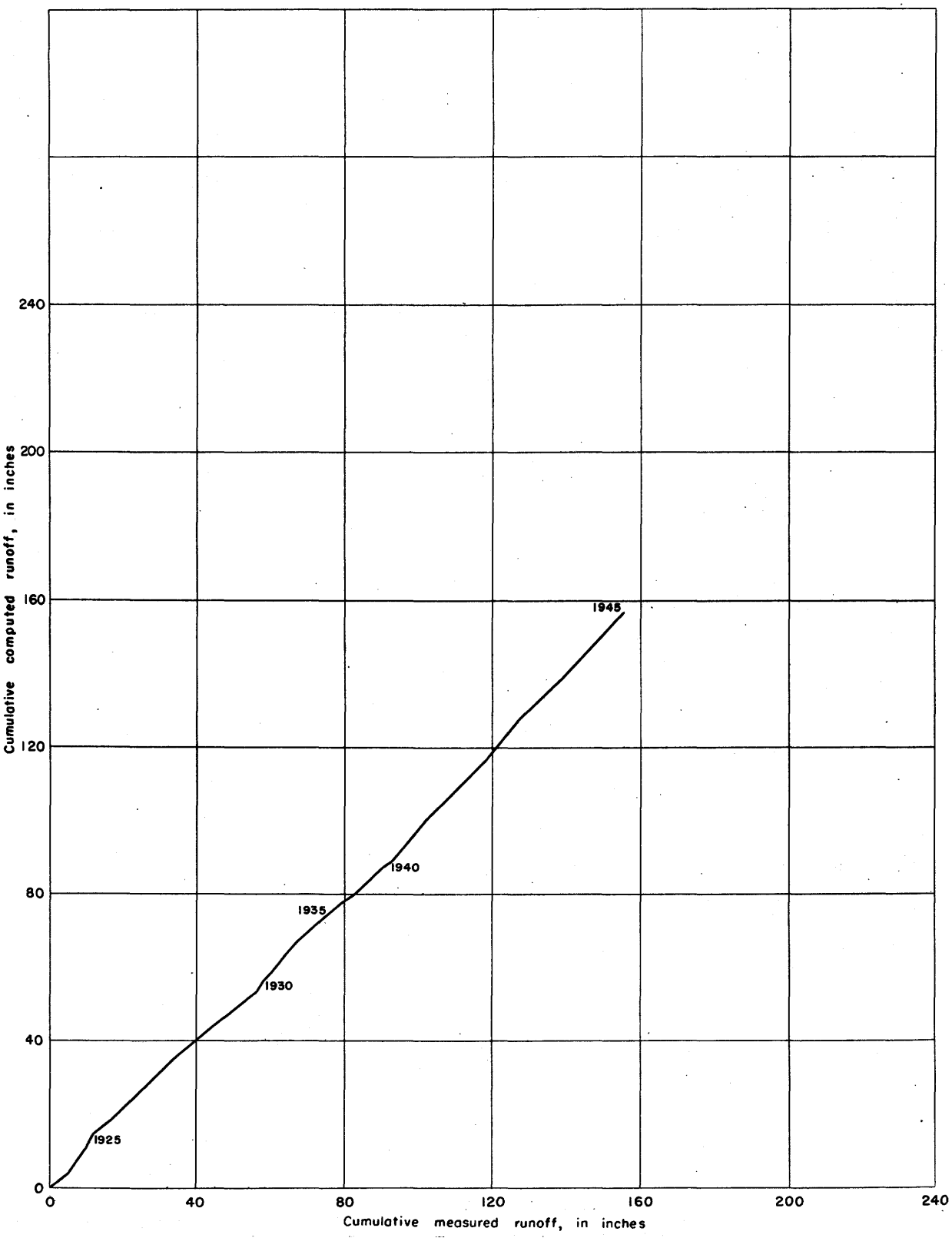

Figure 97. —Double mass curve of measured runoff plotted against computed runoff for Neosho River near Parsons, Kans.

Table 2. —Tributary basins studied for trends in precipitation-runoff relationship

Figure no.	Tributary basin	Period of record	Standard error of estimate (Percent of mean)	Indicated changes in precipitation - runoff relationship	
				Period	Direction
14	Osage - Bagnell, Mo.	1881-1945	24	--	--
16	Beaverhead - Barratts, Mont.	1908-45	18	1925-41	-R
18	Missouri - Ft. Benton, Mont.	1910-45	12	--	--
20	Madison - West Yellowstone, Mont.	1914-45	13	1931-45	-R
22	Tenmile - Rimini, Mont.	1915-45	47	1927-41	-R
24	North Fork Sun - Augusta, Mont.	1906-28	21	--	--
26	Marias - Shelby, Mont.	1912-45	40	1935-42	-R
28	Judith - Utica, Mont.	1920-45	58	1930-41	-R
30	Musselshell - Harlowton, Mont.	1907-45	45	1928-45	-R
32	Yellowstone - Corwin Springs, Mont.	1911-45	16	--	--
34	Bighorn - Thermopolis, Wyo.	1901-45	21	1931-41	-R
36	Powder - Arvada, Wyo.	1917-45	37	1934-45	-R
38	Little Missouri - Alzada, Mont.	1912-45	70	--	--
40	Cannonball - Breien, N. Dak.	1912-18 1922-45	64	--	--
42	Moreau - Promise, S. Dak.	1929-45	75	--	--
44	Cheyenne - Wasta, S. Dak.	1929-45	30	1937-45	-R
46	Rapid - Big Bend, S. Dak.	1915-42	39	1919-25 1938-42	+R -R
48	Belle Fourche - Belle Fourche, S. Dak.	1912-40	49	--	--
50	Bad - Fort Pierre, S. Dak.	1929-45	35	--	--
52	White - Oacoma, S. Dak.	1929-45	33	--	--
54	Niobrara - Dunlap, Nebr.	1924-42	21	1937-42	-R
56	James - Scotland, S. Dak.	1929-45	69	--	--
58	Big Sioux - Akron, Iowa	1929-45	29	--	--
60	North Platte - Saratoga, Wyo.	1904-45	21	1928-45	-R
62	North Fork South Platte - South Platte, Colo.	1914-22 1925-45	28	--	--
64	Clear - Golden, Colo.	1912-22 1925-45	21	--	--
66	Thompson - Drake, Colo.	1918-26 1929-45	21	--	--
68	Cache la Poudre - Ft. Collins, Colo.	1910-45	32	--	--

Table 2.—Tributary basins studied for trends in precipitation-runoff relationship--continued

Figure no.	Tributary basin	Period of record	Standard error of estimate (Percent of mean)	Indicated changes in precipitation - runoff relationship	
				Period	Direction
70	Loup - Columbus, Nebr.	1895-1915 1929-45	14	--	--
72	Elkhorn - Waterloo, Nebr.	1929-45	22	--	--
74	Nishnabotna - Hamburg, Iowa	1929-45	37	--	--
76	Nodaway - Burlington Jct., Mo.	1923-45	33	--	--
78	Platte - Agency, Mo.	1922-45	32	--	--
80	Arickaree - Haigler, Nebr.	1924-45	91	--	--
82	Smoky Hill - Ellsworth, Kans.	1919-45	52	--	--
84	Saline - Tescott, Kans.	1920-45	57	--	--
86	Big Blue - Randolph, Kans.	1919-45	35	--	--
88	Grand - Gallatin, Mo.	1922-45	39	--	--
90	Sac - Stockton, Mo.	1922-45	19	--	--
92	Gasconade - Waynesville, Mo.	1922-45	18	--	--
94	St. Mary - Kimball, Alberta	1912-45	19	--	--
96	Neosho - Parsons, Kans.	1923-45	17	--	--

regions where data on high altitude precipitation are lacking. The effect of this factor must remain unknown. Variations in the orographic effect must also remain an unknown until adequate precipitation records from high-altitude stations are available.

Long-term variations in water tables have been classified as climatic factors because, in basins where ground water is not extensively used for irrigation, most changes in ground-water levels may generally be ascribed to long-term variations in precipitation. The full effect of below-normal precipitation on water tables may not be apparent until many years later - the actual lag in any tributary basin is related to geologic conditions. McDonald and Langbein 4/ showed that, in the Columbia Basin, precipitation for many years back is effective in determining the current year runoff. Unfortunately, lack of long records of precipitation hampers the full exploration of long-term, carry-over effects in some of the tributary basins of the Missouri Valley that showed trends in the precipitation-runoff relationship.

Forest denudation has been shown 5/ to materially increase runoff yield for the first few years after cutting of trees. After the second growth reaches a moderate stage of development the yields will begin to return to normal. In a large drainage basin deforestation would need be on a large scale to show a noticeable effect on the runoff.

Changes in consumptive use due to altered farming methods, new crop types requiring more irrigation water, and the increased growth of wasteful plants in canals and seeped areas could cause an apparent modification in the precipitation - runoff relationship if the increased use were unreported. The extensive construction of small stock ponds may be the cause of part of the declining yield ratio in the Cheyenne River Basin.

Further computations were made in all tributary basins showing a precipitation-runoff relationship trend to determine, if possible, the factors responsible for the change. Figure 98 shows the residual mass curve for the Beaverhead Basin after

4 McDonald, C. C., and Langbein, W. B., Trends in runoff in the Pacific Northwest: Am. Geophys. Union Trans., vol. 29, pp. 387-397, 1948.

5 Hoyt, W. G., and Troxell, H. C., Forests and stream flow: Am. Soc. Civil Eng. Trans., vol. 99, pp. 1-111, 1934.

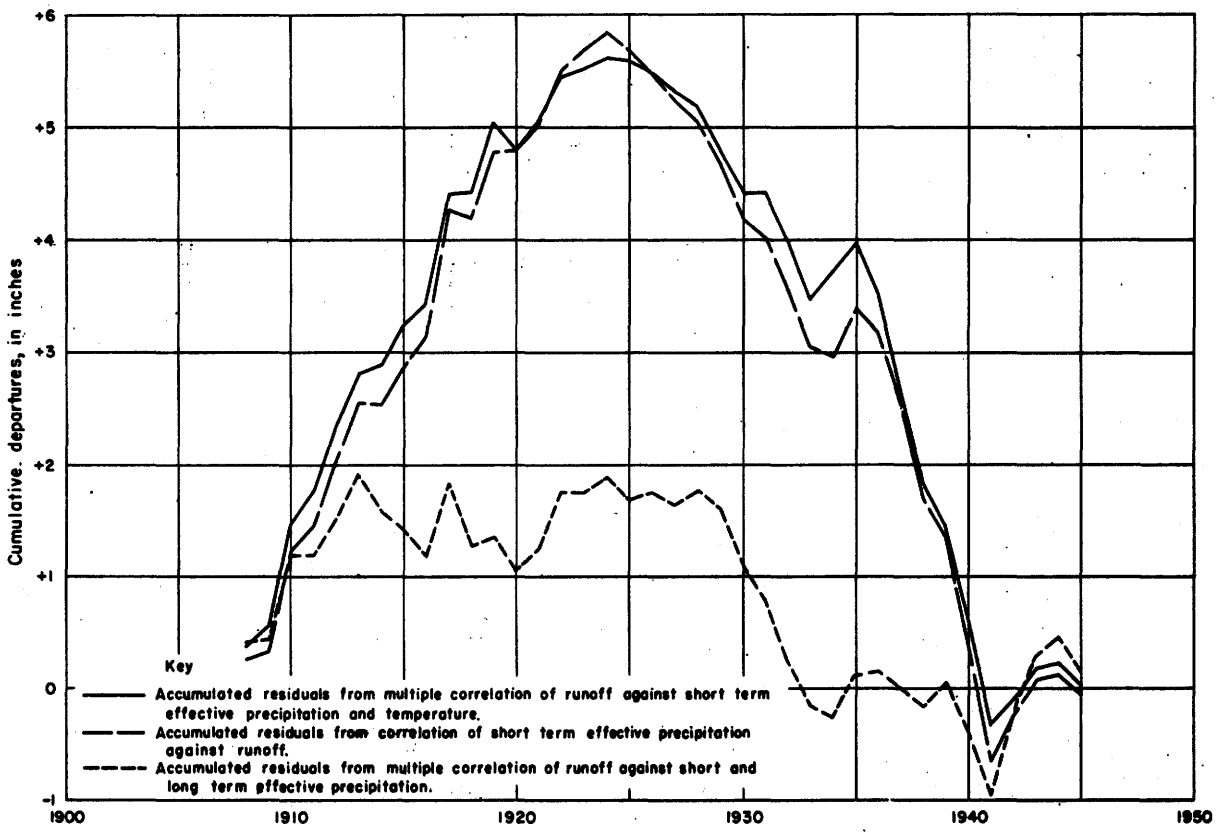

Figure 98.—Residual mass curves for Beaverhead River at Barratts, Mont.

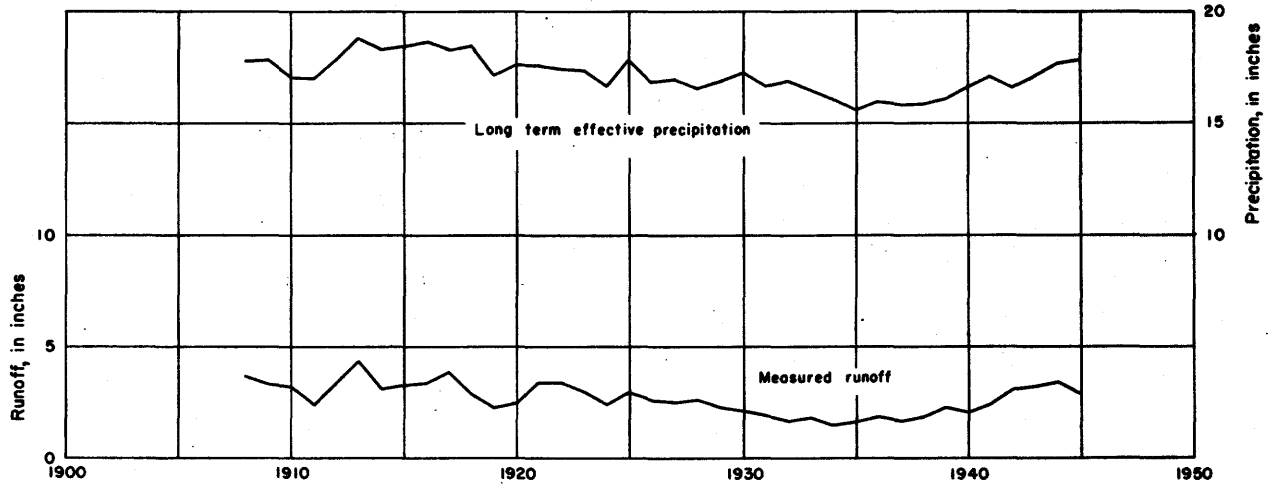

Figure 99.—Comparison of computed long term effective precipitation with measured runoff of Beaverhead River Basin.

mean annual temperature was included in a multiple regression with P_e and R. For comparative purposes the former residual mass curve is drawn on the figure as a dotted line to show the very slight improvement due to inclusion of temperature effects.

Another factor of importance in determining runoff yields in the Beaverhead Basin is fluctuations in water tables. No observation well records for the period 1908-45 are available to appraise the water-table fluctuations in the basin, so an indirect method of showing the probable variations in water table was used. Water-table levels, and hence ground-water contributions to stream flow, are probably determined by precipitation amounts for many years back. A long-term, carry-over effect of precipitation was computed by the use of die-away coefficients as outlined in an article by McDonald and Langbein.6/ Figure 99 shows the computed long-term component of precipitation for the Beaverhead Basin as related to measured runoff. If this long-term component, considered to represent ground-water contributions to stream flow, is included in a multiple regression of observed runoff against annual precipitation, the trend in the precipitation-runoff relationship, found previously, vanishes, indicating that it was due to a combination of declining water-table and temperature effects. The residual mass curve of R vs R_c resulting from the multiple regression, is shown on figure 98.

Similar procedures were used to evaluate the apparent trends in precipitation-runoff relationship in the other tributary basins and all were found due to either or both temperature and declining water-table effects. Figure 100 shows the mean annual discharge plotted as a time series for Big Spring Creek near Lewistown, Mont. The flow measured at this station is almost all spring discharge and is therefore a good indicator of ground-water levels. Follansbee measured the discharge of Big Spring Creek prior to 1909 as 140 c.f.s. The plot shows the rapid decline of the water table for the period 1933-41, and illustrates the time lag between annual precipitation and ground-water outflow by comparison with the Lewistown precipitation record included on the plot. This graphic account of declining ground-water contributions to stream flow in one area of Montana is included to show the importance of an adequate observation-well program in forecasting changes in base flow.

MAP OF LIMITING WATER LOSS

The term "water loss" as used herein refers to that portion of precipitation that does not appear in streams as runoff. Water loss as computed in this way differs from evapotranspiration by (1) the amount of changes in ground-water and soil-moisture storage and (2) the amount of subsurface discharge in or out of a basin. However, changes in storage tend to be compensating.

In an arid or semi-arid climate a larger annual precipitation results usually in a larger annual water loss. But for wet years in a humid climate the water loss tends to remain constant regardless of further increase in precipitation. This water loss, which is close in meaning to Thornthwaite's 8/ potential evapotranspiration, is termed limiting water loss. Although a limiting water loss may be presumed to exist in an arid or semi-arid climate, it may never be reached because precipitation is usually insufficient for all demands. The difference between the limiting water loss and the annual water loss is an indication of the amount of water needed to be supplied by irrigation to fully meet the requirements of vegetation.

In the Missouri Basin only the eastern end and the high-altitude regions of the mountains regularly receive sufficient precipitation to approximate limiting annual water loss during years of high precipitation and runoff. In the greater part of the basin, the limiting annual water loss is seldom, if ever, exceeded by the annual precipitation. If the water from the rapidly melting snow and thunderstorms that produce most of the runoff were made available more slowly no runoff would occur.

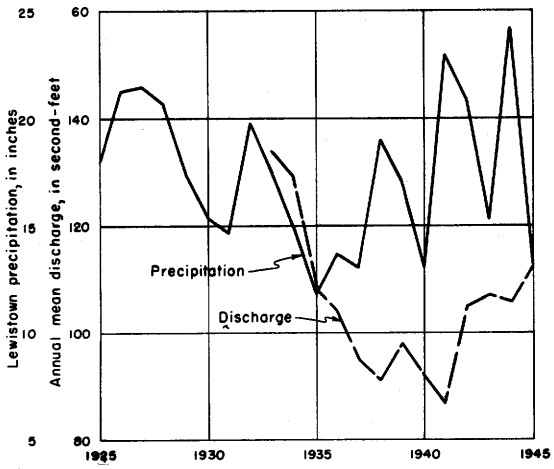

Figure 100.—Decline of base flow during drought years as shown by Big Spring Creek near Lewistown, Mont.

Figure 101 shows the method used to define the limiting annual water loss in the Nodaway River Basin of Iowa-Missouri, as an example for all tributary basins in the humid and subhumid zones. Because of the lack of rain gages in the tributary basins deriving their water from the high mountains, approximate loss values were calculated by using data at mountain snow courses. Figure 102 shows three plots illustrating the relationships of winter precipitation to the total annual precipitation at various rain-gage stations in Colorado, Wyoming, and Montana. These graphs were used to convert snow-survey water contents into usable values of annual precipitation at high altitudes. Figure 103 shows a composite plot of limiting annual water loss against altitude for tributary basins in the Missouri River Basin deriving their water from the mountains. For the semiarid and arid plains region, limiting annual water loss was defined by a temperature-loss relationship modified in light of the known geology of the basin.

6 McDonald, C. C., and Langbein, W. B.. Trends in runoff in the Pacific Northwest: Am. Geophys. Union Trans., pp. 387-397, 1948.

8 Thornthwaite, C. W., in Rept. of Committee on Transpiration and Evaporation, Am. Geophys. Union Trans., vol. 25, pt. 5, pp. 686-693, 1944.

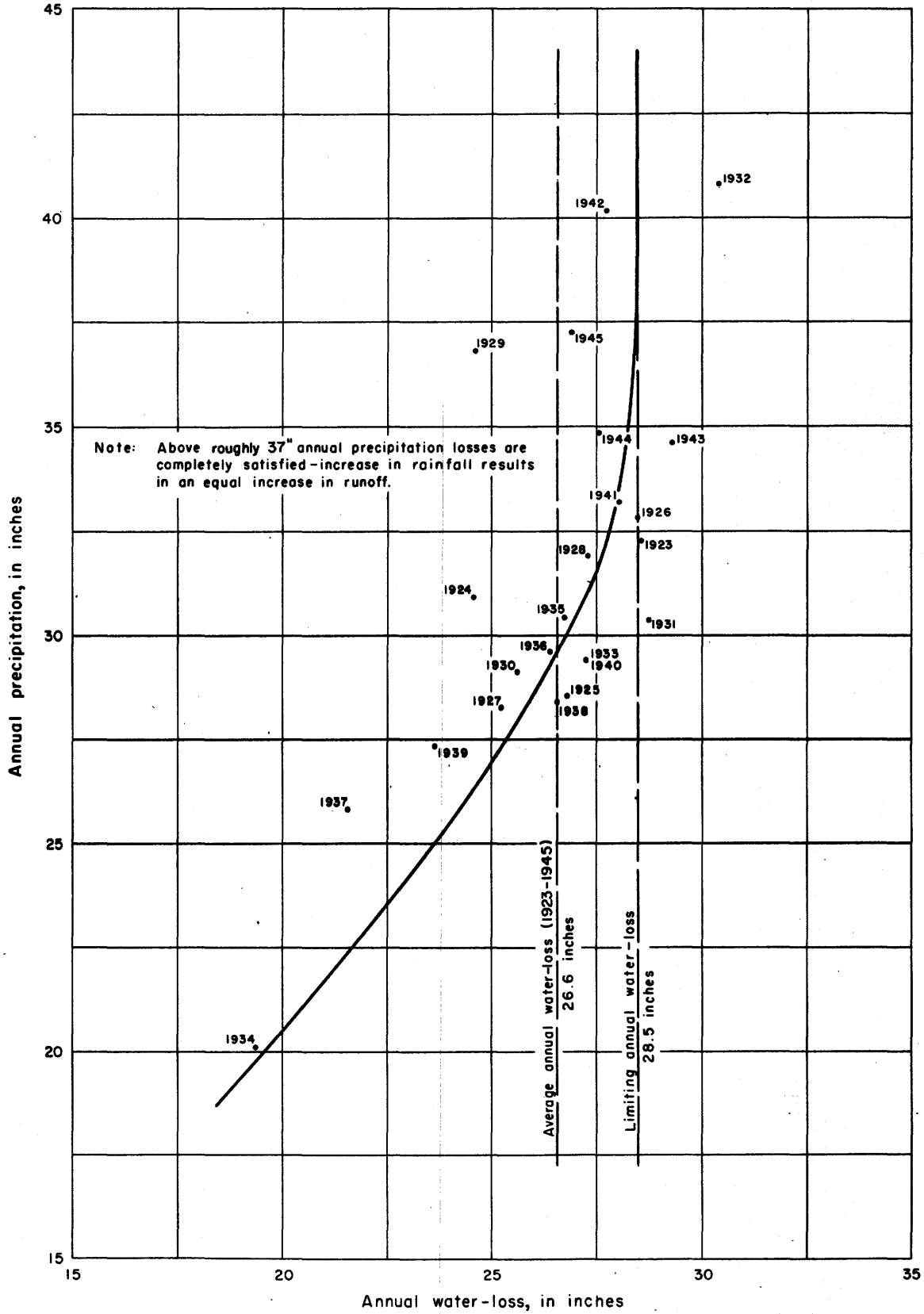

Figure 101.—Determination of limiting annual water-loss for Nodaway River basin above Burlington Junction, Mo.

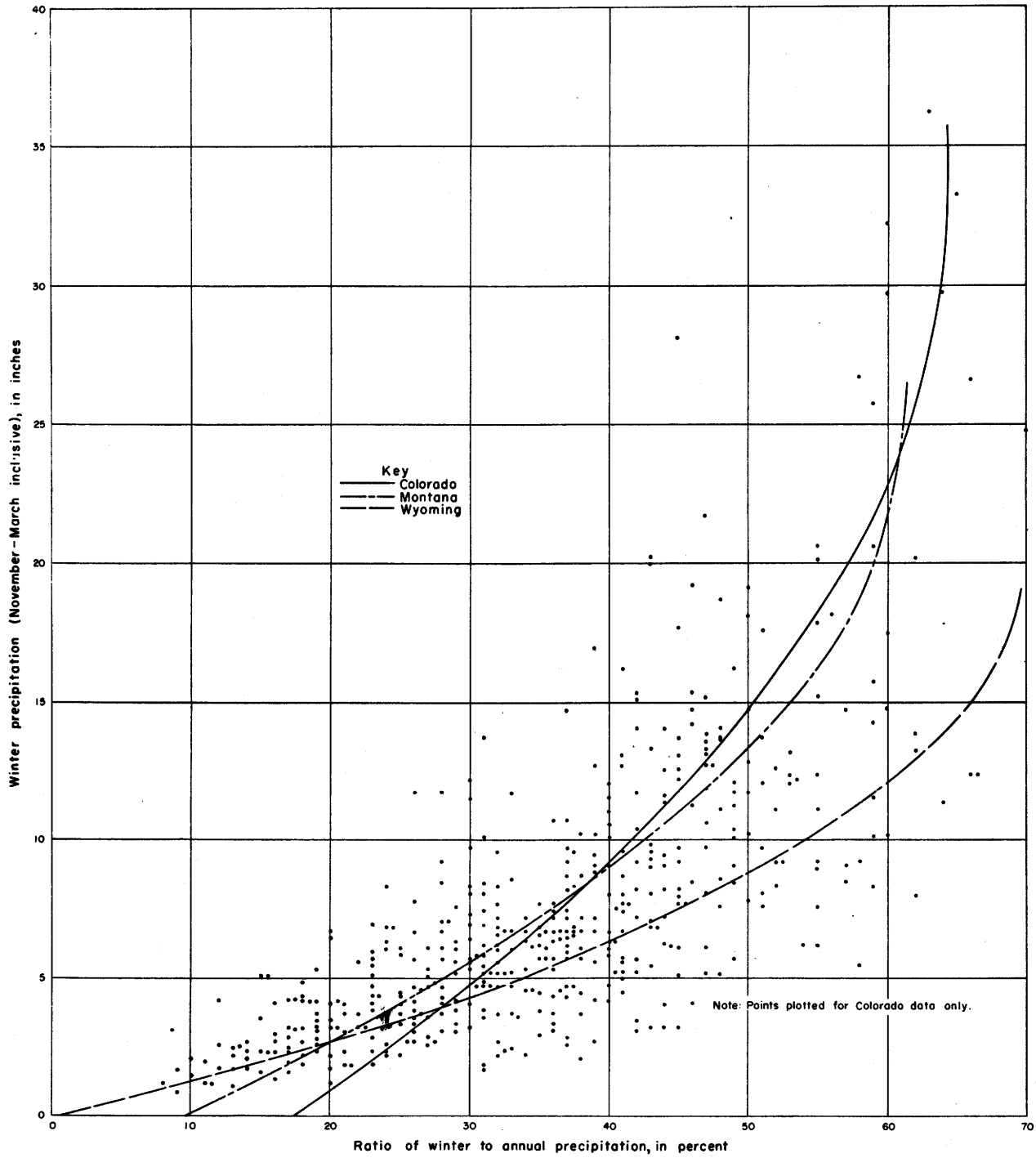

Figure 102.—Relationship of winter precipitation to annual precipitation in Colorado, Wyoming, and Montana.

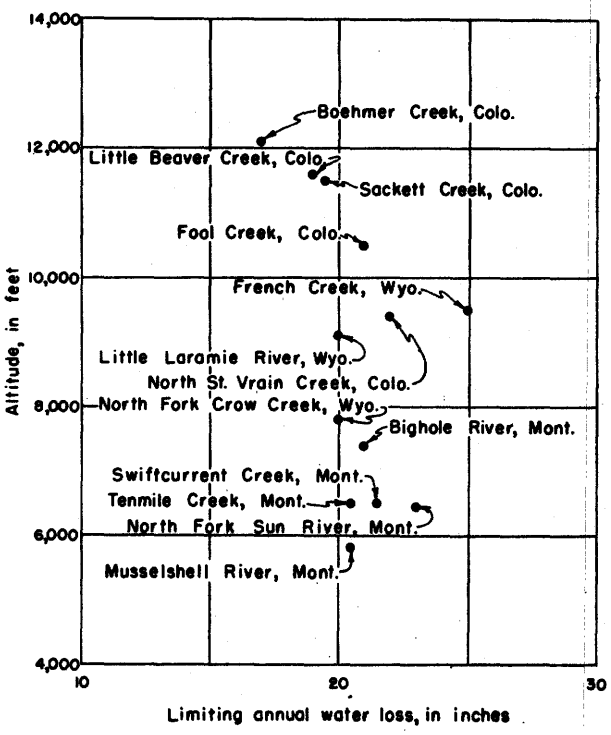

Figure 103.—Variation of limiting annual water loss with altitude.

Figure 104, a map of the Missouri Basin, shows the variation of limiting annual water loss in the basin by means of lines of equal limiting annual water loss. The line locations are roughly similar to the location of lines of equal potential evapotranspiration as defined by Thornthwaite. However, the limiting water loss values were approximated largely from measured runoff, and hence the factors of geology, topography, and surface-drainage patterns are inherent in the loss values. Note the low values surrounding the sand-hill region of Nebraska, and the difference in values on the east and west sides of the Missouri River in the Dakotas; clearly the result of different geologic and topographic conditions. The lines of equal limiting annual water loss on figure 104 are generalized because of local variations and because of the lack of sufficient runoff records.

CONCLUSIONS

During the period of records, annual precipitation has had a downward trend through much of the Missouri Basin. The downward trend may be considered to end with the dry 1930's. Mean annual temperature has trended upward during the period of record. The trend was sharpest during the decade 1930-40. Annual precipitation and mean annual temperature are related although the correlation is poor. If in the future, annual precipitation trends upward, mean annual temperatures may be expected to decline.

There have been long-term trends in the yield of annual runoff from equal annual precipitation during the period of runoff records in several tributary basins of the Missouri Basin. All such trends in the precipitation-runoff relationship were explained by concurrent changes in variables other than current year precipitation, considering ground-water outflow as related to precipitation, for many antecedent years.

The runoff records available for this study were not of sufficient duration really to define long-term trends in the precipitation-runoff relationship. Desirable length of runoff record is at least half a century. Continued gaging at several long-term stations should be considered a necessity for proper evaluation of trends in our water resources. An adequate observation-well program should be maintained to forecast future variations in base flow.

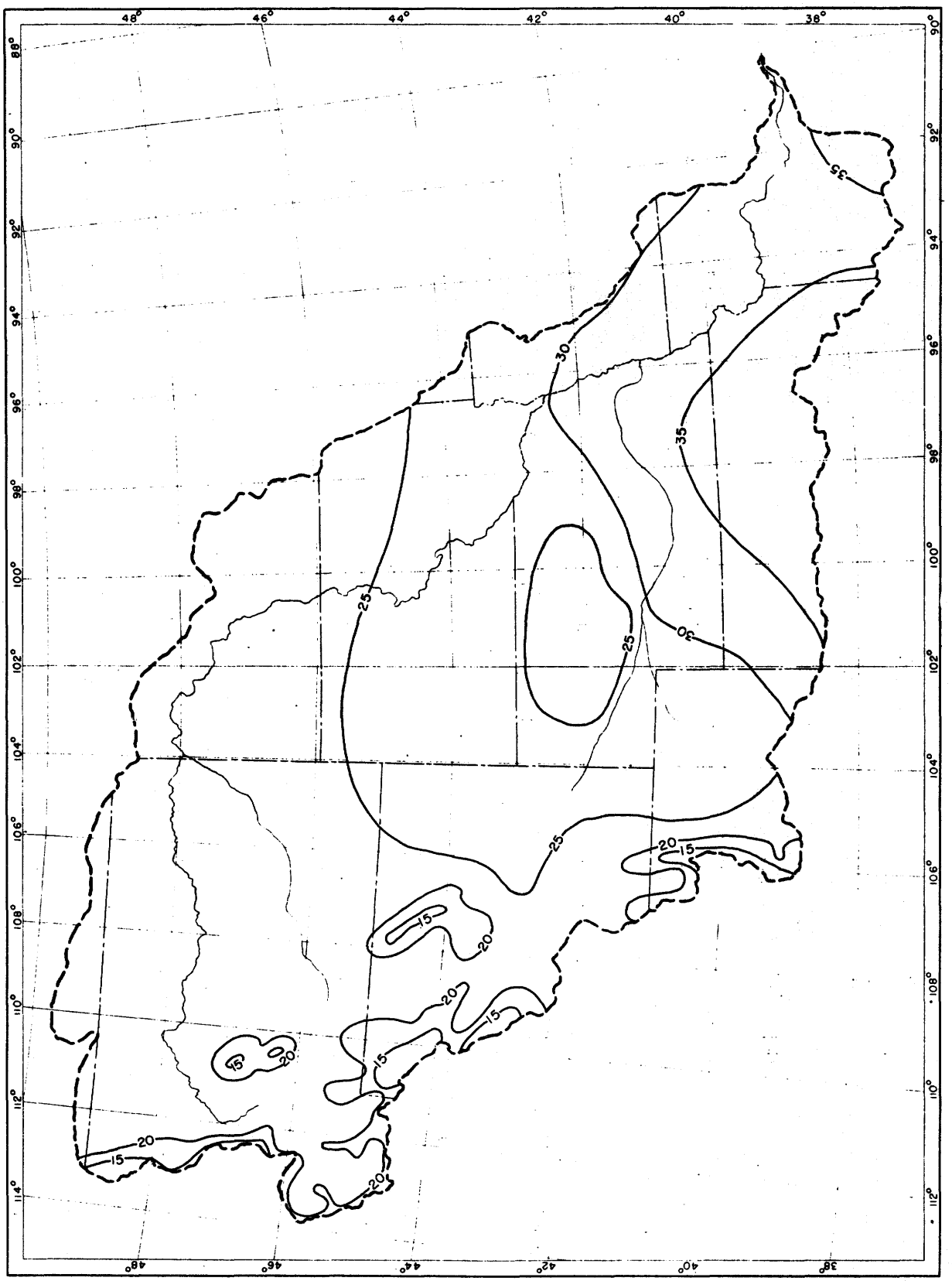

Figure 104.—Limiting annual water loss, in inches, in the Missouri River Basin.

REFERENCES CITED

Clayton, H. H., World weather records, Smithsonian Misc. Cols., vols. 79, 90, and 105, 1944.

Davenport, R. W., Prediction of runoff in Hydrology (edited by O. E. Meinzer), pp. 526-530, Dover Pubs., 1949.

Hoyt, W. G., Droughts in Hydrology (edited by O. E. Meinzer), pp. 579-591, Dover Pubs., 1949.

Hoyt, W. G., and others, Studies of relations of rainfall and run-off in the United States: U. S. Geol. Survey Water Supply Paper 772, 1936.

Hoyt, W. G., and Troxell, H. C., Forests and stream flow: Am. Soc. Civil Eng. Trans., vol. 99, pp. 1-111, 1934.

Kohler, M. A., and Linsley, R. K., Jr., Recent developments in water supply forecasting from precipitation: Am. Geophys. Union Trans., vol. 30, pp. 427-436, 1949.

Langbein, W. B., et al, Annual runoff in the United States, U. S. Geol. Survey Circ. 52, 1949.

Lowry, R. L., Jr., and Johnson, A. F., Consumptive use of water for agriculture: Am. Soc. Civil Eng. Trans., vol. 107, pp. 1243-1266, 1942.

Matthes, F. E., Glaciers in Hydrology (editied by O. E. Meinzer), pp. 149-219, Dover Pubs., 1949.

McDonald, C. C., and Langbein, W. B., Trends in runoff in the Pacific Northwest: Am. Geophys. Union Trans., vol. 29, pp. 387-397, 1948.

Meyer, A. F., The elements of Hydrology, 2d edition, pp. 443-470, 1928.

Soil Conservation Service, U. S. Dept., Agr. Summary of Federal-State cooperative snow surveys and irrigation water forecasts, Missouri-Arkansas Rivers drainage basin, 1936-1947.

Thornthwaite, C. W., An approach toward a rational classification of climate: Geog. Rev., vol. 38, pp. 55-94, Jan. 1948.

Troxell, H. C., and Stafford, H. M., Natural water losses in mountain drainage areas of Southern California: Am. Geophys. Union Trans., vol. 30, pp. 752-758, 1949.

Williams, G. R., and others, Natural water loss in selected drainage basins: U. S. Geol. Survey Water Supply Paper 846, 1940.

Interior—Duplicating Section, Washington, D. C. 95787